Escola de Ciências
Universidade do Minho

Departamento de Biologia

Contributions to the study of the *Pinus pinaster-Botrytis cinerea* interaction

Dissertação apresentada à Escola de Ciências da Universidade do Minho para obtenção do grau de Doutor em Ciencias (Biologia)

Herlânder Anselmo Queirós Pereira Azevedo

Braga, 2005

Declaration

The present PhD thesis was carried out under the supervision of Prof. Dr. Rui Manuel Tavares of the Departamento de Biologia, Escola de Ciências da Universidade do Minho. Work was performed at Centro de Biologia, Escola de Ciências da Universidade do Minho, in Braga, Portugal, between January 2001 and December 2004.

Funding was provided by the FCT (Fundação para a Ciência e Tecnologia), in the form of a PhD grant ref. SFRH/BD/3194/2000.

I declare that I have planned, performed and interpreted the experimental work depicted in the present thesis and submitted for publication.

I authorize the integral reproduction of this thesis for research purposes only.

Herlânder Anselmo Queirós Pereira Azevedo

Braga, 2005

Acknowledgements

I would like to thank Prof. Rui Tavares, my PhD supervisor, for providing me the opportunity to pursue this work. I am most thankful for his teachings, his dedication, and especially the honesty that has been a hallmark of the past four years. • To Prof. Teresa Lino Neto I would like to thank all the wonderful kindness and support, and also the helpful suggestions. • To Prof. Alberto Dias and Prof. Hernâni Gerós I would like to thank all the guidance and the opportunity to have more than a *collaboration*. • I am most grateful to all my lab colleagues and friends, who have been an integral part of this adventure. I thank them all for the help given during the prosecution of this work, and also for the joyful moments spent together. I am particularly thankful to Joana Correia, Carlos Conde and Joana Gonçalves for their direct contribution to this thesis. • I would like to acknowledge Dr. Armand Séguin (Laurentian Forestry Centre, Canada) and Dr. Carola Thöeringer (Martin Luther University, Germany) for providing biological material fundamental to the present work. I thank Dr. Lúcia Guise for her important contribution during nutrient analysis. • I am thankful to Prof. Célia Pais and Prof. Helena Cardoso, Heads of the Biology Department during the course of this thesis, for their commitment in providing the conditions to carry out this thesis. It is also fundamental to acknowledge the teachers and staff of the Biology Department at Minho University who have been an integral part of my life for the past eight years. • To my friends, old and new, my appreciation is endless… A special reference to Amaro who's been a dear companion, to Duarte, most loyal of friends, to Jorge purest of souls, to Sandra e Zé, who are simply the best and also Ana e Nuno, Ana, Sandra and Claudia, Tó, Agostinho, Gonçalo and Tarroso • I believe I should mention Marco, Menezes, Nuno, Paulo, Pedro and Óscar, who've been my best friends for over 20 years, need I say more? • Finally I thank my whole family for being wonderful, caring, and patient, especially Eduardo, who has a special place in my heart, my grandmother, whom I love beyond measure and my parents who are the world to me. • João, thank you for being the love of my life…

Table of contents

Chapter 5 • The *Pinus pinaster-Botrytis cinerea* interaction

Chapter 6 • *Effect of* Botrytis cinerea *elicitation on glucose transport in* Pinus pinaster *suspended cultured cells*

Resumo

O pinheiro bravo (*Pinus pinaster* Ait.) é um espécie que se encontra amplamente distribuida no Sudoeste Europeu. *P. pinaster* é uma espécie pioneira, e a sua adaptabilidade e características fenotípicas tornaram-na numa espécie florestal de elevado interesse económico. *Botrytis cinerea* é um fungo necrotrófico, induzindo a morte das células do hospedeiro para a progressão da infecção. *B. cinerea* é o agente da doença do *bolor cinzento* e um fungo patogénico de amplo espectro, sendo capaz de infectar mais de duzentas espécies vegetais. Populações adultas de pinheiro bravo exibem resistência a *B. cinerea*, enquanto que plântulas em viveiro e plantações jovens são frequentemente atacadas, resultando em acentuadas perdas económicas.

No presente trabalho, vários mecanismos de defesa das plantas from analizados no seu envolvimento na resposta de *Pinus pinaster* ao patogénio *B. cinerea*.

De modo a estabelecer um modelo de elicição para o estudo das interacção *P. pinaster*-*B. cinerea*, culturas heterotróficas de células em supensão de pinheiro bravo foram iniciadas a partir de *calli* de segmentos de raíz, em meio MS modificado. As culturas em suspensão foram caracterizadas no que refere à biomassa, pH, viabilidade celular, e consumo de açúcares, fosfato, nitrato e amónio. Os resultados evidenciaram que o consumo de nutrientes exibe um perfil bifásico no decurso do crescimento quase exponencial. Adicionalmente, a paragem do crescimento das células foi acompanhada por uma curva de morte. Culturas em suspensões de *P. pinaster* depletadas em açúcar exibiram elevada actividade da enzima fosfatase ácida, e evidenciaram degradação do DNA detectada por TUNEL, o que sugere que um mecanismo de morte celular programada por autofagia possa ser responsável pela morte em células de pinheiro privadas de açúcar.

Quando eliciadas com esporos de *B. cinerea*, células em suspensão de *P. pinaster* foram capazes de exibir dois picos de produção ROS, contrariamente ao observado quando a eliciação foi realizada com extractos de micélio de *B. cinerea* e *L. seditiosum*. O primeiro pico foi dependente do influxo de cálcio mas independente da activação de MAPK ou de NADPH oxidases. Contrariamente, MAPK, NADPH oxidase e cálcio parecem estar envolvidos na via de transdução do sinal responsável pelo despoletar do segundo pico de ROS.

A capacidade anti-oxidante de *P. pinaster* no decurso da eliciação com *B. cinerea* foi avaliada pela determinação da actividade das enzimas antioxidantes catalase e superóxido dismutase, e pela análise da transcrição de genes codificantes para enzimas antioxidantes (*FeSod*, *chlCu,Zn-Sod* e *csApx*). A região codificante destes genes foi identificada através da construção de uma biblioteca de cDNA de P. pinaster e rastreio de forma a seleccionar os respectivos clones homólogos de cDNA. Os resultados sugerem que eliciação por *B. cinerea* induz a diminuição da capacidade anti-oxidante das células de *P. pinaster*, o que reflecte uma possível estratégia de *P. pinaster* de favorecer a produção de picos de ROS.

Foi analisado o possível envolvimento do metabolismo dos fenilpropanóides na interacção *P. pinaster-B. cinerea*. Foi observado que células de pinheiro eliciadas exibiam menor quantidade de compostos fenólicos solúveis e de lenhina. Adicionalmente, foram identificados clones de cDNA homólogos a genes que codificam as enzimas PAL e CHS (*Pal1, Pal2, Chs1, Chs2, Ch3*), por rastreio da biblioteca de cDNA. Estudos de expressão dos genes mostraram que a expressão do gene *Pal 1* era reprimida, não tendo sido detectada a presença de transcritos dos genes *Chs1* e *Chs2* em células eliciadas de pinheiro bravo. Estes resultados permitem sugerir que células eliciadas de pinheiro estejam condicionadas quanto à capacidade de promover a síntese de fitoalexinas e o reforço da parede celular.

Tem vindo a ser assinado que o ácido salicílico pode desempenhar uma função importante ao nível da modulação da resposta das plantas ao stresse biótico e abiótico. Em plantulas de pinheiro bravo tratadas com ácido salicílico, este parece ser capaz de induzir a expressão do gene *Cu,Zn-Sod*, que codica a forma cloroplastidial da Cu,Zn-SOD, sugerindo que uma função para esta isoforma possa ser a de contribuir para o aumento de H_2O_2 nos cloroplastos, dependente de SA.

O efeito da eliciação de *B. cinerea* no transporte de glucose em células em suspensão de *Pinus pinaster* foi igualmente avaliado. Células em suspensão de *Pinus pinaster* são capazes de transportar glucose através um simportador de H^+-monosacárido, na ausência de açúcar no meio. Eliciação com esporos de *B. cinerea* também promoveu a indução da actividade do transportador de monosacáridos na ausência de repressão pela glucose, sugerindo que células eliciadas de pinheiro bravo exibem maior capacidade de mobilização de açúcares. Adicionalmente foi observado que a desrepressão do transportador de monosacáridos exercida por condições de depleção parece ser mediada pela NADPH oxidase e cálcio, mas não por MAPK. Todavia as MAPK, conjuntamente com a NADPH oxidase e o cálcio parecem participar na transdução do sinal de eliciação de *B. cinerea*, responsável pela indução do transportador de açúcar.

Abstract

Maritime pine (*Pinus pinast*er Ait.) is a two-needle pine widely distributed throughout SW Europe. *P. pinaster* is a pioneer species and its adaptability and phenotypical characteristics make it an economically important forest species, being considered one of the three most important pines in Europe. *Botrytis cinerea* is a necrotrophic fungus, requiring the killing of plant cells for disease progression. *B. cinerea* is the causal agent of grey mould disease and a broad range pathogen, capable of infecting over two hundred hosts. Adult populations of maritime pine are resistant to *B. cinerea* infection, but seedling nurseries and young plantations are often attacked, resulting in severe economical losses.

In the present work, plant defence mechanisms were analysed for their involvement in the response of *Pinus pinaster* to the non-host necrotrophic pathogen *Botrytis cinerea*.

To establish an elicitation model for the study of *P. pinaster-B. cinerea* interactions, a maritime pine heterotrophic cell suspension culture was initiated from root-derived *calli* in modified MS medium. Suspension cultures were characterized for biomass production, pH, cell viability and the consumption of sugars, phosphate, nitrate, and ammonium. The results indicate that nutrient consumption exhibited a biphasic profile during near exponential growth. Additionally, growth arrest was accompanied by a pronounced death curve. Sugar-starved *P. pinaster* suspended cells exhibited increased acid phosphase activity and DNA degradation, as shown by TUNEL, suggesting than PCD by autophagy accounts for pine cell death in sugar-depleted medium.

When elicited by *B. cinerea* spores, *P. pinaster* suspended cells were able to produce two ROS bursts, contrarily to what was observed when elicitation was performed by *B. cinerea* and *L. seditiosum* mycelia extracts. The first burst of ROS production was shown to be dependent on calcium influx, but independent on the activation of MAPK and NADPH oxidase. However, MAPK, NADPH oxidase, as well calcium, seem to be involved in the transduction pathway responsible for triggering the second ROS burst.

The ROS-scavenging capacity of *P. pinaster* cells during the time course of elicitation with *B. cinerea* was evaluated by determining the activity of the antioxidant enzymes catalase and superoxide dismutase by gel activity assays, and by analysing transcript levels of genes encoding ROS-scavenging enzymes (*FeSod*, *chlCu,Zn-Sod* and *csApx*). For full-length cDNAs isolation, a *P. pinaster* cDNA library was constructed. Taken together, the results suggested that elicitation by *B. cinerea* induces a decrease in the enzymatic ROS-scavenging capacity of pine cells, probably as a strategy for favouring ROS bursts.

Analysis on the role of phenylpropanoid metabolism in the *P. pinaster-B. cinerea* interaction was also performed. Results showed that in elicited pine cells there is a decrease in total phenolics and lignin. Full-length cDNAs (*Pal1, Pal2, Chs1, Chs2, Ch3*) encoding PAL and CHS were identified. *Pal1* is down-regulated, while *Chs1* and *Chs2* were undetected even in non-elicted cells. Is is possible to suggest that elicited maritime pine cells are limited in their capability to promote phytoalexin biosynthesis and cell wall reinforcement.

A major role has been reported for salicylic acid in modulating plant response against abiotic and biotic stresses. Accordingly, the effect of salicylic acid on the up-regulation of the *P. pinaster* chloroplastic *Cu,Zn-Sod* in *P. pinaster* needles was observed, suggesting a role of this SOD isoform in salicylic acid-mediated H_2O_2 increase in chloroplasts.

Effect of *Botrytis cinerea* elicitation on glucose transport in *Pinus pinaster* suspended cultured cells was also evaluated. *P. pinaster* suspended cells were able to transport glucose by a monosaccharide/H^+ symporter, only when sugar was depleted from the culture medium. *B. cinerea* challenging was also able to increase sugar carrier activity, suggesting that elicited pine cells are able to increase sugar mobilization. NADPH oxidase and calcium, but not MAPK seem to play a role in the transduction of

the *B. cinerea* elicitation signal responsible for the induction of the sugar carrier. However, activation of MAPK seems to be required for carrier derepression, induced by low sugar levels.

Abbreviations

Main abbreviations

2,4-D	2,4-dichlorophenoxy acetic acid
$A_{\#\#\#}$	absorbance at ### nm
ABA	abcisic acid
atm	atmosfere
BA	bensylaminopurine
Bisacrylamide	N,N'-methylenebisacrylamide
BLAST	Basic Local Alignment Research Tool
bp	base pairs
BSA	bovine serum albumine
ºC	degrees Celsius
Ci	Curie
CMV	citomegalovirus
c.p.m.	counts per minute
CPU	central processing unit
CTAB	cetyltrimethylammonium bromide
Da	Dalton
d.d.	double deionized
DEAE	diethylaminoethyl
DEPC	diethylpyrocarbonate
DGRF	Direcção Geral dos Recursos Florestais
DMSO	dimethyl sulfoxide
DTT	dithiothreitol
DW	dry weight
EDTA	ethylenediaminetetraacetic acid
EtBr	ethidium bromide
EST	Expressed sequence tag
FW	fresh weight
g	gram
g	gravity acceleration
h	hour
ha	hectare
IAA	isoamyl alcohol
IPTG	isopropyl-ß-D-thiogalactopyranoside

J	Joule
kan	kanamycin
Kin	kinetin
l	Liter
M	Molar
m	Meter
MCS	multiple cloning site
min	minute
MDA	malondialdehyde
MMLV-RT	Moloney murine leukemia virus reverse transcriptase
MOPS	3-(N-morpholino)propane-sulfonic acid
NaAc	sodium acetate
NAA	α-naphtalene acetic acid
NADPH	nicotinamide adenine dinucleotide (reduced form)
NBT	nitroblue tetrazolium
NCBI	National Center for Biotechnology Information
oligo(dT)	oligodeoxythymidylic acid
ORF	open reading frame
PAGE	polyacrylamide gel electrophoresis
PCR	Polymerase chain reaction
p.f.u.	plaque-forming units
Pi	orto-phosphate ion
PS-I	photosystem I
PVPP	polyvinylpolypyrrolidinone
RNase	ribonuclease
ROS	reactive oxygen species
rpm	revolutions per minute
RT-PCR	Reverse transcription polymerase chain reaction
s	second
SA	salicylic acid
SDS	sodium dodecyl sulphate
TEMED	N,N,N',N'-tetramethylethylenediamine
Tris	Tris(hydroxymethyl)aminomethane
Triton X-100	polyoxyethylene-p-isooctylphenol
U	Unit of enzymatic activity
u.p.	ultra pure
UTR	Untranslated region
UV	ultra-violet light
V	Volt
VIS	Visible light
v; vol.	volume
w	weight
X-gal	5-bromo-4-chloro-indolyl-ß-D-galactopyranoside
XTT	3'-(1-[phenylamino-carbonyl]-3,4-tetrazolium)-bis(4-methoxy-6-nitro) benzene-sulfonic acid hydrate

Nucleic acids

DNA		deoxyribonucleic acid
	cDNA	complementary deoxyribonucleic acid
	dsDNA	double stranded deoxyribonucleic acid
	gDNA	genomic deoxyribonucleic acid
	ssDNA	single stranded deoxyribonucleic acid
RNA		ribonucleic acid
	mRNA	messenger ribonucleic acid
	poly(A)-RNA	polyadenylated ribonucleic acid
	rRNA	ribossomal ribonucleic acid
	tRNA	transfer ribonucleic acid

A	Adenine
T	Thymine
C	Cytosine
G	Guanine
dATP	2’-deoxyadenosine-5´-triphosphate
dTTP	2’-deoxycitidine-5´-triphosphate
dCTP	2’-deoxyguanosine-5´-triphosphate
dGTP	2’-deoxythymidine-5´-triphosphate
dNTP	2’-deoxynucleotide-5´-triphosphate

Amino Acids

A	Ala	Alanine	M	Met	Methionine
C	Cys	Cysteine	N	Asn	Asparagine
D	Asp	Aspartic acid	P	Pro	Proline
E	Glu	Glutamic acid	Q	Gln	Glutamine
F	Phe	Phenylalanine	R	Arg	Arginine
G	Gly	Glycine	S	Ser	Serine
H	His	Histidine	T	Thr	Threonine
I	Ile	Isoleucine	V	Val	Valine
K	Lys	Lysine	W	Trp	Tryptophan
L	Leu	Leucine	Y	Tyr	Tyrosine

List of publications

The present thesis includes results that are published, submitted or in preparation for publication with the following collaborators: Rui Manuel Tavares, Teresa Lino Neto, Alberto Dias, Hernani Gerós, Carlos Conde,Joana Gonçalves Published publications are listed bellow:

- **Azevedo H**, Lino-Neto T, Tavares RM. 2003. An improved method for high-quality RNA isolation from needles of adult maritime pine trees. *Plant Molecular Biology Reporter* 21(4): 333-338.

- **Azevedo H**, Lino-Neto, Tavares RM. 2004. Salicylic acid up-regulates the expression of chloroplastic Cu,Zn-superoxide dismutase in needles of maritime pine (*Pinus pinaster* Ait.). *Annals of Forest Science* 61: 847-850.

Chapter 1

General Introduction

1.1. Biology of the forest species *Pinus pinaster*

1.1.1. Maritime pine: general description and morphology

Conifers are dominant forest species spread through most ecosystems, even though they are more representative in boreal areas. They correspond to the largest group of industrial plantation species in the world (Costa et al. 1999). There are approximately 50 species of conifers in Europe, but few are widely distributed and assume both ecological and economical relevance (EUFORGEN, URL no.1).

Maritime pine (*Pinus pinaster* Ait.), a conifer (figure 1.1.1.) originary to the west Mediterranean basin, is a member of the economically important genus *Pinus* that include over 100 species (Costa *et al.* 1999). The species is fairly homogeneous and best recognized as monotypic (Richardson 1998). As a consequence, only two to three subspecies are conventioned (Farjon 1998), with minor differences in leaf anatomy. A complete revision of the species is lacking, but two subspecies (*pinaster* and *atlantica*) are generally accepted (Alía and Martín 2003). Over 15 races are described, including atlantica, mesogeensis, renoui and maghrebiana, being the later sometimes classified as a subspecies (Salvador *et al.* 2000).

Figure 1.1.1. *Pinus pinaster* Ait. (maritime pine) is a predominant forest species of SW Europe. Due to the ecological plasticity of this pioneer species, pine stances have been used for dune fixation in Northern and central Portugal since the XIII century.

Pinus pinaster is a monoic species (Chagné *et al.* 2003). The main aspects concerning the morphology of *P. pinaster* are summarized in table 1.1.1. Data was gathered from Burges *et al.* (1964) and online from the Gymnosperm Database (URL no. 2).

1.1.2. Distribution and ecology of *Pinus pinaster*

Maritime pine can be found throughout Portugal and Spain, in the Mediterranean and southwest Atlantic coasts of France, in the west coast of Italy, along the

Table 1.1.1. Morphological characteristics of *Pinus pinaster*.

	Morphology
Height	30-40 m
Stem	Sinuous. Sometimes straight, especially with subsp. *renoui.*
Bark	Patterned red-brown and black, very thick, scaly and fissured.
Crown	Ovoid to conic in young trees. Develops into an open candelabra form of irregular upswept branches in adult trees.
Branching	Mostly uninodal. Sometimes multinodal in young trees.
Shoots	Yellow-brown. 7-15 mm thick, rough and stout. Foliage buds are large, cylindric-ovoid, with red-brown scales having long free tips, fringed with white hairs.
Adult leaves	Fascicles of two spreading leaves (sometimes three). Green to yellow green. Leaves are 12-25 cm long, with a persistent sheath of 2 cm. 2-2.2 mm thick. Leaves are stout, with serrulate margins, and fine lines of stomata on all faces. Retainance period of 1.5-3 years.
Juvenile leaves	3-6 cm long, on slender (3 mm) shoots. Grown during the first 2-5 years.
Cones	2-3 cones, slightly deflexed on short stout stalks. When closed, cones are ovoid-conic, 9-18 cm long, 4-6 cm broad, symmetrical, hard and heavy. Ripening occurs in April, two years after pollination. Opening occurs the same summer or up to 10 years later. Opened cones are chestnut-brown and 7-11 cm broad.
Cone scales	The scales are stout, thick and woody. The apophysis is rhomboid, 10-16×18-26 mm wide, with a strong raised transverse ridge. The umbo is dorsal, blackish grey and 4-7 mm wide per 3 mm high.
Seeds	Blackish brown above, matt grey below. 7-11×5 mm with an 18-30×10 mm wing, buff, with numerous straight dark brown streaks.

Morocco-Tunisia range of northwest Africa (particularly the Atlas mountains), and in the isles of Malta, Sardinia and Corsica (figure 1.1.2.) (Salvador *et al.* 2000). Recently, the species was introduced for exploitation in South Africa, Australia and New Zealand (Pinto *et al.* 2004). In some situations it has evolved into an invasive plant of shrublands (Andres and Ojeda 2002). *Pinus pinaster* covers over 4 million ha of forest area in SW Europe (Ribeiro *et al.* 2001).

In Portugal, maritime pine occupies wide areas of the North and Center, from the coast to the interior (figure 1.1.3.). In the South, distribution is scattered and mainly located in coastal areas, namely the Setúbal peninsula. Further South, maritime pine is progressively substituted by *P. pinea.* According to the latest inventory of territorial use (DGRF, URL no.3), 38% of the Portuguese territory is occupied by forests, of which 96% come from plantations. This is more than the area devoted to agricultural practice (33%). Maritime pine is the main forest species, occupying 976 000 ha, representing 31% of the Portuguese forest and 23% of the European *P. pinaster* distribution.

Remaining conifers only occupy 3% of the forest, of which 2% is represented by *Pinus pinea* (figure 1.1.3.).

Studies on the variation of maritime pine populations have been performed using terpene analysis, total protein and isozymes (Petit *et al.* 1995; Salvador *et al.* 2000) Genetic approaches have made use of polymorphic chloroplast single sequence repeats (cpSSR) (Vendramin *et al.* 1998; Ribeiro *et al.* 2001). Results indicate no real differentiation between geographically separate Portuguese populations. A high within-population haplotypic diversity was observed in Portuguese pine cultures. However, inter-population variability was almost inexistent (Vendramin *et al.* 1998). In fact, within European pine stances, Portuguese populations presented the lowest haplotypic variability (Vendramin *et al.* 1998). This observation can be explained by extensive gene flow amongst Portuguese populations and also as the result of severe human activity (Ribeiro *et al.* 2001). A maritime pine-based afforestation program was promoted in the early twentieth century by state forestry services, which was responsible for the reforestation of huge areas of grazed shrubland in northern and central Portugal with seeds of unknown origin (Figueiral 1995; Ribeiro *et al.* 2001; Fernandes and Botelho 2004).

Maritime pine is a species of high plasticity, going from sea level to 2100 m of altitude, being able to survive with 350-1400 mm of annual rainfall (Alía and Martín 2003). *P. pinaster* grows well on poor soils, acid and basic. It thrives in calcareous and especially sandy silicate soils (Salvador *et al.* 2000), which constitutes a major commercial advantage.

The major commercial value of maritime pine lies in wood and resin (Chagné *et al.* 2003). It is exploited for resin tapping since it produces high quality resin. In Portugal, 75 000 tons of resin are produced annually, corresponding to over 500 kg ha^{-1} (DGRF, URL no.3). Wood from intensive cultures of pine is used mainly in the paper and pulp industries. Additionally, it is used as a prime source of low-quality timber, which is applied in construction, chipboards, palettes and floor boards. Systematic plantation of pine stances has been performed in Portugal since the XIII century (Ribeiro *et al.* 2001). For many centuries, the ability of maritime pine to grow in poor soils has been used in Portugal in programmes of soil fixation and protection, namely in sandy soils of Northern and central coastal areas (Alía and Martín 2003).

Figure 1.1.2. European distribution of maritime pine (adapted from EUFORGEN; URL no. 1).

The maritime pine population has been in severe decline for the past thirty years, despite a slight increase of the total forest area in Portugal (DGRF, URL no.3). In 1879 it was estimated that *P. pinaster* occupied 5 000 ha, 142 000 ha in 1902, 1 139 000 ha in 1935 and 1 299 000 ha in 1980 (Figueiral 1995). The last land use inventory by the DGRF, using the aerial cover of 1995, estimated 976 000 ha of maritime pine stances. With the escalade of forest fires in recent years it is predictable that this area has fallen

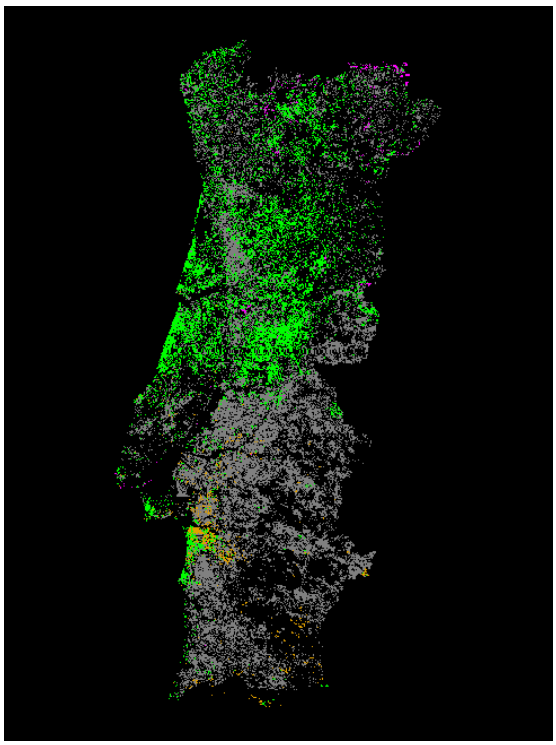

Figure 1.2.3. Distribution of *Pinus pinaster* (green) in Portugal. *Pinus pinea* (orange), other conifers (purple) and other forest species (grey) are also represented. (Adapted from DGRF, URL no. 3)

bellow 1995 values. In the Northern Portuguese coastal area, a region of strong maritime pine implementation, the species represented 81% of the forest area in the 1930's. However, between the first and last national forest inventories (1974-1995) a 46% loss in pine forest was observed.

There are several reasons for the decline of maritime pine, some of which are typified for other threatened species of the Mediterranean basin, and others are related to the strategic use of forest land. Overexploitation of pine stances has created dense, continuous and even-aged populations (Fernandes and Botelho 2004). The appearance of plagues and diseases can be favoured by progressive changes in forest structure and density (e.g. over-population and monoculture stands), and by environmental conditions that directly affect trees (e.g. forest fires, drought) (Sousa and Trigueiros 2001).

There are striking differences between public and private forest management policies, and generally, pine populations have been inadequately installed and accompanied (Sousa and Trigueiros 2001). Poor silvicultural practices not only benefit the appearance of diseases, but have a negative impact on biodiversity (Andres and Ojeda 2002). New silvicultural practises have been hard to impose on producers that never ponder on the impact of biotic factors upon forest populations (Sousa and Trigueiros 2001). Up to now, there is a delay in the establishment of criteria for sustainable forest management, followed by implementation in the field.

Maritime pine decline has not been accompanied by a decrease in forest area since, in the last 30 years, pine has been systematically and consciously substituted by *Eucalyptus* species, due to their higher rentability, and despite the ecological consequences of this policy.

The increasing problem of forest fires has been responsible for the destruction of extensive areas of pine stances (DGRF, URL no.3). Additionally, fire-debilitated pines in border areas become sensitive to plagues and infestations, turning into hotspots for disease spread onto healthy populations. In eight years, forest fires were solely responsible for the destruction of 27.2% of the pine area in Northwest Portugal (DGRF, URL no.3). However, forest fires only account for 28% of pine mortality in this region. Fire proximity is responsible for 14% of the mortality, and phytopathogenic agents are responsible for 44% of *P. pinaster* death (Sousa and Trigueiros 2001). All these conditions have created a high mortality rate amongst adult trees. In addition, an abnormal mortality has been observed in juvenile trees and seedlings. In some cases, young plantations (3-4 years) have suffered 60-70% mortality rates of unknown origins.

High mortality has been systematically affecting pine nurseries, and is conditioning the natural regeneration of pine forests.

1.1.3. *Botrytis cinerea* as a pathogenic fungi of maritime pine

In Northwest Portugal, fungi account for 16% of pathogen derived mortality in *P. pinaster* (Sousa and Trigueiros 2001). Seven species have been described as the main pathogenic fungi affecting *P. pinaster* populations and their incidence risk is summarized in figure 1.1.4. *Botrytis cinerea* has been indicated as one of the main species affecting the early stages of *Pinus pinaster* development. As a consequence, this fungus has severely affected pine nurseries and young populations of maritime pine, affecting the natural regeneration of pine stances.

Botrytis cinerea (Pers.; Fr.) (also designated *Botryotinia fuckeliana*) can be found throughout the world, and although it can live saprophytically, it is a versatile plant pathogen (Rosslenbroich and Stuebler 2000), capable of infecting all plant organs and possessing over 200 hosts (Jarvis 1980; Govrin and Levine 2002). These characteristics make *B. cinerea* the most important phytopathogen of the 22 *Botrytis* species (Rosslenbroich and Stuebler 2000).

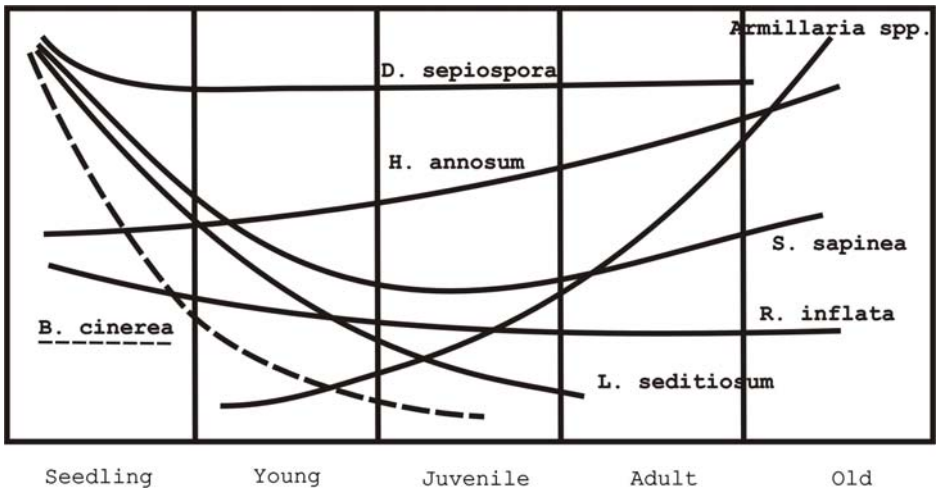

Figure 1.1.4. Incidence risk of the main pathogenic fungi affecting the life span of maritime pine trees. *Botrytis cinerea* (---) infection of *Pinus pinaster* can be observed from the seedling to juvenile stages of development. (Adapted from Sousa and Trigueiros 2001)

B. cinerea is a necrotrophic fungus that requires the death of host cells for the progession of infection (Hoeberichts *et al.* 2003). Its life cycle is summarized in figure 1.1.5. *B. cinerea* is the causal agent of "grey mould" disease, also known as *Botrytis* blight, which is characterized by grey, fuzzy sporulating lesions (Bi *et al.* 1999). Apart from forest species, grey mould can affect many other important crops such as vine, soft fruits, vegetables and flower crops (Hausbeck and Moorman 1996; Choi *et al.* 1997; Bi *et al.* 1999; Rosslenbroich and Stuebler 2000). Like other pathogens, grey mold is favoured by intensive plantations (Rosslenbroich and Stuebler 2000). Addicionally, the agent is favoured by climatic conditions that impose high humidity (Canadian Forest Services, URL no. 4) (Bi *et al.* 1999). These conditions can be artificially generated in greenhouses (Hausbeck and Moorman 1996) or in densely packed seedling populations, such as those found in pine nurseries (Canadian Forest Services, URL no. 4).

For many years, control of grey mould disease has been carried out with limited success using chemical and biological methods. *B. cinerea* has shown an amazing capability to quickly develop tolerance and even resistance to fungal pesticides, which has pushed the need to constantly develop new chemical agents (Forster and Staub 1996; Choi *et al.* 1997; Hilber and Hilber-Bodmer 1998; Bi *et al.* 1999). Furthermore, this practice raises the ecological issue of fungicide residues and the increasing public awareness to pesticide misuse (Hausbeck and Moorman 1996). In this perspective,

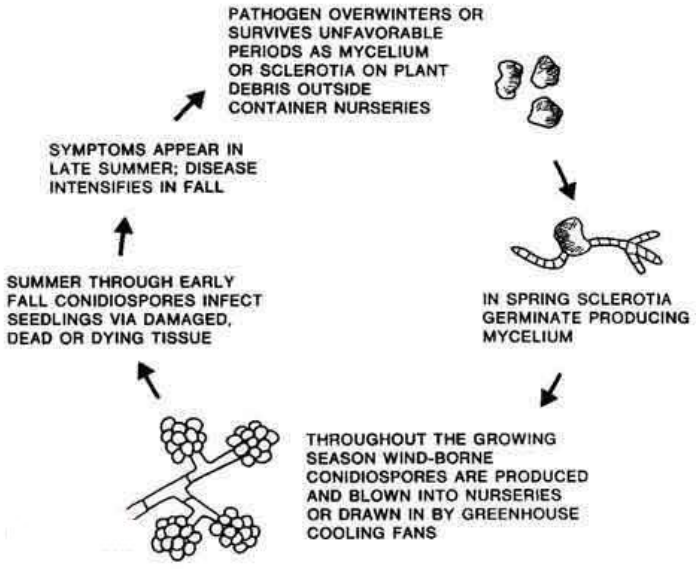

Figure 1.1.5. Life cycle of the pathogenic fungi *Botrytis cinerea*, (Adapted from the Canadian Forest Service; URL no. 4).

biological control offers several advantages over pesticides, but its efficiency is highly dependent on field conditions and infection timing. Moreover, the development of *B. cinerea* resistance to biological control agents is also a concerning problem (Bi *et al.* 1999).

Breeding for resistance has been mainly unsuccessful due to the apparent lack of host resistance to *B. cinerea*. As a result, best hopes for the development of resistance should lay in the introduction of heterologous anti-pathogen mechanisms (Bi *et al.* 1999), or by the improvement of non-host defence mechanisms. Given these circumstances, it is important to understand the mechanisms behind the high adaptability of *B. cinerea* to control measures (Choi *et al.* 1997), as well as to improve the knowledge on the events taking place during the host-*B. cinerea* interaction (Bi *et al.* 1999; Hoeberichts *et al.* 2003).

1.2. Biotic stress and the defence mechanisms of plants

Plants cannot escape environmental challenges such as predation, due to lack of mobility. Also, plants do not have an antibody-based immune system nor specialized mobile cells to combat infection (Lam *et al.* 2001). These are distinctive features to consider when regarding the resistance of superior plants to pathogens (Dangl and Jones 2001; Waterhouse *et al.* 2001). Even though plant defence responses are seemingly generalized when compared to mammalian pathogen combat, plants were capable of developing an effective array of responses to combat the various aspects of biotic stress, such as pathogen attack, insect feeding or animal grazing. As a consequence, most plants are resistant to most pathogens, weather they are insects, fungi, bacteria or viruses, and weather they are biotrophs or necrotrophs (Dangl and Jones 2001).

Several hallmarks of plant defence have had their molecular basis uncovered and new aspects and processes have been recently revealed (Heath 2000; Dangl and Jones 2001; Mysore and Ryu 2004; Van den Ende *et al.* 2004; Van Leeuwen *et al.* 2004). However, an extended degree of complexity is brought by the diverse nature of pathogenic agents, often resulting in seemingly contradictory responses.

When plant resistance to a specific disease is limited to a cultivar or accession, it is often designated host resistance. On the contrary, resistance is considered non-host when it can be found in all members of a species (Holub and Cooper 2004; Mysore and Ryu 2004). Even though non-host resistance determines disease resistance to the majority of plant pathogens (Heath 2000), the mechanisms of non-host resistance are

still much uncovered. This is due to the diversity of mechanisms involved in non-host resistance, and the fact that species level resistance is likely to be a multi-genic trait (Heath 1996; Holub and Cooper 2004). Therefore, the discovery of key genes involved in non-host resistance has been extremely hard, and only now begins to take form (Holub and Cooper 2004). Host-resistance however, is usually determined by a single dominant gene locus: a resistance gene (*R*) (Yang *et al.* 1997).

Resistance genes products interact directly with elicitor proteins of the pathogen, resulting in recognition of the disease agent. Elicitors are often determined by a single locus in the pathogen: an avirulence (*avr*) gene (Dangl and Jones 2001). During the plant-pathogen interaction, the simultaneous presence of *R* and *avr* genes determines an avirulant response, sometimes known as an incompatible interaction. During this type of response, the *R* gene product recognizes an *avr*-dependent signal, but not necessarily the *avr* gene product (reviewed by Dangl and Jones 2001) and triggers a signalling cascade that activates several defence mechanisms, ultimately containing or destroying the pathogen (Hammond-Kosack and Jones 1997). During virulent responses, the inability for *R-Avr* recognition results in disease progression. This mechanism of pathogen recognition is often designated gene-for-gene resistance (Lamb and Dixon 1997).

The first stage of plant defence comprises a series of mechanisms, known as passive defence, that are constitutively involved in impeding the establishment of pathogens through plant tissues (Kobayashi 1992). These mechanisms can be divided into physical barriers and preformed compounds. Physical barriers that prevent pathogen penetration include waxy cuticular skin layers (Dangl and Jones 2001), the cell wall and the cytoskeleton of plant cells, with actin microfilaments taking a part in the defence response against fungal attack (Kobayashi 1992). Additionally, plants constitutively produce a multitude of secondary metabolites, creating a hostile environment to pathogens due to their anti-microbial activity (Dixon 2001).

Once passive defences are surpassed by the pathogen, active resistance against foreign agents requires the coordinated staging of two components: recognition of the pathogen, and deployment of efficient defence responses that minimize or eliminate the threat to plant integrity.

After pathogen recognition, a set of signalling cascades activate the defence response (Baker *et al.* 1997). Three fundamental resistance responses have been shown to occur at the sight of infection (Mysore and Ryu 2004): oxidative bursts, with the rapid generation of reactive oxygen species, the hypersensitive response (HR), a

programmed cell death event and the activation of defence-related genes. These genes are part of various defence responses, which include reinforcement of the cell wall (Smit and Dubery 1997), production of pathogenesis-related (PR) proteins (Bortolotti *et al.* 2005), or the induction of secondary metabolites such as flavonoids/isoflavonoids, alkaloids, isoprenoids and indole derivatives (Dixon 2001). Numerous other genes of the primary and secondary metabolism are up or down-regulated during the defence response (Tao 2003).

Resistance in many interactions is dependant upon the involvement of a complex network of supracellular mechanisms responsible for inducing systemic resistance throughout the plant (Hammerschmidt 2004). Such mechanisms are mediated by low molecular weight signal molecules, such as salicylic acid, jasmonic acid and ethylene (Thomma *et al.* 2001; Hammerschmidt 2004).

Salicylic acid has been implicated in the in the localised expression of resistance and the plant sensitivisation program designated systemic acquired resistance (SAR) (Delaney *et al.* 1984; Sticher *et al.* 1997). Jasmonic acid is a fundamental component in the defence response to herbivore attack and was more recently implicated in the resistance induction of plants to certain types of pathogens, through the induced systemic response (ISR), a mechanisms parallel to SAR (Thomma *et al.* 1998; Pieterse and VanLoon 1999; Ton *et al.* 2002). In fact, there are several indications that SAR and ISR differ on the spectrum of pathogens, with SAR conferring resistance to biotrophic pathogens and ISR protecting against necrotrophic pathogens (Thomma *et al.* 1998; Ton *et al.* 2002). In support of this concept, a reclassification of biotrophs and necrotrophs was recently proposed based on the deployment of defence against fungal pathogens via the salicylate or jasmonate/ethylene pathways, respectively (Oliver and Ipcho 2004). Nevertheless, this classification is seriously limited by being mainly supported in *Arabidopsis* defence research, posing the question of its suitability to other plant systems (Hammerschmidt 2004; Oliver and Ipcho 2004). In addition, extensive crosstalk has been shown to occur between both pathways (Schenk *et al.* 2000; Glazebrook *et al.* 2003; Nickstadt *et al.* 2004). The jasmonate-insensitive *Arabidopsis* mutant *jin1* was shown to possess increased resistance to the necrotrophic pathogen *Botrytis cinerea* as well as the biotrophic pathogen *Pseudomonas syringae* (Nickstadt *et al.* 2004). Moreover, studies concerning resistance of *Cicer arietinum* to the necrotrophic pathogen *Aschochyta rabiei* showed that necrotroph resistance does not

always fall into the pattern of salicylic acid and jasmonate-mediated responses revealed by *Arabidopsis* studies (Cho and Muehlbauer 2004).

In addition to the host resistance, a less-understood mechanism referred to as non-host resistance can provide resistance against pathogens throughout all members of a plant species (Mysore and Ryu 2004). According to these authors, two types of non-host resistance, can be distinguished based on the presence of HR during the defence response. The HR-symptomless response to non-host pathogens is considered Type I resistance, whereas in Type II resistance, non-host parasitic microorganisms induce the hypersensitive response with subsequent cell death (Mysore and Ryu 2004). The form of non-host resistance which is likelier to occur in nature does not trigger the HR in challenged cells (Klement 1999; Lu 2001). In fact, HR is usually considered a visual marker for gene-for-gene resistance (Mysore and Ryu 2004). Nevertheless, non-host resistance has been shown to induce HR (Huckelhoven 2001; Peart 2002; Keith 2003). The same plant species can exhibit both types of response (Peart 2002), and the same pathogen can trigger different non-host resistance types in different plant species (Lindgren 1986; Lu 2001).

Type I non-host resistance occurs when the pathogen tries to enter the plant cell in search of nutrients but is arrested by passive and active defence mechanisms (figure 1.2.1.). Pathogens can be recognized by non-specific or broad spectrum elicitors, such as the flagellin protein in bacteria (Asai 2002), or pathogen-associated molecular patterns (PAMPs), present in the surface of pathogens (Nurnberger and Brunner 2002). If passive defences such as the cell wall and secondary metabolites are overcome by the pathogen, active defence responses are triggered (Thordal-Christensen 2003). These can include cell-wall thickening and lignification, papilla formation, accumulation of phenolics, phytoalexins and other secondary metabolites, as well as the activation of PR genes (Brown 1998; Dixon 2001; Lu 2001).

During type II non-host resistance, the pathogen is able to surpass the primary defences and invades the plant cell (figure 1.2.1.) Plant cells are capable of recognizing pathogen proteins, thus triggering the HR (Mysore and Ryu 2004). The plant surveillance system is active in the cellular membrane and the cytosol, and is capable of recognizing proteins that are involved in the pathogenic process. The proteins that act as elicitors of the defence response are designated avirulance (Avr) proteins (Shan 2000). Because fungi can directly penetrate the cell wall, extracellular and secreted proteins serve as elicitors. Bacteria use the *hrp* gene-encoded type three secretion

system (TTSS) to inject proteins into the plant cell, several of which can be Avr proteins (Hutcheson 2001).

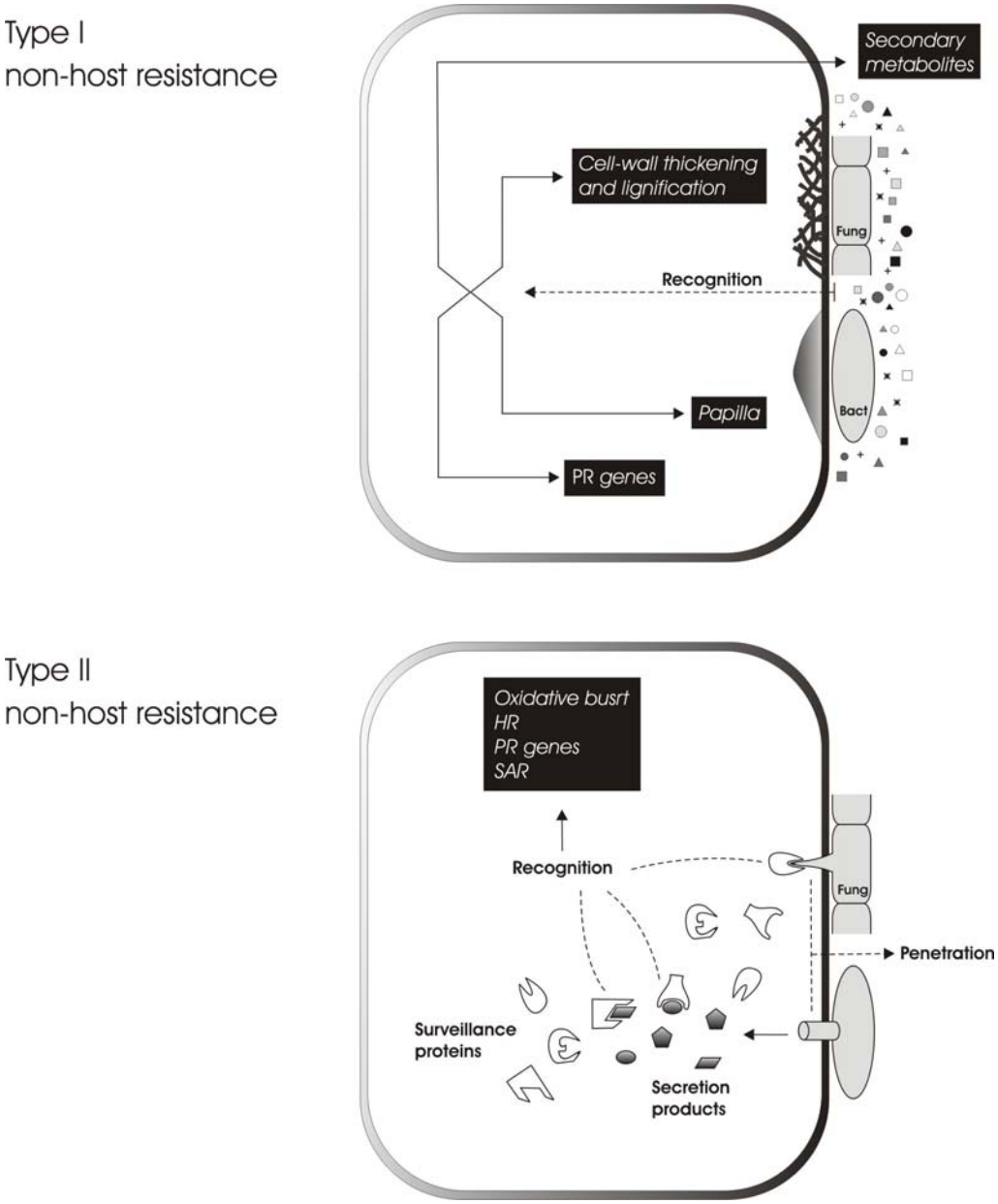

Figure 1.2.1. Mode of action of Type I and Type II non-host resistance during the response of plant cells to fungal and bacterial challenging. (Adapted from Mysore and Ryu 2004).

Type II non-host resistance is very similar to gene-for-gene resistance, in the sense that both processes recognise Avr proteins and may trigger a set of common responses. However, differences exist in the spectrum of pathogen recognition and in

gene activation profiles (Collins 2003; Tao 2003), suggesting different transduction pathways with some contact points (Mysore and Ryu 2004). Passive defences are generally considered non-host mechanisms. However, active responses are often common to host and non-host resistances. Such is the case of HR, ROS production and cell wall reinforcement (Moerschbacher 1990; Vleeshouwers 2000; Huckelhoven 2001; Mysore 2002; Able 2003). Therefore, it is likely that extensive crosstalk exists between both types of resistance, and that they share, to some extent, several signal transduction components. Several genes recently isolated were shown to be determinant in conferring broad-spectrum resistance to non-host parasitic microorganisms (reviewed by Mysore and Ryu 2004). However, functional characterization of these genes is still required for understanding the processes of recognition and signal transduction in non-host resistance.

Pathogen perception is carried out by the recognition of elicitors that differ widely in their chemical nature, and include proteins, oligosaccharides, glycoproteins, and lipids. Elicitor recognition requires the subsequent activation of intracellular signal transduction pathways in order to activate a set of defence responses (reviewed by Suzuki 2002). Protein phosphorylation was shown to be involved the defence response, with protein kinase cascades playing important roles in elicitor signal transduction. Protein kinase inhibitors were shown to block numerous defence responses, including oxidative bursts, accumulation of secondary metabolites, accumulation of transcripts from defence genes, and hypersensitive response cell death. Further evidence showed that within protein kinases, mitogen-activated protein kinase (MAPK) cascades are particularly relevant in elicitor signal transduction (Suzuki 2002; Katou *et al.* 2003). MAPK cascades are highly conserved across all eukaryotes. MAPK are serine/threonine kinases with both cytoplasmic and nuclear substrates, being activated via dual phosphorylation on threonine and tyrosine residues by a MAPK kinase (MAPKK), itself in turn activated by a MAPKK kinase (MAPKKK) (Desikan *et al.* 1999). Apart from MAPK activation being required for signal transduction, a negative regulatory role of putative MAPK cascades has been demonstrated in the activation of plant defence mechanisms. For instance, the *Arabidopsis* mutant, enhanced disease resistance 1 (*edr1*), exhibit increased resistance against bacterial and fungal challenging (Frye and Innes 1998). *EDR1* encodes a putative MAPKK kinase (MAPKKK), and defence responses in *edr1* mutant plants are induced by pathogen signals more rapidly than in wild-type plants (Frye *et al.* 2001).

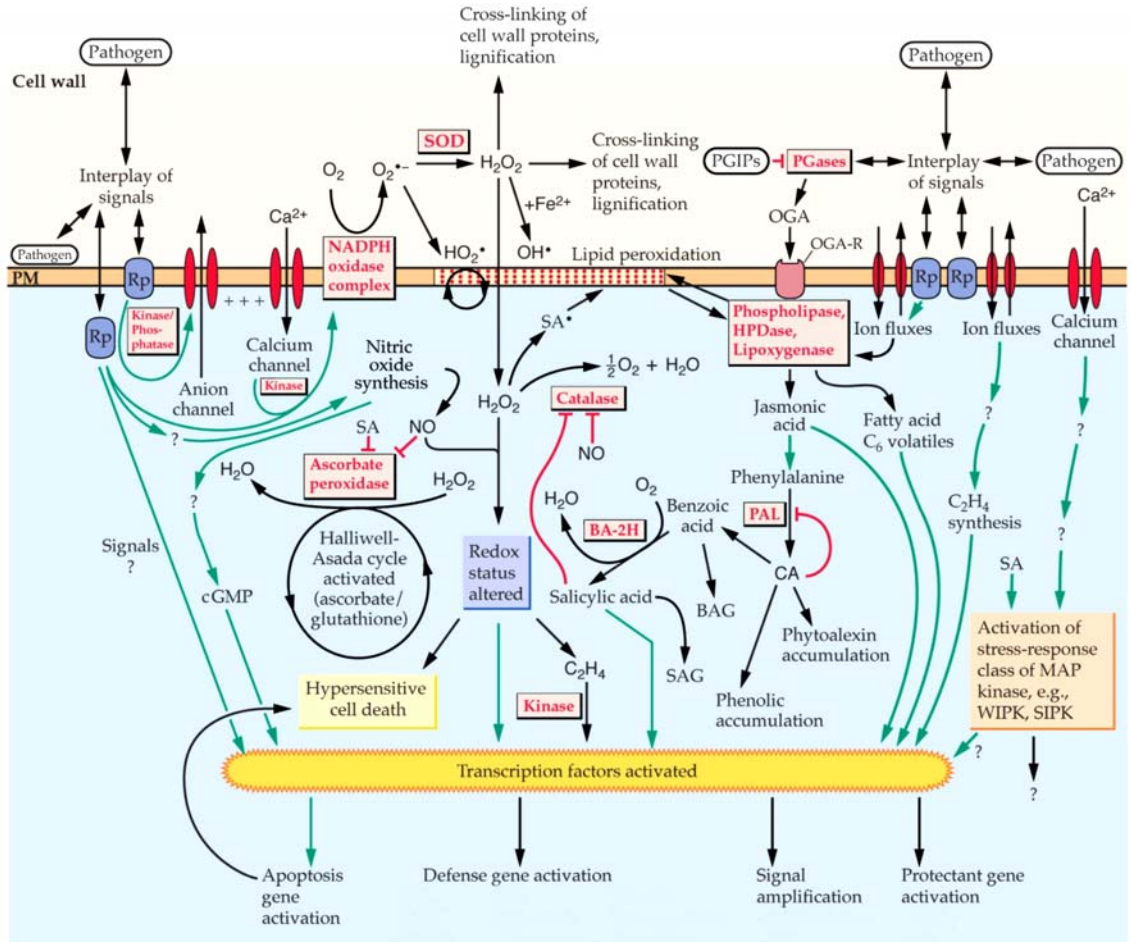

Figure 1.2.2. Overview of signal transduction pathways involved in plant defence responses. The intermediate downstream signalling events are not known but involve kinases, phosphatases, ion fluxes. Several distinct and rapidly activated outcomes are recognized, including ROS, and direct induction of defence gene transcription. Amplification of the initial defence response occurs through the generation of additional signal molecules *(e.g.* other ROS, lipid peroxides, salicylic and jasmonic acids). These, in turn induce other defence–related genes. Concomitant alterations of cellular redox status or cellular damage will activate ROS-scavenging mechanism (e.g., ascorbate-glutathione cycle). Cross-talk between the various induced pathways appears to coordinate the responses. ACC, 1-aminocyclopropane-1-corboxylic acid; BAG, benzoic acid glucoside; BA-2H, benzoid acid 2-hydroxylase; CA, cinnamic acid; cGMP, cyclic guanosine 5'-monophosphate; CHS, chalcone synthase; EFE, ethylene-forming enzyme; GP, glutathione peroxidase; GST, glutathione S-transferase; HMGR, 3'-hydroxy-3-methyl-glutaryl-CoA reductase; $HO_2^{\bullet}$, hydroperoxyl radical; HPDase, hydroxyperoxide dehydrase; MAP, mitogen-activating protein; NO; nitric oxide; $OH^{\bullet}$, hydroxyl radical; OGA and OGA-R, oligogalacturonide fragments and receptor; PAL, phenylalanine ammonia-lyase; PGases, polygalacturonases; PM, plasma membrane; $SA^{\bullet}$, salicylic acid radical; SAG, salicylic acid glucoside; SIPK, salicylic acid-induced protein kinase; WIPK, wound-induced protein kinase. (Hammond-Kosack and Jones 2000)

New perspectives on plant defence signal transduction mechanisms, have been given by the discovery of novel molecules involved in the transduction events. Plant cells have been shown to produce uncommon phospholipids (polyphosphoenosites), when subjected to biotic and abiotic stress (reviewed by Van Leeuwen *et al.* 2004). Apart from their role in energy provision, osmoregulation and stress tolerance, fructan exohydrolases were recently suggested to play a role in plant defence signalling, by preventing the formation of exogenous levan-type fructans from bacterial origin (reviewed by Van den Ende *et al.* 2004). Also recently, plant cell wall polysaccharides seem to play a role in defence signalling, since the high degree of structural complexity of cell wall components suggests they might function as latent elicitors, to be released during pathogen challenging (reviewed by Vorwerk *et al.* 2004).

Part of the present knowledge on the complex network that leads from pathogen recognition to the activation of mediated defence mechanisms is summarized in figure 1.2.2. Recent focus on non-host resistance has highlighted the limitations of the gene-for-gene model (Mysore and Ryu 2004). One example is the fact that resistance genes seem to play a part in non-host resistance (Holub 2001). Thus we face the need to expand our knowledge on how parasitic microorganisms are perceived, and how the defence signal coordinates with the numerous resistance mechanisms.

1.3. Reactive oxygen species: role in plant defence against pathogens

With the onset of aerobic life, cells have had to cope with the by-products of oxygen metabolism: reactive oxygen species (ROS). These species result from the transfer of energy or electrons to ground state oxygen. ROS are extremely toxic to the cell (Amor *et al.* 1998) and thought their affinity is highest to unsaturated fatty acids of membrane lipids, they easily react with proteins and nucleic acids (Lamb and Dixon 1997).

In plants, ROS are mainly composed of four species (Mittler *et al.* 2004): hydrogen peroxide (H_2O_2), superoxide anion (O_2^-), singlet oxygen ($^1O_2$) and the hydroxyl radical (HO•). Most result from the sequential univalent reduction of oxygen into water:

$$O_2 \rightarrow O_2^- \rightarrow H_2O_2 \rightarrow HO\bullet \rightarrow H_2O.$$

The singlet oxygen is formed by the transition of one of the unpaired electrons of ground state oxygen to an orbital of higher energy. Hydrogen peroxide is a potent inhibitor of photosynthesis and its destruction is vital to chloroplast functioning (Kaiser 1979). The hydroxyl radical is the most reactive of ROS, and is normally formed from other oxygen radicals in the presence of a metal ion (Bowler *et al.* 1991). This two-step process is known as the Haber-Weiss reaction. The combined reductive power of one O_2^- molecule

and one H_2O_2 molecule is required to form OH•, through the transient reduction of the metal ion:

$$O_2^- + Fe^{3+} \rightarrow O_2 + Fe^{2+};$$
$$Fe^{2+}\ H_2O_2 \rightarrow Fe^{3+} + OH^- + OH•$$

Other ROS that can be found in the cellular metabolism include the perhydroxy radical (HO_2•), the alkoxy radical (RO•) and the peroxy radical (ROO•) (Thompson *et al.* 1987).

Many of the cellular metabolic processes are directly or indirectly involved in the continuous formation of oxygen radicals, being mitochondria, chloroplasts and peroxisomes the main sites of ROS production due to the presence of strong electron flows or oxygen-involving metabolic reactions (Noctor and Foyer 1998) (figure 1.3.1.). Environmental conditions that impose the disruption of ROS homeostasis usually generate oxygen radicals in these organelles. In contrast, cell-mediated ROS production can be achieved by down-regulating ROS scavenging mechanisms in different cell compartments (Apel and Hirt 2004).

Stress conditions in general are responsible for the increase of ROS. Many abiotic stresses induce the production of O_2^- through PS-I (Asada 1999). O_2^- is rapidly converted to H_2O_2 by chloroplastic superoxide dismutases, and hydrogen peroxide that is formed can be removed by peroxyredoxin, the ascorbate-glutathione cycle or by the glutathione peroxidase cycle (figure 1.3.1.).

Plant cells possess a range of non-enzymatic as well as enzymatic mechanisms to scavenge oxygen radicals. A sensible energetic effort is diverted to the removal of O_2^- and H_2O_2, which are the main oxygen radicals being produced and are the source of HO•. Detoxification of O_2^- and H_2O_2 is possible through enzymatic catalysis (figure 1.3.1.). The main enzymatic mechanisms of scavenging ROS are summarized in table 1.3.1. and include the enzymes superoxide dismutase (SOD), catalase (CAT), ascorbate peroxidase (APX) and glutathione peroxidase (GPX). SODs catalyse the dismutation of O_2^- into H_2O_2, whereas CAT, APX and GPX are involved in H_2O_2 detoxification. Unlike CAT, APX and GPX require reducible substrates (ascorbate and reduced glutathione, respectively). Peroxiredoxin is also capable of H_2O_2 reduction (Rouhier and Jacquot 2002). As a consequence of enzymatic ROS scavenging, the

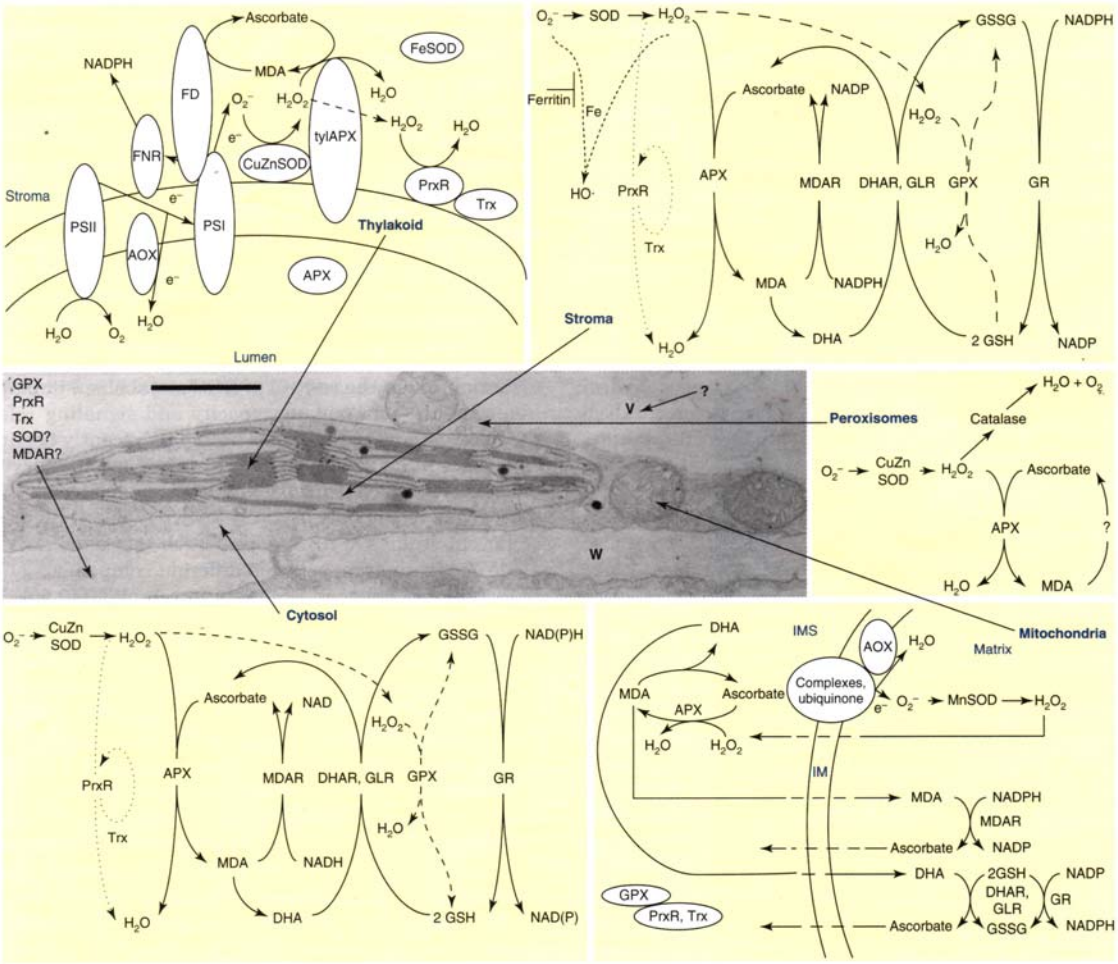

Figure 1.3.1. Schematic representation of the main ROS-scavenging pathways in plant cells and their subcellular localization. The water–water cycle detoxifies O_2^- and H_2O_2, and alternative oxidase (AOX) reduces the production rate of O_2^- in thylakoids (top left). ROS that escape this cycle and/or are produced in the stroma undergo detoxification by Cu,Zn-SOD or Fe-SOD and the stromal ascorbate–glutathione cycle. Peroxiredoxin (PrxR) and glutathione peroxidase (GPX) are also involved in H_2O_2 removal in the stroma (top right). ROS produced in peroxisomes during photorespiration, fatty acid oxidation or other reactions are decomposed by SOD, catalase (CAT) and ascorbate peroxidase (APX) (middle right). SOD and other components of the ascorbate–glutathione cycle are also present in mitochondria. In addition, AOX prevents oxidative damage in mitochondria (bottom right). In principle, the cytosol contains the same set of enzymes found in the stroma (bottom left). However, these are encoded by a different set of genes and the major iron-chelating activity in the cytosol responsible for preventing the formation of HO•radicals is unknown. The enzymatic components responsible for ROS detoxification in the apoplast and cell wall (W) are only partially known, and the ROS-scavenging pathways at the vacuole (V) are unknown. Membrane-bound enzymes are depicted in white, GPX pathways are indicated by dashed lines and PrxR pathways are indicated by dotted lines in the stroma and cytosol. Although the pathways in the different compartments are mostly separated from each other, H_2O_2 can easily diffuse through membranes and antioxidants such as glutathione and ascorbic acid (reduced or oxidized) can be transported between the different compartments. (DHA, dehydroascrobate; DHAR, DHA reductase; FD, ferredoxin; FNR, ferredoxin NADPH reductase; GLR, glutaredoxin; GR, glutathione reductase; GSH, reduced glutathione; GSSG, oxidized glutathione; IM, inner membrane; IMS, IM space; MDA, monodehydroascorbate; MDAR, MDA reductase; PSI, photosystem I; PSII, photosystem II; Trx, thioredoxin; tyl, thylakoid) (Mittler *et al*. 2004).

balance between SODs and H_2O_2-scavenging enzymes is fundamental to maintain ROS homeostasis. Cells maintain a pool of ascorbic acid and glutathione in their reduced states, by the action of NAD(P)H-dependent enzymes in the ascorbate-glutathione and glutathione peroxidase cycles (figure 1.3.1.; table.1.3.1.).

In addition to protecting the cell against oxidative damage, ROS-scavenging pathways regulate the intensity and sub-cellular localization of ROS signals. By maintaining a low-steady state level of oxygen radicals in the cell, the different ROS-mediated signals can be registered against the background (Mittler *et al.* 2004). Since most forms of plant stress involve ROS production, it is likely that oxygen species were initially used in sensing stress, and evolved to take part in the regulation of particular pathways.

Table 1.3.1. Main enzymes involved in the scavenging of oxygen ROS. Chl - chloroplast; Cyt – cytosol; ER – endoplastic reticulum; Mem – membrane; Mit – mitochondria: Per – peroxisome; Sec – secretorial pathway. (reviewed by Lino-Neto 2001)

Enzyme class	**Reaction**	**Gene name**	**Subcellular location**
Superoxide dismutase	$2O_2^- + 2H^+ \rightarrow H_2O_2 + O_2$	FeSOD Cu/ZnSOD MnSOD MnSOD-like	Chl, Per Chl, Cyt, Per Mit Sec
Catalase	$2H_2O_2 \rightarrow 2H_2O + O_2$	CAT	Per
Ascorbate peroxidase	$2Asc + H_2O_2 \rightarrow 2MDA + 2H_2O$	APX Stromal-APX Thylakoid-APX	Chl, Cyt, Mit, Per Chl, Mit Chl
Monodehydroascorbate reductase	$MDA + NAD(P)H + H^+ \rightarrow Asc + NAD(P)^-$	MDAR	Cyt, Mit
Dehydroascorbate reductase	$DHA + 2GSH \rightarrow Asc + GSSG$	DHAR	Chl, Cyt, Mit
Glutathione reductase	$GSSG + NAD(P)H \rightarrow 2GSH + NAD(P)^-$	GR	Chl, Cyt, Mit
Glutathione peroxidase	$H_2O_2 + 2GSH \rightarrow 2H_2O + GSSG$	GPX Phospholipid GPX	Chl, Cyt, ER, Mit Chl, Mit
Ferritin	$Fe + P \rightarrow P\text{-}Fe$	Ferritin	Chl, Mit
Peroxiredoxin	$2P\text{-}SH + H_2O_2 \rightarrow P\text{-}S\text{-}S\text{-}P + H_2O$	PrxR	Chl, Cyt, Mem, Mit, Nuc
Thioredoxin	$P\text{-}S\text{-}S\text{-}P + 2H^+ \rightarrow 2\ P\text{-}SH$	Trx	Chl, Cyt, Mit

Initial perspectives on ROS metabolism were mainly concerned with ROS scavenging mechanisms, capable of converting these species into non-toxic products such as H_2O and O_2. Later on, it became evident that during evolution, ROS were integrated in the cellular metabolism, only to play a central role in regulating many biological processes (Mittler *et al.* 2004). ROS act in the signalling events that control

many aspects of growth, development and of resistance to biotic and abiotic stresses (Kovtun *et al.* 2000; Mittler 2002; Neill *et al.* 2002; Overmyer *et al.* 2003; Rizhsky *et al.* 2003). This has been recently evidenced by knockout and antisense lines (Baier *et al.* 2000; Rizhsky *et al.* 2002; Sagi *et al.* 2004). In plants, the dual role of ROS as toxic metabolic byproducts and signalling molecules has resulted in a complex network of genes: in *Arabidopsis* at least 152 genes are directly associated with ROS (Mittler *et al.* 2004). The modulation of ROS metabolism in plant cells is synthesized in figure 1.3.2. ROS are constantly produced as a consequence of aerobic metabolism, namely through respiration and photosynthesis (Apel and Hirt 2004). In light of this, plants possess a set of anti-oxidant mechanisms that are responsible for the destruction of ROS or their confinement in sub-cellular compartments (Mittler *et al.* 2004). Production of oxygen radicals can be caused by imposed conditions that perturb ROS homeostasis (Apel and Hirt 2004), and in fact most forms of abiotic stresses ultimately result in the production of ROS (*e.g.* high light, salt, drought and cold stresses). Alternatively, developmental or environmental signals (such as pathogen perception) can activate specific ROS-producing pathways.

ROS perception is carried out by different sensors, so that the homeostasis of oxygen species is permanently monitored in all of the cell's compartments. The multitude of ROS mediated signals has an impact on plant growth (e.g. growth arrest during stress), and plays a part in several developmental processes such as seed germination and radicle growth (Gidrol *et al.* 1994). As a result of ROS sensing, several metabolic, developmental or defence pathways can be activated (e.g. rearrangement of the photosynthetic apparatus or the induction of programmed cell death). In most situations, sensing an increase in oxygen species results in the activation of the ROS-scavenging metabolism, though some circumstances might involve modulation by positive feedback mechanisms (figure 1.3.2.). Though a central regulatory role has been attributed to H_2O_2 and O_2^-, a specific transduction pathway for $^1O_2$ was recently proposed (op den Camp *et al.* 2003). However, receptors that bind oxygen radicals and act as sensors have not been discovered.

Fungi and bacteria possess redox sensors in the form of two-component signalling systems involving histidine kinases (Whistler *et al.* 1998). Though plants have similar two-component histidine kinases, a function in redox sensing has yet to be determined (Apel and Hirt 2004). Apart from ROS receptors, two other sensing

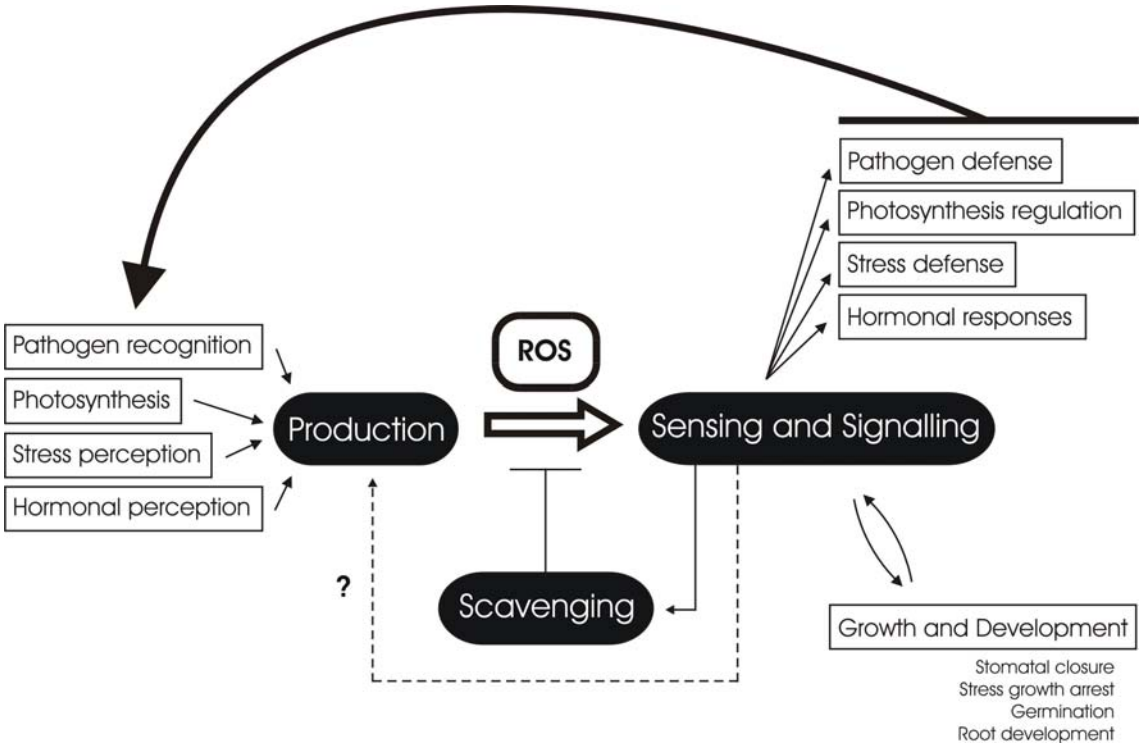

Figure 1.3.2. The modulation of ROS signalling by the ROS gene network of plants. ROS are a natural consequence of aerobic metabolism, but can be induced during environmental conditions that disrupt cellular homeostasis, resulting in increased ROS levels. During plant-microbe interactions, this increase is promoted by ROS-generating mechanisms following pathogen perception (oxidative bursts). ROS sensing is integrated into stress sensing pathways, which dictate the activation of ROS scavenging mechanisms or the induction of positive loops of ROS production. (adapted from Mittler *et al.* 2004)

mechanisms have been proposed: redox-sensitive transcription factors (*e.g.* NPR1 or HSFs) (Mittler 2002; Vranova *et al.* 2002) and direct inhibition of phosphatases containing oxidizable thiol groups (e.g. PTP1) (Gupta and Luan 2003). ROS signalling was shown to involve mechanisms that are common to other transduction pathways, namely G-proteins (Baxter-Burrell *et al.* 2002), Ca^{2+} and Ca^{2+}-binding proteins (Bowler and Fluhr 2000), phospholipid signalling (Anthony *et al.* 2004; Rentel *et al.* 2004) and MAPK (Rentel *et al.* 2004).

In plant-pathogen interactions, the regulatory role of ROS has been extensively substantiated (reviewed by De Gara *et al.* 2003). In contrast to abiotic stress, where ROS generation is usually a consequence of the disruption of electron flows (Asada 1999), plant-microbe interactions are characterized by the increase of ROS levels through the activation of ROS-generating mechanisms following pathogen perception (figure 1.3.2.) (Mittler *et al.* 2004). In plant defence, the production of reactive oxygen

species, also designated an oxidative burst, is common to fungal, bacterial and viral infections, and is usually a biphasic event, with an early and a late stage (Lamb and Dixon 1997). Oxidative bursts are critical in the series of highly localised events that follow cell challenging, leading to the induction of the vast array of plant defence responses and culminating in programmed cell death of plant cells (Apel and Hirt 2004). The timing of both phases can vary significantly, depending on the host and pathogen species (Allan et al. 2001). The early oxidative burst (phase I) occurs few hours, or even minutes after challenging. Phase I do not determine resistance to the pathogen and can be observed in susceptible plants. The second oxidative burst (phase II) occurs within hours or days (Lamb and Dixon 1997). Phase I is considered fundamental in the induction of phase II responses (Baker and Orlandi 1995). However, only phase II correlates with the resistance response to the pathogen, being associated with recognition of the pathogen, followed by the activation of related signalling pathways (Baker and Orlandi 1995). The HR–induced cell death can occur during or after phase II (Allan *et al.* 2001). The kinetics of ROS production varies as a function of the pathogen, weather it is viral, bacterial or fungal. As a consequence, both phases can differ on the type of ROS produced, being hydrogen peroxide (H_2O_2) and superoxide (O_2^-) the main oxygen radicals implicated in the oxidative burst (Mehdy 1994; Baker and Orlandi 1995; Bolwell *et al.* 1995).

In the apoplast, NAPH oxidase-generated superoxide can be rapidly converted to H_2O_2 either by spontaneous dismutation or by apoplastic SODs (De Gara *et al.* 2003) (Mittler *et al.* 2004). Unlike O_2^-, H_2O_2 can diffuse within the cell and was shown to function as a second messenger during the induction of defence genes (Orozco-Cardenas *et al.* 2001). HO• has also been implicated in the defence response. By studying horseradish peroxidase, a new function has been proposed for apoplastic peroxidases as generators of hydroxyl radicals. In the presence of O_2^- and H_2O_2, horseradish peroxidase was shown to produce HO• in a mechanism similar to the Haber-Weiss reaction (Chen and Schopfer 1999).

NADPH oxidases have been involved as the main ROS generating enzymes involved in the early oxidative burst. (Tenhaken *et al.* 1995; Lamb and Dixon 1997; De Gara *et al.* 2003). These enzymes produce superoxide radicals by generating an electron transport chain capable of reducing O_2 and are analogous to mammalian O_2^- generating enzymes (Desikan *et al.* 1996; Groom *et al.* 1996; Murphy and Auh 1996). By disturbing ROS homeostasis, NADPH oxidases take part in activating or amplifying

signalling pathways. Genes coding for ROS-generating enzymes that are induced by pathogen challenging and may contribute to the later massive production of ROS include cell-wall peroxidases, germin-like oxalate oxidases and lipoxygenases (reviewed by Lamb and Dixon 1997). In addition to NAPH oxidase, alternative ROS generating mechanisms responsible for early oxidative burst have been proposed. These include a lipoxygenase acting on polyunsaturated fatty acids, and apoplastic enzymes such as cell wall peroxidases, copper amine oxidase, flavin polyamine oxidases and oxalate oxidase. Some evidence suggests that secretory peroxidase is also able to produce an oxidative burst following pathogen attack (reviewed by Aple and Hirt 2004 and Gara *et al.* 2003).

1.4. Programmed cell death in plants: the case of hypersensitive response

Evidences that a variety of animal cells die with similar morphological features appearing to be the result of an active suicidal process were provided in early 1970's (Kerr *et al.* 1972), leading to the concept of programmed cell death (PCD). A renaissance of PCD research was brought about by the convergence of work on PCD with studies of animal genes involved in oncogenesis such as *Bcl-2*, and genetic research on cell death mutants by Bob Horvitz and his co-workers in the nematode *Caenorhabditis elegans* (reviewed by Lam *et al.* 1999).

Two main categories of programmed cell death have been recognized in animals: apoptosis and autophagy (Clarke 1990; Baehrecke 2003). These categories are based on the morphology of the dying cell and on the main organelle involved. Apoptosis entails engulfment of the dying cell by a live one and degradation in the lysosome of the live cell. By contrast, cellular degradation during autophagy is carried out mainly by the lysosome within the dying cell. A third and less ubiquitous type of metazoan PCD does not involve degradation in the lysosome. To date, the various examples of plant PCD have not been compared in-depth and plant PCD has not been critically compared with the morphology of animal PCD (Van Doorn and Woltering 2005). According to these authors, three morphological types of PCD can be found: autophagy, apoptosis and non-lysosomal PCD.

Autophagy is a major degradation and recycling system in eukaryotic cells, contributing to the turnover of cellular components. This type of PCD has at least two

functions (Klionsky *et al.* 2003): it saves the cell from death (this function occurs during nutrient starvation) and is a mechanism whereby the cell degrades or mobilizes its constituents before death. Among autophagic PCD, three subtypes, not mutually exclusive, are reported. Microautophagy is the sequestration of small portions of the cytoplasm at the vacuolar surface, whereas macroautophagy results in sequestration of larger portions in the cytoplasm. Macro-autophagy entails the formation of a unique double-membrane structure, the autophagosome, which engulfs part of the cytoplasm, with or without large organelles. The autophagosome then merges with a lysosomal vacuole (Otto *et al.* 2003). A role for macro-autophagy in PCD in plants has still to be established. Mega-authopagy occurs when permeabilization or rupture of the lysosome or tonoplast occurs, resulting in the release of vacuolar hydrolases, which can degrade whatever is left in the cell. This permeabilization appears to be common in plant PCD. Tonoplast permeabilization and the subsequent rapid disappearance of the cellular contents has been reported to occur in tracheary element differentiation (Obara *et al.* 2001), and has been observed in PCD during aerenchyma formation (Evans 2003), phloem cell development, formation of root cap cells, and during the senescence of chloroplast-containing cells such as in leaf cells (Gahan 1982). In petals, anthocyanins are often leaked to the apoplast. Because anthocyanins are located in the vacuole, their leakage is probably due to permeabilization of both the tonoplast and the plasma membrane (van Doorn *et al.* 2003).

Apoptosis, the second type of PCD, exhibit three morphological features: nuclear fragmentation, formation of apoptotic bodies, and engulfment and final degradation of the apoptotic bodies in the lysosome of another cell (Baehrecke 2003). Engulfment of apoptotic bodies and degradation in another cell is not found during the PCD of any plant cell, so true apoptosis apparently does not occur in plants. Several other features have often been taken to be characteristic for apoptosis: (i) the role of caspases, (ii) chromatin condensation, (iii) nuclear blebbing, (iv) DNA degradation as shown by the terminal deoxynucleotidyl transferasemediated dUTP nick-end labeling (TUNEL) method, and (v) fragmentation of DNA into internucleosomal fragments (DNA laddering). However, it is now known that caspases can also be regulators of autophagic PCD and that caspases are often absent from systems that are truly apoptotic (Baehrecke 2003; Orrenius *et al.* 2003).

Non-lysosomal PCD, the third morphological type of metazoan PCD involves neither the lysosome of the dying cell itself nor the lysosome of other cells and is called

necrosis-like PCD or non-lysosomal PCD. The cells kill themselves apparently by inhibiting some major biosynthetic pathway, by destabilizing their membranes, or in other unknown ways. Compared with the frequency of PCD by apoptosis or autophagy, in metazoans, this type of PCD occurs in relatively few cells (Baehrecke 2003).

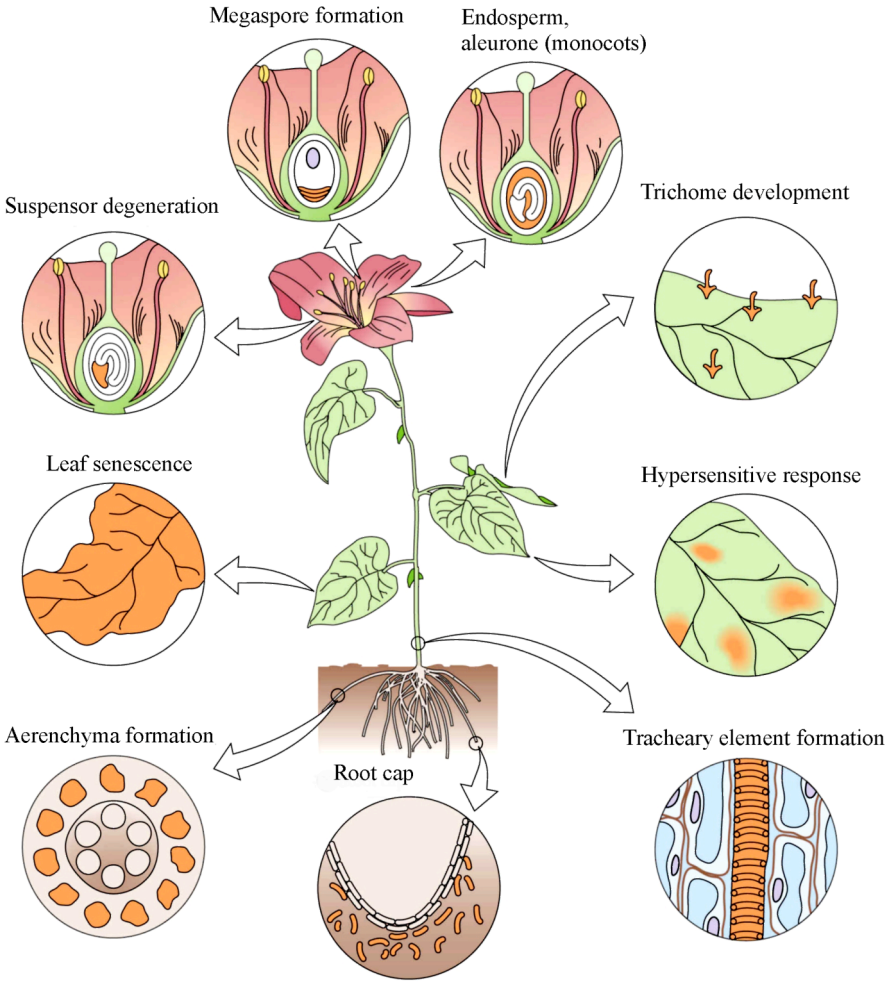

Figure 1.4.1. Examples of developmental and stress-induced processes involving PCD in plants. Root cap formation, xylem differentiation, leaf senescence are programmed cell events that take place during vegetative development. In reproduction, PCD can also occur during megaspore formation and suspensor degradation. Degenerative processes in seeds and fruits also occur through PCD. Environmental signal and pathogens may also induce PCD. (Hammond-Kosack and Jones 2000)

In plants, PCD is commonly found in different aspects of development (figure 1.4.1.). Among them, plant senescence has been intensively studied. The senescence of plant organs is a type of PCD that allows the material that has been used during growth

to be broken down and re-mobilized by developing organs of the plant, such as younger leaves, developing flowers, pods and seeds (Noodén 1988). For instance, leaves senesce prior to freezing or when shadowed by other parts of the plant, and flowers often senesce and die rapidly after opening (Ashman and Schoen 1994). Senescence involves dramatic changes in the major organelles (Dangl *et al.* 2000), but far from undergoing deterioration in structure and function, in which the photosynthetic apparatus is dismantled and nutrients are exported, chloroplasts redifferentiate into gerontoplasts or chromoplasts. In senescing photosynthetic tissues, peroxisomes are converted into glyoxysomes, playing an important role in gluconeogenesis. Also, during senescence of storage tissues, vacuoles suffer serious changes. In contrast, mitochondrial, nuclear, and plasma membranes maintain their integrity until the late stages of cell death (Smart 1994). The molecular mechanisms of senescence are not well understood, but it is clear that increased catabolic activity is observed, including hydrolysis of macromolecules such as proteins, nucleic acids and lipids, loss of chlorophyll and photochemical capability (Thomas and Stoddard 1980; Woolhouse 1984; Noodén 1988).

The declining of photosynthesis dictates that during senescence, the energy demands have to be met from increasingly heterotrophic sources, a trend associated with significant modifications in respiratory and oxidative metabolisms. Additional changes can involve secondary metabolites, and compounds with antimicrobial activity often accumulate in senescing tissues, preventing opportunist pathogens from using such tissues as potential routes of infection (reviewed by Lino-Neto 2001).

Plants have also developed a specialized type of programmed cell death that is specific of resistance responses to pathogen challenging (Heath 2000). This process designated hypersensitive response finds some analogies with animal PCD including a strong connection between PCD and ROS generation. At least three types of microorganisms cause cell death in plants: fungi, bacteria and viruses (reviewed by Van Doorn and Woltering 2005). PCD has been shown to occur during plant–necrotrophs interactions (Lincoln *et al.* 2002). For instance, lily leaf cells challenged with the necrotrophic fungi *Botrytis elliptica* evidenced cytoplasmic shrinkage, loss of mitochondrial membrane potential and no signs of autophagy (Moore *et al.* 1999). Moreover, the hypersensitive response was shown to facilitate plant infection by the necrotrophic pathogen *Botrytis cinerea* (Govrin and Levine 2000).

A characteristic of HR is the fact that cells surrounding the site of pathogen penetration can switch on genes encoding for phytoalexin synthesis and other

pathogenesis related proteins before activating PCD (De Gara *et al.* 2003). Recent progress on plant PCD research suggests that the cellular strategies for programmed death have been conserved between animals and plants (Lam *et al.* 2001), and several hallmarks of plant PCD have similarities to animal apoptosis (Hoeberichts *et al.* 2003). For instance, mitochondria were shown to be involved in the HR cell death (reviewed by Lam *et al.* 2001) and cytochrome *c* leakage has been described in PCD events in plants (Lam *et al.* 1999). Additional support is given by studies involving alternative oxidase (AOX). AOX is a protein that is tightly bound to the inner mitochondrial membrane and diverts electrons from the cytochrome pathway at the level of ubiquinon pool, transferring electrons from ubiquinol to O_2, thus lowering the oxygen levels and preventing the formation of ROS. Evidence suggests a role for inner mitochondrial membrane-derived ROS generation in mitochondria as a signal for PCD activation (reviewed by Lam *et al.* 2001). Hypersensitive response cell death does not show features that are typical of autophagy. In addition, animal cell PCD involves engulfment and hydrolysis of fragments of the dying cell by other cells, which has not been reported in plants. Therefore, pathogen induced PCD in plants does not feature evidences of apoptosis. Despite the fact that few details are known about the ultrastructure of PCD during HR, the present data suggests that it conforms to the non-lysosomal type of PCD (reviewed by Van Doorn and Woltering 2005).

In plants, HR occurs at infection sites in cells that are in contact with the pathogen, and in those in their surrounding (Heath 2000). The main objective is to arrest pathogen spread to the remaining plant tissues. Therefore, HR must occur rapidly and precede pathogen movement. Usually, PCD is accompanied by the activation of other plant defence responses such as the intense production of ROS, which help to contain or kill the pathogen (Lam *et al.* 2001). It seems clear that HR plays a fundamental role in restricting viral progress in plant tissues (Lam *et al.* 2001). An equal part is played in stopping the growth of obligate bacterial and fungal pathogens (Heath 2000).

1.5. Sugar transporters in plant-microbe interactions

Most of the CO_2 fixation process of higher plants takes place in autotrophic cells of the leaf mesophyll tissue. In the Calvin cycle and gluconeogenesis, the fixated CO_2 is converted to sugar monosaccharides such as glucose and fructose, which are pivotal units of the metabolism (Büttner and Sauer 2000). Sugars are nucleotide constituents and the main respiratory substrates that generate energy and metabolic intermediates. Linkage to sugar is required for the functioning of many proteins and lipids, and in plants, polysaccharides are major structural elements (Yu 1999). Sugars constitute the main carbon and energy source of most heterotrophic tissues, and are the main exchangeable form of reduced carbon between different tissues. Therefore, a net flow of sugars is constantly required between carbon "source" tissues and "sink" tissues such as reserve organs, reproducing structures, and developing tissues (Williams *et al.* 2000).

The mechanisms that ensure the supply of sugars to sink tissues can be separated into two components: a long distance transport system, and mechanisms of sugar transfer between cells and across the cellular membrane. In higher plants, long distance transport of solutes is maintained by a vascular system, composed of highly specialized cells: the phloem sieve elements. These cells suffer longitudinal extension and organelle dedifferentiation, including loss of the nuclei and vacuole. They are terminally connected by sieve plates, maintaining a continuum that ensures the vascular function. In the phloem, sieve elements are energetically and functionally maintained by the organelle-enriched companion cells (Williams *et al.* 2000).

In most plants, sucrose is the main carbon hydrate present in the phloem sap (Salisbury and Ross 1994; Lalonde *et al.* 1999), even though other non reducing sugars can be found, like rafinose, and poliols such as mannitol. Near source tissues, sugar accumulation (up to 1 M), creates a concentration gradient and forces the uptake of water, creating an additional pressure gradient (Williams *et al.* 2000). Transport events from the sieve elements to sink cells contribute to phloem unloading (Patrick 1997).

There are two mechanisms responsible for the unloading of sucrose from the phloem sap to sink cells. During *apoplastic* transport, sugars are exported by carrier proteins, diffuse into the intercellular space and suffer protein-mediated uptake into sink cells. In *symplastic* transport, the carbon sources diffuse between plasmodesmata, reaching targets cells through a cytoplasmic continuum (lalonde *et al.* 1999). Symplastic transport is often the main mechanism of sieve element unloading (Patrick 1997), even though phloem unloading always includes an apoplastic component due to the large difference in transmembrane sucrose concentrations (Patrick 1990).

The nature of phloem unloading varies widely due to the large array of sink tissues and functions (Taiz and Zeiger 1998), which can include roots, stem and root elongation zones, fruits, developing seeds, and terminal vegetative storage sinks. Moreover, the unloading path seems to be highly influenced by sink development, in a dynamic rather than static process (Patrick 1997). In the *apoplastic mechanism*, sucrose can leave the sieve element-companion cell complex (SE-CC) by facilitated diffusion through efflux carriers, and enter cells directly via disaccharide transporters (DST) (figure 1.5.1.), where it can suffer hydrolysis by cytosolic invertases or be translocated into the vacuole (Williams *et al.* 2000; Koch 2004). However, in the most common process, apoplastic sucrose is hydrolysed by extracellular or cell-wall-bound invertases into glucose and fructose (Damon *et al.* 1988; Taiz and Zeiger 1998; Koch 2004). The process helps to maintain a steep transmembrane sucrose gradient between the SE-CC and the apoplastic space (Patrick 1997). Hexoses are then imported by monosaccharide transporters (MST) (figure1.5.1.) (Williams *et al.* 2000).

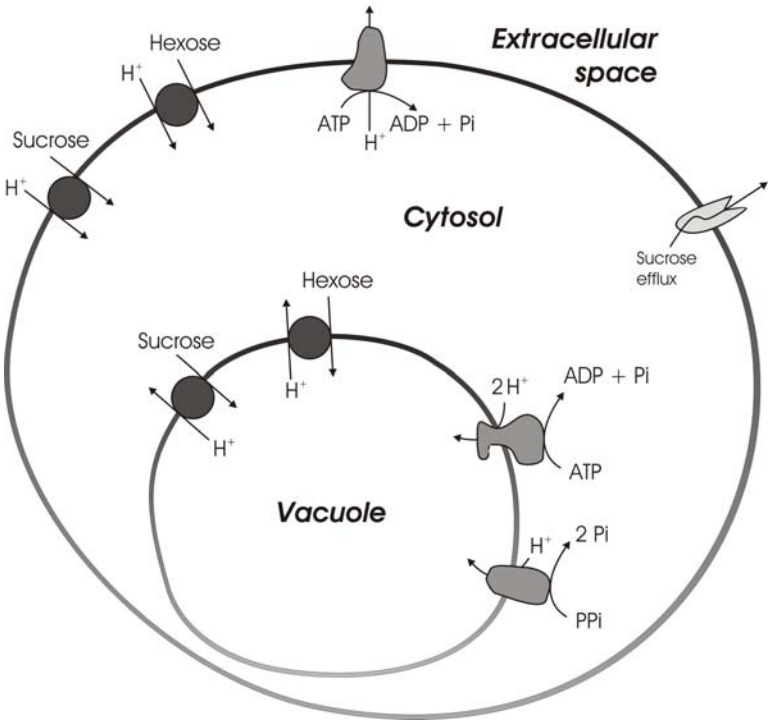

Figure 1.5.1. Schematic representation of carrier-mediated sugar transport across plant cell membranes. At low extracellular sugar concentrations, uptake is supported by H^+-symporters. Due to the electrochemical gradient, sugar accumulation in the vacuole requires the presence of tonoplast H^+-antiporters. Primary active transport generates a proton motive force, by action of plasma membrane H^+-ATPase, vacuolar H^+-ATPase and H^+-pyrophosphatase (Rea and Poole 1993; Sussman 1994; Lüttge and Ratajczak 1997; Palma *et al.* 2000). Sucrose unloading from the cell can occur through facilitated diffusion, by action of efflux carriers. (adapted from Taiz and Zeiger 1998)

Sugars have very limited diffusion capabilities due to their polarity. Even though passive transport mechanisms are involved in sugar translocation across the lipid bilayer, the prominent role in sugar uptake is carried out by taken by secondary active transport (MST and DST carrier proteins) (figure 1.5.1.). Twenty six MSTs and at least seven DSTs are identified in *A. thaliana*. MSTs belong to the major facilitator superfamily, whereas DSTs seem to be plant specific (Williams *et al.* 2000). MST protein structure possesses 12 transmembrane domains with a long internal loop. Prediction was performed based on the hydrophobicity pattern of the aminoacidic sequences. This structure is thought to have evolved from an ancestral transporter with 6 transmembrane domains that was subjected to duplication or genetic fusion in the course of evolution. Conserved motifs in MST promoter regions suggest that these genes are differentially regulated by various transduction signals. (Saier *et al.* 1999).

Heterologous expression studies using MST coding genes has contributed to the understanding of the functional and kinetical properties of these carrier proteins (Büttner and Sauer 2000). These approaches have showed that MST activity in plants is dependent of the membrane potencial ($\Delta\psi$) and the proton gradient ($\Delta\mu H^+$). This evidence supports that mediated sugar uptake takes place by a proton-symport mechanism (Oliveira *et al.* 2002). Even though transporters are usually highly specific as to the kind of solute, they are often capable of transporting a family of related substances (Taiz and Zeiger 1998). The range of monosaccharides recognised by MST proteins include D-glucose, 3-*O*-methyl-D-glucose, 2-deoxy-D-glucose, D-mannose and D-fructose. The K_m for the substrates ranges from 10-100 μM (Williams *et al.* 2000).

MST expression can be regulated by several signalling molecules like ethylene, absisic acid and sugars, and by abiotic stress factors such as salinity and temperature, (Truernit *et al.* 1996; Büttner and Sauer 2000). Recently, sugar carriers were implicated in the sugar signalling mechanism, working as sensors that promote the activation of signalling transduction pathways, and ultimately regulate genes involved in the metabolism of sugar uptake (Rolland *et al.* 2001).

During plant-pathogen interaction, there is a strong competition for nutrients, since fungi are heterotrophs for reduced carbon. Therefore, phytopathogens become an additional sink tissue, and a competition for solutes is set in the apoplast. (Clark and Hall 1998; Sutton *et al.* 1999). Evidences have been provided for the involvement of sugar transporters in resistance to pathogens. In *A. thaliana* suspension cultures, the expression of the sink-specific, wound induced, high affinity H^+-monosaccharide symporter, *AtSTP4* (MST) was shown to be induced by fungal and bacterial elicitors (Truernit *et al.* 1996; Fotopoulos *et al.* 2003). According to Truernit *et al.* (1996), the increase in the host sugar uptake capacity allows the recovering of sugar from the apoplast, thus reducing the loss of carbohydrate to pathogen. In contrast, it has also been reported that during plant-pathogen interactions, inhibition of sugar transporters may occur. It was shown that the fungal elicitor cryptogein, a protein secreted by *Phytophthora cryptogea*, is able to rapidly inhibit glucose transport in tobacco suspended cells (Bourque *et al.* 2002). According to these authors, toxins/elicitors released from the fungus may affect directly or indirectly the host´s glucose carrier activity, thus decreasing the ability of the plant to absorb/retrieve these compounds from the apoplast.

Sugar transporters seem also to pay an important role in plant-symbiont interactions. Colonization of *Medicago truncatula* roots with the mycorrhizal fungus *Glomus versiforme*, induces expression of the monosaccharide transporter gene, *MtST1* (MST), in cortical cells of the root that correlates with regions that are heavily colonized by the fungus (Taiz and Zeiger 1998). The effect is localized to cells within the immediate vicinity of the fungus, either in cells containing an arbuscule, or cells that are frequently in contact with intercellular hyphae. Thus, sugar transporters seem to be important for carbon transfer to mycorrhizal fungi (Taiz and Zeiger 1998). The nature of the signal for the induction of plant sugar-carriers during microorganism interactions is not yet clear.

1.6. Aims and outline of the thesis

In the early twentieth century, a massive afforestation program promoted by state forestry services set maritime pine as the main forest species in Portugal for over one century. However, the *Pinus pinaster* population has been in severe decline for the past thirty years (Figueiral 1995; Ribeiro *et al.* 2001; Fernandes and Botelho 2004). Phytopathogenic agents are responsible for 44% of *P. pinaster* death in Northwest Portugal (Sousa and Trigueiros 2001), with an abnormal mortality being observed in juvenile trees and seedlings. *Botrytis cinerea* is one of the main pathogens affecting the early stages of *Pinus pinaster* development. This fungus attacks both pine nurseries and young populations of maritime pine, affecting the natural regeneration of pine stances. *B. cinerea* is a versatile necrotrophic fungi that can be found throughout the world infecting numerous important crops species (Hausbeck and Moorman 1996; Choi *et al.* 1997; Bi *et al.* 1999; Rosslenbroich and Stuebler 2000). Chemical and biological control measures have proved ineffective due to the quick development of tolerance or resistance (Forster and Staub 1996; Choi *et al.* 1997; Hilber and Hilber-Bodmer 1998; Bi *et al.* 1999). Breeding for resistance has been unsuccessful due to the apparent lack of host resistance to *B. cinerea*. Therefore, the development of plant resistance strategies lay on the improvement of non-host defence mechanisms, and the importance of understanding the mechanisms underlying *B. cinerea* pathogenicity have been emphasized (Choi et al. 1997; Bi et al. 1999; Hoeberichts et al. 2003).

Substantial progress has been made in recent years on plant non-host defence mechanisms (Holub and Cooper 2004; Mysore and Ryu 2004). However, proposed non-host resistance models are more adequate to the better understood plant-biotroph systems. It has recently been evidenced that necrotrophs can use HR and ROS-mediated cellular disruption in their advantage (Bolwell *et al.* 1999; Mittler *et al.* 1999). *B cinerea* has been shown to make use of this strategy for the progress of infection (Williamson *et al.* 1995; ten Have *et al.* 1998; Muckenschnabel *et al.* 2002).

This work aims to contribute to the understanding of *P. pinaster-Botrytis cinerea* interaction. Specific aims are included in thesis outline.

Chapter 1 includes a general introduction to maritime pine biology, distribution and economic importance. In addition, a review on the plant-defence strategies against pathogens, including the role oxidative stress metabolism, programmed cell death and sugar transporters, is reported.

Chapter 3 describes the establishment of an efficient method for isolation of high-quality RNA from maritime pine tissues and the construction of a cDNA library.

Chapter 4 includes the establishment of a *P. pinaster* suspension cell cultures to be used as a plant model for elicitation with *Botrytis cinerea*. Additionally, the characterization of pine suspension cultures, in what concerns biomass production, viability and nutrient consumption are also included. Data supporting the occurrence of a programmed cell death process of pine cell under sugar starvation is also reported.

Chapter 5 includes the results from the quantification of ROS in elicited cells and the dependence of ROS bursts upon the activation of known components of the elicitor signal transduction pathway, evaluation of ROS-enzymatic scavenging capacity of elicited pine cells, the evaluation of cells capacity in activating phenylpropanoid metabolism as a defence strategy, the occurrence of hypersensitive response and the study of the capacity of pathogen for inducing hypersensitive response in pine cells. Additionally, the effect of salicylic acid in regulating the expression of genes encoding antioxidant enzymes in maritime pine seedlings was also reported.

Chapter 6 includes the kinetics and energetics characterization of a *P. pinaster* active sugar transport, its regulation by sugar levels and by *B. cinerea* elicitation. Insights on signal transduction components putatively involved in elicitor-dependent sugar carrier regulation are also given.

Chapter 2

Materials and Methods

2.1. Biological materials, reagents and culture media

2.1.1. Plant material

Pinus pinaster Ait. seeds were obtained from CENASEF (Centro Nacional de Sementes Florestais of the DGRF, Amarante, Portugal; URL no. 3). Seeds were collected from 20-40 year old premium specimens in the Melgaço region (northwest Portugal), and stored at 4ºC.

For cDNA library construction, needles from 30-year-old maritime pine trees were harvested in Braga (Northwest Portugal) in March 2000. After collection, needles were immediately frozen in liquid nitrogen and stored at -80 ºC.

Maritime pine seedlings were obtained by germinating seeds in sterile soil in plastic pots. In order to break dormancy, seeds were water-embedded overnight, placed in the soil, and maintained at 4ºC for 1 week. Seedlings were grown in a culture chamber at 26 ºC with a 16/8 h photoperiod (cool white fluorescent light of 450-500 $\mu W/cm^2$), and watered weekly.

Seedlings were also obtained under sterile conditions. One-year old *P. pinaster* seeds were water embedded overnight and surface disinfected by immersion in 35% H_2O_2 for 20 min, followed by thorough rinsing using sterile H_2O. Two to three seeds were placed per each sterile germination tube containing 10 ml of gMS medium.

To break dormancy, tubes were placed for one week at 4 ºC in the dark and then subjected to a 16/8 h photoperiod under continuous cool white fluorescent light

(450-500 μW/cm^2), at 26 ºC in a growth chamber. To prevent dehydration of the medium, cotton corks were partially flamed and double capped with aluminium foil. Seedlings were allowed to develop for 6 weeks.

2.1.2. Fungal strains

Botrytis cinerea (also referenced as *Botryotinia fuckeliana* Whetzel) was obtained from CECT - The Spanish Type Culture Collection (Valencia; URL no. 5), accession no. 2850. *Lophodermium seditiosum* Minter. Was obtained from DSMZ - The German Type Culture Collection, accession no. DSM 5029.

2.1.3. *Escherichia coli* strains

In the present work, *E. coli* strains that were used in several molecular biology procedures, including cDNA library construction and cell transformation, are listed in table 2.1.1.

Table 2.1.1. *Escherichia coli* strains used in this work

Strain	Genotipe	Reference
XL1 Blue MRF'	Δ(mcrA)183 Δ(mcrCB-hsdSMR-mrr)173 endA1 supE44 thi-1 recA1 gyrA96 relA1 lac [F' proAB lacI^{q}ZΔM15 Tn10 (tet^r)]	(Jerpseth *et al.* 1992)
XLOLR	Δ(mcrA)183 Δ(mcrCB-hsdSMR-mrr)173 endA1 thi-1 recA1 gyrA96 relA1 lac [F' proAB lacI^{q}ZΔM15 Tn10 (Tet^r)] Su$^-$ (nonsuppressing) λ^r (lambda resistant)	(Short and Sorge 1992)
JM109	e14$^-$(McrA$^-$) recA1 endA1 gyrA96 thi-1 hsdR17 (r_k^- m_k^+) supE44 relA1 Δ(lac-proAB) [F'traD36 proAB lacI^{q}ZΔM15]	(Yanish-Perron *et al.* 1985)

2.1.4. Vectors and bacteriophages

Construction of the *P. pinaster* cDNA library was performed on the *ZAP Express* vector, provided with the *ZAP Express cDNA Synthesis Kit* (Stratagene). This vector possesses increased cloning capacity and the ability of both eukaryotic and prokaryotic expression. The main characteristic of lambda ZAP vectors is the ability to excise the cDNA insert in a phagemid (pBK-CMV), without the requirement for subcloning (Short and Sorge 1992).

The ZAP Express vector was packaged into the *Gigapack III Gold* packaging extract (Stratagene) in order to create bacteriophage particles.

The *ExAssist* helper bacteriophage (Stratagene) was used to auxiliate the *in vivo* excision of the phagemid pBK-CMV from the Zap Express vector (Stratagene). This bacteriophage was provided with the *ZAP Express cDNA Synthesis Kit* (Stratagene).

DNA fragments obtained from PCR amplifications using degenerate primers were cloned onto the *pGEM-T Easy vector* (Promega), which is designed to conveniently clone PCR products.

2.1.5. Culture media

2.1.5.1. Media for growing P. pinaster

A cell culture medium was developed in order to induce *P. pinaster calli* and subsequently produce and maintain a cell suspension culture. The medium was designated *MSPS* medium, and was based on the Murashige and Skoog (MS) medium (Murashige and Skoog 1962). The hormonal composition was adapted from the medium composition described by Lange et al. (1994) for *Pinus sylvestris* cell cultures.

Suspension cells were established and regularly maintained in 3% (w/v) sucrose. References to MSPS medium assume this carbon source concentration unless otherwise stated. Through the course of the thesis other carbon sources at different concentrations were used. Several experiments required the use of a simplified form of MSPS,

designated *modMSPS*. Glucose uptake experiments required the use of a carbon source-deprived modMSPS medium.

Calli induction was promoted from root segments of *P. pinaster* seedlings. Seedlings were germinated in sterile culture tubes in *gMS*. Medium.

The detailed composition MS-based mediums used in this work is depicted in table 2.1.2. The culture media were sterilized by autoclaving recipients for 15 min at 121 ºC and 1 atm.

Table 2.1.2. Composition of MS-based culture media used for growing *P. pinaster calli* and suspended cells

	Medium components	MSPS	modMSPS	gMS
Macronutrients	$MgSO_4.7H_2O$	0.37 $g.l^{-1}$	0.37 $g.l^{-1}$	0.185 $g.l^{-1}$
	$CaCl_2.2H_2O$	0.44 $g.l^{-1}$	0.44 $g.l^{-1}$	0.22 $g.l^{-1}$
	KNO_3	1.9 $g.l^{-1}$	1.9 $g.l^{-1}$	0.95 $g.l^{-1}$
	NH_4NO_3	1.65 $g.l^{-1}$	1.65 $g.l^{-1}$	0.825 $g.l^{-1}$
	KH_2PO_4	0.17 $g.l^{-1}$	0.17 $g.l^{-1}$	0.085 $g.l^{-1}$
Micronutrients	$MnSO_4.H_2O$	16.9 $mg.l^{-1}$	16.9 $mg.l^{-1}$	16.9 $mg.l^{-1}$
	KI	0.83 $mg.l^{-1}$	0.83 $mg.l^{-1}$	0.83 $mg.l^{-1}$
	$CoCL_2.6H_2O$	0.025 $g.l^{-1}$	0.025 $g.l^{-1}$	0.025 $g.l^{-1}$
	$ZnSO_4.7H_2O$	8.6 $mg.l^{-1}$	8.6 $mg.l^{-1}$	8.6 $mg.l^{-1}$
	$CuSO_4.5H_2O$	0.025 $mg.l^{-1}$	0.025 $mg.l^{-1}$	0.025 $mg.l^{-1}$
	H_3BO_3	6.2 $mg.l^{-1}$	6.2 $mg.l^{-1}$	6.2 $mg.l^{-1}$
	$Na_2MoO_4.2H_2O$	0.25 $mg.l^{-1}$	0.25 $mg.l^{-1}$	0.25 $mg.l^{-1}$
Fe/EDTA	$FeSO_4.7H_2O$	0.0278 $g.l^{-1}$	0.0278 $g.l^{-1}$	0.0278 $g.l^{-1}$
	$Na_2EDTA.2H_2O$	0.0413 $g.l^{-1}$	0.0413 $g.l^{-1}$	0.0413 $g.l^{-1}$
Vitamines	Nicotinic acid	0.5 $mg.l^{-1}$		
	Tiamine-HCl	0.1 $mg.l^{-1}$		
	Piridoxine-HCl	0.5 $mg.l^{-1}$		
	Glicine	2 $mg.l^{-1}$		
	Myo-inositol	0.1 $g.l^{-1}$		
Hormones	BA	1 $mg.l^{-1}$	1 $mg.l^{-1}$	
	2,4-D	2 $mg.l^{-1}$	2 $mg.l^{-1}$	
Carbon source	Sucrose/Glucose	30/12/5 $g.l^{-1}$	20 $g.l^{-1}$ *sucrose*	20 $g.l^{-1}$ *sucrose*
Other components	Dithiothreitol	5 $mg.l^{-1}$		
	Agar	7 $g.l^{-1}$		7 $g.l^{-1}$
pH 6.0				

2.1.5.2. Microbiology culture media

Composition of the culture media used in growing, maintaining or operating fungal mycelium and *E. coli* strains is depicted in table 2.1.3. All agarized media were

obtained by adding 1.5% (w/v) agar to the medium's broth composition. Recombinant selection using the *lacZ* gene was performed by supplementing the appropriate agar

Table 2.1.3. Composition of culture media used for growing fungi and bacteria strains.

Culture medium	Composition	Aim	Strain
LB	1% (w/v) NaCl 1% (w/v) bacto-tryptone 0.5% (w/v) yeast extract pH 7.0	Growth and maintenace	*E. coli*
LB^{++}	LB 10 mM $MgSO_4.7H_2O$ 0.2% (w/v) maltose	Phage infection	*E. coli* XL1 Blue MRF'
LB-Tet	LB 12.5 μg ml^{-1} tetracyclin	Growth and maintenance	*E. coli* XL1 Blue MRF' E. coli XLOLR
LB-Kan	LB 50 μg ml^{-1} kanamycin	Maintenance of transformants carrying Kan resistance mark	E. coli XLOLR E. coli JM109
LB-Amp	LB 100 μg ml^{-1} Ampicillin	Maintenance of transformants carrying Amp resistance mark	E. coli JM109
NZY	0.5% (w/v) NaCl 0.2% (w/v) $MgSO_4.7H_2O$ 0.5% (w/v) yeast extract 1% (w/v) NZ amine (casein hydrolysate), pH 7.5	Phage infection	*E. coli* XL1 Blue MRF' E. coli XLOLR
NZY Top agarose	NZY 0.7% (w/v) agarose	Phage infection	*E. coli* XL1 Blue MRF'
$M9^{++}$	0.6% (w/v) Na_2HPO_4 0.3% (w/v) KH_2PO_4 0.1% (w/v) NH_4Cl 0.05% (w/v) NaCl After sterilization the medium was supplemented with: 1 mM $MgSO4.7H_2O$ 0.2% (w/v) glucose 0.1 mM $CaCl_2$ 1 mM thiamine-HCl, pH 7.4	Growth and maintenance	*E. coli* JM109
PD	0.4% (w/v) potato infusion 2% (w/v) dextrose	Growth for elicitation assays	*B. cinerea*
PDA	PD liquid broth 1.5% (w/v) agar	Growth and maintenance	*B. cinerea*
YM	0.3% (w/v) yeast extract 0.3% (w/v) malt extract 0.5% (w/v) peptone 1% (w/v) dextrose 1.5% (w/v) agar	Growth for elicitation assays	*L. seditiosum*
YMA	YM 1.5% (w/v) agar	Growth and maintenance	*L. seditiosum*

plaques with 40 μg ml^{-1} of IPTG (0.5 M in water) and 40 μg ml^{-1} of X-gal (50 mg ml^{-1} in DMF). The culture media were sterilized by autoclaving for 20 min at 121 ºC and 1 atm.

2.1.6. Establishment and maintenance of *Pinus pinaster* suspension cell cultures

Pinus pinaster suspension cells were established after induction of *calli* tissue in agarized medium. For this, 10 mm length sections of roots and hypocotyls were obtained under aseptic conditions, and five to six explants were transferred to each culture flask containing 25 ml of agarized MSPS medium. *Calli* were allowed to develop for 4 weeks and were subcultured every 8-10 weeks.

Suspension cultures were initiated from 8-week *callus* by transferring 0.5-2 g to 250 ml erlenmeyer flasks containing 25 ml of MSPS liquid medium and incubating in the dark, at 25°C on a orbital shaker at 100 rpm. Additional 25 ml were added when biomass started to increase. Subcultures were performed at late exponential phase (every 12-14 days), by transferring 10 ml of the culture into 70 ml of fresh medium. After four subculture cycles, suspension cultures were considered stabilized.

For nutrient starvation studies, *P. pinaster* cells grown in mid exponential phase were washed twice in sterile d.d. water, by centrifugation at 5000 *g* for 4 min and half strength deceleration in order to avoid cell resuspension. Cells were resuspended at 0.2 g ml^{-1} FW in sugar-free, phosphate-free modMSPS medium (P^-S^-) or in the same media supplemented with: 60 mg l^{-1} phosphate (P^+S^-), 30 g l^{-1} sucrose (P^-S^+) or 60 mg l^{-1} phosphate + 30 g l^{-1} sucrose (P^+S^+).

For sugar transport studies, *P. pinaster* suspended cells were grown in MSPS medium containing 3% (w/v) glucose. Cells were allowed to adapt for four growth cycles. When required, suspended cells were transferred to MSPS medium containing 1.5% glucose.

2.1.7. Growing of fungi strains

Botrytis cinerea cultures were maintained in PDA plates (DIFCO) at room temperature, and subcultured by mycelium transfer to fresh medium every 20 days. For long term storage, glycerol stocks were created (section 2.1.11.).

To induce sporulation, *B. cinerea* was grown in PDA plates for 20-30 days. The mycelium was recovered and resuspended in sterile 0.03% (v/v) tween-20. Hyphae removal was performed by filtrating the suspension through gauze. Spore concentration was determined using a haemocytometer.

Lophodermium seditiosum cultures were maintained in YM agarized medium (DIFCO) at room temperature, and subcultured by mycelium transfer to fresh medium every 20 days.

2.1.8. Elicitation of *P. pinaster* suspended cells with fungi

Pinus pinaster suspended cells in end exponential phase were harvested and washed twice by centrifugation (5000 *g*, 5 min, no deceleration) and resuspended in modMSPS medium, at a final density of 0.1 g FW ml^{-1}.

For the quantification of superoxide radical by the XTT method, cells were awshed in 10 mM potassium phosphate buffer (pH 7.8) and resuspended at a final density of 0.1 g FW ml^{-1} in 10 mM potassium phosphate buffer (pH 7.5) containing 2% (w/v) sucrose.

For the determination of intracellular calcium, cells were washed twice in 10 mM sodium phosphate buffer (pH 7.0) and resuspended at a final density of 0.1 g FW ml^{-1} in the same buffer containing 2% (w/v) sucrose.

Elicitation by *B. cinerea* spores was performed by transferring spore suspension aliquots a final concentration of up to 6 10^4 spores ml^{-1} (Mazel and Levine 2002). Cells were subsequently incubated at 25ºC in the dark with agitation (100 rpm).

P. pinaster suspended cells were also elicited by mycelia extracts. *B. cinerea* and *L. seditiosum* mycelia was respectively subcultured in PD and YM liquid medium, and grown at 25ºC with agitation (150 rpm). Cultures at mid exponential growth phase were

centrifuged at 5000 g for 5 min, and the mycelia was washed by resuspension in sterile water. Mycelia was lyophilised for 48 h in a *Christ Alpha RVC Lyophilizer* (B-Braun) and grinded with a mortar and pestle to a fine powder. Extracts were transferred to pine suspended cultures to a final concentration of 2 mg ml^{-1}.

2.1.9. Treatment of *P. pinaster* seedling with salicylic acid

Two month-old *Pinus pinaster* seedlings were sprayed with 5 mM salicylic acid. Twenty randomly picked seedlings were removed daily for one week. The harvested material was immediately frozen in liquid nitrogen and stored at –80 ºC.

2.1.10. Growing of *E.coli* strains

E. coli strains were grown in the appropriate medium as indicated in table 2.1.3. For isolating single colonies, the strains were striked onto an appropriate agarized medium and incubated overnight at 37ºC. Liquid cultures were obtained by inoculating a single colony into the medium and incubating at 37°C, with agitation (150-250 rpm).

2.1.11. Glycerol stock preparation

Long term viable stocks of *E. coli* strains were prepared by inoculating single colonies in the appropriate liquid medium (table 2.1.3.), followed by growth in the appropriate conditions (section 2.1.10.) until reaching late exponential growth phase. Culture aliquots was then added to sterile glycerol-containing criotubes to a final 20% (v/v) glycerol concentration.

Botrytis cinerea and *L. seditiosum* glycerol stocks were prepared by growing mycelium cultures in PD medium or YM medium, respectively for 30 days, when a reasonable amount of biomass had accumulated. Mycelium aliquots were then

transferred to sterile glycerol-containing criotubes at a final 30% (v/v) glycerol concentration.

The vials were immediately stored at -80°C. To maintain cell viability, stocks were recovered by scraping off splinters of solid ice with a sterile wire loop.

2.1.12. Reagents

All chemicals used for molecular biology methods and nucleic acid extractions were *Molecular Biology* grade. The remaining chemicals were ***p.a.*** grade.

2.1.13. Material treatment

RNA manipulation was carried out under special conditions to prevent RNase contamination. The specifications are described in table 2.1.4. DEPC was destroyed by autoclaving at for 20 min at 121 ºC and 1 atm.

Table 2.1.4. Listing of laboratory practises to promote an RNase free environment.

Reagents and Material	Treatment
Water	u.p. treated overnight with 0.1% (v/v) DEPC and autoclaved.
Solutions	Prepared using u.p. water. Treated overnight with 0.1% (v/v) DEPC and autoclaved.
Tris solutions	Incompatible with DEPC. Prepared using DEPC-treated u.p. water and autoclaved.
Glass and ceramics	Treated at 180ºC for 6 h.
Disposable material	Autoclaved at 1 atm for 1 h.
Electrophoresis material	Treated overnight with 0.1% (v/v) DEPC or for 2 h with 0.1 M NaOH. Washed thoroughly with DEPC treated water.

2.2. Biochemical methods

2.2.1. Characterization of *P. pinaster* suspension cell cultures

2.2.1.1. Determination of dry weight

Four independent *P. pinaster* suspension cultures in MSPS medium were started using the same inoculum, grown under the conditions described in section 2.1.6. Aliquots of 3 ml of suspended cells were harvested every 3 days under sterile conditions, over a total period of 24 days. Samples were centrifuged at 5000 *g* for 4 min using half strength deceleration to avoid cell resuspension. The supernatant was separated and cells were filtered using pre-weighted *GF/C glass microfiber filter* (Whatman). Dry weight was determined after oven drying the cells at 60ºC for 48 h. The pH value of each supernatant was immediately measured. The remaining supernatants were stored at -20ºC.

2.2.1.2. Determination of cell viability

Viability of *P. pinaster* suspended cells was determined using the trypan blue exclusion method. Aliquots of the cell culture were mixed with identical volume of 0.4% (w/v) trypan blue, and incubated in the dark, for 10 min. Cells were observed under a light microscope. Non-viable cells were stained in blue.

2.2.1.3. HPLC quantification of sugar content

Sucrose, fructose and glucose levels were determined by HPLC in a *Gilson* system composed of a *piston pump model 307* and a *refractive index detector model 132*, coupled with a *block heater model 7970* (Jones Chromatography). The HPLC system was connected through the *Gilson 506C System Interface Module* to a CPU containing the *System Controller Gilson 712* software. The mobile phase consisted in a solution of 0.125 g l^{-1} calcium nitrate in u.p. water, filtrated through a 0.2 μm nylon membrane and vacuum degasified. Samples were filtrated for cell debris removal, and an equal volume of 10 g l^{-1} arabinose was added, serving as the internal standard. For sample running, 20 μl were injected through a 0.5 ml min^{-1} flow into a *HyperRez* H^+ *Carbohydrate LG* column (Hypersyl) at 37ºC.

2.2.1.4. Determination of glucose concentration

Glucose levels were determined by the glucose oxidase (GOD) method (*Test-Combination*, Boehringer Mannheim), according to the supplier's instructions.

2.2.1.5. Phosphate quantification

The orto-phosphate ion was quantified spectrophotometrically using the ascorbic acid method, as described by Adams (1991). To prepare a working solution, 50 ml of Armstrong reagent were added to 10 ml of freshly made 3% (w/v) ascorbic acid. Samples obtained in section 2.2.1.1 were unfrozen and diluted 3-20 fold. A one-ml aliquot was added to 120 μl of working reagent, vortexed and allowed to react for 20 min. The presence of phosphate in the sample was detected by the appearance of blue coloration, and absorbance was determined at 880 nm, in a UV-VIS double beam spectrophotometer *Cary 1E UV-Vis Spectrophotometer* (Varian). A calibration curve was produced using KH_2PO_4 solutions with linearity being observed between 30-4500 μg l^{-1}.

Armstrong reagent: 11.8% (v/v) H_2SO_4; 0.03% (w/v) $K(SbO)C_4H_4O_6.1/2H_2O$; 1.05% (w/v) ammonium molibdate.

2.2.1.6. Nitrate and ammonium quantification

Nitrate and ammonium ions were quantified using selective electrodes as described by Eaton *et al.* (1995). Samples (section 2.2.1.1.) were diluted 50-100-fold in u.p. water at 4ºC. Nitrate was quantified using a NO_3^- selective electrode (*Elit 21 Model 900100*: Orion Research Incorporated, Boston, USA) in 1% $KAl(SO_4)_2$. A standard curve was obtained using defined amounts of KNO_3. Ammonium was quantified using a selective electrode (*Ammonia Electrode Model 95-12*, Orion Research Incorporated, Boston, USA). A standard curve was created using defined amounts of NH_4Cl.

An ionic strength adjustor (*ISA sol. no. 951211*, Orion) was added to all samples. Readings were performed in a pH/ISE metter (*Model 720 A*, Orion) at 25 ºC (*Temperature Probe 917005*, Orion).

2.2.2. Determination of lignin content

The lignin content in cell walls of *P. pinaster* suspension cell cultures was determined through the acetyl bromide method, adapted from Fukushima and Hatfield (2001). *P. pinaster* suspension cells were harvested, washed twice in d.d. water by centrifugation at 5000 *g* for 5 min, lyophilised for 48 h in a *Christ Alpha RVC Lyophilizer* (B-Braun) and grinded to a fine powder. Between 0.1-0.2 g of cell material were transferred onto a 15 ml Falcon tube and precision weighted. Cells were added 5 ml of 90% (v/v) methanol and allowed to extract for 24 h in the dark at room temperature. The methanol extract was removed by centrifugation (5000 *g* for 5 min). Cell material was consecutively extracted with water, acetone and hexane as previously described, after which it was dried overnight at 60ºC. Ten mg of cell wall were added to 500 µl of acetic acid and 500 µl of 25% (v/v) acetyl bromide in acetic acid and incubated at 50ºC for 2 hours with agitation. Samples were centrifuged and 100 µl of the supernatant were mixed with 200 µl of acetic acid, 150 µl of 3 M NaOH and 50 µl of 0,5 M hydroxylamine hydrochloride. Finally, 500 µl of acetic acid were added, and the absorbance was determined at 280 nm in a spectrophotometer. A standard calibration curve was generated with lignin (Aldrich), showing linearity within the range 0.005-0.1 mg.

2.2.3. Determination of the total soluble phenolics content

The total content of soluble phenolics was determined in pine cell extracts by the Folin method (Waterman and Mole 1994). *P. pinaster* suspended cells were harvested, washed twice in d.d. water by centrifugation at 5000 *g* for 5 min, lyophilised for 48 h in a *Christ Alpha RVC Lyophilizer* (B-Braun) and grinded to a fine powder. Aliquots of 0.1-0.2 g of cell material were transferred onto a 15 ml Falcon tube and precision weighted. Cells were added 5 ml of 90% (v/v) methanol and allowed to extract for 24 h in the dark at room temperature. The methanol extract was recovered by centrifugation (5000 *g* for 5 min). Quantification of the phenolics content was initiated by adding 5 ml of H_2O and 0.5 ml of Folin-Denis' reagent (Fluka) to 0.1 ml of methanol extract. The mixture was mixed thoroughly and allowed to react for 5 min, after which 1.5 ml of 35% (w/v) sodium carbonate was added. The reaction was carried out in the dark for 2 h, by the end of which, 2.9 ml of H_2O were added and absorbance was read at 760 nm. A calibration curve was generated using quercetin (Sigma).

2.2.4. Quantification of reactive oxygen species

2.2.4.1. Detection of O_2^-

The intracellular production of the superoxide radical (O_2^-) was quantified by the reduction of the tetrazolium dye sodium,3'-(1-[phenylamino-carbonyl]-3, 4-tetrazolium)-bis(4-methoxy-6-nitro) benzene-sulfonic acid hydrate (XTT) to a soluble formazan (Able et al. 1998).

Immediately before suspended cell elicitation with *B. cinerea*, pine cells were added 0.5 mM XTT and incubated in the dark at room temperature with agitation. Aliquots were removed periodically, and the reduced XTT form was readily quantified by reading the absorbance of the supernatant at A_{470}.

2.2.4.2. Detection of total ROS

The overall oxidative stress of the cell was quantified using the cell-permeant 2',7'-dichlorodihydrofluorescein diacetate (H_2DCFDA; Molecular Probes) as previously described (Parsons et al. 1999; Allan et al. 2001). H_2DCFDA is converted by non-specific cellular esterases to H_2DCF, which oxidizes in the presence of H_2O_2 and other reactive oxygen intermediates. The end product 2',7'-dichlorofluorescein is highly fluorescent (Cathcart et al. 1983) and able to diffuse out of the cell. We used this property to quantify the intracellular production of 2',7'-dichlorofluorescein, by performing a spectrofluorimetric analysis of the supernatant.

During the time course of the pine suspended cells elicitation with *B. cinerea* spores, 1 ml aliquots were removed and mixed with 10 µl of 20 µM H_2DCFDA. Cells were incubated in the dark, at room temperature, for 30 min with agitation. Samples were centrifuged at 8000 *g* for 5 min and the supernatant recovered. Relative fluorescence was quantified using a *LS 50 Luminescence Spectrometer* (Perkin Elmer) at an excitation wavelength of A_{488} and an emission wavelength of A_{525}.

In identical assays, cells were separately added 5 µM staurosporine, 50 µM DPI, 1 mM lanthanum (III) chloride heptahydrate, 250 µM α-amanitin and 50 µg ml^{-1} cyclohexamide, 15 min prior to elicitation with *B. cinerea* spores.

2.2.4.3. Detection of H_2O_2

The quantification of H_2O_2 concentration in cell suspension medium was performed spectrophotometrically by the xylenol orange method (Bellincampi *et al.* 2000). The reaction is based on the peroxide-mediated oxidation of Fe^{2+}, followed by the formation of a complex between Fe^{3+} and xylenol orange (*o*-cresosulfonephthalein 3',3''-bis[methyl-imino] diacetic acid, sodium salt).

Aliquots of pine suspended cells were harvested during the time course of the elicitation with *B. cinerea* spores and the supernatant recovered after centrifugation at 8000 *g* for 5 min. A 500 µl aliquot of cell medium was added to 500 µl of assay solution (500 µM ammonium ferrous sulfate, 50 mM H_2SO_4, 200 µM xylenol orange, 200 mM sorbitol). The reaction mixture was incubated for 45 min at room temperature and analysed in a spectrophotometer (A_{560}). A calibration curve was constructed using H_2O_2 dilutions in cell medium.

2.2.5. Detection of lipid peroxidation

Lipid peroxidation was quantified spectrophotometrically by the MDA-TBA method (Loreto and Velikova 2001), which quantifies the end product of lipid peroxidation malondialdehyde (MDA) by reaction at low pH and high temperature with 2-thiobarbituric acid (TBA). The reaction was initiated by adding 75 µl of protein extract from *B. cinerea* spore-challenged pine suspension cells, to 250 µl of chilled reaction mixture, composed of 0.5% (w/v) TBA in 20% (w/v) TCA. The mixture was incubated at 95ºC for 30 min and placed immediately on ice. Samples were centrifuged at 10000 *g* for 5 min at 4ºC, and the supernatant was recovered. Quantification of the MDA-TBA complex was performed by determining the absorbance of the supernatant at 532 nm and deducting non-specific absorbance at 600 nm. The molar extinction coefficient of MDA-TBA complex, at 532 nm, is 155 $mM^{-1}.cm^{-1}$.

2.2.6. Detection of intracellular calcium

Intracellular calcium was detected using the intracellular probe *fluo-3, AM* (Molecular Probes). When exited at 488 nm, Ca^{2+}-binded fluo-3 molecules present a large increase in fluorescence intensity (>100 fold). Maximum emission of calcium-bound probe occurs at 526 nm. The cell permeant AM ester allows for intracellular specificity.

The procedure was performed according to the manufacturer's instructions. *P. pinaster* suspended cells were collected according to section 2.1.8. and allowed to adapt to the medium by incubating for 60 min in reaction buffer containing: 10 mM sodium phosphate (pH 7.0) and 2% (w/v) sucrose with agitation (100 rpm). For cell loading, fluo-3 probe (stored in a 1 mM stock solution in DMSO) was added in the dark, to a final concentration of 2 µM in reaction buffer. Cells were incubated for 30 min at 25ºC and washed, to remove excess dye. After incubation for 30 min at 25ºC to allow complete de-esterification of the intracellular probe, a *B. cinerea* spore suspension was added.

During the time course of elicitation, cells were removed periodically and observed under UV light using an excitation wavelength of 450-490 nm and an emission filter of 510 nm. in a fluorescence microscope *Leitz Laborlux S* (detection range of Fluo-3 is 492-577 nm - green).

Control reactions were performed in the absence of *B. cinerea* elicitation, as well as in challenged cells in the presence of $LaCl_3$, a blocker of calcium channels. For the purpose, 1 mM $LaCl_3$ was added to cells 10 min prior to elicitation.

2.2.7. TUNEL assay

TUNEL assay was performed according to the procedure described by Gavrieli *et al.* (1992). The reaction is based on the presence of single and double-stranded breaks in genomic DNA during apoptosis. Terminal deoxynucleotidyl transferase (TdT) polymerizes fluorescein labelled nucleotides to free 3'-OH termini, in a template independent manner. The TUNEL reaction was performed using the In Situ *Cell Death Detection Kit - Fluorescein* (Roche Applied Science), according to the manufacturer's instructions, and as described by Sgonc *et al.* (1994).

P. pinaster suspended cells were washed once with PBS and subsequently fixated for 1 h at 20ºC in newly prepared fixation solution. Cells were washed in PBS and incubated for 10 min at 20ºC in blocking solution. After washing in PBS, permeabilisation solution was added, followed by a 2 min incubation on ice. The TUNEL reaction solution was prepared by mixing *Label* and *Enzyme solution* (Roche Applied Science). Suspended cells were washed twice in PBS and carefully dried, after which 50 µl of TUNEL solution were added to ~50 µl of cells. The mixture was incubated for 60 min at 37ºC in the dark. Finally, cells were washed three times with PBS and transferred to a glass slide. Fluorescein has a detection range of 515-565 nm (green). Cells were analysed for TUNEL reaction under a UV light with an excitation wavelength of 450-490 nm and an emission filter of 510 nm in a fluorescence microscope.

PBS: 8 $g.l^{-1}$ NaCl; 0.2 $g.l^{-1}$ KCl; 1.44 $g.l^{-1}$ Na_2HPO_4; 0.24 $g.l^{-1}$ KH_2PO_4.
Fixation solution: 4% Paraformaldehyde in PBS, pH 7.4.
Blocking solution: 3% H_2O_2 in methanol.

Permeabilisation solution: 0.1% (v/v) Triton X-100 in 0.1% (w/v) sodium citrate.

2.2.8. Protein extraction and quantification

Pinus pinaster plant material were grinded to a fine powder in liquid nitrogen with a mortar and stored at -80ºC. Samples (~1 g of fresh weight) were thawed in 2-3 ml of protein extraction buffer and incubated on ice for 5 min. After centrifugation for at 15000 *g* 15 min at 4ºC, the supernatant was recovered and immediately used for enzyme assays or stored at -80ºC.

Protein was quantified using the Coomassie Blue method (Sedmak and Grossberg 1977). The reaction mixture consisted of 1 ml of Coomassie Blue reagent and 100 µl of a suitable dilution of protein extract. Samples were incubated for 10 min at room temperature in the dark, after which absorbance was read at 595 nm. BSA (0.5-10 µg) was used as standard.

Protein extraction buffer: 50 mM Na_2HPO_4 (pH 7.0), 1mM benzamidine, 0.1% (v/v) 2-mercaptoethanol and 1% (w/v) PVPP.
Coomassie Blue reagent: 0.06% (w/v) Coomassie Brilliant Blue G 250; 1.9 % (v/v) perchloric acid. After filtrating with Whatman® No.1 filter paper, the solution was stored in the dark at room temperature.

2.2.9. Protein electrophoretic separation by Native-PAGE

The electrophoretic separation of proteins in native conditions was performed using a polyacrylamide vertical slab gel apparatus (*Protean II xi Cell*; BioRAD) in a discontinuous buffer system. The acrylamide concentration was chosen according to the predicted native molecular weight. Prior to loading, proteins samples were mixed with 0.1 vol of loading buffer. Electrophoresis was carried out overnight, at 50 V and 4°C.

10% Acrylamide resolving gel: 375 mM Tris-HCl (pH 8.8); 10 % (w/v) acrylamide; 0.26 % (w/v) bisacrylamide; 0.075 % (w/v) ammonium persulphate. Add 0.05 % (v/v) TEMED to begin polymerization.
7.5% Acrylamide resolving gel: 375 mM Tris-HCl (pH 8.8); 7.5 % (w/v) acrylamide; 0.2 % (w/v) bisacrylamide; 0.075 % (w/v) ammonium persulphate. Add 0.05 % (v/v) TEMED to begin polymerization.

Stacking gel solution: 125 mM Tris-HCl (pH 6.8); 3.75 % (w/v) acrylamide; 0.1 % (w/v) bisacrylamide ; 0.075 % (w/v) ammonium persulphate. Add 0.05 % (v/v) TEMED to begin polymerization.
Reservoir buffer: 0.025 M Tris; 0.192 M glycine.
Loading buffer: 50% (v/v) glycerol; 0.05% (w/v) bromophenol blue.

2.2.10. Enzyme assays

2.2.10.1. Acid phosphatase

Acid phosphatase activity was determined using a spectrofotometric assay according to (Moriyasu and Ohsumi 1996). Protein extracts were thawed and maintained at 4ºC until the beginning of the reaction. The assay was started by adding 50 µl of protein solution to 250 µl of 0.1 M Tris-maleate (pH 5.0), 190 µl of water and 10 µl of 50 mM *p*-nitrophenylphosphate. After incubation at 37ºC for 15 min, the reaction was stopped by adding 0.8 ml of 1 M sodium carbonate and the absorbance was read at 405 nm. One unit (U) of acid phosphatase activity was defined as the protein amount responsible for the production of 1 mmole *p*-nitrophenylphenol min^{-1} , at 37 °C (molar extinction coefficient of *p*-nitrophenylphenol = $1.78x10^4$ M^{-1} cm^{-1}).

In addition, the cytochemical localization of acid phosphatase activity was performed on suspended cells, according to Moryasu and Ohsumi (1996). Aliquots of cell cultures were harvested and cells were washed in PBS medium using a centrifugation at 5000 *g* for 5 min. Cells were fixed in 1% (w/v) formaldehyde (obtained by de-polimerization of paraformaldehyde) in PBS (pH 7.4) for 1 h at room temperature. The cells were subsequently washed in 0.1 M sodium acetate (pH 5.0) and incubated in a reaction medium, containing 50 mM sodium acetate (pH 5.0), 0.1% Fast Garnet GBC and 1 mM *p*-nitrophenylphosphate. After incubation in the dark for 10 min at room temperature, cells were observed under a light microscope.

PBS: 8 $g.l^{-1}$ NaCl; 0.2 $g.l^{-1}$ KCl; 1.44 $g.l^{-1}$ Na_2HPO_4; 0.24 $g.l^{-1}$ KH_2PO_4.

2.2.10.2. Superoxide dismutase

SOD activity was determined after Native-PAGE electrophoresis on a 10% acrylamide gel, according to the method of Wendel and Weeden (1989), a procedure

modified after Beauchamp and Fridovich (1971). Aliquots of 30 μg of protein were loaded per well.

Once the electrophoretic separation was carried out, the gel was incubated in SOD reaction solution for 30 min, in the dark, with agitation. SOD isoforms were differentiated according to their sensitivity to KCN and H_2O_2 (Wendel and Weeden 1989). CuZn-SODs are inhibited by KCN and H_2O_2, Fe-SODs are resistant to KCN and inhibited by H_2O_2, Mn-SODs are resistant to both KCN and H_2O_2. Inhibition assays were carried out using gel replicas. The gels were pre-incubated for 30 min in 50 mM Tris-HCl (pH 8.0), containing 2 mM KCN or 5 mM H_2O_2, followed by incubation in SOD reaction solution for 30 min, in the dark, with agitation. After incubation, the gels were finally transferred to light box and exposed to white light. SOD activity was revealed as achromatic bands against a dark purple background.

SOD reaction medium: 50 mM Tris-HCl (pH 8.0); 0.106 mM riboflavin; 53.7 μM EDTA; 0.245 mM NBT.

2.2.10.3. Catalase

CAT activity was determined after Native-PAGE gel electrophoresis, on a 7.5% acrylamide gel as described by Woodbury (1984). Aliquots of 20 μg of protein were loaded per well.

After electrophoresis, the gel was incubated in 0.01% (w/v) H_2O_2 for 10 min and immediately transferred to freshly prepared CAT reaction medium. The gel became uniformly dark blue stained. Zones corresponding to CAT enzymatic activity were revealed as achromatic bands.

CAT reaction medium: 1% (w/v) $FeCl_3.6H_20$; 1% (w/v) $K_3[Fe(CN)_6]$.

2.2.11. Glucose uptake studies in *Pinus pinaster* suspended cells

2.2.11.1. Estimation of initial D-[^{14}C]glucose uptake rates

P. pinaster cells were harvested, washed twice by centrifugation at 5000 g for 5 min and resuspended in modMSPS medium without sugar, at pH 5.0 and 4ºC at a final

concentration of about 4 mg ml^{-1} DW. To estimate initial uptake rates of D-[^{14}C]glucose (Radiochemical Centre, Amersham), 1 ml aliquots were transferred to 10 ml flasks, with agitation (100 rpm) at 25°C. After a 3 min incubation, the reaction was started by the addition of 40 µl of an aqueous solution of radiolabelled sugar (500 dpm $nmol^{-1}$). Sampling times were 0, 180, 360 and 540 s, time periods during which the uptake was linear. The reaction was stopped by adding 5 ml of ice-cold modified sugar-free MS medium and the mixtures were immediately filtered through GF/C filters (Whatman, Clifton, NJ, U.S.A.). The filters were washed with additional 10 ml of the same medium and transferred to a vial containing scintillation fluid (*OptiPhase HiSafe II*; LKB Scintillation Products). The radioactivity was quantified using a *Packard Tri-Carb 2200 CA* liquid scintillation counter (Packard Instruments Co., Inc., Rockville, MD, U.S.A.). Results were corrected for non-specific binding of labelled sugars to the filters and/or the cells, by diluting the cells with 5 ml ice-cold modified MS medium without sugar, before the addition of labelled sugar.

2.2.11.2. Determination of substrate specificity

The specificity of the glucose carrier was determined by measuring 0.02-0.2 mM labelled glucose uptake in the presence of non-labelled substrates. The final cold substrate concentration was at least 10-fold higher than the K_m value estimated for the glucose transporter.

2.2.11.3. Accumulation studies

For accumulation studies, 10 ml of cell suspension were transferred to a 50 ml Erlenmeyer flask under agitation (100 rpm). After 3 min of incubation at 25°C, the reaction was started by the addition of an aqueous solution of radiolabelled 3-*O*-methyl-D-glucose (3-*O*-MG specific activity of 3000 dpm $nmol^{-1}$) at a final concentration of 0.1 mM. One-ml aliquots were taken from the reaction medium into 5 ml of ice-cold modified MS medium without sugar and filtered immediately through Whatman GF/C membranes. The filters were washed with 10 ml of the same medium, and the radioactivity was determined as indicated above.

2.2.11.4. Determination of intracellular volume

Intracellular water volume was based on the quantification of the relative distribution of two radioactive compounds in a cellular suspension: inulin-[^{14}C]methoxy to which biomembranes are impermeable and [^{3}H]H_2O that equilibrates across biomembranes. After washing with modified MS medium without sugar, 2 ml of cell suspension were incubated with 5 µl of 250 mCi ml^{-1} [^{3}H]H_2O (Amersham; 5 Ci ml^{-1}), and 5 µl of 0.22 mg ml^{-1} inulin-[^{14}C]methoxy (New England Nuclear; 5.2 mCi g^{-1}). The mixture was incubated for 30 min, and the cells were pelleted by centrifugation at 4000 *g*, for 1 min. The supernatant (100 µl) was added to 5 ml of 1% (w/v) SDS and the same volume of SDS was added to the pellet. After overnight incubation, the mixtures were centrifuged, and the radioactivity of 40 µl of each supernatant was measured as described above. Intracellular water volume (V_{int}) was determined according to the expression: $V_{int} = V_{sup} [(^{3}H_{pel} / {}^{3}H_{sup}) - (^{14}C_{pel} / {}^{14}C_{sup})]$, where V_{sup} corresponds to the volume of supernatant, $^{3}H_{pel}$ and $^{3}H_{sup}$ correspond to the ^{3}H counts in the pellet and in the supernatant, respectively, and $^{14}C_{pel}$ and $^{14}C_{sup}$ correspond to the ^{14}C counts in the pellet and in the supernatant, respectively. A value of 7.6 ± 2 µl intracellular water mg^{-1} DW was obtained.

2.2.11.5. Calculation of kinetic parameters

The data of the initial uptake rates of labelled glucose were analyzed by a computer-assisted non-linear regression analysis (GraphPad software; San Diego, CA). By this method, the transport kinetics best fitting to the experimental initial uptake rates was determined, and then estimates for the kinetic parameters were obtained. Error bars indicate the standard error (SE) of triplicate independent experiments.

2.2.11.6. Study of glucose transport upon elicitation of pine suspended cells by B. cinerea

Botrytis cinerea was grown in PDA plates for 20-30 days until extensive sporulation occurred. Spores were recovered by adding 10 ml of 0.03% tween-20 to each plate. The suspension was filtered through gauze to remove contaminating hyphae. Spores concentration was determined using a haemocytometer. For elicitation experiments, 1.5% glucose-grown *P. pinaster* cells were harvested from culture at day

9, when glucose in the medium had fallen to around 0.7% (w/v), and washed in sugar-free MS medium. Cells were resuspended in the same medium in the absence or in the presence of 2% glucose. *Botrytis cinerea* spores were added to a final concentration of $6x10^4$ or $2x10^4$ spore ml^{-1}. Staurosporine (5 μM), DPI (50 μM), $LaCl_3$ (1 mM), cycloheximide (50 μg ml^{-1}) and α-amanitin (250 μM) were added independently to pine cell suspensions 15 min prior to elicitation with *B. cinerea* spores. Transport experiments were performed as described above.

2.2.12. Statistical analysis

All experiments were performed using 3-4 four independent experiments.

For rate determination during the characterization of *P. pinaster* suspension cell cultures (section 2.2.1.), the original data sets for growth and nutrient uptake were used. Biomass levels were transformed into their natural logarithm for specific growth rate (μ) calculation. All data for the determination of nutrient consumption rates for phosphate ion (qP), carbon source (total sugar, qC; glucose, qC_{glu}; fructose, qC_{fru}) and nitrogen source (ammonium ion, qN_{amm}; nitrate ion, qN_{nit}) were divided by the corresponding biomass value. Transformed values were plotted against the time course of the experiment, and a fit curve was generated using a *cubic spline* calculation with 100 data points (GraphPad Prism software, v4.0). Instant rates were calculated by determining slope values for every adjacent points.

2.3. Molecular biology methods

2.3.1. RNA purification

2.3.1.1. Total RNA purification

This protocol is developed for the purification of high-quality RNA from needles of 30-year-old maritime pines. The protocol is also suitable for RNA extraction of seedling material, and is easily adapted for the extraction of quality RNA of cell suspensions.

Needled were ground to a fine powder in liquid nitrogen with a mortar and pestle. In a 50-mL Falcon tube, 15 ml of the extraction buffer were mixed with 2% (w/v) PVPP and 2% (v/v) 2-mercaptoethanol. Proteinase K was then added to a final concentration of 1.5 mg ml^{-1} After incubation of the extraction medium for 10 min at 42°C, ~1.3 g of ground frozen tissue were added. The mixture was vigorously mixed in a vortex and incubated for 90 min at 42°C with occasional mixing.

The sample was extracted by adding 1 vol of chloroform-isoamyl alcohol (24:1 [v/v]), followed by thorough vortexing and centrifuged at 15000 *g* for 15 min at 4°C to separate phases. The top aqueous phase was transferred to another tube, extracted again with chloroform-isoamyl alcohol and centrifuged in the same conditions. The top phase was recovered and 1/4 vol of 10 M $LiCl_2$ was added. RNA precipitation was promoted by overnight incubation at 4°C. The sample was centrifuged at 15000 *g* for 25 min at 4°C and the supernatant discarded. The RNA pellet was washed by resuspension in 2 ml of 2 M LiCl and centrifuged at 15,000 *g* for 25 min at 4°C. The pellet was dissolved in

100-200 µL of DEPC-treated water and the RNA's concentration and purity were determined spectrophotometrically. RNA samples were immediately frozen in liquid nitrogen and stored at –80°C.

Extraction medium: 100 mM Tris-HCl (pH 8), 2% (w/v) CTAB, 30 mM EDTA, 2 M NaCl, 0.05% (w/v) spermidine. Add 2% (w/v) polyvinylpolypyrrolidinone (PVPP, Sigma P-6755), 2% (v/v) 2-mercaptoethanol and 1.5 mg ml^{-1} prior to use.

2.3.1.2. mRNA purification

Isolation of mRNA from total RNA was carried out using the *Dynabeads® Oligo(dT)$_{25}$ Biomagnetic Separation System* (Dynal), according to the supplier's instructions. Five aliquots of 75 µg of total RNA in 100 µl of DEPC-treated water were used. For disruption of secondary structures, the samples were incubated at 65°C for 2 min. Each sample was then combined with 200 µl (1.0 mg) of Dynabeads Oligo(dT)$_{25}$, previously washed twice with 100 µl of 2x binding buffer. After gentle mixing, hybridization was promoted by incubating the mixture for 5 min, at room temperature.

Beads were concentrated by placing the tubes in the *Dynal MPC-E magnet stand* (Dynal) for 30 seconds and the supernatan was discarded. The beads were washed twice in 200 µl of 1x washing buffer. mRNA was eluted from the beads, by adding to each tube 7.5 µl of 1x elution buffer, followed by incubation at 65°C for 2 min. After concentrating the beads in the magnetic stand for 30 seconds, the mRNA sample was recovered. A second elution was performed, using 5 µl of 1x elution buffer. Aliquots from the first and second elutions were used for RNA quantification. The mRNA solutions were immediately frozen in liquid nitrogen and stored at -80°C.

2x Binding buffer: 20 mM Tris-HCl (pH 7.5); 1.0 M LiCl; 2 mM EDTA.
1x Washing buffer: 10 mM Tris-HCl (pH 7.5); 0.15 M LiCl; 1 mM EDTA.
1x Elution buffer: 2 mM EDTA.

2.3.2. cDNA library construction and screening

All steps of constructing the *P. pinaster* cDNA library were performed according to the supplier's instructions, provided with the *ZAP Express™ Synthesis Kit* (Stratagene) and the *ZAP Express™ Gigapack® III Gold Cloning Kit* (Stratagene).

2.3.2.1. First-strand cDNA synthesis

To synthesize the first-strand cDNA, the *P. pinaster* mRNA was primed with a hybrid molecule containing a linker (GAGA sequence), the *Xho* I restriction site and an oligo(dT) sequence:

5'-GAGAGAGAGAGAGAGAGAGAACTAGT**CTCGAG**TTTTTTTTTTTTTTTTT-3'

Reverse transcription was promoted using the enzyme MMLV-RT (Moloney murine leukemia virus reverse transcriptase). The reaction mixture contained 5-methyl dCTP, which promoted hemimethylation of the cDNA strand, thus preventing future digestion of the cDNA strand during the *Xho* I restriction step. The mRNA was denaturized at 70°C for 10 min and placed on ice for 5 min prior to adding to the reaction mixture. The reverse transcription reaction was incubated at room temperature for 10 min to permit annealing of the primer to the template poly(A), and 1.5 µl of MMLV-RT were added. After transferring 5µl of this reaction mixture to a first-strand control tube containing 0.5 µl of [α-32P] dATP (800Ci/mmol), both reactions were incubated at 37°C for 1 h. Another control reaction was performed with test 1.8 Kbp RNA, provided by the kit.

First strand reaction mixture:

5 µl of first-strand buffer (10x)
3 µl of first-strand methyl nucleotide mixture
(10 mM dATP, dGTP, dTTP and 5 mM 5-methyl dCTP)
2 µl of linker-primer (1.4 µg/µl)
1 µl of RNase Block Ribonuclease Inhibitor (40 U/µl)
37.5 µl of leaf mRNA (5.2 µg)

2.3.2.2. Second-strand cDNA synthesis

Synthesis of first-strand DNA resulted in a hybrid double stranded RNA-DNA molecule. For second-strand synthesis, RNA was digested by RNase H. The resulting

fragments served as primers for DNA polymerase I. The second strand nucleotide mixture was supplemented with dCTP to reduce the probability of 5-methyl dCTP becoming incorporated into the second strand. This ensured that the restriction sites in the linker-primer would be susceptible to restriction enzyme digestion. The first-strand reaction mixture was cooled on ice, after which the second-strand reaction components were added. The solution was incubated at 16°C for 2.5 h and immediately placed on ice. A control reaction was also performed using the 1.8 Kbp test RNA.

Second strand reaction mixture:

20 µl of second-strand buffer (10x)
6 µl of second-strand nucleotide mixture
(10 mM dATP, dGTP, dTTP and 26 mM dCTP)
114 µl of sterile water
2 µl of [α-32P] dATP (800Ci/mmol)
2 µl of RNase H (1.5 U/µl)
11 µl of DNA polymerase I (9.0 U/µl)

2.3.2.3. Blunting of cDNA termini and ligation of EcoR *I adapters*

The uneven termini of the double stranded cDNA were filled in by incubating the cDNA with a blunt end generating polymerase. The reaction was performed by adding 23 µl of blunting dNTP mixture (2.5 mM dNTP) and 2 µl of cloned *Pfu* DNA polymerase (2.5 U/µl) to the total volume of the second-strand reaction mixture, followed by incubation at 72°C for 30 min. The cDNA was then purified by performing a phenol/chloroform/IAA [25:24:1 (v/v/v)] extraction, followed by a chloroform/IAA [24:1 (v/v)] extraction. DNA was precipitated overnight at –20°C after addition of 20 µl of 3 M sodium acetate and 400 µl of ethanol. The solution was centrifuged at 12000 *g* for 60 min at 4°C, and the pellet was washed with 500 µl of 70% (v/v) ethanol and resuspended in 9 µl of the *Eco*R I adapters solution (0.4 µg μl^{-1}).

*Eco*R I adapters were composed of small dsDNA fragments containing a phosphorylated blunt end and an *Eco*R I cohesive end:

5’ – OH – **AATTC**GGCACGAG-3’
3’ – **G**CCGTGCTCp - 5’
(*Eco*R I site)

The blunt end’s 5’ nucleotide is phosphorylated in order to allow the ligation to cDNA blunt ends, whereas the *Eco*R I cohesive end has a dephosphorylated 5’ nucleotide to prevent ligation to cohesive ends of other adaptors. Ligation was

promoted by adding to 8 µl of the *Eco*R I adapters/cDNA solution, the following components: 1 µl of ligase buffer (10x); 1 µl of rATP (10 mM); 1 µl of T4 DNA ligase (4 U/µl). The reaction was incubated at 4°C for 2 days. Ligase was subsequently heat inactivated by incubation at 70°C for 30 min.

After adapter ligation to blunt ends, phosphorylation of the *Eco*R I cohesive end was promoted in order to enable its ligation to the dephosphorylated vector arms. Phosphorylation was performed by adding to the previous reaction solution the following components: 1 µl of ligase buffer (10x); 2 µl of rATP (10 mM); 6 µl of sterile water; 1 µl of T4 polynucleotide kinase (10 U/µl). The solution was incubated at 37°C for 30 min. The kinase enzyme was subsequently inactivated by heat as previously described.

2.3.2.4. Digestion with Xho *I*

The cDNA molecule now contained an *Eco*R I adapter at both ends. To release the adapter from the 3' end and create a *Xho* I cohesive end that permits orientated ligation to the vector arms, the cDNA was digested with *Xho* I. Digestion was performed by adding to the total volume of the previous reaction the following components: 28 µl of *Xho* I buffer supplement; 3 µl of *Xho* I (40 U/µl). The mixture was incubated at 37°C for 1.5 h.

The cDNA was purified by adding 5 µl of 10xSTE and 125 µl of etanol and incubating overnight at –20°C. Recovery of the cDNA was performed by centrifugation at 12000 *g* for 60 min, at 4°C, and resuspension of the pellet in 14 µl of 1x STE buffer.

10x STE buffer: 200 mM Tris-HCl (pH 7.5); 100 mM EDTA; 1M NaCl.

2.3.2.5. cDNA size fractionation

Size fractionation of the cDNA was performed by gel filtration chromatography. A drip column was prepared from a 1 ml pipette connected on it's top to a sterile 10 ml syringe, and loaded with *Sepharose CL-2B* gel filtration medium. After equilibrating the column with 10 ml of 1x STE buffer, the cDNA sample (14 µl mixed with 3.5 µl of column loading dye) was loaded at the top of the column. Separation was promoted by gravity flow by adding 3 ml of 1x STE. Fifteen fractions of approximately 100 µl (three drops) were collected and monitored for the presence of radioactivity in a

scintillation counter (*Scintillation Counter LS 7500*, Beckman Instruments). We then selected seven fractions corresponding to the first fractions showing radioactivity. For each fraction an 8 µl sample was removed for use in nondenaturing acrylamide gel electrophoresis.

The cDNA from selected fractions was purified through a phenol/chloroform/IAA [25:24:1 (v/v/v)] extraction followed by a chloroform/IAA [24:1 (v/v)] extraction. DNA was precipitated overnight after addition of 200 µl of ethanol and recovered by centrifugation at 12000 *g* for 60 min at 4°C. The pellet was washed with 200 µl of 80% (v/v) ethanol and resuspended in 10 µl of sterile water.

1x STE buffer: 20 mM Tris-HCl (pH 7.5); 10 mM EDTA; 100 mM NaCl.

2.3.2.6. cDNA ligation to the ZAP Express vector

The cDNA was quantified spectrophotometrically and the ligation of cDNA fragments to the vector was promoted by the enzyme T4 DNA ligase, using 100 ng of cDNA and 1 µg of ZAP Express vector in a final reaction volume of 5 µl. The reaction mixture was incubated for 2 days at 4°C. A parallel control ligation was performed using 1 µg of *ZAP Express* vector and 0.4 µg of test insert (provided by the kit).

Ligation reaction mixture:

2.5 µl of cDNA
1 µl of the ZAP Express vector (1 µg/µl)
0.5 µl of ligase buffer (10x)
0.5 µl of 10 mM rATP (pH 7.5)
0.5 µl of T4 DNA ligase (4 U/µl)

2.3.2.7. Packaging of the cDNA library

Using the *Gigapack® III Gold Packaging Extract* (Stratagene), 2 µl of the ligation reaction mixture were used for packaging of the vector into the λ phage. The remaining solution was stored at -80ºC, in the event of future packaging needs. Two packaging extracts were partially thawed, and 1 µl of vector-containing solution was added to each extract. The reaction mixture was gently stirred and incubated at room temperature for 2 h. After incubation, 500 µl of SM buffer and 20 µl of chloroform were added. As a control for packaging efficiency, a *Gigapack III* packaging extract was used with 1 µl (≈0.2 µg) of lambda control DNA.

SM buffer: 50 mM Tris-HCl (pH 7.5); 100 mM NaCl; 10 mM $MgSO_4.7H_2O$; 0.01% gelatine.

2.3.2.8. cDNA library amplification

Most *E. coli* strains contain the mcrA and mcrB restriction systems, which are responsible for digesting hemimethylated DNA. Therefore, an *E. coli* strain (XL1-Blue MRF') lacking this system was necessary to plate the *ZAP Express* cDNA library. Once the library is amplified using XL1-Blue MRF' cells, the DNA is no longer hemimethylated and can be grown on strains like XLOLR, that contain the mcrA and mcrB restriction systems.

After determining the titer of the primary library, aliquots containing ~$5x10^4$ p.f.u. were added to 600 µl of XL1-Blue MRF' cell suspension. For this purpose, XL1-Blue MRF' cells were grown in LB^{++} and harvested when A_{600} had reached 0.5-1.0. The cells were centrifuged at 500 *g* for 10 min, and resuspended in 10 mM $MgSO_4$ to a final A_{600} of 0.5. After phage infection, the samples were incubated at 37°C for 15 min, and 6.5 ml of melted Top Agarose NZY medium were added. The mixture was quickly distributed onto 150-mm NZY agar plates. After an incubation at 37°C for 12 hours, the phages were eluted by overlaying the agar plates with 10 ml of SM buffer and incubating overnight at 4°C with agitation. The phage containing SM buffer was recovered and the plates were rinsed with additional 2 ml of SM buffer. To kill *E. coli*, precipitate cell debris and prevent further library contamination, chloroform at a final 5% (v/v) concentration was added to the phage suspension in SM buffer, followed by incubation for 15 min at room temperature. The suspension was centrifuged for 10 min at 500 *g* and the supernatant recovered. For long-term storage, DMSO to a final 7% (v/v) was added to the phage suspension. The *P. pinaster* cDNA library was distributed in aliquots and stored at –80°C.

SM buffer: 50 mM Tris-HCl (pH 7.5); 100 mM NaCl; 10 mM $MgSO_4.7H_2O$; 0.01% gelatine.

2.3.2.9. Plating and titering the cDNA library

For platting the primary library, serial dilutions (10^{-2}-10^{-5}) of packaged reaction mixture was performed. Aliquots of 100 µl of each dilution were added to 200 µl of XL1-Blue MRF' cells. For this purpose, XL1-Blue MRF' cells were prepared as previously described (section 2.3.2.8.). The tubes were incubated at 37°C for 15 min, to

allow the adsorption of the phage particles to bacterial cell walls. Then, 3 ml of melted Top Agarose NZY medium supplemented with 15 µl of 0.5 M IPTG and 50 µl of X-gal (250 mg ml^{-1} in dimethylformamide) were added to each sample, and immediately poured onto NZY agar plates. After incubation at 37°C for 12 h, phage plaques were counted to determine the library's titer. Phagic plaques containing non-recombinant clones were stained in blue coloration.

To titer the amplified secondary library, 25 µl aliquots of dilutions 10^{-6}-10^{-11} were incubated with XL1-Blue MRF' cells under the conditions described for primary library, with the exception that Top Agarose NZY was not supplemented with IPTG and X-gal.

2.3.2.10. cDNA library screening

Amplified *P. pinaster* cDNA library was plated at a density of ~$5x10^4$ plaques in 150 mm NZY agar plates. The phage suspension was combined with 600 µl of XL1-Blue MRF' cells. For this purpose, XL1-Blue MRF' cells were prepared as previously described (section 2.3.2.8.).. The tubes were incubated at 37°C for 15 min, and 6.5 ml of melted Top Agarose NZY medium were added. The mixture was quickly distributed onto the NZY agar plates, incubated at 37°C for 12 hours and then transferred to 4ºC for 2h.

Phage particles were transferred from plaques to duplicate nylon filter discs (*Hybond-N+*; Amersham). The first disc was placed onto the agarized plaque for 2 minutes to allow the transfer of phage particles to the membrane. The replica disc was placed for 4 min to compensate for the smaller number of phage particles. Release of the phage DNA from the phage particled was promoted by incubating the membrane in denaturation solution for 2 min. Plaque lifts were then transferred to the neutralization solution for 5 min, rinsed in washing solution for 30 seconds and air dried on Whatman® 3MM paper. DNA was crosslinked to the membranes by UV light in a *Stratalinker® UV crosslinker* (Model 1800, Stratagene) using a autocrosslink setting (1200 mJ). Hybrization with a radiolabeled probe was identical to what is describe in section 2.3.8. Positive signals matching in both replicas were removed from the NZY agar plaque and resuspended in 500 µl of SM buffer containing 20 µl of chloroform. Tubes were vortexed. Lambda phages were re-plated at low density in 100 mm agar plaques, using for the purpose 200 µl of XL1-Blue MRF' cells and 3 ml of melted Top

Agarose NZY in the conditions previously described. For second screening *Hybond-N* (Amersham) nylon filter discs were used, but no duplicates were performed. Positive individualized clones were cored from the agar plates and resuspended in 500 µl of SM buffer containing 20 µl of chloroform and vortexed.

Denaturation solution: 1.5 M NaCl; 0.5 M NaOH.
Neutralization solution: 0.5 M Tris-HCl (pH 8.0); 1.5 M NaCl.
Washing solution: 0.2 M Tris-HCl (7.5); 2x SSC.
SM buffer: 50 mM Tris-HCl (pH 7.5); 100 mM NaCl; 10 mM $MgSO_4.7H_2O$; 0.01% gelatine.

2.3.2.11. In vivo *excision of recombinat pBK-CMV phagemids*

The excision *in vivo* of the pBK-CMV phagemid from the *ZAP Express* vector was initiated by combining 250 µl of the previously isolated single-clone λ phage solution, with 1 µl of *ExAssist* helper phage ($1x10^6$ pfu/µl) and 200 µl of XL1-Blue MRF' cells. These cells were prepared as previously described (section 2.3.2.8.) but were resuspended to a final A_{600} of 1.0. The mixture was incubated at 37°C for 15 min to permit phage attachment to the bacterial cell wall, and 3 ml of NZY medium were added. After growing overnight at 37ºC with agitation, the cultures were heated at 70°C for 20 min to inactivate the parent lambda phage and kill XL1-Blue MRF' cells. The samples were centrifuged at 1000 *g* for 15 min. The supernatant contained the recombinant pBK-CMV phagemid packaged in f1 phage particles, as well as the f1 helper phage.

To eliminate the helper phage, 25 µl of the supernatant were combined with 200 µl of XLOLR cells. These had been grown in NZY and resuspended in $MgSO_4$, as previously described for XL1-Blue MRF' cells. The mixture was incubated at 37°C for 15 min. After adding 300 µl of NZY broth, the samples were incubated at 37ºC for 45 min with agitation. LB-Kan plates were used to plate 25 µl of the cell suspension. Colonies containing the pBK-CMV phagemid were obtained after incubation of the cultures at 37ºC for 12 h.

2.3.2.12. Selection of cDNA clones of interest

To discard the false-positive clones among the putative positive cDNA clones obtained by cDNA library screening, the corresponding phagemids were isolated by the quick boiling miniprep method and digested with *EcoR* I and *Xho* I restriction

endonucleases. Digestion products were separated through a 1.2% (w/v) agarose gel electrophoresis and transferred to nylon membranes (*Hybond-N+*, Amersham) and hybridized with the same labelled probe used for library screening. The cDNA inserts of positive clones of interest were then sequenced.

2.3.3. DNA purification

2.3.3.1. Genomic DNA purification

Genomic DNA (gDNA) purification was performed using a modification of the method describe by (Doyle and Doyle 1990) and (Csaikl *et al.* 1998).

*P. pinaste*r material was ground in liquid nitrogen to fine powder with a mortar and a pestle. Approximately 1 g of fresh weigh was added to 10 ml of preheated (65ºC) extraction buffer. The mixture was incubated at 65ºC for 1 h with occasional swirling. After incubation, an extraction was performed, by adding 1 vol of chloroform-isoamyl alcohol (24:1 [v/v]) with gentle swirling. The samples were centrifuged at 7500 *g* for 5 min at 4°C, and the top aqueous phase recovered. After adding 2 ml of 5x CTAB solution, chloroform-isoamyl alcohol extraction was repeated in the same conditions.

To precipitate gDNA, the aqueous phase was added 0.7 vol of isopropanol with gentle swirling, and incubated at room temperature for 10 min. The DNA was recovered by centrifugation at 7500 *g* for 10 min at 4ºC and briefly washed with 70% (v/v) ethanol. The pellet was then resuspended in 250 µl of TE buffer containing 0.1 mg ml^{-1} RNase A and incubated for 30 min at 37ºC. After extraction with 1 vol of phenol-chloroform-isoamyl alcohol (25:24:1 [v/v/v]), the mixture was centrifuged at 7500 *g* for 5 min at 4ºC and the aqueous phase recovered.

Genomic DNA was precipitated by adding 2 vol of 96% (v/v) ethanol and 0.1 vol of 3 M NaAc (pH 5.2), followed by overnight incubation at 4ºC. The sample was centrifuged for 10 min at 7500 *g* and 4ºC. The pellet was briefly washed with 70% (v/v) ethanol and allowed to dry. Finally, the gDNA was resuspended in 100 µl of TE buffer and stored at 4ºC. An aliquot was removed for spectrophotometric quantification.

Extraction buffer: 2% (w/v) CTAB; 1.4 M NaCl; 100 mM Tris-HCl (pH 8.0); 20 mM EDTA (pH 8.0) Add 2% (w/v) polyvinylpolypyrrolidinone (PVPP, Sigma P-6755) and 2% (v/v) 2-mercaptoethanol prior to use.
5x CTAB solution: 5% (w/v) CTAB; 0.7 NaCl.
TE buffer: 50 mM Tris-HCl (pH 8.0); 10 mM EDTA (pH 8.0).

2.3.3.2. Plasmid isolation - quick boiling miniprep

For purifying small amounts of DNA, the boiling method (Holmes and Quigley 1981) was used. Bacteria were grown in appropriate culture medium, until end exponential phase was reached. An aliquot of 1.5 ml of the culture was removed and centrifuged at 8000 *g* for 5 min to collect the cells. The pellet was resuspended in 400 µl of STET supplemented with 25 µl of freshly prepared lysozyme solution. Lysis was promoted by incubation at room temperature for 10 min. followed by incubation at 95ºC for 1 min. Denaturated proteins and chromosomal DNA was removed by centrifugation at 14000 *g* for 15 min The supernatant was recovered and mixed with 300 µl of isopropanol to precipitate plasmid DNA. After centrifugation under the same conditions, the supernatant was discarded and the plasmid was resuspended in 20-100 µl of TE.

STET: 10 mM Tris-HCl (pH 8.0); 100 mM NaCl; 1 mM EDTA; 5% (v/v) Triton X-100.
Lysozyme solution: 10 mM Tris-HCl (pH 8.0); 10 mg ml^{-1} lysozime.
TE: 10 mM Tris-HCl (pH 8.0); 1 mM EDTA.

2.3.3.3. Plasmid purification - miniprep kit

Small scale isolation of high purity plasmid DNA was performed using the *QUIAGEN Plasmid Mini Kit* (Quiagen), according to the supplier's instructions. Bacteria were grown in appropriate culture medium, until end exponential phase was reached.

A 3 ml sample was centrifuged at 8000 *g* for 5 min to collect the cells. The bacterial pellet was resuspended in 300 µl of resuspension buffer and an equal volume of lysis buffer was added, followed by gentle mixing and incubation at room temperature for 5 min. The lysate was neutralized by the addition of 300 µl of neutralization buffer, followed by gentle mixing and incubation on ice for 5 min. Cell debris, denatured proteins and chromosomal DNA were removed by centrifugation at 14000 *g* for 10 min.

The supernatant was loaded onto a *Quiagen-tip 20* column (Quiagen), previously equilibrated with 1 ml of equilibration buffer. The column was washed with 4 x 1 ml of wash buffer and plasmid DNA was eluted by loading 800 µl of elution buffer. To precipitate plasmid DNA 0.7 vol. of isopropanol were added. After centrifugation at 8000 *g* for 15 min, the supernatant was discarded and the plasmid pellet briefly washed in 70% (v/v) ethanol. Plasmid DNA was resuspended in 20-50 µl of u.p. sterile water and stored at -20ºC.

Resuspension buffer: 50 mM Tris-HCl (pH 8.0); 10 mM EDTA; 100 µg ml^{-1} of RNase A.
Lysis buffer: 200 mM NaOH, 1% (w/v) SDS.
Neutralization buffer: 3.0 M KOAc (pH 5.5).
Equilibration buffer: 50 mM MOPS (pH 7.0); 750 mM NaCl; 15% (v/v) isopropanol; 0.15% (v/v) Triton X-100.
Wash buffer: 50 mM MOPS (pH 7.0); 1 M NaCl; 15% (v/v) isopropanol.
Elution buffer: 50 mM Tris-HCl (pH 8.5); 1.25 M NaCl; 15% (v/v) isopropanol.

2.3.3.4. Plasmid purification – midiprep kit

Medium scale isolation of high purity plasmid DNA was performed using the *Wizard™ Plus Midipreps DNA Purification System* (Promega), according to the supplier's instructions. Bacteria were grown in appropriate culture media until end exponential phase was reached.

The bacterial culture (100 ml) was centrifuged at 8000 *g* for 5 min. The cells were resuspended in 3 ml of resuspension buffer and an equal volume of lysis buffer was added, followed by gentle mixing and incubation until the cell suspension cleared. The lysate was neutralized by the addition of 3 ml of neutralization buffer, followed by gentle mixing. Cell debris were removed by centrifugation at 14000 *g* for 15 min at 4ºC.

The supernatant was combined with 10 ml of the *Wizard® Midiprep DNA Purification Resin* (Promega) and loaded onto the midicolumn. Vacuum was applied to the column to promote packaging of the resin and 2x15 ml of washing buffer were subsequently added. The midicolumn was placed inside a 1.5 ml microtube and centrifuged at 8000 *g* for 2 min to remove any residual wash buffer. The midicolumn was transferred to a new microtube and plasmid DNA was eluted by loading 300 µl of u.p. sterile water at 70ºC. After a 1 min incubation, the column was centrifuged at 8000 *g* for 20 sec to collect the eluted plasmid. The column was discarded and the

plasmid DNA solution was centrifuged at 8000 *g* for 5 min to precipitate column debris. The supernatant was stored at -20ºC.

Resuspension buffer: 50 mM Tris-HCl (pH 7.5); 10 mM EDTA; 100 μg ml^{-1} of RNase A.
Lysis buffer: 200 mM NaOH, 1% (w/v) SDS.
Neutralization buffer: 1.32 M KOAc (pH 4.8).
Washing buffer: 8.3 mM Tris-HCl (pH 7.5); 80 mM KOAc; 40 μM EDTA; 55% (v/v) ethanol.

2.3.3.5. cDNA purification from a phage library

The DNA from *P. pinaster* cDNA library was isolated by adding 1 vol of phenol-chloroform-isoamyl alcohol (25:24:1 [v/v/v]) to 1 ml phage suspension. The mixture was vortexed, centrifuged at 7500 *g*, for 5 min and the aqueous phase recovered. The DNA was precipitated, by adding 2 vol. of ethanol and 1/10 vol of 3 M NaAc (pH 5.2), and incubating the mixture at -20ºC for 4 h. The sample was centrifuged at 7500 *g*, for 10 min at 4ºC and the pellet resuspended in u.p. water and stored at -20ºC.

2.3.4. Spectrophotometric quantification of nucleic acids

Quantification of nucleic acids was performed spectrophotometrically by measuring the A_{260} of sample solution on a *Cary 1E UV-Vis Spectrophotometer* (Varian) using quartz cuvettes. For estimation of the nucleic concentration, it was considered that 1 A_{260} = 50 ng/μl DNA; 1 A_{260} = 40 ng/μl RNA. To determine the purity of the samples these the values of A_{230} and A_{280} were also determined (Sambrook *et al.* 1989; Krieg 1996).

2.3.5. Digestion with endonucleases

The digestion of DNA with restriction endonucleases was performed according to standard procedures (Sambrook *et al.* 1989; Ausubel *et al.* 1996) and to the supplier's instructions. Acetylated BSA (Stratagene) was used in both reaction volumes to stabilize endonuclease activity. Enzyme buffers were chosen according to standard

buffer efficiency tables supplied by the manufacturers. Reactions were performed at 37°C for 1.5 h to overnight, depending on experimental needs.

20 µl reaction: 2 µl enzyme buffer (10x); 2 µl BSA (5 mg ml^{-1}); x µl DNA; 0.5 µl restriction enzyme; complete with H_2O.
50 µl reaction: 5 µl enzyme buffer (10x); 5 µl BSA (5 mg ml^{-1}); x µl DNA; 1 µl restriction enzyme; complete with H_2O.

2.3.6. Nucleic acid electrophoretic separation

2.3.6.1. Agarose gel electrophoresis

DNA fragments were resolved by electrophoretic separation using horizontal slab gel apparatus. Agarose concentration (0.5% - 1.2%) was chosen depending of the fragment length range. Gels were made by melting agarose in 0.5x TBE, also used as running buffer. DNA samples, including molecular weight markers (*1 kb DNA Ladder*, Invitrogen) were mixed with 0.25 vol. of loading buffer and 1 µl of EtBr (1 mg ml^{-1}). Electrophoresis was carried out at 50-100 V, until the bromophenol blue dye had migrated two thirds the length of the gel.

10x TBE buffer: 0.89 M Tris; 0.89 M boric acid; 20 mM EDTA.
Loading buffer: 30% (w/v) Glicerol; 0.1 M EDTA; 0.25% (w/v) bromophenol blue.

2.3.6.2. Alkaline gel electrophoresis

An alkaline gel electrophoresis (McDonell *et al.* 1977) was used to determine the size range of the first and second cDNA synthesis controls, during the cDNA library construction. Electrophoresis was carried out in a horizontal gel system. An alkaline agarose gel was allowed to equilibrate for 3 h in running buffer. Samples of the radiolabelled first and second cDNA strands used for construction of the cDNA library and the molecular weight marker (*1 kb DNA Ladder*, Invitrogen) were mixed with 1 vol. of loading buffer and loaded onto the gel. Electrophoresis was carried out at 50 V for 5 h. The lane containing the *1 kb DNA Ladder* was separated from the remaining gel and stained using a 5 µg ml^{-1} EtBr solution in alkaline running buffer. The remaining gel was dehydrated using a vacuum gel dryer system (*Gel Dryer Model 583*, BIORAD) and analysed by autoradiography. DNA agarose gels were visualized under long wave UV

light (Transilluminator 2020E, Stratagene) and analyzed using the *Eagle Eye® II Still Video System* (Stratagene) through corresponding software (EagleSight™ 3.2, Stratagene).

Alkaline agarose gel: 1.4% (w/v) agarose; 30 mM NaOH; 2 mM EDTA.
Alkaline running buffer: 30 mM NaOH, 2 mM EDTA .
2x Loading buffer: 60 mM NaOH; 20 mM EDTA; 0.02% (w/v) bromophenol blue; 20% (v/v) glycerol.

2.3.6.3. Nondenaturing polyacrylamide gel electrophoresis

Nondenaturing polyacrylamide gel electrophoresis (Sambrook *et al.* 1989) was performed to determine the size of cDNA fragments collected after gel filtration fractioning, during the cDNA library construction. This procedure allowed the selection of the cDNA fractions containing cDNA with adequate size to be ligated to *ZAP Express*™. (section 2.3.2.).

A 5% (w/v) acrylamide/bisacrylamide vertical slab gel was prepared. Fractionated cDNA samples (8 µl) and the molecular weight marker (*1 kb DNA Ladder*, Invitrogen) were combined with 0.5 vol. of loading buffer and loaded onto the gel. Electrophoresis was carried out in 1x TBE running buffer at 100 V for 6 h. The lane containing the *1 kb DNA Ladder* was separated from the remaining gel and stained in a 5 µg ml^{-1} EtBr solution in 1x TBE. The remaining gel was fixated in 7% (v/v) acetic acid for 5 min, dehydrated using a vacuum gel dryer system (*Gel Dryer Model 583*, BIORAD) and analysed by autoradiography.

5% (w/v) Acrylamide/bisacrylamide gel: 5% (w/v) acrylamide/bisacrylamide; 1x TBE; 0.07% (w/v) ammonium persulfate; 0.035% (v/v) TEMED.
30% Acrylamide/bisacrylamide solution: 29% (w/v) acrylamide; 1 % (w/v) bisacrylamide.
10x TBE buffer: 0.89 M Tris; 0.89 M boric acid; 20 mM EDTA.
Loading buffer: 20% (w/v) Ficoll 400; 0.1 M EDTA; 0.25% (w/v) bromophenol blue.

2.3.6.4. Denaturing formaldehyde agarose gel electrophoresis

The electrophoretic separation of RNA was performed on a denaturing formaldehyde agarose gel to prevent the formation of secondary structures (Krieg 1996). Samples were added an equal volume of loading buffer and, when required for visualization, 1 µl of 1 mg $ml^{-1}$of EtBr. Denaturation was promoted by incubating samples at 65°C for 10 min, followed by cooling on ice. After loading samples into the gel, electrophoresis was carried out at 60 V until the dye front had migrated two-thirds

the length of the gel. EtBr-stained DNA agarose gels were rinsed several times in DEPC-treated water to remove formaldehyde, visualized under long wave UV light (Transilluminator 2020E, Stratagene) and analyzed using the *Eagle Eye® II Still Video System* (Stratagene) through corresponding software (EagleSight™ 3.2, Stratagene).

Agarose gel: 0.8% or 1,2% (w/v) agarose; 1× MOPS (pH 8.0); 6,7% (v/v) formaldehyde.
Loading buffer: 66% (v/v) formamide; 3% (v/v) formaldehyde; 0,1% (p/v) bromofenol blue; 1× MOPS (pH 7.0).
Running buffer: 1× MOPS (pH 7.0).
10x MOPS: 2 M MOPS; 0.5 M NaAc; 100 mM EDTA.

2.3.7. Nucleic acid blotting

2.3.7.1. Southern blotting

Transfer of DNA from agarose gels nylon membranes (*Hybond N^+*, Amersham) was performed by the capillary transfer method (Ausubel *et al.* 1996),

After electrophoresis, denaturation was promoted by rinsing the agarose gel in 0.4 M NaOH for 20 min. An apparatus was set up by placing a platform inside a reservoir that contained transfer solution (0.4 M NaOH). A sheet of Whatman® 3MM paper soaked in transfer solution was laid on the platform and in contact with the reservoir's transfer solution. The agarose gel was placed on the paper sheet. On top of the agarose gel and cut to gel size were successively layered: a nylon membrane; three sheets of Whatman® 3MM paper; paper towels to a thickness of 7 cm. Finally a small weight (0.6-1 Kg) was placed on top to promote capillary transfer of reservoir liquid to the absorbing paper towels. Capillary transfer was allowed to perform overnight. Nucleic acids were crosslinked to the membranes with UV light (120 mJ) on the *Stratalinker® UV crosslinker* (Model 1800, Stratagene).

2.3.7.2. Northern blotting

For Northern blot analysis, 20 μg of RNA were separated by denaturing formaldehyde agarose gel electrophoresis. The agarose gel was rinsed in DEPC-treated water (2 x 20 min) to remove formaldehyde, and equilibrated in 20x SSC for 30 min.

RNA was transferred to *Hybond-N*$^+$ nylon membranes (Amersham) by capillary transfer using a 20x SSC solution. An identical apparatus used for Southern blotting (section 2.3.7.1.) was mounted, but using 20x SSC as transfer solution. RNA was crosslinked to the filters by UV light, according to what was described in section 2.3.7.1.

20x SSC: 0.3 M Na citrate (pH 7.0); 3 M NaCl

.

2.3.7. Hybridization with ^{32}P-labelled DNA probes

2.3.7.1. Labelling of DNA probes

In the present work, DNA heterologous and homologous probes used for cDNA library screening and for hybridization after Southern or Northern blotting are listed in table 2.3.1.

Table 2.3.1. Plasmid inserts used for synthesis of ^{32}P-labeled probes used in this work

Insert	Acc. no.	Plasmid	Restrict. sites	Use
Zantedeschia aethiopica chlCu,Zn-Sod4	AF054151	pBK-CMV (Stratagene)	*Eco*R I; *Xho* I	cDNA library screening
Zantedeschia aethiopica Fe-Sod	AF094831	pBK-CMV (Stratagene)	*Eco*R I; *Xho* I	cDNA library screening
*Zantedeschia aethiopica csApx*1	AF053474	pBK-CMV (Stratagene)	*Eco*R I; *Xho* I	cDNA library screening
Digitalis lanata Pal	AJ002221	pBluescript SK (+/-) (Stratagene)	*Eco*R I; *Xho* I	Southern blot
Pinus pinaster genomic *Pal* fragment	-	pGEM-T Easy (Promega)	*Eco*R I	cDNA library screening
Picea mariana Chs1	AF227922	pCR2.1 (Invitrogen)	*Eco*R I	cDNA library screening
Pinus pinaster Fe-Sod1	AY536055	pGEM-T Easy (Promega)	*Eco*R I; *Xho* I	Northen blot
Pinus pinaster Apx1	AY485994	pGEM-T Easy (Promega)	*Eco*R I; *Xho* I	Northen blot
Pinus pinaster Pal1	AY321088	pGEM-T Easy (Promega)	*Eco*R I; *Xho* I	Northen blot
Pinus pinaster Chs1	AY168850	pGEM-T Easy (Promega)	*Eco*R I; *Xho* I	Northen blot
Pinus pinaster Chs2	AY168851	pGEM-T Easy (Promega)	*Eco*R I; *Xho* I	Northen blot
Pinus pinaster chlCu,Zn-Sod	AF434186	pGEM-T Easy (Promega)	*Eco*R I; *Xho* I	Northen blot

Plasmids containing DNA inserts to be used as probes were digested using restriction enzymes belonging to the corresponding polylinker sites.

Digestion products were separated through gel electrophoresis and the fragments of interest were recovered from the agarose gel using DEAE membranes, quantified spectrophotometrically and stored at -20ºC.

DNA fragments were ^{32}P-labeled by random oligonucleotide priming, using the *Rediprime II DNA labelling system* (Amersham) and [α-^{32}P] dCTP (*Redivue*, Amersham). Each DNA probe (100-200 ng) was diluted to a final volume of 45 µl in TE buffer, denaturated at 95°C for 5 min and cooled on ice for 5 min. The solution was then used to reconstitute the *Rediprime II* labelling mix, after which 5 µl of [α-^{32}P] dCTP (50 µCi) were added. Radioactive nucleotide incorporation was promoted by incubating the reaction mixture at 37°C for 1 h.

TE buffer: 10 mM Tris-HCl (pH 7.6); 1 mM EDTA.

2.3.7.2. Purification of ^{32}P-labeled DNA probes

Radiolabelled probes were purified from unincorporated nucleotides, by gel filtration trough a *Sephadex G-50* (Pharmacia) mini column (Sambrook *et al.* 1989). A sterile Pasteur pipette was partially blocked with a glass pearl and filled with the resin equilibrated in TE buffer. The column was washed with 3 ml of TE and the radiolabelled probe loaded. Size separation by gravity flow was promoted by loading into the column one 450 µl TEN fraction followed by twelve 150 µl TEN fractions. All fractions were successively collected in microcentrifuge tubes and evaluated for radioactivity with a mini-monitor (*Series 900*, Morgan). The first 4-5 fractions to present radioactivity were pooled.

TE buffer: 10 mM Tris-HCl (pH 7.6); 1 mM EDTA.
TEN buffer: 10 mM Tris-HCl (pH 7.6); 1 mM EDTA; 100 mM NaCl.

2.3.7.3. Hybridization and washings

Membrane filters were pre-hybridized in hybridization buffer at 42°C, for 3 h, in a hybridization oven (Amersham). The probe was heat denatured for 5 min, cooled on

ice and added to the hybridization buffer. Hybridization was allowed to proceed overnight at 42ºC, with shaking.

After hybridization, filters were successively washed for 20 min in the following solutions: 2x SSC, 0.1% SDS, at 45°C; 2x SSC, 0.1% SDS, at 50°C; 1x SSC, 0.1% SDS, at 50°C. For heterologous probes, the final washing step was 1x SSC, 0.1% SDS, at 55°C. For homologous probes, the final washing step was 0.5x SSC, 0.1% SDS, at 65°C.

Hybridization buffer: 50 mM sodium phosphate (pH 7.0), 0.9 M NaCl, 5 mM EDTA, 10x Denhardt reagent, 0.1% SDS, 250 μg ml^{-1} denatured salmon sperm DNA and 30% (v/v) formamide.(heterologous probe) or 50% (v/v) formamide (homologous probe)
50x Denhardt's Reagent: 5% (w/v) Ficoll 400; 5% (w/v) polyvinylpyrrolydone 360; 5% (w/v) BSA (fraction V).
20x SSC: 0.3 M Na citrate (pH 7.0); 3 M NaCl.

2.3.7.4. Autoradiography

Radioactive dried agarose gel and membrane filters were enveloped in plastic film and placed in cassetes (*Hypercassete*, Amersham) in direct contact with autoradiographic film (*BioMax MS*, Kodak; *BioMax MR*, Kodak; *Cronex ortho-S*, Sterling), within two intensifying screens (*Hyperscreen*, Amersham). Exposure was performed at –80°C for a suitable time (overnight to 1 month). The autoradiographic film was developed in a dark room by submerging in *X-ray Developer D-19* (Kodak) for up to 5 min. Development was stopped by rinsing in 3% (v/v) acetic acid stop solution and fixation was performed by submerging the film in *Rapid Fixer* (Ilford) for 5 min. After rinsing with running water for 5 min, the film was dried at room temperature.

2.3.8. DNA fragment recovery from agarose gels

2.3.8.1. DEAE membrane-based method

Recovery and purification of DNA fragments was performed using DEAE membranes (Dretzen *et al.* 1981). After electrophoresis, incisions were made on the

agarose gel, above and below the DNA fragment band of interest. Strips of DEAE membrane (*NA-45*, Schleicher & Schuell) were placed in the incisions. Membranes had been previously activated by soaking in 10 mM EDTA (pH 7.6) for 10 min, followed by soaking in 0.5 M NaOH for 5 min and extensive washing in u.p. sterile water. The eletrophoresis was then resumed until the DNA fragment reached the lower DEAE membrane. This membrane strip was removed from the gel and briefly washed in LSB to remove any agarose debris. The DNA fragment was recovered by incubating the membrane strip in 400 µl of HSB at 60°C for 1 h. The isolated fragment was further purified by performing a phenol/chloroform/IAA [25:24:1 (v/v/v)] extraction followed by an ethanol precipitation (2 vol. ethanol, 1/10 vol. 3M NaAc pH 5.2).

LSB: 20 mM Tris-HCl (pH 8.0); 0.15 M NaCl; 0.1 mM EDTA.
HSB: 20 mM Tris-HCl (pH 8.0); 1.0 M NaCl; 0.1 mM EDTA.

2.3.8.2. GFX DNA purification kit

Recovery of DNA from agarose gels was also performed using the *GFX PCR DNA and Gel Band Purification Kit* (Amersham). A maximum of 300 mg of agarose gel, containing the DNA band of interest, were sliced in small pieces and placed in a microcentrifuge tube. An equal volume (1 mg = 1 µl) of capture buffer was added. After vortexing vigorously, the mixture was incubated at 60ºC until the agarose gel was completely dissolved (~10 min). During the incubation, a GFX column was placed in a collection tube.

The sample was loaded onto the GFX column and incubated at room temperature for 1 min, followed by centrifugation at 8000 *g* for 30 sec. The flow-through was discarded by emptying the collection tube. The GFX column was placed back into the collection tube and 500 µl of washing buffer were loaded. After centrifugation at 8000 *g* for 30 sec the collection tube containing the washing buffer was discarded and the GFX column placed in a new microcentrifuge tube. DNA recovery was promoted by applying 50 µl of autoclaved u.p. water directly to the top of the glass fibber matrix in the GFX column. The sample was incubated at room temperature for 1 min and eluted by centrifugation at 8000 *g* for 1 min.

2.3.9. Amplification of DNA fragments by PCR

P. pinaster cDNA was used as template in a polymerase chain reaction (PCR) using degenerate primers. Degenerate primers were designed based on conserved gene regions, as determined by the multiple sequence alignment of homologous genes. Primer design obeyed several parameters as suggested by Griffin and Griffin (1994) and was performed with the assistance of specific software. Primers were 18-25 bases long and 3' ends contained G/C nucleotides to ensure correct annealing (G.C clamp). The G/C content was maintained between 45%-55%, and melting temperatures (T_m) between primer pairs were as similar as possible. Annealing sites between primer pairs were distanced between 200-700 bp. The extent of primer self-homology was minimized with the aid of software analysis. Redundancy in degenerate primers (combination of nucleotide sequences synthesized) was kept as low as possible, and always inferior to 512×. In order to minimize sequencing errors, primers were designed ~100 bp prior to the end of the template sequence. Primers were synthesized by Pharmacia and MWG.

Each 20 µl PCR reaction mixture contained 40 ng of cDNA, 1 µM of each primer, 200 µM of dNTP mix (Boehringer Mannheim), 2 mM $MgSO_4$ (Invitrogen) and 1x PCR buffer (Invitrogen). The enzymatic reaction was started by adding 0.5 µl of *Taq* polymerase (Invitrogen). PCR amplification was carried out on a *Mastercycler Gradient* (Eppendorf) with a gradient of 5 annealing temperatures. PCR steps were as follows: (1) denaturation for 5 min at 94°C; (2) 35 cycles of denaturation for 1 min, at 94°C, annealing for 1 min at 40.1ºC, 44.2ºC, 49.4ºC, 54.7ºC or 60.2ºC, polymerization for 1 min of at 72°C; (3) extension for 10 min at 72°C.

2.3.10. DNA sequencing

Plasmid inserts were sequenced by BigDye terminator chemistry (ABI Prism), using universal primers that flank the plasmid's polylinker. cDNA inserts in the pBK-CMV plasmid were sequenced in both directions using T3 and T7 primers. When required for obtaining full sequence, new specific primers were designed.

2.3.11. Cloning of PCR fragments into an expression vector

PCR fragments were separated by agarose gel electrophoresis and the fragments of interest recovered using the GFX DNA purification kit. DNA fragments were cloned onto the *pGEM-T Easy vector* (Promega), an expression vector suited to efficiently clone PCR products. pGEM-T vectors contain 3'-T overhangs at the insertion site that prevent recircularization of the vector and provide a compatible ligation site to PCR products obtained from A-tailing thermostable DNA polymerases such as *Taq* polymerase.

In 0.5 ml tubes, a 10 µl ligation reaction was set up using 5 µl of 2× *Rapid Ligation Buffer* (Promega), 1 µl of pGEM-T Easy vector (50 ng), 3 µl of purified PCR product and 1 µl of T4 DNA Ligase. The reaction was incubated overnight at 4ºC to maximize the number of transformants.

An aliquot of the ligation reaction (5 µl) was used to transform *E. coli* JM109 cells. Cells were transformed using the method described (section 2.3.13.) and plated onto selective LB-Amp plates containing X-gal and IPTG for recombinant selection.

2.3.12. Transformation of *E. coli* cells

E. coli JM109 competent cells were obtained by inoculating 250 ml of SOB medium with a single colony of *E. coli* JM109. Cells were grown at 18°C with vigorous shaking (200-250 rpm) until A_{600} = 0.6 was observed. The medium was placed on ice for 10 min and cells were collected by centrifugation at 2500 *g* for 10 min at 4ºC. The pellet was resuspended in 80 ml of ice-cold TB medium, and left on ice for 10 min. Cells were centrifuged for at 2500 *g* for 10 min at 4ºC, and gently resuspended in 20 ml of ice-cold TB medium. DMSO to a final concentration of 7% (v/v) was carefully added. The preparation was left on ice for 10 minutes and distributed in 200 µl aliquots. Competent cells were immediately place in liquid nitrogen and stored at -80°C.

Transformation of *E. coli* cells was initiated by thawing competent cells at room temperature and immediately placing them on ice. The DNA sample (1-20 µl) was added to 200 µl of competent cells by gentle mixing, and the mixture were incubated at

4°C for 30 minutes. Cells were heat-shocked by incubation at 42°C for 30 s with agitation, followed by 10 min on ice. After addition of 0.8 ml of SOC medium and incubation for 1 hour at 37°C with vigorous shaking (200-250 rpm), cells were spinned down for a few seconds at 10000 *g* and the pellet resuspended in 50 µl of the supernatant. Finally, cells were transferred to selective plates containing X-gal and IPTG, and grow overnight at 37°C.

TB: 10 mM Pipes; 15 mM $CaCl_2$; 250 mM KCl; 55 mM $MnCl_2$. Mix all components except $MnCl_2$ and adjust pH to 6.7 with KOH. Dissolve $MnCl_2$ and sterilize solution through a 0.45 µm filter.
SOC: 2% (w/v) Tryptone peptone; 0.5% Yeast extract; 2.5 mM KCl; 10 mM NaCl; 10 mM $MgSO_4$; 10 mM $MgCl_2$; 20 mM glucose.
SOB: Identical to SOC but deprived of glucose.

2.3.13. Bioinformatics

2.3.13.1. Sequence analysis

Nucleotide and amino acid sequence editing and analysis were performed using the *Lasergene* suit of sequence analysis software from DNASTAR. Within the software package, *EditSeq* was used to edit, translate and back-translate sequences, locate ORFs, as well as create base-files for the remaining softwares. *MegAlign* produced multiple sequence alignments and less robust phylogenetic trees. *Protean* served in predicting protean physico-chemical properties and *SeqMan II* was used to manage and order contigs.

2.3.13.2. NCBI Tools and GenBank Database

All nucleotide sequences isolated from the *P. pinaster* cDNA library, as well as the corresponding amino acid sequences, were submitted to the GenBank Database at NCBI (URL no. 6). Database search for specific nucleotide and protean sequences was performed using Entrez (URL no. 7). The database search for highly similar sequences was carried out using the BLAST algorithm (URL no. 8) (Altschul *et al.* 1997)

2.3.13.3. Construction of phylogenetic trees

Unrooted phylogenetic trees, based on the alignment of selected sequences, were constructed using the PHYLIP software suit (URL no. 9) (Felsenstein 1989). Multiple sequence alignment was carried out using the Clustal algorithm (Jeanmougin *et al.* 1998). The ClustalW server at GenomeNet (URL no. 10) was used to produce a PHYLIP sequence alignment input file.

From the models of phylogenetic inference provided in the PHYLIP software package, maximum likelihood (Doyle and Gaut 2000) proved the most adequate to resolve phylogenetic relationships between maritime pine accessions and the remaining selected sequences, and was used through the PROML and DNAML softwares to calculate phylogenetic distances between protein and nucleotide sequences, respectively. Unrooted trees were plotted using PHYLIP's DrawTree software.

2.3.13.4. Protein targeting prediction

Prediction of the final subcellular localization of proteins, based on their amino acidic sequence, was carried out using TargetP (URL no. 11) (Emanuelsson *et al.* 2000) and further confirmed using PSORT (URL no. 12) (Nakai and Kanehisa 1992).

Chapter 3

Pinus pinaster RNA isolation and cDNA library construction

3.1. Isolation of *P. pinaster* RNA

Adapted from:

Azevedo H, Lino-Neto T, Tavares RM. 2003. An improved method for high-quality RNA isolation from needles of adult maritime pine trees. *Plant Molecular Biology Reporter* 21(4):333-338.

3.1.1. Introduction

Isolation of intact, high-quality RNA from conifers, suitable for gene isolation with RT-PCR, cDNA library construction, and gene expression studies, is difficult because of the high levels of phenolics, polysaccharides, and endogenous RNases. Phenolics are readily oxidized to form covalently linked quinones and easily bind nucleic acids (Loomis 1974). In addition to phenolics and other secondary metabolites, polysaccharide contamination hinders resuspension of precipitated RNA, interferes with absorbance-based quantification, and may inhibit enzymatic manipulations, poly(A)-RNA isolation, and electrophoretic migration (Wilkins and Smart 1996). Endogenous ribonucleases may also drastically reduce the integrity of RNA, particularly when their amount is increased, such as during senescence, wounding, and pathogen attack (Logemann *et al.* 1987; López-Gómes and Gómes-Lim 1992; Green 1994). To overcome these problems, specific protocols for the isolation of RNA from pine embryos and seedlings have been developed (Chang *et al.* 1993; Xu *et al.* 1997; Claros and Cánovas 1998; Avila and Cánovas 2000). However, few methods for RNA isolation from adult pine needles are available.

We established a protocol that can produce high-purity and high-integrity RNA from needles of 30-year-old maritime pine trees and from 2-month-old seedlings (section 2.3.1.). The procedure is suitable for reverse transcription and cDNA library

construction. This protocol is easily adaptable for the isolation of quality RNA from *P. pinaster* suspension cells.

3.1.2. Results and discussion

Standard methods for RNA isolation, including the hot-borate method (Wilkins and Smart 1996) and the CTAB/NaCl method (Chang *et al.* 1993), have been applied in the isolation of RNA from 30-year-old *P. pinaster* needles. Both protocols failed to yield high-quality RNA for downstream enzymatic procedures, such as RT-PCR or cDNA synthesis, mainly because of RNA degradation and contamination by polysaccharides. We devised a new method for isolating RNA from adult maritime pine needles using a high concentration of proteinase K combined with prolonged 42°C incubation for enzymatic digestion of ribonucleases. The inclusion of proteinase K is critical for obtaining intact RNA (figure 3.1.1.). When proteinase K was not added to

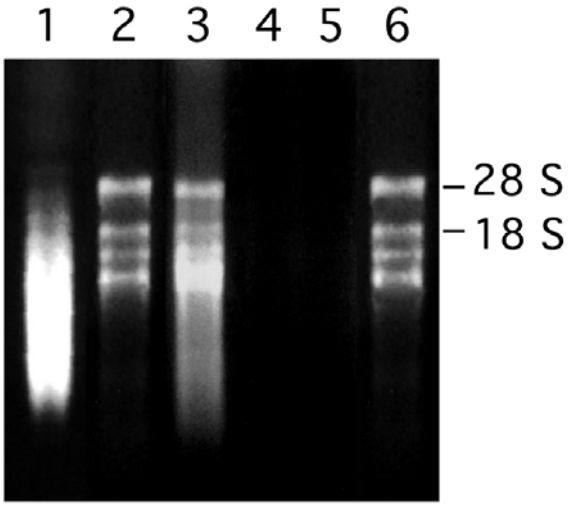

Figure 3.1.1. Electrophoretic analysis of *Pinus pinaster* RNA isolated by using different extraction procedures. Total RNA preparations (5 µg) were analyzed on 0.8% formaldehyde-denaturing agarose gel stained with ethidium bromide. RNA from needles of 30-year-old pine trees was isolated by using the described protocol without the addition of proteinase K (1) or in the presence of proteinase K at a ratio of FW to extraction buffer of 1.3 g/15 ml (2), 2 g/15 ml (3), 2.6 g/15 ml (4), and 3.3 g/15 ml (5). RNA from seedlings was isolated in the presence of proteinase K at a ratio of FW to extraction buffer of 1.3 g/15 ml (6).

the extraction buffer, the integrity of isolated RNA was extremely low. Even in the presence of proteinase K, the integrity of RNA highly depends on the ratio of the amount of plant material (FW) to the volume of extraction buffer, being significantly reduced as the amount of starting material increases (figure 3.1.1., lanes 2-5). In addition to high integrity, RNA isolated from this method also had high purity, as judged by the A_{260}/A_{230} and A_{260}/A_{280} ratios, which indicated low polysaccharide levels and reduced protein contamination, respectively (table 3.1.1.). To verify the applicability of this method, 2-month-old seedlings were used, and high-quality RNA was obtained (figure 3.1.1., lane 6). The RNA yield of 143 $\mu g.g^{-1}$ FW obtained using this protocol for adult *P. pinaster* needles is lower than that obtained for seedlings (table 3.1.1.) but is higher than that referred by Chang *et al.* (1993) for 5-year-old loblolly pine needles.

Table 3.1.1. Purity and yield of the two isolation methods used for isolating RNA from *Pinus pinaster* needles.

Method	Plant Material	A_{260}/A_{230}	A_{260}/A_{280}	RNA Yield, µg/g FW
Chang *et al.* (1993)	Needles from adult trees	1.73 ± 0.06	1.94 ± 0.05	113 ± 12
Current method	Needles from adult trees	2.12 ± 0.09	2.07 ± 0.14	143 ± 20
Current method	Needles from seedlings	2.14 ± 0.03	1.92 ± 0.10	340 ± 17

To evaluate the suitability of isolated RNA in downstream enzymatic procedures, RNA prepared from adult pine needles was used for cDNA library preparation. Biomagnetic separation with beads coupled to oligo(dT) was used to isolate poly(A)-RNA from RNA, with a mRNA yield of 34 µg/mg total RNA. After synthesizing the first and second cDNA strands, the bulk of radioactive cDNA fragments lay between 1 kb and 3 kb, which indicated that the cDNA synthesis was effective and that high-quality mRNA was used as starting material. After size fractionation on a *Sepharose CL-2B* gel filtration column, the longer cDNA fragments were used for cloning in the *ZAP Express* vector (Stratagene). An efficiency of 3.5×10^5 p.f.u./µg of packaged cDNA library was obtained, from which recombinant clones comprised about 96%, as determined by color selection with IPTG and X-gal. As a

result, after cDNA library preparation, a total number of 4.5×10^6 recombinant clones were obtained, which can be considered as a good representational primary library size.

Because the high quality of a cDNA library depends not only on the number of clones but also on the size of their inserts, the cloning efficiency of long cDNAs was evaluated by determining the insert size from 33 randomly chosen clones. The analyzed recombinant clones had inserts with an average size of about 2 kb and a modal size of 1-1.5 kb (figure 3.2.6.). This indicates that the cDNA library prepared from the RNA isolated by means of the described protocol fulfils two key characteristics of a high-quality cDNA library: (1) it is large enough to contain representatives of all genes being expressed, and (2) it has a reduced number of clones containing small cDNA inserts (<10% of random clones contained cDNA inserts <1 kb), increasing the probability of finding full-length cDNAs.

The method described is an efficient, simple, and reproducible procedure for the isolation of RNA from needles of adult maritime pine trees. The isolated RNA is of high quality and could serve as a robust template for reverse transcription, as indicated by the construction of a good-quality cDNA library. By using a high concentration of proteinase K combined with prolonged 42°C incubation, enzymatic digestion of ribonucleases can occur, avoiding the need for phenol extraction to denature and partition proteins and thereby inhibiting RNases. Because phenol extraction can damage poly(A)-RNA, the devised method becomes more suitable when isolated RNA is to be used for RT-PCR or for synthesis of cDNA libraries.

3.2. Construction of a *P. pinaster* cDNA library

3.2.1. Introduction

3.2.1.1. cDNA and gDNA libraries

One of the most frequent methods for searching and cloning genes of interest is the construction of genomic DNA (gDNA) libraries. These libraries consist of digested gDNA fragments (normally 20 Kbp long) that are inserted on an appropriate vector. To guarantee a fully representative library, the number of clones which are required are proportional to the genome size. This means that plant gDNA libraries must be considerably larger than their bacterial or fungal counterparts (Brown 1995).

Another versatile tool is the cDNA library, which is constructed by reverse transcribing mRNA. Due to the presence in pluricellular organisms of tissue differentiation and extensive cellular specialization, not all of the genetic information is simultaneously translated at a given moment or physiological condition. Therefore, cDNA libraries allow the cloning of integral gene coding regions, which are being translated in cells of a given tissue or organ, at a given moment, or as a consequence of an imposed experimental situation.

When searching for genes of interest, there are several advantages of using a cDNA library over a genomic library. First, the number of clones required per screening is significantly smaller. This is particularly relevant given the large *P. pinaster* genome,

which sizes 25,000–30,000 Mb 1C (Wakayima *et al.* 1993) and has a large low copy fraction (Chagné *et al.* 2003). Secondly, a cDNA clone contains the complete intron-free coding sequence of a specific gene. As a consequence the aminoacidic sequence is directly deducible, and the cDNA can immediately serve as a homologous probe in northern blot experiments. Finally, gDNA clones are extremely large (10-40 Kbp) when compared to cDNA clones (1.5-3 Kbp). As a result, sequencing becomes time consuming, requiring a costly chromosome–walking approach, or clone digestion with further subcloning. Nonetheless, gDNA libraries can be advantageous given the fact that they contain the whole gene pool of a species and allow the identification of promoter and regulatory regions.

As an initial strategy to isolate *P. pinaster* genes we chose to construct a cDNA library. RNA was isolated from leaf tissue of adult pine trees because of the higher diversity in gene transcripts. This permitted the isolation of genes involved in metabolic processes as different as primary, secondary and ROS scavenging metabolism. The clones were fundamental in performing expression profiles of genes of interest

3.2.1.2. Construction of a cDNA library

In the past most cDNA libraries were constructed using plasmid vectors, which were maintained in independently transformed bacterial colonies. These were stored at -80ºC and amplified whenever required (Sambrook *et al.* 1989). Amongst other problems, these libraries presented low viability and limited re-screening capability. With the advancement of DNA technology (high efficiency cDNA synthesis, linkers, methylases, adapters and packaging mixtures), it was possible to take advantage of the bacteriophage λ to create more resourceful libraries. The benefits include a 100-fold increase in packaging efficiency and the possibility to store and amplify libraries almost indefinitely without loss in viability (Short *et al.* 1988). The use of lytic phages allowed for DNA fragments of heterogeneous dimensions to be inserted with equal efficiency, and also circumvented the potential cytotoxic effect of insert translation products in bacteria (Alting-Mees *et al.* 1992).

The *P. pinaster* cDNA was inserted into the *ZAP Express cloning vector* (Strategene) (figure 3.2.1.). *ZAP Express* can accommodate up to 12 Kbp DNA inserts and has twelve unique cloning sites. These include the *Eco*R I and *Xho* I restriction

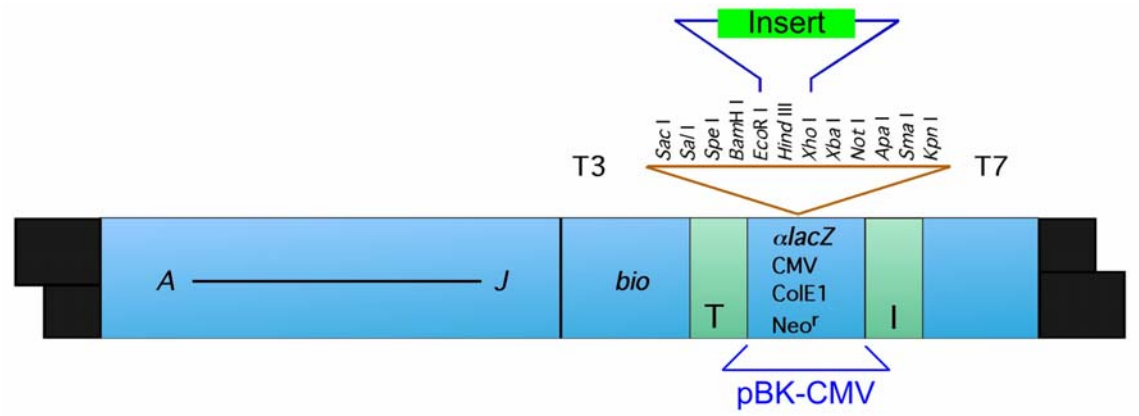

Figure 3.2.1. Map of the *ZAP Express* cloning vector. Bacteriophage-f1-derived sequences T and I flank the pBK-CMV plasmid, in which cDNA clones are inserted.

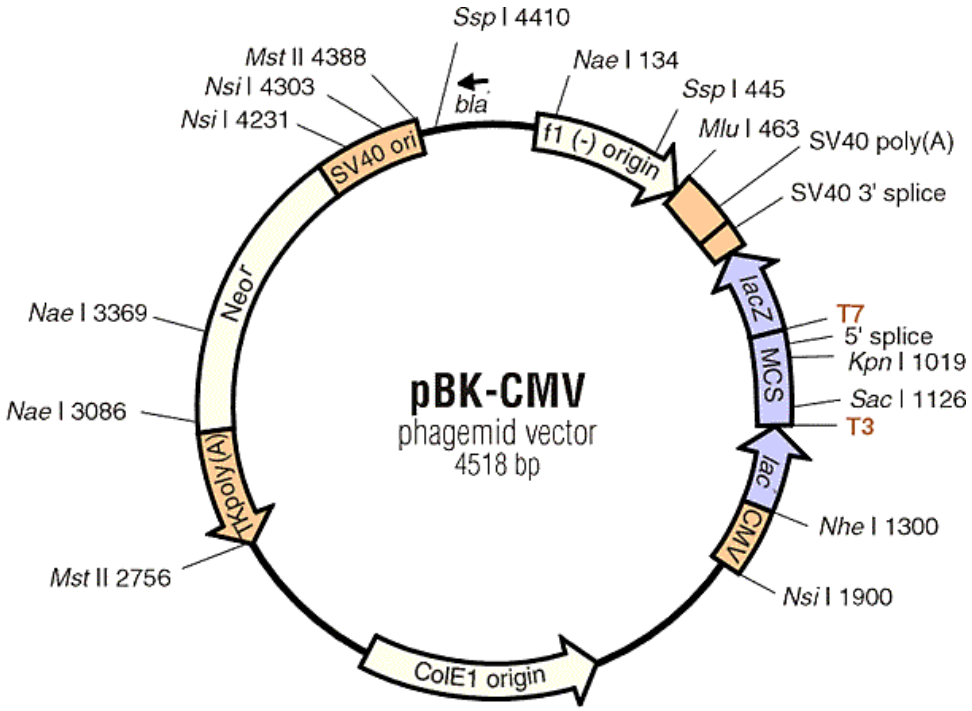

Figure 3.2.2. Map of the pBK-CM vector. The 4518 bp phagemid results from the *in vivo* excision of the *ZAP Express* vector. The plasmid contains three origins of replication: phagic f1(-) origin (2-462 bp); prokaryotic ColE1 origin (2759-1896 bp); eukaryotic SV40 origin (4393-4036 bp). Expression is possible in eukaryotes through the CMV promoter upstream of the MCS, and the SV40 terminator downstream. In prokaryotes expression is induced by the β-galactosidase promoter (P_{lac}). Selection of recombinant plasmids is possible due to the *lacZ* gene (1183-810 bp) immediately downstream of the MCS.

sites, which are used to ligate cDNA inserts in a vector-oriented manner. This system belongs to a generation of vectors that simplify recovery and manipulation of cDNA inserts (Alting-Mees *et al.* 1992; Short and Sorge 1992). The *ZAP Express* contains bacteriophage-f1-derived sequences flanking a phagemid vector: pBK-CMV. As a consequence, cloned inserts can be easily excised out of the phage in the form of the kanamycin-resistant pBK-CMV phagemid (figure 3.2.2.). The polylinker is flanked by T3 and T7 promoters and has three standardized primer sites for DNA sequencing. Heterologous expression is facilitated in pBK-CMV by the presence of both prokaryotic and eukaryotic origins of replication, promoters and terminators, as well as neomycin and kanamycin-resistance genes (Alting-Mees *et al.* 1992).

3.2.2. Results and Discussion

3.2.2.1. mRNA purification and cDNA synthesis

RNA is mostly composed of rRNA (75%). Depending on the cell type and physiological conditions, mRNA can constitute 1-5% of the total RNA pool (Speirs and Longhurst 1993; Wilkins and Smart 1996). As a consequence, isolation of this fraction from rRNA and tRNA considerably enhances the efficiency of first-strand cDNA synthesis.

Quality mRNA was purified using magnetic bead technology (Dynabeads®), consisting of extremely small polystyrene beads (0.5 μm), incorporated with a Fe_2O_3 core, which grants them paramagnetic properties (Cunningham 1992). Beads could now be instantly recovered using a magneto. The procedure makes use of the poly(A)-tail of eukaryotic mRNA: up to 300 adenosine residues, present at the 3'-end of the molecule. The poly(A)-tail can specifically hybridize oligo$(dT)_{25}$-molecules covalently attached to magnetic beads (Hornes and Korsnes 1990; Bosnes *et al.* 1997), each bead containing approximately $9x10^5$ oligo$(dT)_{25}$ sequences. All RNA molecules lacking a poly(A)-tail will not hybridise and can be readily washed off.

RNA from adult leaves of *P. pinaster* was extracted and checked for purity and integrity. A total of 375 μg were used for mRNA isolation. The elution step resulted in the recovery of 9.18 μg of RNA for an expected 10 μg according to the supplier's

instructions. A second elution allowed the recovery of 40% more RNA (3.75 μg). Approximately 5 μg of *P. pinaster* mRNA were used to initiate the construction of the cDNA library.

Synthesis of the first cDNA strand was performed by reverse transcribing the mRNA, resulting in a hybrid double stranded RNA/DNA molecule. Polymerization was performed using a *Xho* I linker-primer containing a GAGA sequence, the *Xho* I restriction site and an oligo(dT) sequence that hybridized to the mRNA's poly(A)-tail. As a positive control to the first synthesis, 1.8 Kbp test RNA was used. A parallel first synthesis reaction was performed in the presence of [α-^{32}P]dATP, to permit the autoradiographic detection of first synthesis efficiency (figure 3.2.3.).

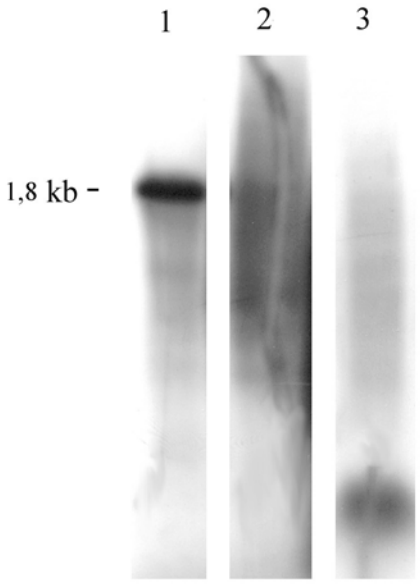

Figure 3.2.3. Autoradiography of the alkaline agarose gel separation of first and second strand cDNA. (1) Control reaction of first strand synthesis from test 1.8 Kb RNA. (2) First strand synthesis. (3) Second strand synthesis.

Synthesis of the second cDNA strand was performed by digesting the RNA strand and using the resulting fragments as primers for DNA polymerase. Second strand synthesis already included [α-^{32}P]dATP which meant that a parallel reaction was unnecessary. Following the creation of blunt ends by incubation with *Pfu* DNA polymerase, *Eco*R I adapters were ligated to both ends of the cDNA molecules. A subsequent digestion of the cDNA with *Xho* I led to the release of a low

molecular weight fragment, containing one *Eco*R I adapter and the GAGA sequence of the linker-primer. Fractionation was then required to separate these fragments from the cDNA molecules. At this point an aliquot was removed to test the efficiency of the second strand synthesis and the subsequent reactions (figure 3.2.3.). Electrophoretic separation was performed on an alkaline gel that promoted double chain denaturation and eliminated secondary structures.

Results indicate that synthesis of first strand cDNA occurred when using both the *P. pinaster* and the test RNA-poly(A) (figure 3.2.3.). The integrity of the 1.8 Kbp band indicates that no nucleic acid degradation occurred during the first synthesis reaction and the electrophoretic separation. *P. pinaster* cDNA fragments were averagely sized around 1.5 kbp. This is a good indicator as to the quality of the RNA extraction, mRNA isolation and cDNA synthesis steps. Intensity differences between first and second cDNA strands are explained by the different ratios of radiolabelled nucleotides that were incorporated in both reactions (10-20 fold difference according to the supplier). Lane 3 also revealed an intense spot of low molecular weight fragments, which are the result of *Xho I* digestion. These ascertain the efficiency of the blunting, ligation and digestion reactions.

3.2.2.2. cDNA fractioning and packaging

Double-stranded cDNA was size fractionated by gel filtration chromatography in a *Sepharose CL-2B* column. This allowed the separation of high molecular weigh cDNA from *Xho* I digestion products, *Eco*R I adapters, oligo(dT) linker-primers and residual nucleotides. Fractions were analyzed for their radioactive strength using a scintillation counter (*Tri-Carb® 2200CA*, Packard). The results showed the presence of two peaks of radioactivity (figure 3.2.4.). The first peak (fractions 4-7) contained cDNA and a second much stronger peak (fractions 9-14) contained low molecular weight fragments and mainly unincorporated nucleotides.

The length of cDNA molecules contained in fractions 3-9 was determined by non-denaturing polyacrylamide gel electrophoresis (figure 3.2.5.). Fractions containing low molecular weight cDNA fragments were discarded, since they increase the proportion of incomplete ORFs in the library.

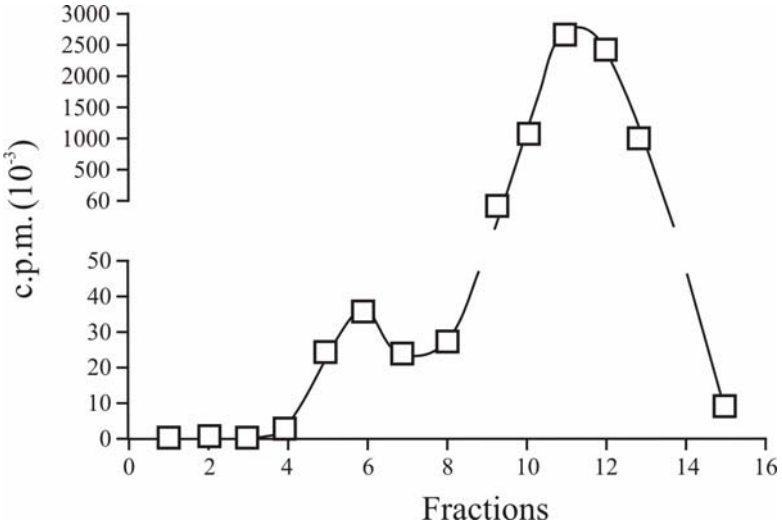

Figure 3.2.4. Radioactivity quantification after size fractionation of the *P. pinaster* cDNA by gel filtration cromatography.

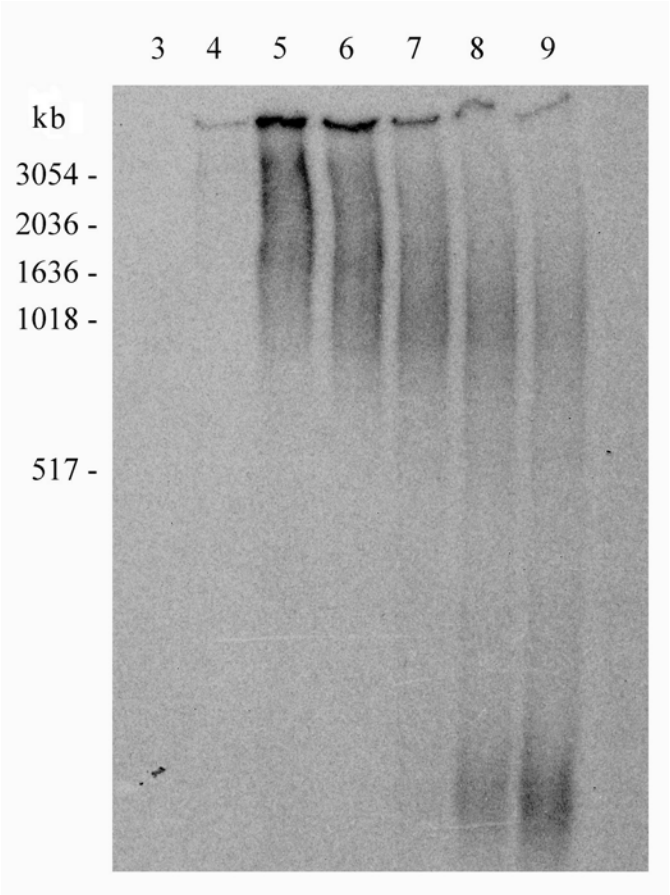

Figure 3.2.5. Non-denaturing polyacrylamide gel electrophoresis of fractions 3-9, obtained by gel filtration column cromatography of *P. pinaster* cDNA.

Results demonstrated the efficiency of size fractioning and revealed that fractions 5 and 6 were enriched with 1-5 kbp fragments. These fractions were selected for insertion onto the *ZAP Express*™ vector. The samples were mixed and digested with *Eco*R I, to permit the ligation of the cDNA fragments to the expression vector in an *Eco*R I (5')-*Xho* I (3') orientated manner. An aliquot of the reaction was then removed to perform a first packaging of clones into the λ phage, while the remaining solution was stored at -80ºC. The phage solution was titrated in *E. coli* biofilms in order to determine the representativity of the library and the packaging efficiency. The bacterial growing medium contained X-gal and IPTG, to allow determining of the recombination efficiency. A positive control was performed using the pBR322 plasmid. Results for both reactions are presented in table 3.2.1.

Table 3.2.1. Library titer and recombination and packaging efficiencies, for packaging *P. pinaster* clones and pBR322 into the λ fage.

	Library titer (p.f.u./µl)	**DNA ammount (ng)**	**Recombination efficiency (%)**	**Packaging efficiency (p.f.u./µg DNA)**
P. pinaster	3.2×10^3	100	96	$3{,}5 \times 10^5$
pBR322	3.7×10^3	400	100	$3{,}27 \times 10^5$

The observed 96% recombination efficiency was well into the standard values advanced by the supplier (91-99%). This data evidenced the efficiency of all reactions previously performed on cDNA fragments, namely the ligation of *Eco*R I adapters, fosforilation of 5' ends and digestion with *Xho* I. As expected, the recombination efficiency of the purified plasmid pBR322 was 100%. The packaging efficiency of *P. pinaster* clones was identical to that of pBR322, even though the control reaction had 4 times more DNA. The first packaging library had a titer of 3.2×10^3 p.f.u/µl. Taking into account the total reaction volume and the recombination efficiency, the library contained ~1.6×10^6 *P. pinaster* cDNA clones. Even though a cDNA library is considered as being representative of the genome when it contains 1×10^6 independent clones, and taking into account the *P. pinaster* genome size, a second packaging was performed. Both packaging reactions were combined into a primary library, which was titrated, resulting in a total number of ~4.5×10^6 independent clones.

The primary library was amplified, as is recommended for phage stabilization. Amplification was performed by growing plaques from individual phages in an *E. coli* biofilm. The resulting secondary library presented a titer of 1×10^9 p.f.u. ml^{-1} in a total volume of ~400 ml, and was stored at -80ºC being ready to use. Considering the final size of the library, the possibility of phage reamplification and of repackaging stored cDNA clones, the use capability of the *P. pinaster* cDNA library is almost unlimited.

To once more ascertain the quality of the *P. pinaster* cDNA library, 33 randomly picked clones were removed from the *ZAP Express* vector by *in vivo* excision. The end-product of excision was the phagemid pBK-CMV, which contained the cDNA fragment inserted into the multiple cloning site. pBK-CMV was digested with *Xho* I and *Eco*R I and the resulting fragments were analysed on an agarose gel (not shown). Insert length was determined using a molecular weight marker. The results of the frequency distribution of the insert length for all 33 clones are depicted in figure 3.2.6.

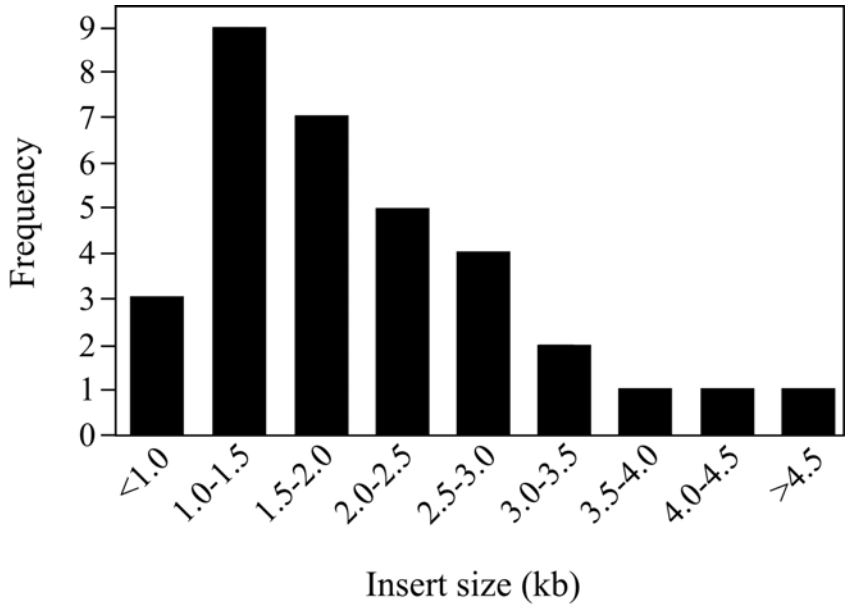

Fig 3.2.6. Frequency distribution of the insert length of 33 *P. pinaster* cDNA clones, randomly isolated from the cDNA library.

Insert length ranges between 0.7-6.4 kb, of which 50% can be found in the interval 1.3-2.2 kbp, suggesting that most of the clones in the *P. pinaster* library are within the size range for what has been considered a good cDNA library (Sambrook *et al.* 1989).

Chapter 4

Establishment and characterization of *Pinus pinaster* suspension cell cultures

4. Establishment and characterization of *Pinus pinaster* suspension cell cultures

4.1. Introduction

Cell suspension cultures are advantageous in the study of multiple aspects of plant physiology and molecular biology, given that in a simplified unicellular system, cells respond in a concerted way, minimizing variability (Eshita *et al.* 2000). Cell suspensions also possess increased accessibility and provide a fully controllable environment to carry out experimentation (McCabe and Leaver 2000). This aspect becomes most relevant when investigating tree species, due to the inherent limitations of the plant material. Despite some reservations that should be maintained when extrapolating results to a multicellular level, the applicability of this model system has been well supported (Butland *et al.* 1998; Chiron *et al.* 2000; Cooney *et al.* 2000; Fornalè *et al.* 2002).

Forest research has focused mainly on species such as *Populus* sp. and the gymnosperms *Pinus sylvestris* and *Picea abies*. Despite the relevance of *P. pinaster* as a forest species, tool development and fundamental studies remain scarce.

Studies on plant nutrition focus mostly on nitrogen since it is the most required nutrient and is generally associated with growth limitations (Warren and Adams 2002). Carbon and nitrogen are two essential components of the primary metabolism of cell suspensions, and the interaction between these nutrients is a valuable tool to decipher

cell culture behaviour (Durzan 1976). Nonetheless, although nitrogen is a common limiting factor for tree growth, the effect of nitrogen supplementation on growth and metabolism is poorly understood in woody plants, particularly in what concerns gymnosperms (Suarez *et al.* 2002). In suspension cells, nitrogen nutrition is also of extreme significance, since the amount and particularly the nitrogen source can dramatically affect the cell's morphology, totipotency and growth rate (Thorpe 1980).

Growth conditions for establishment of suspension cell cultures have already been proposed for several gymnosperms (Jelaska 1987) despite the recalcitrant nature of these species. Even though, work with conifer species is scarce when compared to the remaining superior plants, gymnosperm cell suspensions have been successfully used in many studies addressing the biochemistry and molecular biology of primary (Ishii and Teasdale 1997) and secondary metabolism (Heerden *et al.* 1996; Butland *et al.* 1998; Fornalè *et al.* 2002), biotic stress (Popp *et al.* 1996; Hotter 1997; Cooney *et al.* 2000) and abiotic stress (Chiron *et al.* 2000). More often, suspension cell cultures are the first step in the establishment of plant regeneration systems (Tang and Ouyang 1999; Ingram and Mavituna 2000). For *P. pinaster* only *calli* cultures were previously established (Jelaska 1987), and no report of suspension cultures was published to our knowledge. In addition, no extensive characterization of nutrient uptake kinetics of major nutrients has been reported in suspension cultures of *Pinus sp.*, resulting in a lack of insight into the behavior of *Pinus* cells in culture.

Here, the establishment of stable suspension cultures of *Pinus pinaster* cells in MS-based medium is reported. The cultures were analysed for biomass, cell viability, pH, and consumption of the main nutrients (sugars, phosphate, nitrate and ammonium). In addition, nitrate consumption was also determined when cells were grown in a ammonium-free medium. Since death phase was achieved after phosphate and sugar exhaustion from the medium, and as programmed cell death (PCD) can be triggered during nutrient starvation (Moriyasu and Ohsumi 1996; Singh et al. 2003), the occurrence of PCD was evaluated in phosphate- and sugar-starved pine cells.

4.2. Results and Discussion

4.2.1. Establishment of P. pinaster *suspension cell cultures*

P. pinaster suspension cell cultures were obtained from *calli* tissue grown in agarized medium. To initially establish *calli* cultures, different nutrient based media and different hormonal supplementations were tested, using hypocotyl and root segments of seedlings as starting material (figure 4.1.-A). *P. pinaster callus* had been previously established in MS medium (Murashige and Skoog 1962) supplemented with 5 mg ml^{-1} 2,4-D and 0.5 mg ml^{-1} Kin, originated from root segments and trunk tissue of adult trees (Jelaska 1987). The need for high concentrations of auxin seemed to be a requirement for *callus* establishment in *Pinus* species (Jelaska 1987). However, *calli* failed to be induced in this medium, or when the same hormonal supplementation was used in B5 medium (Gamborg *et al.* 1968). *Calli* were slightly induced when hormone levels were switched to 1 $mg.ml^{-1}$ NAA and 0,5 $mg.ml^{-1}$ Kin in both B5 and MS mediums, with better results in B5. Effective *P. pinaster calli* production was obtained from root segments in a modified MS medium supplemented with 2 mg ml^{-1} 2,4-D and 1 mg ml^{-1} BA (Lange *et al.* 1994) (figure 4.1.-B). The auxin concentration was considerably lower than that previously reported for *P. pinaster calli* (Jelaska 1987). *Calli* were obtained after 3-4 weeks, presenting a white to cream coloration and moderate friability (figure 4.1.-B). Cultures were steadily maintained by subculturing to fresh medium every 8 to 12 weeks, after which rapid browning and necrosis occurred.

Maritime pine suspension cell cultures (figure 4.1.-C,D) was initiated transferring friable callus from agarized medium to liquid medium of identical composition, in a stepwise process, keeping a minimal cell concentration to allow the culture to surpass lag phase. Suspended cells were approximately isodiametric and highly vacuolated (figure 4.1.-D), showing moderate tendency for aggregation (figures 4.1.-C,D).

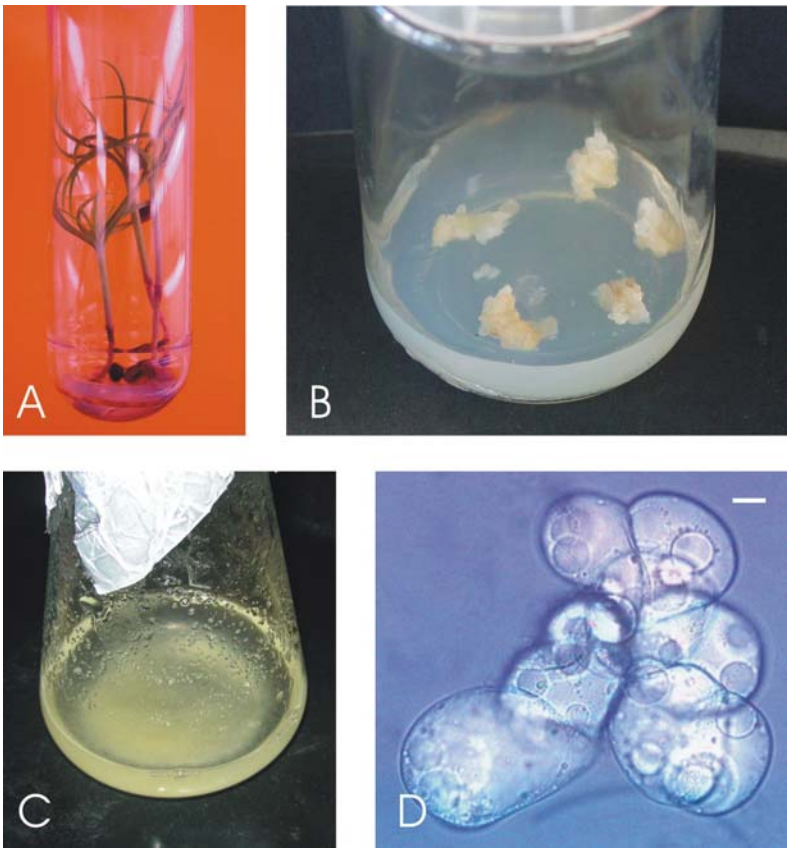

Figure 4.1. Establishment of *P. pinaster* suspension cultures. **A** – 1-month old sterile seedlings were used for *calli* induction. **B** – *calli* was induced in culture flasks using root segments as explant. **C** – suspension cell cultures were obtained by *calli* transfer to liquid medium. **D** – suspended cells are approximately isodiametric, showing moderate tendency for aggregation. In figure D, bar indicates 10 μm.

4.2.2. Analysis on P. pinaster *suspended cells growth*

In batch cultures, growth tends to occur according to a sigmoid curve (King *et al.* 1973). After inoculation, a lag phase is ususally observed, reflecting an adaptation period of the cells to the new medium, when strong biosynthetic activity occurs (Wilson 1971). New *P. pinaster* suspension cultures were initiated by transferring cells growing at the end of the exponential phase (12-14 days) to new medium. According to results depicted in figure 4.2.-A, no lag phase was apparently observed. This observation was also described in *Fragaria ananassa* (Zhang *et al.* 1998) and *Symphytum officinale* (Shimon-Kerner *et al.* 2000) suspension cell cultures. A continuous exponential phase

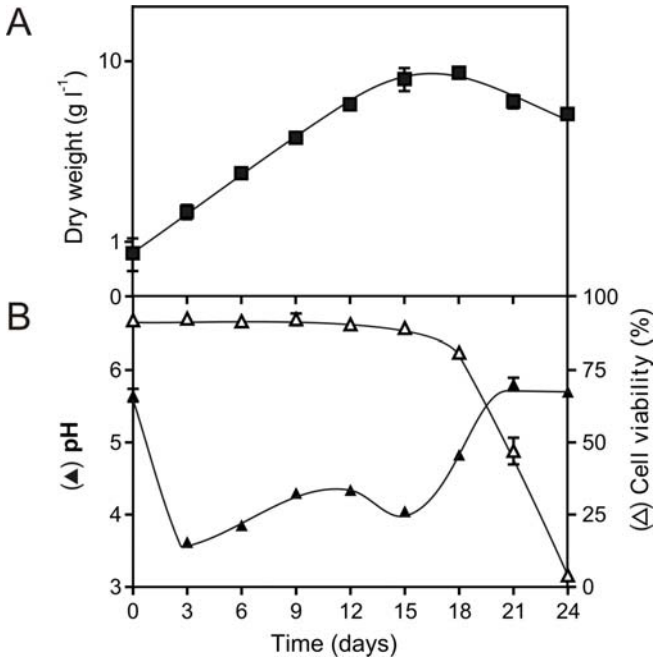

Figure 4.2. Dry weight (**A**), pH and cell viability (**B**) in suspension cultures of *P. pinaster* grown in MSPS medium with 3% sucrose.

should derive from a strong acclimatization to the medium and the absence of significant modifications in nutrient availability with every subculturing (Zhang *et al.* 1998). In *P. pinaster* suspension cultures, growth was kept nearly exponential for a period of 15 days, reaching a maximum of biomass production at day 18 (figure 4.2.-A). During this period, a maximum growth rate (μ) of 0.18 d^{-1} was observed. This corresponds to a cell duplication time of approximately 4 days, which is slightly lower than the 5-day period observed in *Hypericum androsaemum* (Dias 2000). However, it is not as fast as the duplication periods observed in *Fragaria ananassa* (2.5 days) (Zhang *et al.* 1998) and tobacco (less than a day) (Kato and Nagai 1979).

Cell viability of *P. pinaster* cultures remained constant (~92%) up to day 15 (figure 4.2.-B). After day 18, a pronounced decline in cell viability was observed, becoming 50% of the initial value by day 21. These results suggest that the stationary phase was extremely short, as cell death rapidly followed exponential growth phase. These results do not agree with those reported by (Fornalè *et al.* 2002), that suggest that despite the decrease in cell division during the stationary phase, cell viability should remain high, if not superior to the exponential phase

During the growth of *P. pinaster* suspension cell cultures, changes in pH of the medium were observed (figure 4.2.-B). Accordingly, at the third day of the culture pH had decreased from 5.7 to 3.5. This observation has been described for other cell

cultures (Srinivasan *et al.* 1995; Mühlbach 1998; Dias 2000). These authors suggested that the decrease of pH resulted from loss in cell viability, due to the release of cell content. The results obtained for *P. pinaster* suspensions are inconsistent with this hypothesis, since the decrease of pH is not accompanied by loss in cell viability (figure 4.2.-B). It was shown that cells will grow efficiently within a wide range of initial pH (4.0-7.0) and will tend to shift pH to their optimal levels by the end of the culture (Butenko *et al.* 1984) It was also shown that the regulation of intracellular pH, which is tightly kept within a 6.5-7.5 range, begins to fail below extracellular levels of 4.5 (Smith 1984; Torimitsu *et al.* 1984), due to the increased net influx of H^+ that leads to acidification of the cytoplasm. In *P. pinaster* cells, this steep decrease did not affect biomass production, as growth was kept near exponential from the start of the culture. It is suggested that the decrease in pH value of the medium should result from an immediate response of pine suspension cells to the newly established growth conditions. After pH reduction, a steady increase in pH was observed throughout the exponential phase, until a 4.2 value was observed around day 9 (figures 4.2.-B). This should be considered the optimal pH for *P. pinaster* cells under these growth conditions, since cell cultures tend to the optimal pH value in the course of the cycle (Hahlbroc and Kuhlen 1972).

4.2.3. Analysis on sugar consumption

In *P. pinaster* suspension cell cultures, sucrose (3%) was used as the sole energy and carbon source, since it was successfully used in other *Pinus sp.* suspension cultures (Heerden *et al.* 1996; Hotter 1997; Fornalè *et al.* 2002). Sucrose has been frequently considered the best carbon and energy source, since the utilization of other sources usually results in lesser growth (Thompson and Thorpe 1987). Additionally, growth rates do not seem to be affected by sucrose concentrations ranging between 2-5% (Matsumoto *et al.* 1971). The use of lower amounts of sugar would have resulted in less biomass accumulation, and increasing the concentration to 4-5% sucrose may not result in significant gains in biomass production (Grey *et al.* 1987).

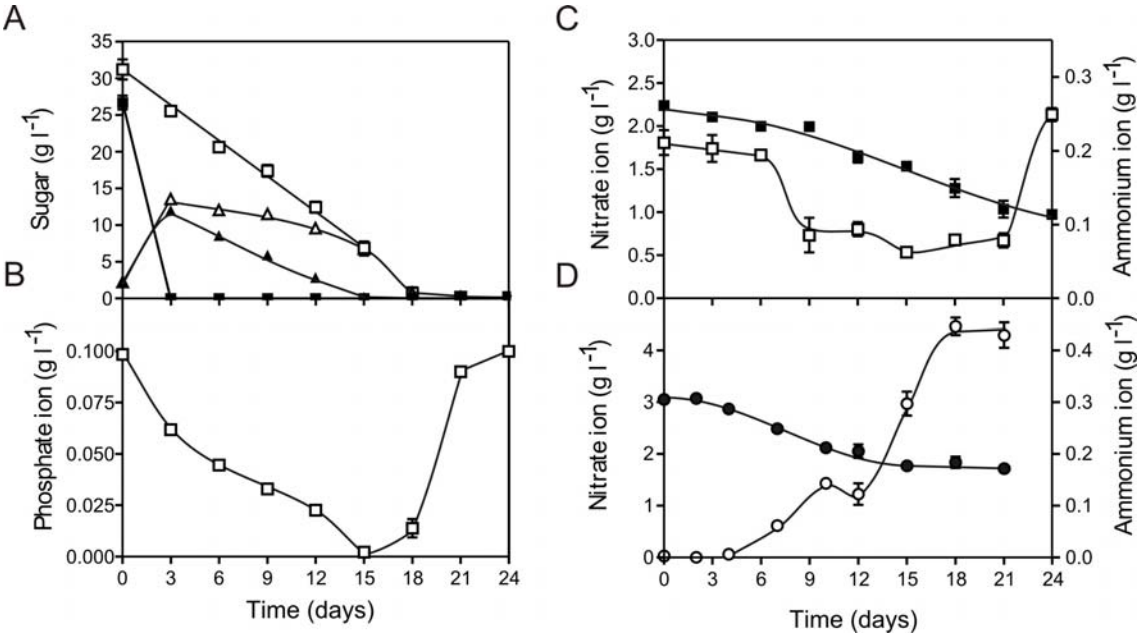

Figure 4.3. Kinetics of nutrient uptake by *P. pinaster* suspended cells. **A** – sugar concentration: total sugar (□), sucrose (■), glucose (▲) and fructose (Δ). **B** – phosphate concentration. **C** – concentration of nitrate (■) and ammonium (□). **D** – concentration of nitrate (●) and ammonium (○) in an ammonium-free medium.

Sugar consumption in *P. pinaster* suspension cell cultures is depicted in figure 4.3-A. At day 0, residual amounts of glucose and fructose were detected, resulting from the hydrolysis of sucrose induced by the autoclaving procedure. Results shown that sucrose is rapidly hydrolyzed into glucose and fructose, which can be explained by the action of extracellular invertases (Masuda *et al.* 1988).

During the exponential phase of pine suspension cell cultures, glucose and fructose were progressively consumed, with preference for glucose (figure 4.3.-A). This behaviour was also referred for other species (Ilieva and Pavlov 1997; Krook *et al.* 2000; Oliveira *et al.* 2002). The phosphorylation reaction in glycolysis has been pointed as the limiting step for hexose utilization at high sugar concentrations (Krook *et al.* 2000). Fructokinase is responsible for the highly specific phosphorylation of fructose into fructose-6-phosphate (F-6-P). Glucose is converted into glucose-6-phosphate by hexokinase, which is also capable of generating F-6-P only with less affinity (Doehlert 1989). Krook and co-workers (2000) showed that in *Daucus carota* suspensions cells, different affinities of hexose phosphorylating enzymes for fructose and glucose were also involved in the preferable consumption of glucose.

In *P. pinaster* suspension cell cultures, growth was near exponential as depicted by the specific growth rate (figure 4.4.-A). A low yet steady decrease in μ values was observed, ranging from 0.18 d^{-1}, at the beginning of the experiment, to 0.14 d^{-1}, at day 12. This behaviour is characteristic of a batch culture where growth conditions differ along time, and might reflect the experimental procedure, since a small volume for sampling was removed systematically. After day 12, μ decreased considerably, resulting in a very short stationary phase (between days 15-18) and a rapid transition to death phase, being 0 at day 18. At day 15, corresponding to the end of the growth phase, total glucose depletion from the medium was observed but 0.8% fructose was still present (figure 4.3.-A). At day 18, fructose was still residually present in the medium but cell death was already underway, suggesting that sugar depletion is not involved in growth arrest.

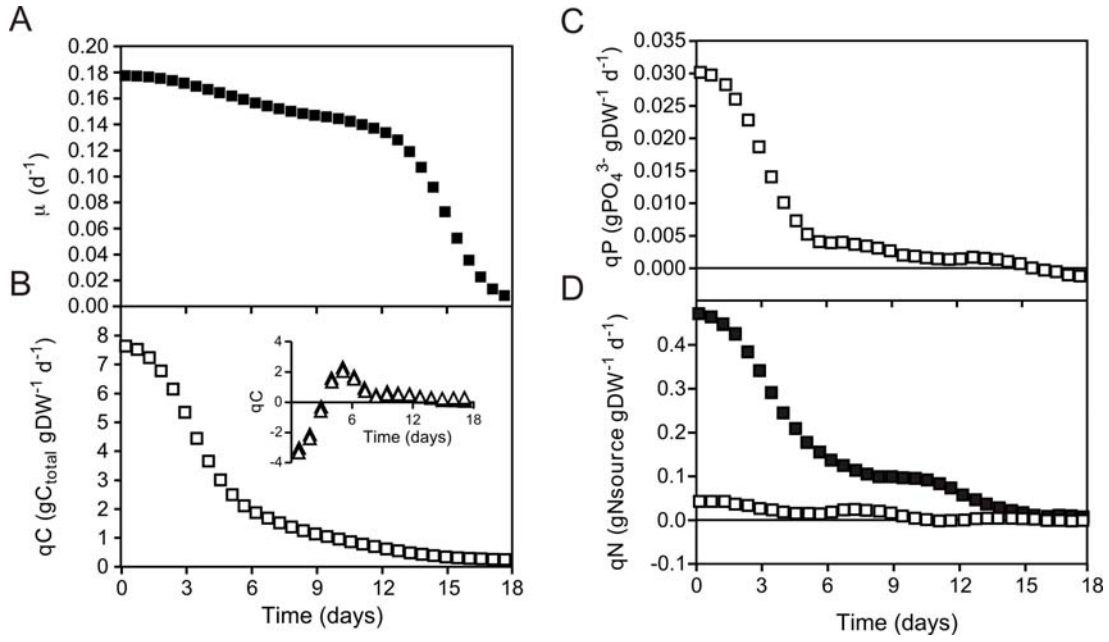

Figure 4.4. Variation of the specific growth rates (μ) and nutrient consumptionr rates (q), during the exponential and stationary phases of growth of *P. pinaster* suspended cells. **A** – specific growth rate. **B** – sugar consumption rate for total sugar (□), glucose (*insert*; ▲) and fructose (*insert*; Δ). **C** - phosphate consumption rate. **D** – consumption rates of nitrate (■) and ammonium (□).

4.2.4. Analysis on phosphate consumption

Phosphate in the medium should be consumed in a descending sigmoid curve, accompanying the upward growth curve (Dias 2000). The results depicted in figures 4.3.-B and 4.4 –C suggest that consumption of phosphate was fast, with a maximum qP level of 0.03 $gPO_4^{3-}g\ DW^{-1}\ d^{-1}$ at the beginning of the culture. As a consequence, by day 15 all phosphate was depleted from the medium. This coincides with the end of the near exponential phase, the subsequent loss of cell viability, and is prior to complete glucose exhaustion from medium (figure 4.1.3.-A). At day 24, when cell viability reached 0, soluble phosphate levels were restored to their initial values (figure 4.3.-B). Cell suspensions of different species growing in MS medium have caused phosphate depletion prior to growth arrest. Such is the case of *Saponaria officinalis*, with depletion at day 9 of a 14 day growing period (Morard *et al.* 1998) or even within day 4 of a 10 day growing period in *Fragaria ananassa* (Zhang *et al.* 1998). In both situations phosphate starvation had no effect on growth arrest, witch could only be observed after sugar depletion. Still, *S. officinalis* suspension cells presented higher biomass accumulation when grown in the phosphate reinforced MH2 medium rather than the MS based MSA medium (Morard *et al.* 1998). A similar behaviour was observed in *Ginkgo biloba* cells (Carrier *et al.* 1990). In light of this, the present results are insufficient to ascertain a definite role of phosphate depletion on growth arrest.

4.2.5. Analysis on nitrate and ammonium consumptions

Nitrate (NO_3^-) and ammonium (NH_4^+) ions are the most common nitrogen sources in cell suspension media composition, even though it has been shown that suspended cells can adapt to other nitrogen sources (*e.g.* urea, casein hydrolysate and α-aminobutyric acid) (Leustek and Lee 1987). When isolatedly used, both NO_3^- and NH_4^+ tend to be insufficient as a nitrogen source, especially NH_4^+ in the case of gymnosperms (Leustek and Lee 1987). NH_4^+ in high concentrations can inhibit secondary metabolism, also requiring tricarboxylic cycle acids supplementation (Zhao *et al.* 2001). In *Pinus strobus, callus* growth is inhibited by the use of NH_4^+ due to its toxicity (Kaul and Hoffman 1993), resulting in quick browning. Still, it has been shown that the addition of even small amounts of NH_4^+ to media containing solely NO_3^- can increase growth (Sargent and King 1974; Rose and Martin 1975). Moreover, the NO_3^-/NH_4^+ ratio can have dramatic effects on secondary metabolite productivity (Zhao *et al.*

2001). Conifer forests are characterized by low pH soils with reduced nitrification capability, which leads to NH_4^+ being the main nitrogen source available (Suarez *et al.* 2002). This has led to the development of mycorrizal associations that increase nitrogen uptake efficiency (Suarez *et al.* 2002). In conifer trees, and contrary to herbaceous species, this has also led to a preferable uptake of NH_4^+ over NO_3^- (Bedell *et al.* 1999).

In medium used for growing *P. pinaster* suspended cells, initial NO_3^- levels were almost 10-fold higher that those of NH_4^+ (figure 4.3.-C), and a preference for NO_3^- consumption was observed (figure 4.4.-D). NO_3^- was steadily depleted from the medium (figure 4.3.-C) during growth, and qN was always higher for NO_3^-, with a maximum of 0.48 gNO_3^- g DW^{-1} d^{-1} at the beginning of the culture (figure 4.4.-D).

When *P. pinaster* suspended cells were subcultured to medium containing solely NO_3^- (figure 4.3.-D), accumulation of NH_4^+ was observed in the medium, starting at day 3, when pH had dropped to 3.5 (figure 4.2.-B) and reaching a maximum value at day 18. Leakage of NH_4^+ at low pH levels has been previously reported (Martin and Rose 1976). In both experimental situations (figure 4.3-C,D), the final levels of NH_4^+ surpassed the initial ones, were as NO_3^- levels were substantially reduced. These results not only support the preferable consumption of nitrate, but suggest a net flow towards metabolization of nitrogen. The present observations can be explained by the nutrient balance in the medium. In *Pinus*, nitrogen:phosphate ratios of 12:1 to 14:1 are associated with better growth and nutrient balance (Lebourgeois *et al.* 1997). For *P. pinaster* suspension cultures, the ratio is 24:1. It was shown that in *P. pinaster*, high nitrogen availability, low phosphate supply or imbalance between nitrogen and other nutrients can lead to nitrogen accumulation either in the form of N-rich amino-acids or NH_4^+ (Warren and Adams 2002). In addition, the incapability to efficiently metabolize NH_4^+ seems to be common in the *Pinus* genus (Flaig and Mohr 1992; Kaul and Hoffman 1993).

The analysis on nutrient uptake rates indicates that qC, qN and qP possess a similar biphasic profile (figure 4.4.). Meanwhile, μ levels are nearly constant. Until day 6, the nutrient uptake capability per biomass produced is significantly higher than that observed from day 6 to day 15. The initial 6 day period might allow maritime pine suspension cells to satisfy the nutrient and energetic requirements of maintaining exponential growth from the beginning of the culture while meeting the demands of adaptability to the new medium, which usually result in growth delay at the beginning of the culture (lag phase).

4.2.6. Evidences for programmed cell death in sugar-starved P. pinaster *cells*

Results were uncertain as to the preponderance of sugar and phosphate depletions in determining growth arrest. Moreover, growth arrest was immediately followed by a pronounced death curve, which suggests the involvement of programmed cell death events at the end of the culture. Therefore, *P. pinaster* suspended cells were transferred to several media combining phosphate and sugar supplementations, and analysed for biomass levels, for the concentration of phosphate in the medium and for the activity of the PCD marker enzyme acid phosphatase (APase) (figure 4.5.). Results for biomass levels (figure 4.5.-A) showed that biomass loss was observed in cultures where sugar was removed from medium. Compared to P^+S^+, P^-S^+ only accounted for a partial growth inhibition. The simultaneous removal of phosphate and sugar had a synergistic effect that resulted in a more rapid loss of biomass. These results suggest that sugar is the sole responsible for the loss of biomass observed in maritime pine suspensions at the end of the culture (figure 4.2.-A). Previously, it was shown that

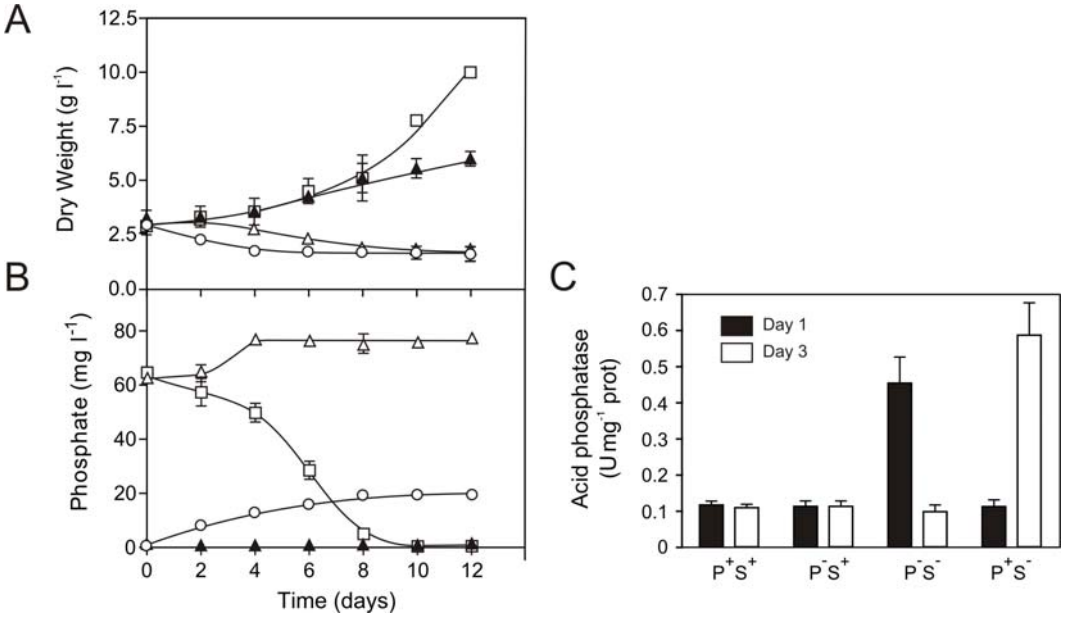

Figure 4.5. Effect of phosphate and sugar starvation on *P. pinaster* suspended cells. Cells were harvested during exponential growth phase and transferred to identical medium without either phosphate [P^-S^+ (▲)], or sucrose [P^+S^- (Δ)], or both [P^-S^- (○)]. As a control, cells were transferred to identical medium containing both phosphate and sucrose [P^+S^+ (□)]. **A** - biomass. **B** - phosphate content. **C** – acid phosphatase activity was determined at days 1 and 3 after subculture.

biomass loss was accompanied by an increase in soluble phosphate in the cellular medium (figure 4.3.-B). The determination of phosphate concentrations in the medium (figure 4.5.-B) completely corroborate the previous results (figure 4.5.-A) and suggest that biomass loss is accompanied by the release of phosphate. Moreover, final phosphate levels were higher than the initial amounts, which suggests that death by sugar starvation is accompanied by the mobilization of phosphate, a process that is characteristic of PCD events, in which nutrient recovery is favoured (reviewed by Lino-Neto 2001).

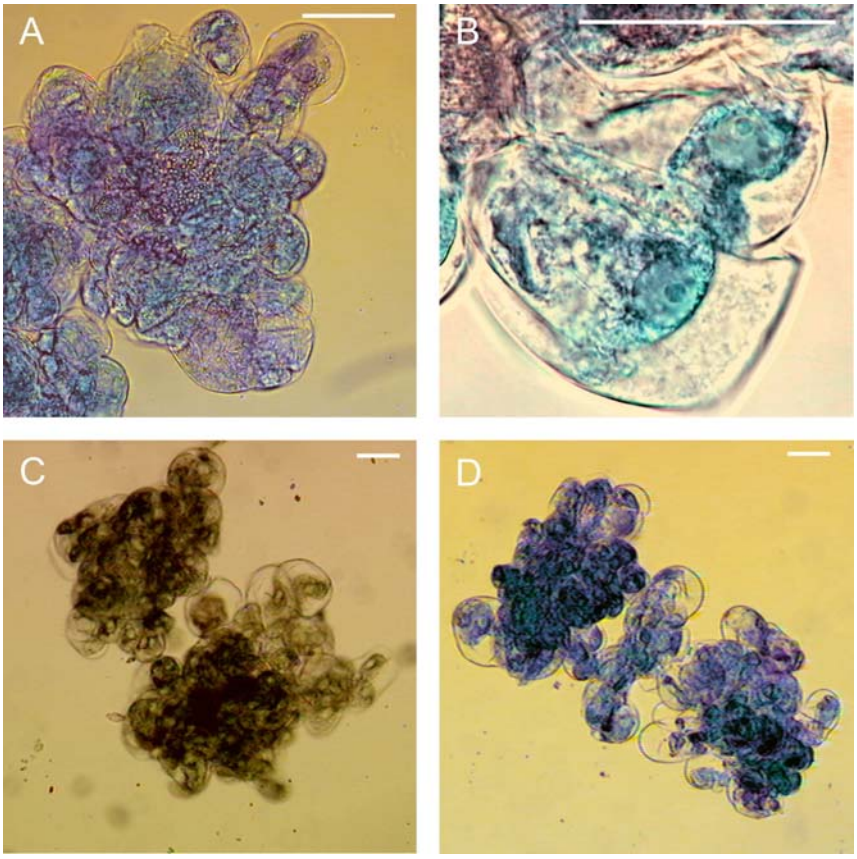

Figure 4.6. Cytochemical localization of acid phosphatase activity in sugar- and/or phosphate-starved *P. pinaster* suspended cells. **A,B** - cells grown in $P^{+}S^{-}$ medium for three days. C – cells grown in $P^{-}S^{+}$medium for three days. **D** – cells grown in $P^{-}S^{-}$ medium for one day.

Analysis on the activity of acid phosphatase during sugar and phosphate depletion (figure 4.5.-C) evidenced that an increase in APase activity was only observed in cells cultivated in sugar-free medium. Cells grown in P^-S^- evidenced a four fold increase in APase activity at day 1, decreasing for control levels at day 3, while cells grown in P^+S^- evidenced increased APase activity at day 3. These results are in accordance with those shown in figures 4.1.5.-A,B, and corroborate the hypothesis that sugar-deplition is responsible for the induction of cell death, and phosphate-starvation is strictly responsible for a synergistic effect in death induction by sugar-starvation.

The activity of acid phosphatase was also determined by cytochemical analysis under light microscopy (figure 4.6.). Results for specific blue staining resulting from APase activity were only observed in sugar-starved cells, and are in accordance with previous results (figure 4.5.)

DNA cleavage, detected by TUNEL assay, was used as a definite marker for the presence of programmed cell death by nutrient depletion (figure 4.7.). DNA cleavage occurs in the early stages of PCD and results from the endonuclease attack of internucleosomal linker regions between nucleossomes, with the subsequent creation of ~200 bp gDNA fragments (Yen and Yang 1998). As expected, pine cells grown in P^+S^+ medium did not exhibit TUNEL staining after 5 days in culture P^+S^+ (figure 4.7.-A). Moreover, P^-S^+ cells where also incapable of evidencing DNA cleavage, even after 5 days of phosphate depletion (figure 4.7.-B). Cells did not present evidence of PCD when placed in P^+S^- medium for 1 day (figure 4.7.-C), which is consistent with the evidence that biomass loss and phosphate leakage only occurred within two days of starvation (figure 4.5.-A,B). Therefore intense nuclei labelling by TUNEL was observed in these cells after three days of sugar deprival (figure 4.7.-D), when the death process was underway. Once more, the synergistic effect of combining sugar and phosphate depletion was demonstrated, since P^-S^--growing cells showed evidence of TUNEL reaction within 1 day of starvation (figure 4.7.-E). This evidence is also in accordance with previous biomass and phosphate leakage indications (figure 4.5.-A,B). Nuclei specificity of the TUNEL labelling was shown by the visualization of positively stained cells under visible light (figure 4.7.-F).

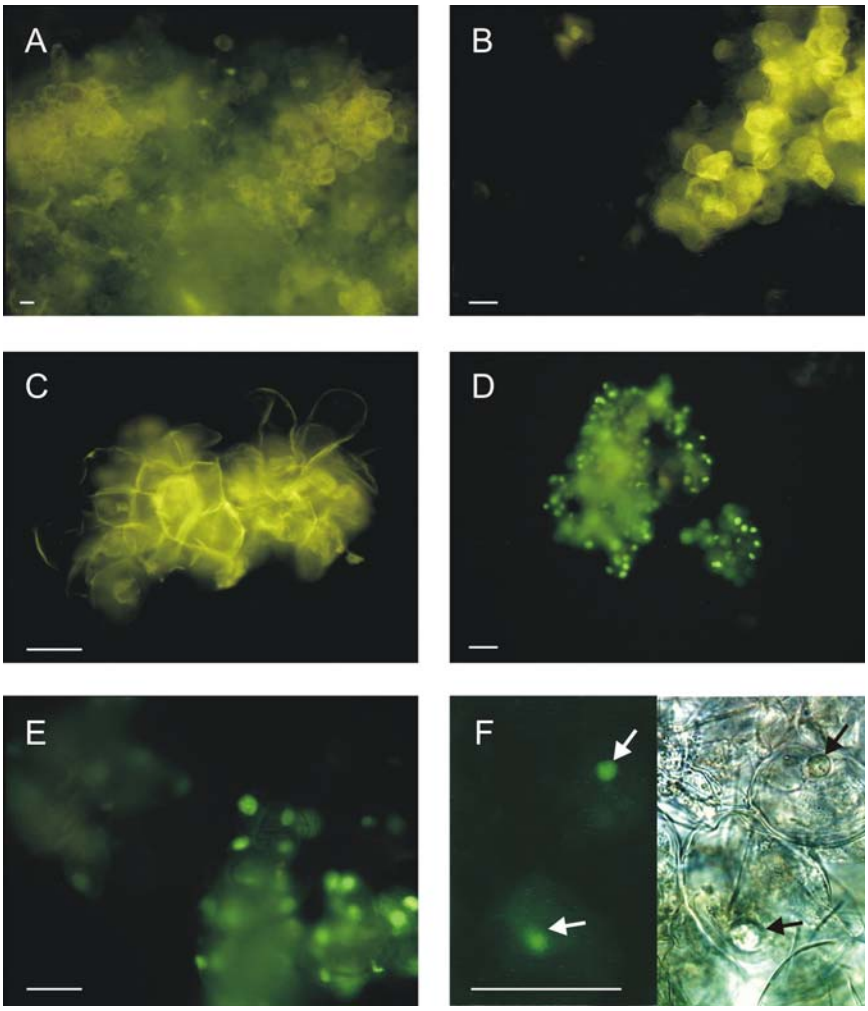

Figure 4.7. TUNEL assay performed on sugar- and/or phosphate-starved *P. pinaster* suspended cells. **A** - cells grown in P^+S^+ medium for 5 days. **B** - cells grown in P^-S^+ medium for 5 days. **C** - cells grown in P^+S^- medium for 1 day. **D** - cells grown in P^+S^- medium for 3 days. **E,F** - cells grown in P^-S^- medium for 1 day. Positive TUNEL staining was specific for nuclei (arrows). In figures, bar indicates 50 μm.

Programmed cell death has been shown to occur during nutrient depletion in yeasts (Baba et al. 1994; Granot et al. 2003) and plant cells (Moriyasu and Ohsumi 1996; Singh *et al.* 2003). Both sugar and phosphate starvation have been shown to induce extensive changes in cell morphology, which correlate with the PCD process (Moriyasu and Ohsumi 1996; Devaux *et al.* 2003; Singh *et al.* 2003). According to Singh *et al.* (2003), *Brassica napus* cells required over three weeks under phosphate starvation to exhibit PCD, but PCD could be observed earlier (at day 9) when *B. napus* cells were grown in a medium containing the non-metabolizable phosphate analog phosphite. At the contrarily, phosphate-starved *P. pinaster* suspended cells showed no

evidence of PCD up 3 days (nor up to 12 days, even when cells were grown in a medium phosphate-free medium containing the non-metabolizable phosphite.

Two types of PCD can be found in plant, the first involving autophagy and the other being of non-lysosomal origin (Van Doorn and Woltering 2005). According to these authors, autophagy is a major degradation and recycling system in eukaryotic cells, contributing to the turnover of cellular components. Among autophagic-dependant PCD, the extent of cell self-degradation could vary, reaching full cytoplasm degradation. It has been suggested that if autophagy occur at sub-lethal extent, it could constitutes a mechanism that defend the starved cell from death. (Klionsky *et al.* 2003). These authors also referred that another possible role for autophagic PCD is the degradation and mobilization of nutrients before death, thus sharing some features common to senescence.

Results shown that in sugar-starved *P. pinaster* cell cultures an increase in phophaste levels in the medium takes place. Theses results, together with those reporting an increase in acid phosphatase activity and positive TUNEL labelling, suggest that sugar-starved pine cells exhibit increased hydrolytic capacity and DNA degradation and strongly suggests that death occur through an autophagic programmed process.

Chapter 5

The *Pinus pinaster-Botrytis cinerea* interaction

5.1. Evaluation of the role of ROS and hypersensitive response in the *P. pinaster-B. cinerea* interaction

5.1.1. Introduction

Plants are continually exposed to a vast number of potential pathogens and, as a result, they have evolved intricate defence mechanisms to recognize and defend themselves against a wide array of these disease-causing agents, namely by inducing a set of defence responses that can defeat the invading pathogens. (Yang *et al.* 1997). Typical defence responses include oxidative bursts, hypersensitive response and increased expression of defence-related genes (Lamb and Dixon 1997; Heath 2000; Dixon 2001). Host resistance is cultivar or accession specific, while non-host resistance provides broad-spectrum defence against pathogens. Two types of non-host resistance can be distinguished. The type I does not produce any visible necrosis while the type II is always associated with hypersensitive response (Mysore and Ryu 2004). Host (gene-for-gene) and type II non-host resistance share some similarities, and the same pathogen can induce both in different plant species; however it is still questionable if they involve the same signal transduction pathways.

ROS has been shown to play a fundamental part in the complexity of events that characterize biotic stress resistance. In incompatible interactions, two bursts of ROS are produced, being the second considered an indicator of recognition and mediated response to the pathogen (Lamb and Dixon 1997). It has also been suggested that coordination of ROS-scavenging mechanisms is fundamental during the defence

response (Apel and Hirt 2004). Evidences that have been given for the involvement of ROS in non-host interactions suggest that despite the similarities to host resistance, responses may vary in terms of the intensity and timing of ROS bursts (Huckelhoven 2001; Able 2003). Additionally, it has been suggested that HR induction is dependant upon the suppression of ROS-scavenging systems, that permit accumulation of the necessary levels of ROS required to induce programmed cell death (De Gara *et al.* 2003; Apel and Hirt 2004).

Here, we evaluate the production of ROS and ROS-scavenging capacity of *P. pinaster* suspended cells when elicited by the necrotroph *B. cinerea*. The involvement of transduction pathway components on the triggering of ROS bursts was also studied. In addition, it was evaluated the occurrence of hypersensitive response in maritime pine cells during the time course of elicitation.

5.1.2. Results and Discussion

5.1.2.1. Quantification of ROS in P. pinaster *suspended cells challenged by* necrotrophic fungi

Reduction of the tetrazolium dye XTT was used to measure the intracellular production of superoxide radical (O_2^-), in the presence of a *B. cinerea* spore suspension and mycelium extract. Since XTT is added at the beginning of the experiment, the production of XTT-reduced form (formazan) is accumulative. The results showed that only *B. cinerea* spore challenging was able to induce two bursts of O_2^- production in pine cells (figure 5.1.1.-A). A first burst started almost immediately after challenging and prolonged for 5 hours. A second burst of O_2^- production, at least 5-fold higher than the first started 9 h after elicitation. When elicited by *B. cinerea* mycelium extract, no oxidative bursts were observed in pine suspension cells (figure 5.1.1.-A *insert*). Non-elicited pine cells, spores and mycelium suspensions exhibited residual O_2^- levels through the time course of the experiment.

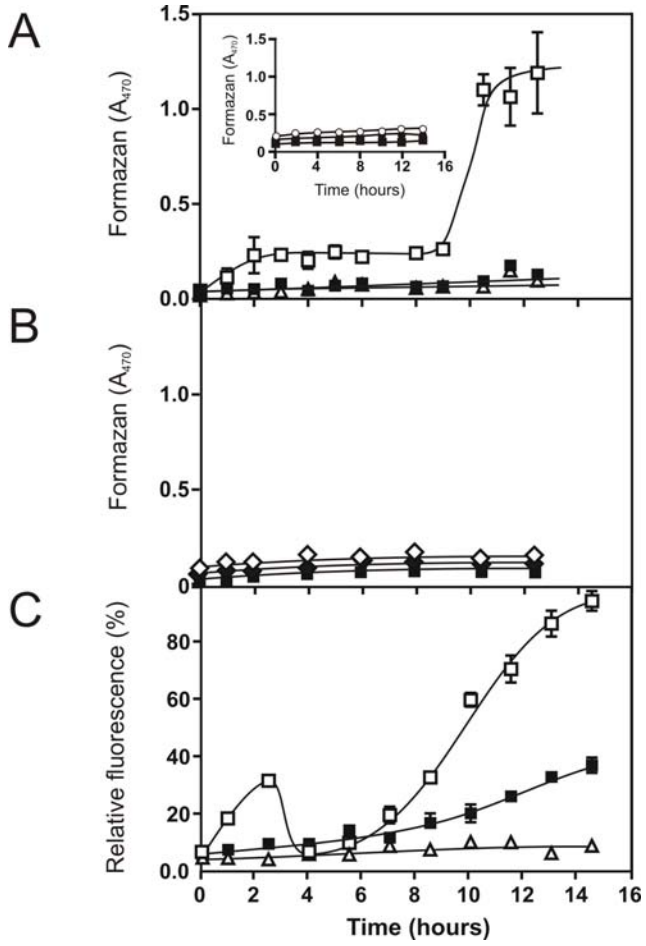

Figure 5.1.1. Quantification of intracellular ROS in *P. pinaster* suspended cells after challenging with the pathogenic fungi *Botrytis cinerea* and *Lophodermium seditiosum.* **A** – XTT quantification of superoxide radical in unchallenged cells (■), cells elicited with *B. cinerea* spores (□), and *B. cinerea* spores suspension (Δ). Insert: XTT quantification of superoxide radical in unchallenged cells (■), cells elicited with *B. cinerea* mycelium (○) and in mycelium suspension (●). **B** – XTT quantification of superoxide radical in unchallenged cells (■), cells elicited with *L. seditiosum* mycelium extract (◇) and in *L. seditiosum* mycelium extract suspension (◆).**C** – H_2DCFDA quantification of ROS in unchallenged cells (■), cells elicited with *B. cinerea* spores (□), and *B. cinerea* spores suspension (Δ).

The capacity of O_2^- production was further evaluated in *P. pinaster* cell suspensions challenged with mycelium extract of *Lophodermium seditiosum*. This necrotrophic fungus is also a pathogen of *P. pinaster*, particularly of seedlings in nurseries. Elicitation of *P. pinaster* cells with *L. seditiosum* mycelium extract did not result in the induction of intracellular oxidative bursts (figure 5.1.1.-B). The results

suggest that a mediated response of *P. pinaster* cells to challenging requires the specific recognition of *B. cinerea* spores.

The analysis on intracellular levels of ROS was further complemented using H_2DCFDA for assessing the overall oxidative stress. The results are depicted in figure 5.1.1.-C and were similar to those referred for XTT. When compared to non-elicited cells, pine cells elicited by *B. cinerea* spores evidenced two oxidative bursts, the initial peak within 3 h and the a second peak after 7 h. At 8 h of elicitation, the increase in ROS increased 3-fold when compared to the initial oxidative burst.

Oxidative bursts observed in *B. cinerea*-challenged maritime pine cells followed the generally accepted two peaks of ROS production observed in incompatible interactions (reviewed by Lamb and Dixon 1997). While phase I of ROS production is a very rapid response (within minutes or hours after elicitation), not always correlated with plant disease resistance, phase II of ROS production will extend from hours (or days) after challenging and correlates with resistance/susceptibility of the plant to the pathogen (Allan *et al.* 2001). According to these authors, phase I and II bursts can differ kinetically in different plant-pathogen systems, as to the source of ROS and/or the type of ROS produced. The exact kinetics of ROS induction is a function of the biology of the invading pathogen.

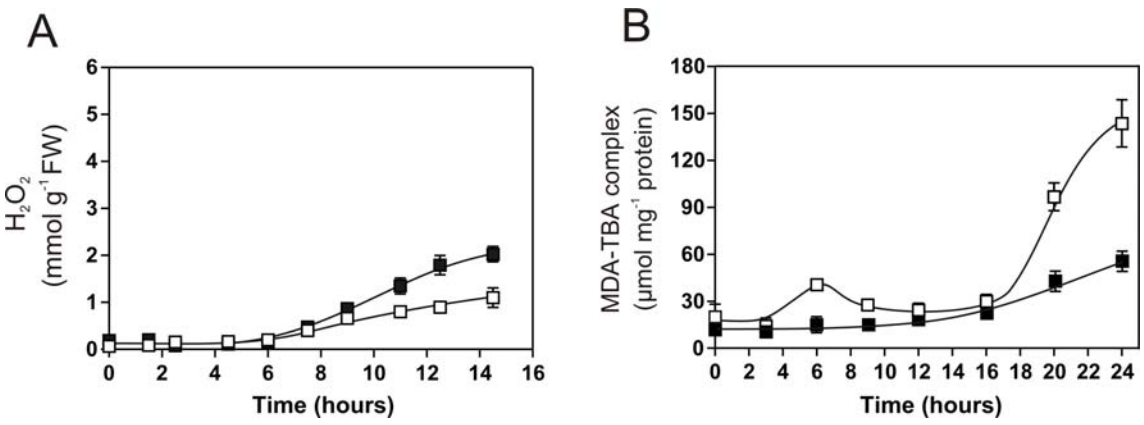

Figure 5.1.2. Determination of extracellular H_2O_2 content (**A**) and lipid peroxide formation (**B**) in unchallenged *P. pinaster* suspended cells (■) and in cells elicited with *B. cinerea* spores (□).

Oxygen radicals are highly limited in the capacity to diffuse within the cell. Exceptionally, the chemical properties and higher stability of H_2O_2 allows it to cross cellular membranes, serve as a localized signalling molecule, or be used extracellularly in the defence response (Henzler and Steudle 2000; Heitefuss 2001). Extracellular levels

of H_2O_2 were quantified during the maritime pine-*B. cinerea* interaction (figure 5.1.2.-A), making use of the peroxide-mediated oxidation of Fe^{2+}, followed by the formation of a complex between Fe^{3+} and xylenol orange (Bellincampi *et al.* 2000). The results indicate that when pine suspended cells were elicited with *B. cinerea* spores, there was a near 50% reduction in H_2O_2 content in the medium, compared to what was observed in non-elicited cells, suggesting that elicitation does not induce the extracellular production of this reactive species.

Lipid peroxidation is generally considered a marker for extensive oxidative stress and occurs as a consequence of ROS production (Liu *et al.* 1997; Petersen *et al.* 1999). The levels of lipid peroxides during challenging of *P. pinaster* cells by *B. cinerea* were evaluated by the quantification of MDA-TBA complexes (figure 5.1.2.-B). According to this figure, lipid peroxide levels increased after challenging, with two peaks of production being observed within 3 and 16 h of elicitation. The results were consistent with those depicted in figures 5.1.1.-A and 5.1.1.-C, as lipid peroxide formation was observed after intracellular levels of ROS had increased in two oxidative bursts.

Detection of fungal pathogens by the recognition of specific or unspecific elicitors has been shown to induce both an extracellular oxidative burst and an intracellular ROS increase (Heitefuss 2001). Results indicate that only intracellular ROS production was observed in *P. pinaster* suspensions challenged by *B. cinerea*. It has become evident in recent years that successful pathogenicity of necrotrophs is correlated with the disruption of challenged cells, particularly cellular membranes, by action of the plant's oxidative bursts (Bolwell *et al.* 1999; Mittler *et al.* 1999). *B. cinerea* challenging has been shown to induce the intracellular production of ROS in *Capsicum annuum*, *Phasheolus vulgaris* and *Arabidopsis thaliana* cells (Deighton *et al.* 1999; Muckenschnabel *et al.* 2001; Muckenschnabel *et al.* 2002). ROS generation was often accompanied by a decrease in the pool of antioxidants (namely ascorbic acid) and an increase in Fe(III).

Reports considering the extent of lipid peroxidation observed after *B. cinerea* challenging have been contradictory. MDA levels were shown to increase in elicited *P. vulgaris* cells, which are in accordance with the results observed in *B. cinerea*-elicited maritime pine suspensions. In contrast, lipid peroxide levels were unaffected by *B. cinerea* in *C. annuum* fruits, and even decreased in elicited *Arabidopsis* plants (Deighton *et al.* 1999; Muckenschnabel *et al.* 2001; Muckenschnabel *et al.* 2002).

5.1.2.2. Analysis on the involvement of MAPK, NADPH oxidase and calcium on the transduction of B. cinerea *elicitation signal*

It was evaluated the dependency of *B. cinerea*-induced oxidative bursts on known components of defence signal transduction pathways, as well as protein synthesis. For this purpose, staurosporine (MAPK inhibitor), DPI (NAPH oxidase inhibitor), $LaCl_3$ (calcium influx inhibitor), and cycloheximide (inhibitor of protein synthesis) were added prior to elicitation and intracellular ROS accumulation was monitored using H_2DCFDA. As can be seen in figure 5.1.3.-A, from all inhibitors tested only $LaCl_3$, a blocker of calcium channels, was able to suppress the first oxidative burst. The results suggest that in elicited pine cells, the production of the first ROS peak does not depend upon the occurrence of *de novo* protein synthesis, as cyclohexamide did not have a significant inhibitory effect. In addition, MAPKs and NADP oxidases did not correlate with the first oxidative burst. Contrary to what was observed for the first ROS peak, all the compounds markedly inhibited the second oxidative burst in elicited pine cells (figure 5.1.3.-B). The results indicate that phase II oxidative burst requires *de novo* protein synthesis to operate and the involvement of MAPK activation and calcium influx event. In addition, phase II ROS production seems to be dependent of NADPH oxidase activity. In plant-pathogen interactions, the phase I oxidative burst has been attributed to the activity of membrane NADPH oxidases (Tenhaken *et al.* 1995; Lamb and Dixon 1997; De Gara *et al.* 2003). The results depicted in figure 5.1.3-A are not in accordance with this observation, since inhibition by DPI did not prevent phase I ROS production in elicited pine cells. NAPH oxidases produce superoxide radicals by generating an electron transport chain capable of reducing O_2 and are analogous to mammalian O_2^- generating enzymes (Desikan *et al.* 1996; Groom *et al.* 1996; Murphy and Auh 1996). By generating oxygen oxygen radiclas, NADPH oxidases are capable of disturbing ROS homeostasis, thus activating or amplifying ROS sensitive signalling pathways (Mittler *et al.* 2004). NADPH oxidases were initially shown to play a fundamental role in ROS signalling events during biotic stress, (Desikan *et al.* 1996; Lamb and Dixon 1997; Dat *et al.* 2003) and were subsequently involved in abiotic stress signalling (Cazale *et al.* 1998; Pellinen *et al.* 1999). The results depicted in figure 5.1.3-B suggest that NAPH oxidase activity is fundamental for triggering the second oxidative burst, imparting a role for this enzyme in the defence response to *B. cinerea*.

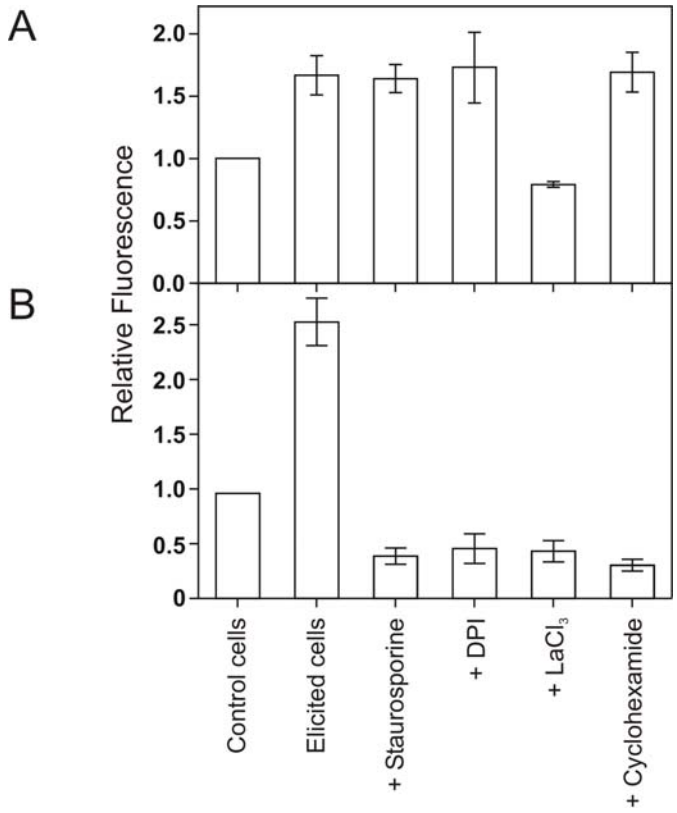

Figure 5.1.3. Effect of staurosporine (MAPK inhibitor), DPI (NADPH oxidases inhibitor), $LaCl_3$ (calcium channels inhibitor), and cyclohexamide (protein synthesis inhibitor) on the oxidative bursts produced during elicitation of *P. pinaster* suspended cells with *B. cinerea* spores. The intracellular levels of ROS were determined using the fluorescent probe H_2DCFDA, and samples were taken during the first (**A**) and second (**B**) oxidative burst, 3 h and 12 h after elicitation, respectively.

Other mechanisms of ROS generation, alternative to NADPH oxidase, have been reported, such as those including lipoxygenase, which acts on polyunsaturated fatty acids, and apoplastic enzymes, such as copper amine oxidase, flavin polyamine oxidases, oxalate oxidase or a secretory peroxidase (reviewed by De Gara *et al.* 2003). In the apoplast, NAPH oxidase-generated superoxide can be rapidly converted to H_2O_2 either by spontaneous dismutation or by apoplastic SODs (De Gara *et al.*; Mittler *et al.* 2004). Unlike O_2^-, H_2O_2 can diffuse within the cell and was shown to function as a second messenger during the induction of defence genes (Orozco-Cardenas *et al.* 2001). HO• has also been involved in the defence response. By studying horseradish peroxidase, a new function has been proposed for apoplastic peroxidases as generators

of hydroxyl radicals. In the presence of O_2^- and H_2O_2, horseradish peroxidase was shown to produce HO• in a mechanism similar to the Haber-Weiss reaction (Chen and Schopfer 1999).

DPI inhibition of NADPH oxidase was already shown to severely diminish ROS production in *B. cinerea*-infected *Arabidopsis*, and to arrest cell death in *Arabidopsis*, tobacco, soybean and parsley (Tenhaken *et al.* 1995; Naton *et al.* 1996; Govrin and Levine 2000). Still, signal transduction pathways involving ROS signalling events are still poorly understood in plants. Though a central role has been attributed to H_2O_2 and O_2^-, a specific transduction pathway for $^1O_2$ has been recently proposed (op den Camp *et al.* 2003). However, receptors that bind oxygen radicals and act as sensors have not been discovered. Fungi and bacteria possess redox sensors in the form of two-component signalling systems involving histidine kinases (Whistler *et al.* 1998). Though plants have similar two-component histidine kinases, a function in redox sensing has yet to be determined (Apel and Hirt 2004).

MAPK inhibition also demonstrated a role for MAPK in the signal transduction cascade that leads to phase II, but not phase I oxidative burst in *B. cinerea*-elicited *P. pinaster* cells. The initial burst is therefore likely to precede the activation of kinases. The involvement of ROS-activated MAPK in regulating various stress responses has been previously described. In *Arabidopsis*, H_2O_2 was shown to activate MAPK 3 and 6 via MAPKKK ANP1 (Kovtun *et al.* 2000). MAPK 3 and 6 are involved in the modulation of several defence mechanisms with ROS production (Kovtun *et al.* 2000). OXI1, a serine/threonine kinase, was shown to be fundamental in coordinating Ca^{2+} and ROS sensing with the activation of MAPK 3 and 6 (Rentel *et al.* 2004). OXI1 is also activated by PDK1 through the phospholipase-C/D–phosphatidic-acid pathway (Anthony *et al.* 2004).

Several transcription factors have been associated with ROS production. They include members of WRKY, RAV, Myb, GRAS and Zat families (Mittler *et al.* 2004). Transcription factors should be responsible for the activation of adaptative responses (e.g. defence mechanisms, rearrangement of the photosynthetic apparatus). These responses include the activation ROS scavenging metabolism, which ultimately controls the intensity, duration and cellular localization of ROS bursts.

Ca^{2+} channel blocking conditioned both phase I and II oxidative bursts (figure 5.2.3.), which is consistent with the observation that most defence responses are dependant upon calcium influx, including early signal transduction events such as

NADPH oxidase-dependant early ROS production and the activation of MAPK (Tavernier *et al.* 1995; Lecourieux *et al.* 2002; Suzuki 2002).

Results from the assays performed using the calcium channels blocker $LaCl_3$ suggested that during *B. cinerea* challenging, maritime pine suspended cells required calcium influx to be able to induce the generation of ROS. To demonstrate the

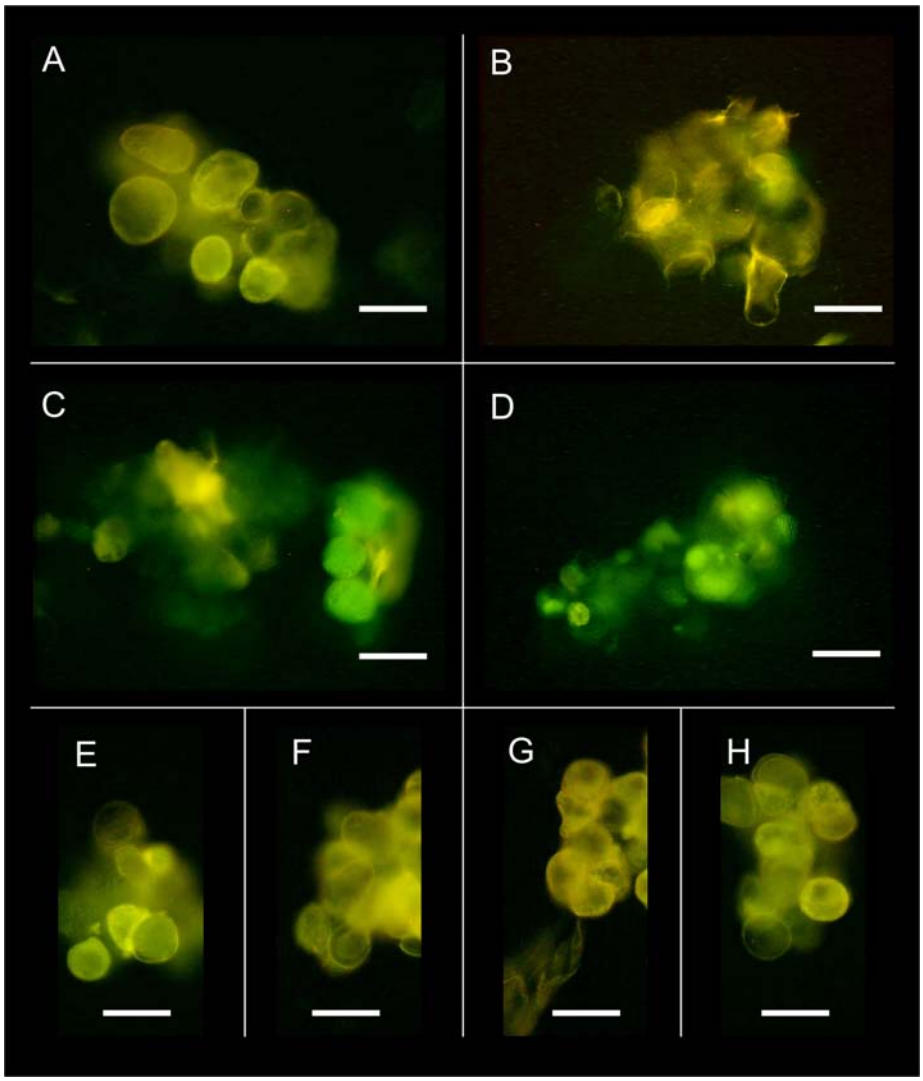

Figure 5.1.4. Fluorescence microscopy analysis of the intracellular calcium concentration in *P. pinaster* suspended cells challenged by *B. cinerea* spores, as revealed by the emission of green fluorescence, after probing with Ca^{2+}-binding probe fluo-3. Cells loaded with fluo-3 were immediately challenged with *B. cinerea* spores and were observed after 10 min (**A**), 20 min (**B**), 30 min (**C**) and 60 min (**D**). The effect of $LaCl_3$ (calcium channels blocker) on the intracellular calcium concentration in elicited maritime pine cells was also analysed for the presence of green fluorescence, 30 min (**E**) and 60 min (**F**) after elicitation. As a control, non-elicited pine cells were analysed for the presence of green fluorescence 30 min (**G**) and 60 min (**H**) after probe loading. In figures, bar indicates 50 µm.

occurrence of calcium influx following the elicitation of maritime pine cells, the intracellular concentration of calcium ion in the initial stages of challenging was monitored. Apart from the defence response, calcium influx can be involved in numerous signal transduction pathways (Barker *et al.* 1998; Iwata *et al.* 1998). Therefore, prior to probe loading and elicitation with *B. cinerea* spores, pine suspended cells were allowed to adapt to the new experimental conditions for 1 h. Suspended cells were incubated with the Ca^{2+}-binding probe fluo-3 and observed under a fluorescence microscope (figure 5.1.4.).

At the early stages of elicitation (10 and 20 min after challenging), no evident increase in intracellular calcium was observed in pine suspended cells (figures 5.1.4.-A,B). However, a marked calcium influx was observed approximately 30 min after challenging, as intense green fluorescence was observed in ~60% of suspension cells (figure 5.1.4.-C). Within 60 min of challenging, all cells were positively stained with Ca^{2+}-binded fluo-3 (figure 5.1.4.-D). Two control reactions were performed, using unchallenged pine cells and elicited cells in the presence of the Ca^{2+}-channel blocker: $LaCl_3$. Controls performed 30 and 60 min after challenging were negatively stained and only evidenced autofluorescence of *P. pinaster* suspensions (figures 5.1.4.-E,F,G,H).

Calcium is a ubiquitous internal second messenger (Trewavas and Malhó 1998) which was shown to be induced in response to biotic stress (Knight *et al.* 1991; Pugin *et al.* 1997; Blume *et al.* 2000; Lecourieux *et al.* 2002). It has been evidenced that, in plant cells, an alteration of the ionic homeostasis in the cytosol is crucial for the signal transduction pathway that leads to HR activation (reviewed by Lam *et al.* 2001). For instance, the *Arabidopsis* mutant *Dnd1* (defence, no death), which is involved in HR activation in response to various pathogens, was shown to code for a cyclic-nucleotide-dependant calcium channel (Clough 2000). Calcium influx events have been shown to differ in lag time, peak time, intensity, and duration, depending on factors such as the elicitor type, elicitor concentration and extracellular calcium concentration (Blume *et al.*; Lecourieux *et al.* 2002).

5.1.2.3. Evidences for the induction of the hypersensitive response following B. cinerea *challenging of* P. pinaster *cells*

ROS production has been consistently linked to the induction of the hypersensitive response. ROS, namely H_2O_2, were implicated as a local threshold

trigger of programmed cell death, acting also as inter-cellular signal molecules of defence, promoters of the cross-linking of cell-wall structural proteins, and toxic effector molecules acting upon the pathogen (Tenhaken *et al.* 1995; Govrin and Levine 2000; De Gara *et al.* 2003).

Previous results of quantification of ROS in *P. pinaster* cells elicited with *B. cinerea* gave evidences for the induction of two oxidative bursts during the time course of elicitation. Therefore, the occurrence of HR was further investigated.

Cell death was evaluated by measuring cell viability in the course of *P. pinaster* cells elicitation by *B. cinerea*. The results, depicted in figure 5.1.5., show that cell viability remained constant up to 24 h after elicitation, and 30% loss in cell viability was observed 48 h after elicitation. Similar results were observed for protein content (figure 5.1.5.-B). Decrease of protein levels occurred after 24 h of elicitation. A reduction in protein content of approximately 25% was observed 48 h after *B. cinerea* challenging. These results are in agreement with those referred for cell viability.

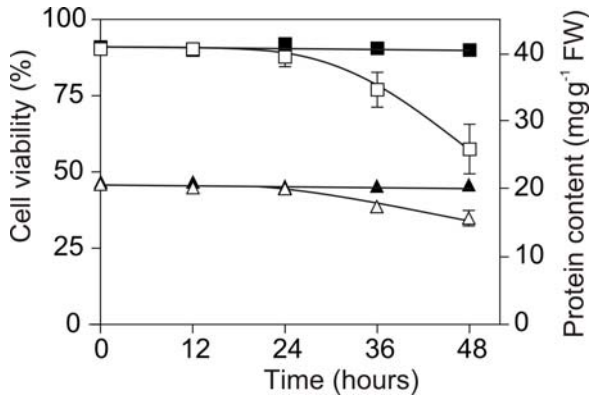

Figure 5.1.5. Cell viability and protein content of *P. pinaster* suspended cells during the time course of *B. cinerea* challenging. Cell viability of elicited (□) and non-elicited (■) pine cells; protein content of elicited (Δ) and non-elicited (▲) pine cells.

The TUNEL assay was performed to evaluate the occurrence of programmed cell death in elicited *P. pinaster* suspended cells. The results depicted in figure 5.1.6 show that prior to elicitation, pine cells did not evidence DNA cleavage (figure 5.1.6.-A). After 24 h of challenging, more than 95% of pine cells showed intense nuclei green fluorescence, while non-elicited cells did not present positive TUNEL

staining (figure 5.1.6.-C). It is worthwhile to refer that at 12 h of elicitation, 10% of elicited cells exhibited positive TUNEL signal, and after 48 h of elicitation, 40% of cell exhibited positive nuclei staining (not shown). In cells exhibiting negative TUNEL staining, only yellow autofluorescence was observed (figure 5.1.6.-A,C).

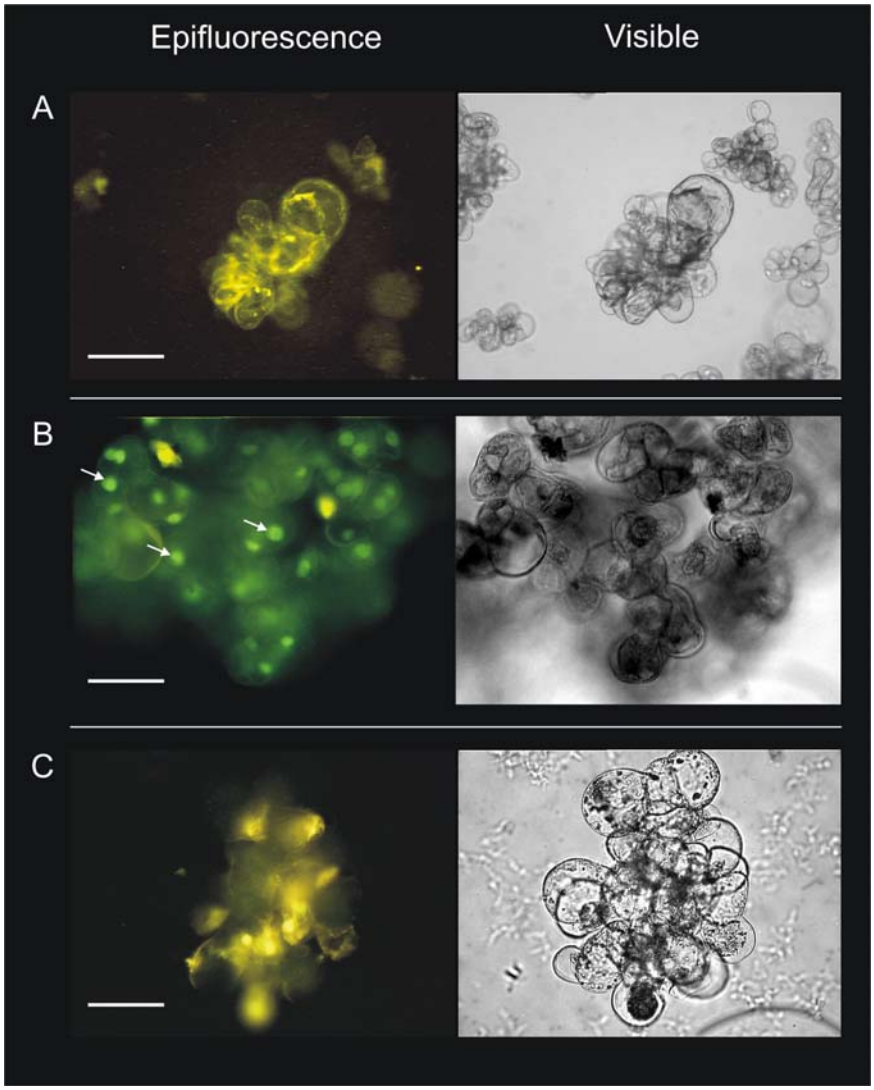

Figure 5.1.6. TUNEL assay performed on *P. pinaster* cells elicited with *B. cinerea* spores. Pine suspended cells undergoing apoptosis exhibited intense nuclei green fluorescence (arrows), after excitation with UV light. Cells were also visualized under visible light. Cells containing nonfluorescent nuclei and yellow autofluorescence indicated the absence of DNA cleavage. TUNEL analysis was performed in cells suspensions immediately before challenging (**A**) and 24 h after elicitation (**B**). As a control, TUNEL assay was performed on non-elicited cells, 24 h after the beginning of the experiment (**C**). In figures, bar indicates 50 μm.

H_2O_2 accumulation was shown to be fundamental in triggering the programmed cell death that occurs at infection sites during the defence response (Dangl and Jones 2001). *B. cinerea* and *L. seditiosum* mycelia were incapable of inducing an oxidative burst in *P. pinaster* suspended cells, suggesting the absence of elicitor motifs susceptible of recognition by pine cells. Being both necrotrophic fungi, the absence of plant cell penetration mechanisms should make detection by intracellular disease resistance associated genes unfeasible. *B. cinerea* spore germination was observed 48 h after placement in the reaction medium, when hyphae first developed from the spore wall. Therefore, *B. cinerea* hyphae developed by the time *P. pinaster* cells underwent cell death, ruling out the possibility for recognition of hyphal motifs or hyphal metabolic processes. Recognition by plant cells of *B. cinerea* conidia is likely to be determined by the presence of elicitor proteins in spore walls rather than by spore metabolic activity.

There is good support to the hypothesis that HR impairs biotroph infection but can assist necrotrophs during pathogen challenging (Lucas 1998; Govrin and Levine 2000). Mechanistically, HR helps necrotrophs due to their reduced capability to penetrate plant cells. In this context, the oxidative burst is involved not only in triggering HR, but also in helping pathogen progress by leading to the peroxidation of membranes and inducing cell leakage (Adam *et al.* 1989; Smirnoff 1993). It was shown that when challenged with *B. cinerea* spores, maritime pine suspension cells were capable of inducing both the hypersensitive response cell death and oxidative bursts. However, the present elicitation model is insufficient to determine weather HR triggering is detrimental to the plant, despite the evidence that *B. cinerea* is capable of using HR induction to its advantage. Grovin and Levine (2000) previously showed that in *Arabidopsis* plants, the non-host pathogen *Botrytis cinerea* was capable of using HR in benefit of pathogen progression. Infection of wild type *Arabidopsis* plants with *B. cinerea* evidenced HR-derived necrotic lesions, which expanded throughout infected leaves simultaneously to fungal expansion. Meanwhile, *dnd1* (defence, no death) mutant plants, being HR-impaired, were capable to resist pathogen progress.

When considering the HR, one of the main questions that is evoked is weather HR induction is a key process of pathogen resistance, or it is just induced as part of the generalized defence response, regardless of its particular efficacy (Lam *et al.* 2001). Even though the importance of HR in several plant-pathogen models is unquestionable (Gilchrist 1998; Piffanelli *et al.* 1999), it has been previously shown that the HR is not

essential in the deployment of effective resistance. In tomato, effective defence against *Cladosporium fulvum* is mediated by *Cf* resistance genes in the absence of HR (Hammond-Kosack *et al.* 1996). The *dnd1* (defence, no death) mutant in *Arabidopsis* mounts a HR-impaired resistance response to several pathogens which are capable of inducing the HR in wild-type plants (Clough 2000). Type I non-host resistance is effective in restricting the deployment of most plant pathogens in a non-HR manner.

It was also suggested that HR was activated only at a final stage of the resistance process, when a certain threshold of defence stress signals is reached (Morel and Dangl 1997). In the model proposed by Mysore and Ryu (2004) for HR-inducing type II non-host resistance, this threshold is set at cell-breach level. This is inconsistent with the challenging of *P. pinaster* cells with *B. cinerea* spores. It is suggested that in the *P. pinaster-B. cinerea* interaction, elicitors such as those typical of type I non-host pathogen recognition (Mysore and Ryu 2004) are capable of activating the HR in an cell-breach-independent manner during necrotroph attack.

5.1.2.4. Evaluation of ROS-scavenging capacity in P. Pinaster *cells elicited by* B. cinerea

Maritime pine suspended cells elicited by *B. cinerea* were capable of generating two intracellular bursts of ROS production and simultaneously produce O_2^- and H_2O_2 (as detected by XTT and H_2DCFDA, respectively), but no extracellular ROS accumulation was evident. To further investigate the role of ROS-scavenging metabolism in elicited pine cells, superoxide dismutase and catalase activities were determined.

Superoxide dismutase activity was evaluated in protein extracts of pine suspended cells, after elicitation with *B. cinerea* spores for 48 h. According to figure 5.1.7.-A, six isoforms of SOD are present in *P. pinaster* cells growing in a medium containing sucrose. Specific inhibition by KCN and H_2O_2, performed on replica gels, allowed the identification of four MnSOD, one FeSOD and one Cu,ZnSOD isoforms. Although monomeric SOD forms can be found in prokaryotes (Pesce *et al.* 1997), plant isoforms are usually homodimeric or homotetrameric. Cu,ZnSOD homodimers usually range the 32 KDa size, while FeSOD and MnSOD, much closely related enzymes, present homodimers sized around 42 KDa (Kanematsu and Asada 1994). According to

our results, three MnSOD homotetramers, one Cu,ZnSOD homotetramer, one MnSOD homodimer and one FeSOD homodimer (high to low MW) are present in pine cells.

The results depicted in figure 5.1.7.-A indicate that superoxide dismutase activity decreases in pine cells during elicitation with *B. cinerea* spores. FeSOD activity decreased to undetectable levels, after 6 h of challenging, while Cu,ZnSOD activity was not observed 48 h after challenging. Although the activity of MnSOD isoforms deferentially decreased during elicitation, being activity of MnSOD homotetramers not

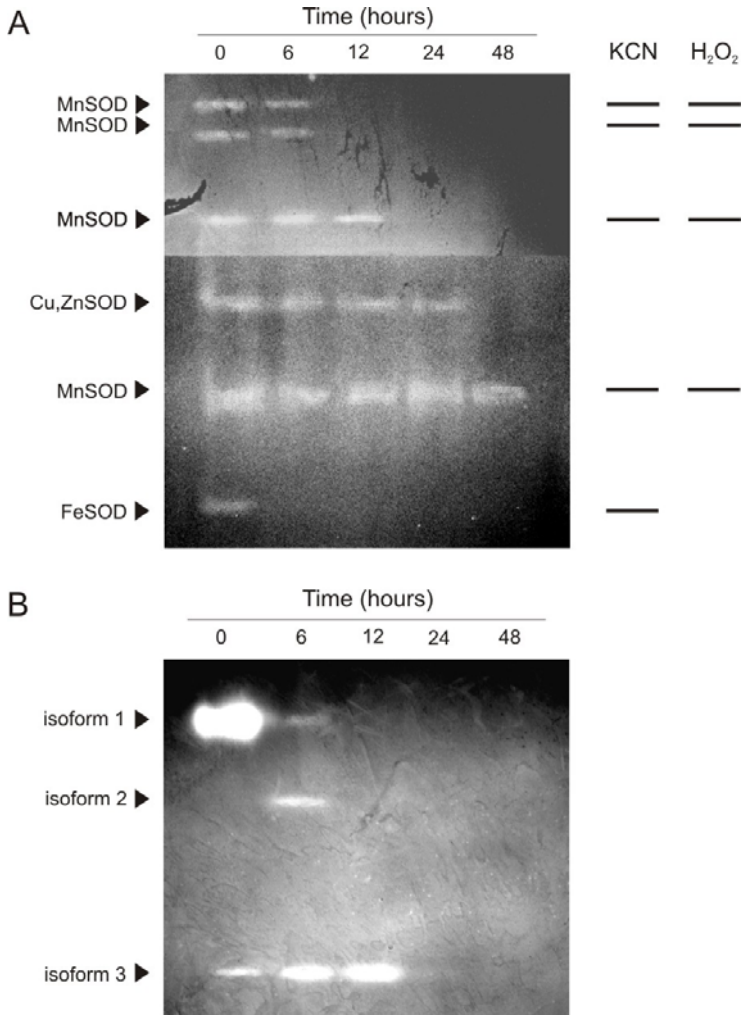

Figure 5.1.7. In-gel activity assay of superoxide dismutase and catalase after Native PAGE of protein extracts of *P. pinaster* cells during the time course of elicitation with *B. cinerea* spores. **A** – superoxide dismutase activity is depicted as achromatic bands in a dark background. Diagrammatic representation of gel replicas (t = 0), after incubation with KCN and H_2O_2 and SOD assay. **B** – catalase activity is depicted as achromatic bands in a dark-blue background.

detected in pine suspended cells after 24 h of elicitation, the MnSOD homodimer activity was still observed after 48 h of elicitation.

Catalase activity was also evaluated in protein extracts of pine suspended cells, following elicitation with *B. cinerea* spores for 48 h. The results depicted in figure 5.1.7.-B showed the existence of three isoforms with different molecular weight. Non-elicited cells only exhibit isoforms 1 and 3, the former accounting for more than 95% of catalase activity. During the time course of elicitation, the activity of isoform 1 markedly decresead, being non-detected after 12 hours. Activity of isoform 2 was transiently detected, after 6 hours of challenging. In what concerns isoform 3, an increase in activity was observed until 12 hours of elicitation, after which activity was non-detected. The results showed that both SOD and catalase activities decline during elicitation of pine cells with *B. cinerea*.

The catalase multigene family was shown to be comprised of three genes in the angiosperms *Arabidopsis thaliana*, *Nicotiana plumbaginifolia*, *Zea mays*, and *Oryza sativa* (Willekens *et al.* 1994; Frugoli *et al.* 1996; Guan and Scandalios 1996; Iwamoto *et al.* 1998). The existence of a complex catalase isozyme system was long ago established through enzyme assays after electrophoretic separation (Drumm and Schopfer 1974). CAT isoforms are usually found as homotetramers, although heterotetramers can be observed, and as a consequence, the three CAT genes of *Arabidopsis* can combine into at least six isozymes (Frugoli *et al.* 1996). Therefore, a correlation between the observed pine isoforms and the existence of corresponding genes should not be made.

CAT isoforms were shown to be differentially regulated in many physiological conditions. In maize, catalases show complex expression patterns during plant development (reviewed by Frugoli *et al.* 1998). Transcript analysis of the different CAT genes in *Nicotiana plumbaginifolia* showed that temporal and spatial patterns of gene expression were differential regulated in response to light, suggesting the association of each specific gene product to a particular H_2O_2-producing process (Willekens *et al.* 1994). CAT gene expression in response to various stress factors was addressed in *Arabidopsis* using microarray analysis (Mittler *et al.* 2004). The *Arabidopsis* genome comprises three catalase genes, responsible for H_2O_2 scavenging in peroxissomes. In response to heat, drought, salt, cold and high light, *CAT1* transcripts are up-regulated with the exception of down-regulation by cold. On the contrary, *CAT3* is

down-regulated with the exception of up-regulation by heat. Finally, *CAT2* transcripts increase with drought and cold and decrease with the remaining stresses.

The antioxidant capacity of *P. pinaster* cells during elicitation by *B. cinerea* was also analysed at the transcript level, by studding the expression of genes encoding Fe-SOD, Cu,Zn-SOD and APX. The corresponding full-coding sequences were identified by screening the *P. pinaster* cDNA library with heterologous *Zantedeschia aethiopica* probes coding for Fe-SOD, Cu/Zn-SOD and APX. Each screening resulted in the excision of 7-12 independent pBK-CMV plasmids containing the putative cDNAs of interest. Inserts were digested from the plasmid and confirmed for positive clones by southern blot analysis using the same ^{32}P-labeled heterologous probe.

Positive clones were sequenced using T3 and T7 universal flanking primers and the corresponding nucleotide and deduced amino acid sequences were analysed by BLAST (URL no. 8), and the sequences were edited in GenBank database (URL no. 6).

The following *P. pinaster* genes were identified: *chlCu,Zn-Sod1* (acc. no. AF434186), *Fe-Sod1* (acc. no. AY536055) and *Apx1* (acc. no. AY485994). A detailed characterization of *chlCu,Zn-Sod1* is performed in section 5.3.

Pine *Fe-Sod1* contained a 929 bp insert with a putative 750 bp open reading frame. The predicted protein of 249 amino acid residues has a molecular mass of 28.6 kDa and a 7.63 isoelectric point. Comparison with full-sequence *Fe*-Sod genes using multiple nucleotide sequence alignment was carried out with ClustalW (URL no. 10) (data not shown), indicating the presence of a putative N-terminal signaling peptide.

Protein targeting prediction using TargetP (URL no. 11) (Emanuelsson *et al.* 2000) and PSORT (URL no. 12) (Nakai and Kanehisa 1992) did not allow to ascertain the subcellular location of *P. pinaster FeSod1*. TargetP presented a positive score of chloroplastic targetting, while PSORT analysis evidenced a strong score for peroxissomes. FeSOD are usually assumed to be plastid targeted (Kitayama *et al.* 1999), namely by the presence of a putative transit peptide typical of plastids (enriched in hydrophobic and basic residues) (Keegstra *et al.* 1989). However, it has suggested other subcellular locations, namely peroxisomes (Salin 1988; Droillard and Paulin 1990), but also mitochondria (Droillard and Paulin 1990) and the cytosol (Becana *et al.* 1989). Even though a N-terminus transit peptide can be observed in *P. pinaster* Fe-SOD1, the amino acid sequence also presented a C-terminus peroxisomal-matrix targeting sequence, PST1 [(S/A/C)(K/R/H)L], also described as the SKL motif (Volokita 1991), with the presence of the tripeptide ARL at residue positions 239-241.

In fact, PSORT analysis has suggested a peroxisomal targeting for most putative FeSODs available at the database (Lino-Neto 2001).

P. pinaster Fe-Sod1 was the first described nucleotide sequence encoding a chloroplastic Fe-SOD in gymnosperms. The phylogenetic analysis of this sequence was performed considering *Fe-Sod* sequences from other plant species, bacteria and the *Fe-Sod* sequence from *Entamoeba histolytica* as outroot. Analysis was performed using maximum likelihood for tree computation (Doyle and Gaut 2000) and DrawTree for visualization (Felsenstein 1989). The analysis of the unrooted phylogenetic tree (figure 5.1.8.) clearly showed that plant Fe-SOD proteins clustered together in a distinct

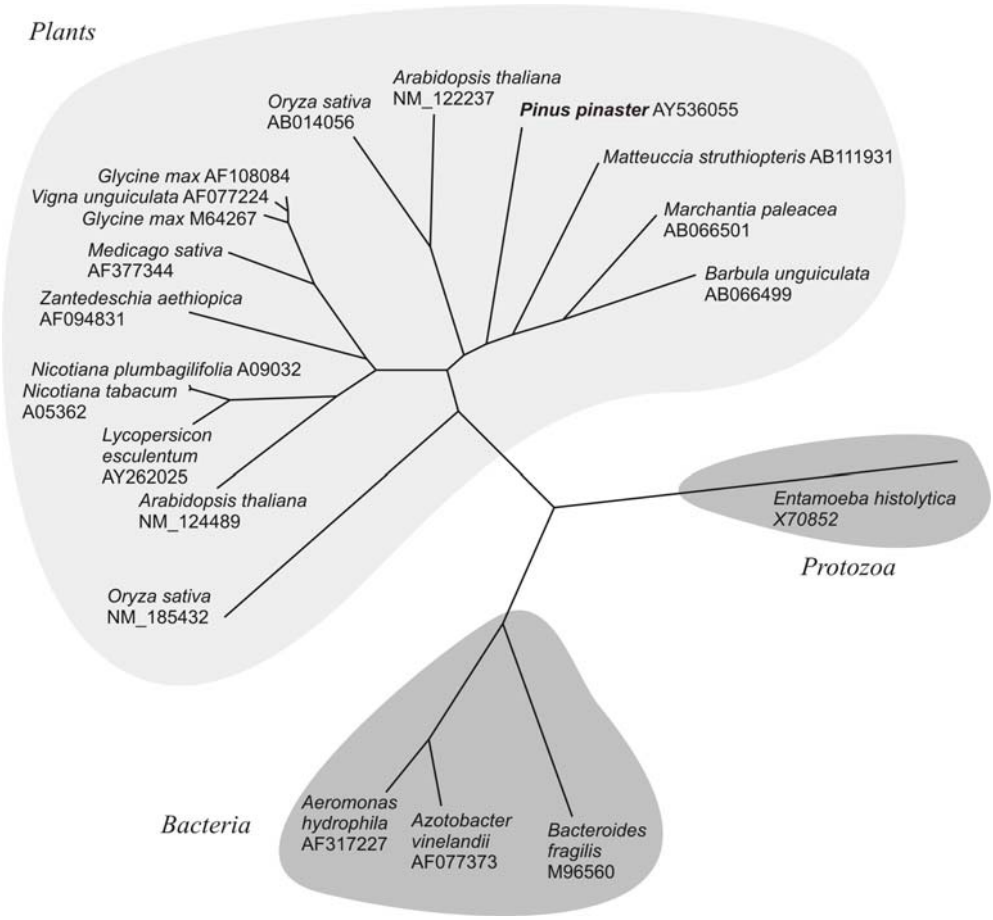

Figure 5.1.8. Unrooted tree representing the phylogenetic relationship between *P. pinaster* Fe-SOD and Fe-SOD's from other plants, Bacteria and Protozoa. The corresponding coding nucleotide sequences were analyzed using ClustalW and maximum-likelihood algorithms. GenBank Accession numbers are indicated for all sequences. The *P. pinaster* Fe-SOD sequence is depicted in bold. GenBank accession numbers are indicated.

subclade. *P. pinaster Fe-Sod* presents 47.5-63.6% identity to angiosperms sequences and 53.7-59.7% identity to seedless plants. From figure 5.1.8 is can also be seen that *A. thaliana* and *O. sativa* Fe-SOD sequences have distinct clustering patterns, suggesting that moderately unrelated Fe-SODs exist in the same plant species. It could then be conjectured that several gene duplications might have occurred in different stages of evolution before the complete transference of plastidial *FeSod* gene to the nucleus (Bridges and Salin 1981; Lino-Neto 2001).

By secreening the *P. pinaster* cDNA library a full-length cDNA (*Apx1*) was identified. This mucleotide sequence (1084 bp) exhibits a predicted open reading frame of 750 bp. The deduced amino acid sequence of 249 residues presented a 27.3 kDa mass and a 5.44 isoelectric point. Multiple sequence alignment of the full coding regions and the deduced amino acid sequence were performed, together with higher plants coding regions and the deduced amino acid sequence, respectively. *P. pinaster Apx1* deduced amino acid sequence was also analysed by Targeting prediction software (TargetP and PSORT), as previously described. The results indicated the absence of protein signalling peptides or of membrane-spanning regions, suggesting a cytosolic localization for pine APX1 protein.

Ascorbate peroxidase is a multigenic family of major H_2O_2 scavenging proteins, with isoforms that can be found in diferent cell compartments (table 1.3.1) and is involved in the ascorbate-gluthatione cycle (Asada 1994). APX is abundant in chloroplasts, where it is involved in the important detoxification of photosynthesis-derived ROS (Asada 1999). Nevertheless, the ascorbate-glutathione cycle enzymes play a fundamental ROS-scavenging role in nonphotosynthetic tissues, being mainly present in the cytosol (figure 1.3.1.) where APX activity prevents H_2O_2-dependent inhibition of cytosolic enzymes (Kaiser 1979; Tanaka *et al.* 1982; Verniquet *et al.* 1991). It was shown that cytosolic APX can occur in two forms with distinct targeting: csAPX are cytosol-soluble proteins (Mittler and Zilinskas 1991; Webb and Allen 1995), whereas cmAPX were suggested to be localized on the membranes of peroxisomes (Yamaguchi *et al.* 1995; Bunkelmann and Trelease 1996; Ishikawa *et al.* 1998).

P. pinaster Apx1 was the first database-available nucleotide sequence encoding a cytosolic APX in gymnosperms. A phylogenetic analysis, similar to that described for *P. pinaster Fe-Sod1*, was carried out for *P. pinaster* clone *Apx1*, together with other higher plants *Apx*. The yeast cytochrome c peroxidase (CCP) was used as outroot, since

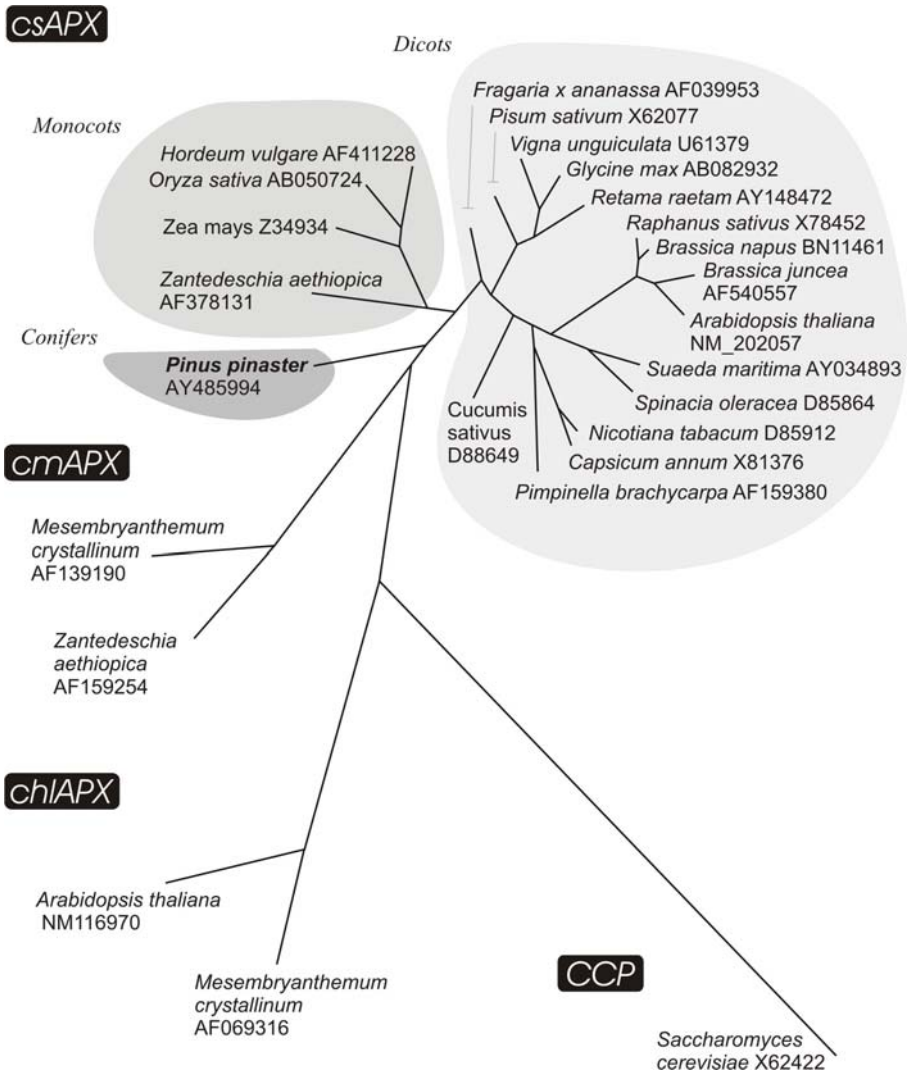

Figure 5.1.9. Unrooted tree representing the phylogenetic relationship between *P. pinaster* csAPX and APX's from other higher plants. Isoforms are indicated as chloroplastic (chl), cytosolic soluble (cs) and cytosolic membrane-bound (cm) APX, as well as the outroot cytochrome *c* oxidase (CCP) from *S. cereviseae*. The *P. pinaster* sequence is depicted in bold; GenBank accession numbers are indicated.

it exhibits higher identity to APX than to plant peroxidases (Ishikawa *et al.* 1998; Lino-Neto 2001). The analysis of the unrooted phylogenetic tree (figure 5.1.9) shows that the *csApx*s cluster together in a clade distinct form those of *cmApx* or *chlApx*. It is also observed distinct sub-clades for monocot and dicot *csApx* sequences. The results suggest that *P. pinaster Apx1*codes for a csAPX isoform, since it clustered together with higher plant *csApx* sequences. This is corroborated by the identity percentages observed between *P. pinaster APX1* and *csApx* (73.3-76.9) in contrast to *cmApx* (58.7-58.8).

Expression analysis of *P. pinaster Fe-Sod1*, *Cu,Zn-Sod1* and *Apx1* genes was performed by Northern blotting and incubation in ^{32}P-labeled homologous probes. For this, total RNA were isolated from pine suspended cells during the time course of elicitation by *B. cinerea* spores. As can bee seen in figure 5.1.10, the expression of all the genes studied decreased during elicitation, suggesting that they are down-regulated during elicitation by *B. cinerea*. *P. pinaster Fe-Sod1* transcript levels markedly decreased upon elicitation, being non-detected at 12 h of elicitation. The expression levels of *Apx1* also decreased significantly after 12 h of elicitation. In what concerns *chlCu,Zn-Sod1*, transcript levels maintained for 12 h and subsequently decreased. Even though *chlCu,Zn-Sod* is naturally expressed in photosynthetic tissues, the corresponding isoform was identified in other plastids, such as those found in *calli*, etiolated leaves and roots (Kaminaka *et al.* 1997; Kurepa *et al.* 1997).

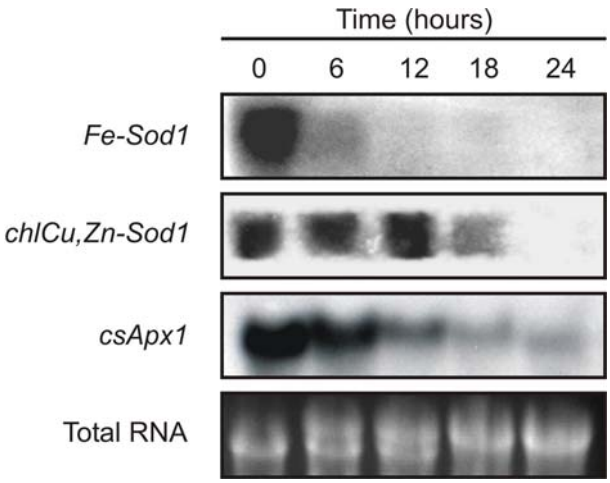

Figure 5.1.10. Expression analysis of *P. pinaster Fe-Sod1*, *chlCu,Zn-Sod1* and *csApx1* during time course of elicitation of pine suspended cells with *B. cinerea* spores. Total RNA samples were separated on a denaturing formaldehyde gel, blotted and hybridized with homologous cDNA ^{32}P-labeled probes. Total RNA was used as loading control.

Results did not allow ascertaining weather *P. pinaster Fe-Sod1* products are targeted to plastids or to peroxisomes. Fe-SOD has been found in photosynthetic tissues (Kitayama et al., 1999), as well as in non-photosynthetic tissues, such as *Glycine max* cultured cells and *Oryza sativa* etiolated seedlings (Crowell and Amasino 1991; Kaminaka *et al.* 1999). In *Nicotiana plumbaginifolia*, the expression of *Fe-Sod* was shown to be controlled by the cellular oxidative state (Tsang *et al.* 1991). In fact, Fe-SOD has been previously implicated as the major enzyme involved in the control of cellular O_2^- levels, in comparison to other SOD isoforms. A predominant role for Fe-SOD was observed in the protection of tobacco cells to oxidative stress

(Kurepa *et al.* 1997). A role of peroxisomal Fe-SOD in senescence was also referred (Droillard and Paulin 1990; Lino-Neto 2001). This data is supportive of an important role played by FeSOD in regulating maritime pine cellular ROS levels during challenging by *B. cinerea*, as evidenced by the rapid down-regulation of *P. pinaster FeSod1* transcripts (figure 5.1.10.) and FeSOD enzymatic activity (figure 5.1.7.-A).

It was previously suggested that during the oxidative burst, the large amount of ROS have an overwhelming effect on cellular antioxidative defences (Lamb and Dixon 1997). However, the present results are consistent with the hypothesis that a fine regulation of antioxidant systems is part of the signalling pathways activating defence responses (De Gara *et al.* 2003; Mittler *et al.* 2004). The pool of antioxidants was shown to be determinant to the oxidative level of challenged cells (reviewed by De Gara *et al.* 2003). Evidence previously suggested that a suppression of APX was required in cells undergoing HR, and a decrease in the GSH content was observed in tomato leaves infected with the *B. cinerea* (Mittler *et al.* 1998; Kuzniak and Sklodowska 1999; Bestwick *et al.* 2001). It has been difficult to establish a general model for the response of anti-oxidative systems to pathogen attack, due to the existence of too many variables, including the pathogen type and pathogenicity, the plant-pathogen model and the range of mechanisms studied (reviewed by De Gara *et al.* 2003). However, and in support of the present results, evidence clearly points out that the coordinated production of ROS and the down-regulation of ROS scavenging mechanisms is an absolute requirement for hypersensitive response cell death to be observed during plant-pathogen interactions (De Gara *et al.* 2003; Apel and Hirt 2004).

5.2. Analysis on the role of phenylpropanoid metabolism in the *P. pinaster-B. cinerea* interaction

5.2.1. Introduction

Secondary metabolites are generally defined as molecules that are not part of the essential metabolic processes of cells. Their importance however, should not be minimized, since the diversity of chemical constituents constitutes the major advantage of plants against pathogens. Over 100 000 low-molecular-weight secondary metabolites are known to be produced by plants. Even though some classes of chemicals seem to be specific to related plant families, the use of other classes like phenylpropanoid derivatives seems to have become generalized in the course of plant evolution (Dixon 2001).

Phytoalexins are defined as secondary metabolites that are synthesized as part of the defence response, and their importance in conferring resistance to pathogen attack has been confirmed (VanEtten *et al.* 1994). Most of these secondary metabolites have relatively broad-spectrum activities against pathogens and do not constitute targeted responses to specific pathogens. Therefore, genetic approaches using knock-outs or overexpression of enzymes that alter the metabolic profile have led to the conclusion that individual compounds or metabolite classes are essentially incapable of

single-handedly conferring resistance, and complex multi-compound responses are often required reviewed by Dixon (2001).

Progress on the identification and functional characterization of important genes involved in phytoalexin biosynthesis has increased the knowledge on the metabolic networks of defence secondary metabolites (Dixon *et al.* 1995; Bohlmann *et al.* 1998; Lange *et al.* 1998; Jung 2000). Phytoalexin biosynthesis occurs after primary metabolic precursors are diverted to secondary metabolic pathways. Diversion has been shown to occur by the *de novo* induction of enzymes such as PAL (Hammond-Kosack *et al.* 1996).

As depicted in figure 5.2.1., most plant natural products containing antimicrobial activity can be grouped within four chemical classes: flavonoids/isoflavonoids, alkaloids, isoprenoids and indole derivatives. The main contact point between these metabolic pathways and primary metabolism is established through the shikimic acid pathway (figure 5.2.1.). Isoprenoid biosynthesis also involves glucose and acetylCoA of the primary metabolism (Dixon 2001). Flavonoid and isoflavonoid biosynthesis is the best established metabolic pathway within phytoalexin metabolism, with virtually every enzyme already isolated (Dixon *et al.* 1995). Apart from the defence role as phytoalexins, flavonoids are also committed to interaction with *Rhyzobia*, UV protection, pigment biosynthesis and pollen viability (Durbin *et al.* 2000; Schröder 2000).

Phenylpropanoid metabolism is a fundamental component of the plant defense response (Ehness *et al.* 1997) because the reactions involved lead to various defense-related products that are functionally very diverse. Two chemical classes of phytoalexins are derived from phenylpropanoids: the isoprenoids and the flavonoids/isoflavonoids (figure 5.2.1.). Phenylpropanoid metabolism additionally leads to the synthesis of the cell-wall component lignin, and of salicylic acid, a crucial signalling molecule in the plant defence response (Durbin *et al.* 2000; Thomma *et al.* 2001). Phenylalanine ammonia-lyase (PAL) and chalcone synthase (CHS) are both key enzymes of the phenylpropanoid metabolism. PAL catalyzes the deamination of phenylalanine into cinnamic acid, and is the branch point enzyme between primary (shikimate pathway) and secondary (phenylpropanoid) metabolism (Dixon *et al.* 1995; Dvornyk *et al.* 2002). Chalcone synthase (CHS) is the first committed step of the flavonoid biosynthetic pathway (Yamakaki *et al.* 2001), generating the 15-carbon ring

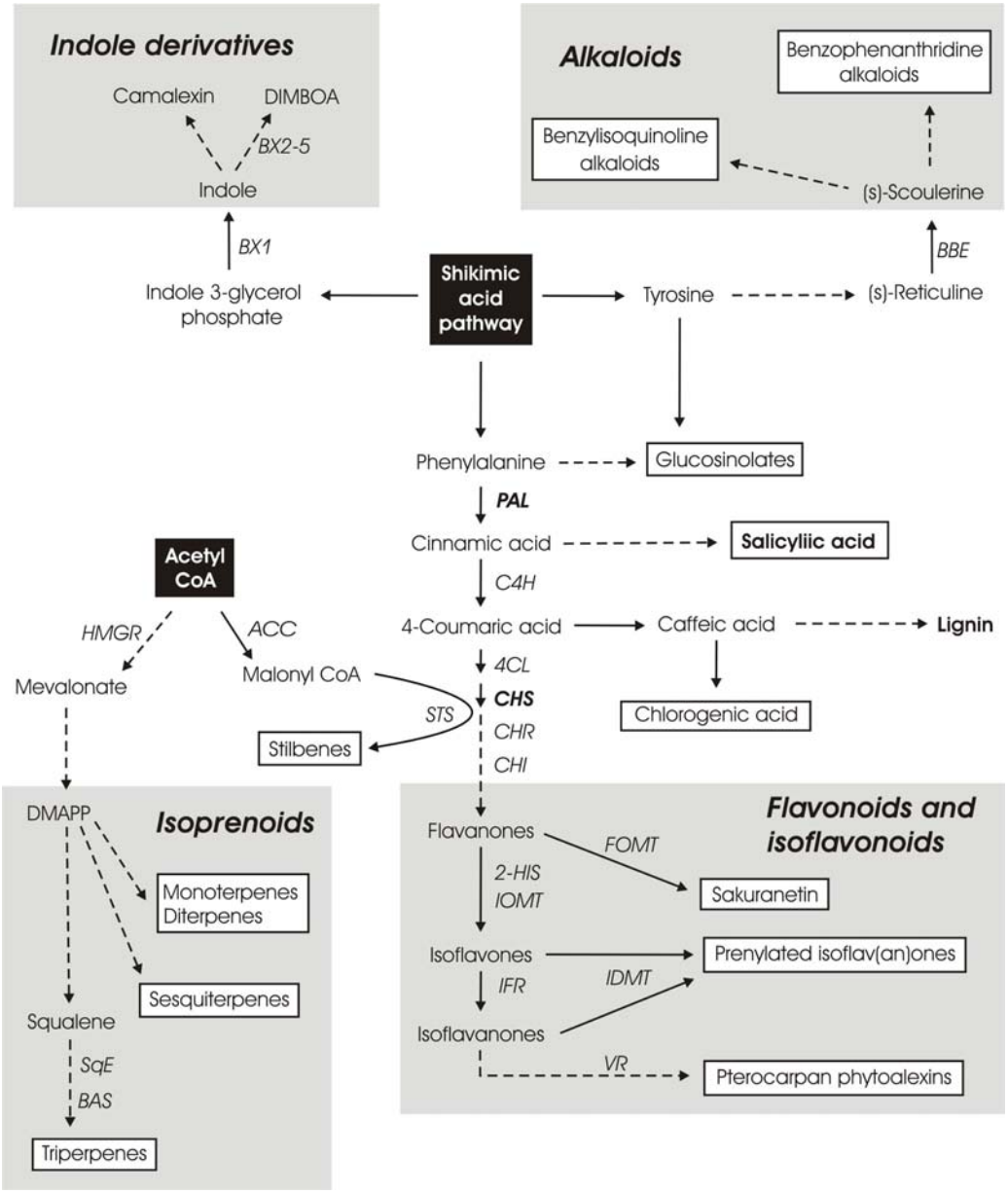

Figure 5.2.1. Biosynthetic network leading to the production of the main antimicrobial molecules in plants. Grey boxes highlight the four major groups: flavonoids/isoflavonoids, alkaloids, isoprenoids and indole derivatives. Black boxes indicate contact points with the primary metabolism of plants. Indications in bold illustrate metabolic compounds that were subject of analysis in the present work. Key enzymes are referred in italic. ACC – acetyl CoA carboxylase; βAS – β-amyrin synthase; BBE – berberine bridge enzyme; BX1 – indole-3-glycerol phosphate lyase; BX2-5 – four consecutive cytochrome P450 enzymes of DIMBOA biosynthesis; CHI – chalcone isomerase; CHR – chalcone (polyketide) reductase; CHS – chalcone synthase; C4H – cinnamate 4-hydroxylase; FOMT – flavanone 7-*O*-methyltransferase; HMGR – 3-hydroxy-3-methylglutaryl CoA reductase; IDMT – isoflavone or isoflavanone dimethylallyl transferase; IFR – isoflavone reductase; IOMT – isoflavone 4´-*O*-methyltransferase; PAL – L-phenylalanine ammonia-lyase; SqE – squalene epoxidase; STS – stilbene synthase; VR – vestitone reductase; 2HIS – 2-hydroxyisoflavanone synthase; 4CL – 4-coumarate CoA ligase. (adapted from (Dixon 2001).

structure that is the backbone of flavonoid biosynthesys (Durbin *et al.* 2000; Farzad *et al.* 2005). CHS is a member of the CHS superfamily of condensing enzymes. These enzymes vary significantly in substrate specificity (accepting a variety of CoA-esters), in the number of condensation reactions and in the type of ring closure of the released products (Schröder 2000). CHS catalyses the repetitive decarboxytive condensation of a phenylpropanoid-derived starter CoA with three C_2-units from malonyl-CoA and regiospecific cyclization to give chalcone (Yamakaki *et al.* 2001).

Maritime pine suspension cells challenged with *Botrytis cinerea* conidia were analysed by measuring the soluble phenolics and lignin content. In addition, genes coding for key metabolic enzymes PAL and CHS were isolated from a *P. pinaster* cDNA library and used in transcript profiling.

5.2.2. Results and Discussion

5.2.2.1. Determination of lignin and total phenolics contents

Pinus pinaster suspension cells were elicited with *Botrytis cinerea* ($6\ 10^4$ spores.ml^{-1}) and analysed for their capacity to counteract fungal challenging by mobilizing phytoalexin production and inducing cell wall reinforcement.

Challenged maritime pine suspended cells were extracted for their phenolic component and analysed by HPLC (not shown). Results evidenced a reduced number of simple phenolic acids, presenting no qualitative difference between challenged and non-elicited cells. Maritime pine suspensions were then analysed in terms of their total soluble phenolics content. As can be seen in figure 5.2.2.-A, non-elicited cells displayed a slight increase in phenolics during the 48 h period. In contrast, elicited cells evidenced an almost immediate reduction in the soluble phenolics content. Within 12 h of challenging, a 20% reduction was observed, which increased to 40% by hour 24. The results are in contrast with the observation that phenolic compounds accumulate around *B. cinerea* infection sites in *Arabidopsis* (Govrin and Levine 2002), that in pines, phenolics are induced upon fungal challenging (Lange *et al.* 1994), and that in general, the phenolics content increases upon pathogen challenging (Matta 1969; Nicholson and Hammerschmidt 1992; Singh *et al.* 2003).

The lignin content of the cell wall was analysed in challenged maritime pine suspensions. Results depicted in figure 5.2.2.-B show that in non-elicted *P. pinaster* cells a steady increase in lignin was observed, which accounted for ~0.44% of the cell wall by the end of the experiment. In contrast, in cell walls of pine cells challenged by *B. cinerea* spores, the total lignin content was 20% inferior to control cells. These results suggested that a reduction of cell capacity to reinforce the cell wall may have occurred. The present data is in contrast with the evidence that plant cells induced cell wall lignification after pathogen challenge (Smit and Dubery 1997). For instance, elicited *Pinus banksiana* suspensions were shown to rapidly promote lignin biosynthesis, with maximum concentrations being observed 48 h after challenging (Campbell and Ellis 1992). It should be taken into consideration that necrotrophs are seriously limited or even impaired in their capability to penetrate plant cells, and that cell wall reinforcement is a typical response to biotrophs (Lucas 1998).

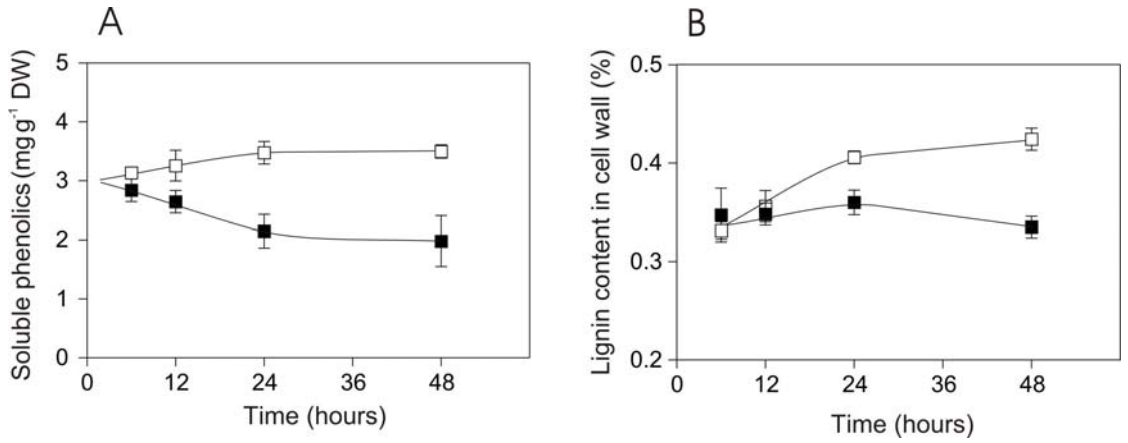

Figure 5.2.2. Determination of the content of total soluble phenolics (**A**) and lignin percentage in the cell wall (**B**) in *P. pinaster* cells non-elicited (□) and elicited with *B. cinerea* spores (■).

5.2.2.2. Identification of genes encoding key phenylpropanoid enzymes

P. pinaster genes coding for phenylalanine ammonia lyase and chalcone synthase, key-enzymes of the phenylpropanoid pathway, were identified by screening the maritime pine cDNA library.

For the isolation of genes coding for PAL in *P. pinaster*, a heterologous probe from the dycot *Digitalis lanata* was used in screening the cDNA library. This

methodology was unsuccessful in producing positive clones, probably due to low similarity percentage between the *D. lanata* and *P. pinaster* PAL sequences or the low copy number of PAL clones in the library. Taking into account that no *Pinus pinaster* sequences were available at the Genbank database (URL no. 6), PCR amplification of gDNA with degenerate primers was performed. For this, gDNA was purified from pine suspended cells and used as template in a PCR reaction, carried out at annealing temperatures in the range of 40-60ºC. For primers design, a multiple sequence alignment of deduced PAL amino acid sequences from higher plants [*Arabidopsis thaliana* (acc. no. NM111869), *Camellia sinensis* (acc. no. D26596), *Digitalis lanata* (acc. no. AJ002221), *Nicotiana tabacum* (acc. no. AB008200), *Pinus taeda* (acc. no. U39792), *Pinus banksiana* (acc. no. AF013482) allowed the identification of conserved regions. Two forward and two reverse primers were designed taking into account the analysis of the multiple nucleotide sequence alignment of the referred sequences. All combinations of forward/reverse primers were tested. Primer sequences were as follows:

PalFo1	23 bases	Degenerescency: 128×
	TAT GG(T/C) GT(T/C) AC(T/C) AC(T/C) GGI TT(T/C) GG	
PalFo2	23 bases	Degenerescency: 384×
	AC(A/C/G) AG(A/G) GC(A/T) GC(A/T) ATG CTI GTI AG	
PalRe1	20 bases	Degenerescency: 256×
	TG(C/T) TCI GC(A/G) CT(C/T) TGI AC(A/G) TG	
PalRe2	22 bases	Degenerescency: 128×
	AAI AC(A/G) TC(C/T) TG(A/G) TG(A/G) TG(C/T) TG	

Amplification products were resolved by electrophoresis. For the identification of putative *Pal* fragment(s) among the amplification products, PCR products were blotted onto nylon membranes and hybridized with the ^{32}P-labeled *D. lanata* probe. The autoradiogram, depicted in figure 5.2.3.-A, showed a single positive band (0.75 Kbp) that was obtained using the pair of primers PalFo2/PalRe1, at 55ºC. Also the primer combination PalFo2/PalRe2, at 55ºC, allowed the amplification of a 1 Kbp fragment (not shown). Both fragment lengths are in the range of expected fragment sizes, as deduced by multiple sequence alignment.

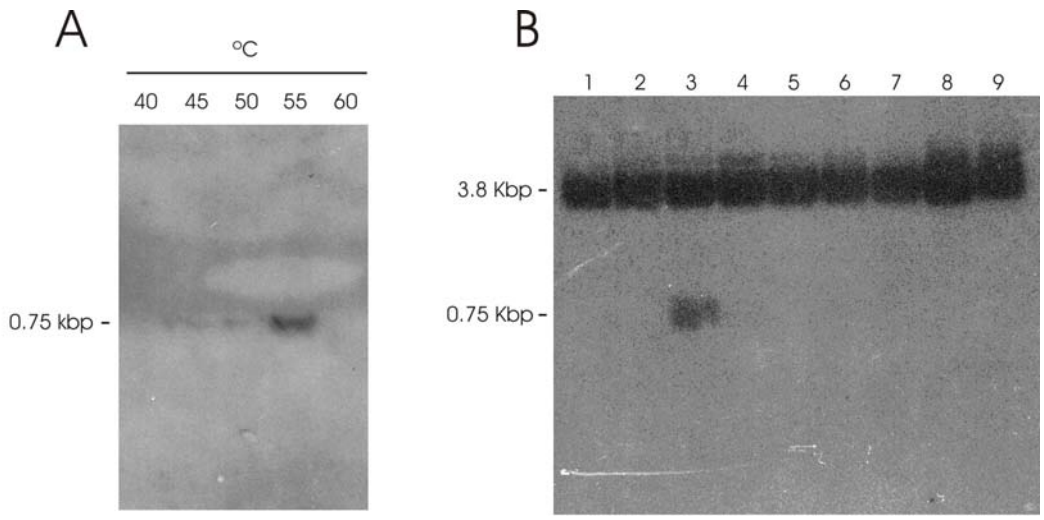

Figure 5.2.3. - Cloning of putative *P. pinaster Pal* fragments onto the pGEM-T Easy vector. **A** – Autoradiogram of PCR products after termocyclic gDNA amplification with PalFo2/PalRe1 primers, Southern bloting and hybridization with a ^{32}P-labeled *Digitalis lanata Pal* probe (acc. no. AJ002221). **B** – Autoradiogram of pGEM-T Easy plasmid after ligation of the PCR product depicted in A. The plasmid was digested with *Eco*R I, and the digestion product was Southern blotted and hybridized with a ^{32}P-labeled *Digitalis lanata Pal* probe (acc. no. AJ002221).

The 0.75 kbp PCR fragment was isolated from the agarose gel, cloned into the pGEM-T Easy vector, and subsequently used to transform *E. coli* JM109 cells. Nine recombinant clones were selected, and their plasmids were purified and digested. The digestion products were separated electrophoretically, blotted onto nylon membranes and hybridized with the ^{32}P-labeled *D. lanata* probe. The results (figure 5.2.3.-B) evidenced that clone 3 contained a single positive insert. After sequencing, this fragment was shown to have 738 bp and BLAST analysis revealed high homology with other *Pal sequences.* This fragment was then used as a homologous probe to screen the *P. pinaster* cDNA library. Ten putative positive spots were considered, and the corresponding pBK-CMV plasmids inserts were analyzed by Southern blotting, followed by hibridization with the radiolabeled *D. lanata* probe. Full sequencing was performed using T3 and T7 universal primers and custom designed primers, allowing the identification of two distinct *Pal* sequences, as confirmed by BLAST (URL no. 8). Full-length cDNA sequences, designated as *P. pinaster Pal1* and *P. pinaster Pal2*, were edited in the GenBank database (acc. no. AY321088 and AY321089, respectively).

P. pinaster Pal1 and *Pal2* contained an open reading frame of 2184 bp, coding for a 727 amino acid sequence of estimated 57 KDa. *P. pinaster Pal* sequences

presented nearly identical gene coding regions, with differing UTR regions. Despite the fact that *Pal* exist in pines as a multigene family (Butland *et al.* 1998; Kumar and Ellis 2001), both sequences are most likely the result of allelic variation, has they have 99.7% of coding nucleotide identity and presented only silent nucleotide substitutions, resulting in identical deduced amino acid sequences (figure 5.2.4.).

Figure 5.2.4. Deduced amino acid sequence alignment of *Pinus pinaster* PAL1 (acc. no. AY321088) and PAL2 (acc. no. AY321089) with *Arabidopsis thaliana* PAL (acc. no. NM111869) and *Cicer arientum* PAL (acc. no. AJ250836). The single letter code is used for amino acid depiction, and conserved residues are shadowed in black. Conserved egions used for degenerate primer design are indicated (arrows).

Phylogenetic analyses was carried out by comparing maritime pine *Pal* full-coding sequences with *Pal* sequences from angiosperms and *Pinus taeda Pal* (the only *Pal* conifer accession edited in database). The fern *Blechnum spicant Pal* sequence was used as outroot. Maximum likelihood was the algorithm of phylogenetic inference. DNAML and DrawTree from the PHYLIP software package (URL no. 9) were used for phylogenetic distance computation and tree plotting, respectively. The analysis of the unrooted phylogenetic tree (figure 5.2.5.) suggests that *Pal* genes present a highly consistent molecular evolutionary rate, as can be depicted by phylogenetic distances and the branching pattern. These should reflect the fact that PAL is a highly conserved protein, as can be observed by the multiple amino acid residue alignment depicted in figure 5.2.4. An extremely low rate of nucleotide diversity was attributed to pines in the *pal* locus (Dvornyk *et al.* 2002). Selective evolutionary constraint is likely the consequence of the pivotal role of PAL as the first committed step of the phenylpropanoid pathway, by which the carbon flux is controlled into this pathway (Kumar and Ellis 2001).

Figure 5.2.5. Unrooted tree representing the phylogenetic relationship between *Pinus pinaster Pal1* (acc. no. AY321088) and *Pal2* (acc. no. AY321089) and other plant *Pal* coding sequences. Coding sequences were analyzed using ClustalW and maximum-likelihood algorithms. GenBank accession numbers are indicated for all entries. *P. pinaster Pal* sequences are depicted in bold.

For the identification of genes encoding chalcone synthase in *P. pinaster*, the cDNA library was secreened using *Picea mariana Chs* as heterologous probe. Fourteen positive clones were considered, and their plasmids purified. Positive inserts were detected by Southern blotting, followed by hybridization with the ^{32}P-labeled *P. mariana* probe. Full cDNA sequencing revealed the presence of three unique *Chs* genes. The cDNA sequences were designed as *P. pinaster Chs1* (acc. no. AY168850), *Chs2* (acc. no. AY168851) and *Chs3* (acc. no. AY321087). Each ORF corresponded to fragments of 1189 bp, and coded for a 395 polypeptide with 39 kDa. The analysis of multiple sequence alignment of amino acid residues (figure 5.2.6.) evidenced the presence of five conserved active site amino acids (Cys^{169}, Phe^{220}, Phe^{270}, His^{308} and Asn^{341}), as well as the motif G^{377}(F/L)GPG which was referred as a signature common in the CHS superfamily (Yamakaki *et al.* 2001).

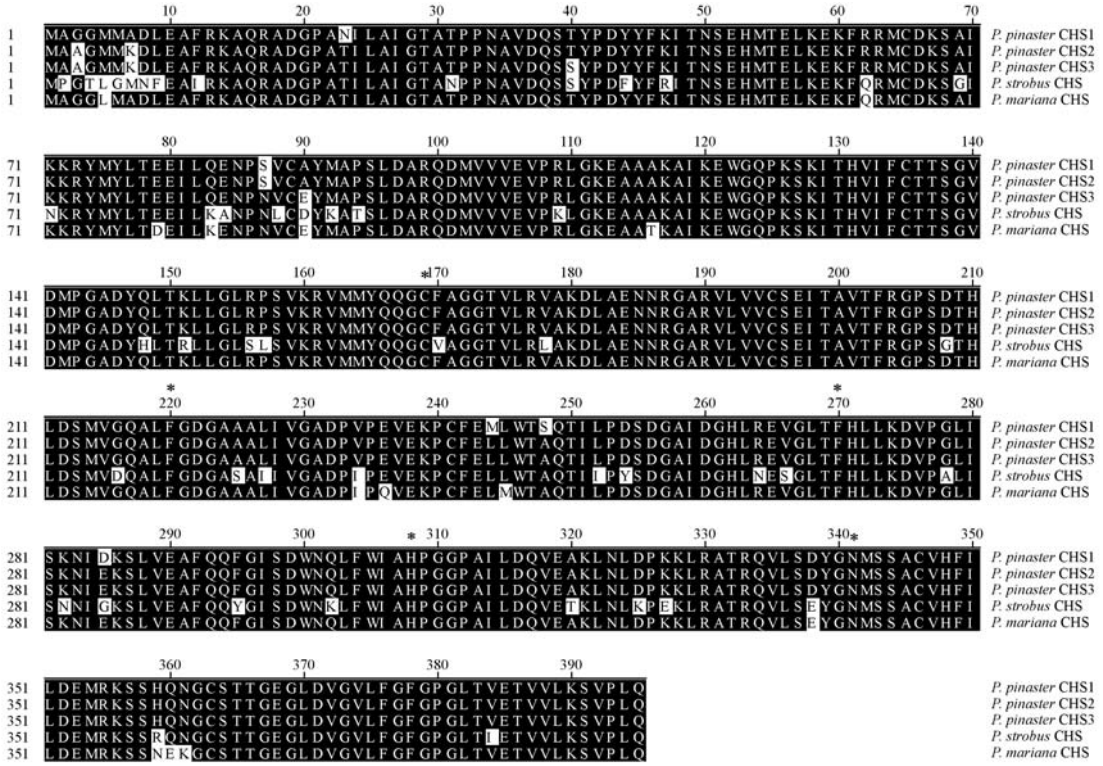

Figure 5.2.6. Deduced amino acid sequence alignment of *P. pinaster* CHS1 (acc. AY168850), CHS2 (acc no. AY168851) and CHS3 (acc. no. AY321087) with *Pinus strobus* CHS (acc. no. AJ002156) and *Picea mariana* CHS (acc. no. AF227627). The single letter code is used for amino acid depiction, and conserved residues are shadowed in black. Conserved active-site residues are indicated (asteriscs).

The phylogenetic analysis of *P. pinaster Chs* sequences was performed together with *Chs* sequences from other higher plant species. The fern *Psilotum nudum Chs* sequence was used as outroot. Analysis was performed using maximum likelihood (DNAML) for tree computation (Doyle and Gaut 2000) and DrawTree for visualization (Felsenstein 1989). The analysis of the unrooted phylogenetic tree, depicted in figure 5.2.7., shows that conifer *Chs* sequences are clustered together in a clade distinct from that of angiosperms, and monocot and dicot *Chs* sequences clustered together in distinct subclades as referred by (Yamakaki *et al.* 2001). According to figures 5.2.7. phylogenetic tree analysis points to at least five distinct branches with apparently high variability, as depicted by the distribution of *P. pinaster* and *P. strobes* sequences. This is consistent with the dynamic and complex evolutionary process that has been observed in CHS related enzymes, with CHS being the prototype and the likely evolutionary basis for a wide range of condensing enzymes: the CHS superfamily (Schröder 2000). In the course of plant evolution, CHS superfamily gene members have evolved from repeated branching steps (Durbin *et al.* 2000). As a consequence, functional prediction from primary nucleotide sequences is uncertain and functional characterization is required through heterologous expression (Schröder 2000).

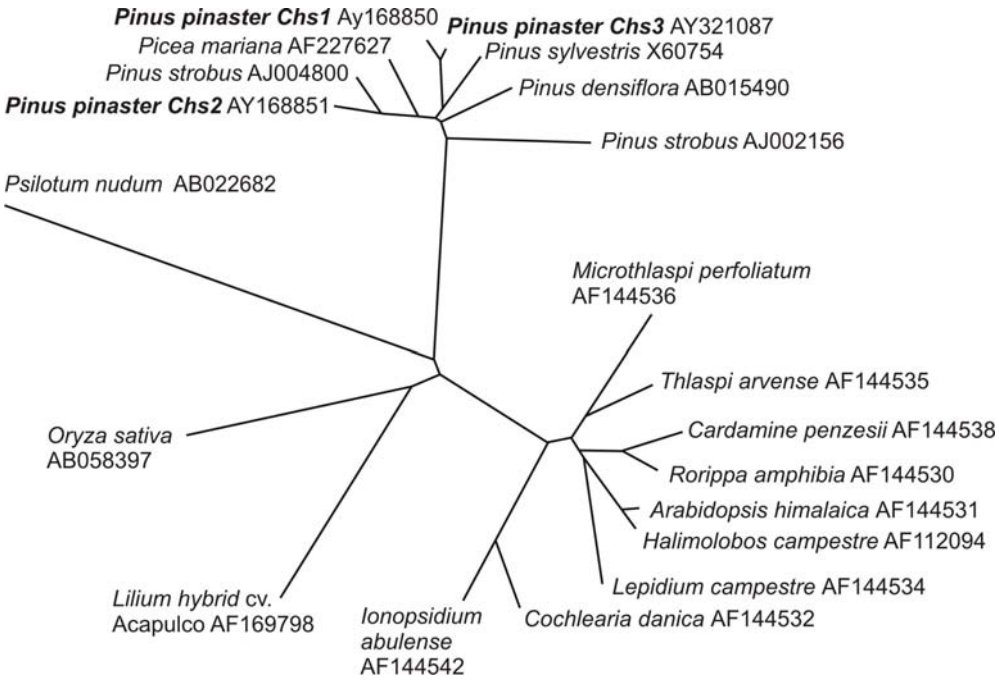

Figure 5.2.7. Unrooted tree representing the phylogenetic relationship between *Pinus pinaster Chs1*, *Chs2* and *Chs3* and other plant *Chs* coding sequences. Coding nucleotide sequences were analyzed using ClustalW and maximum-likelihood algorithms. GenBank accession numbers are indicated for all sequences. *P. pinaster Chs* sequences are indicated in bold

A frequent divergence has been the shift to genes encoding proteins exhibiting stilbene synthase (STS) activity, which is responsible for the branching of phenylpropanoid metabolism towards the production of stilbenes (Durbin *et al.* 2000). It was previously shown that even within conifers, high protein similarity of CHS might not correspond to identical enzyme activity. According to Yamakaki *et al.* (2001), the phylogenetic analysis of CHS superfamily genes revealed that *Pinus strobus* STS clustered together with its CHS paralog, rather than with *Vitis vinifera* and *Psilotum nudum* STS orthologs. The results obtained for *P. pinaster Chs* sequences, based on sequence comparison, do not unequivocally allow the determination of the enzyme activity characteristics of the corresponding enzymes, and further functional characterization will be needed.

P. pinaster Chs sequences presented nucleotide identity percentages as follows: 92.6% (*Chs1-2*), 91.3% (*Chs1-3*) and 97.8% (*Chs1-2*). Considering the phylogenetic analysis which placed *Chs1* away from *Chs2* and *Chs3* (figure 5.2.7.), and the thumb-rule that determines sequences presenting over 95% identity as identical forms of the same gene, we considered *maritime pine Chs2* and *Chs3* as being allelic forms.

5.2.2.3. Expression analysis of genes encoding key phenylpropanoid enzymes

Expression analysis of *P. pinaster Pal1, Chs1 and Chs2* genes were performed by Northern blotting, followed by hybridization with the corresponding homologous probes. According to the autoradiogram, depicted in figure 5.2.8., during the *P. pinaster-B. cinerea* interaction, low transcript levels of *Pal1*, compared to those observed in needles were observed until 6 h or elicitation, declining then to non-detectable levels. In *P. pinaster* unchallenged and elicited cells, no expression of *Chs1* and *Chs2* was observed.

Lignification of cell walls and the accumulation of phenolic compounds are characteristic responses of plant defence (Nicholson and Hammerschmidt 1992; Ryals *et al.* 1996; Smit and Dubery 1997; Chen and Chen 2000). Activation of the phenylpropanoid metabolism, usually observed by the induction of PAL and CHS activities, has been a hallmark of the plant biotic stress response (Lange *et al.* 1994; Ryals *et al.* 1996; Ehness *et al.* 1997; Smith-Becker *et al.* 1998; Wang and Wu 2004), and in fact PAL has been used as a marker enzyme for the defence metabolism (Ehness *et al.* 1997). Our results are in clear contrast with the observation that carrot cells

challenged with a necrotrophic fungus induce phenylpropanoid metabolism and cell wall reinforcement while rapidly undergoing HR (Koch *et al.* 1998). The present data also suggests that in *P. pinaster* cells elicited by B. cinerea, *Pal1* downregulation is likely to account for the observed reduction in lignin content, since as referred by Bernards *et al.* (2000) for *Pinus taeda,* the lignification process in suspended cells involves a steep induction of the entry point to phenylpropanoid metabolism.

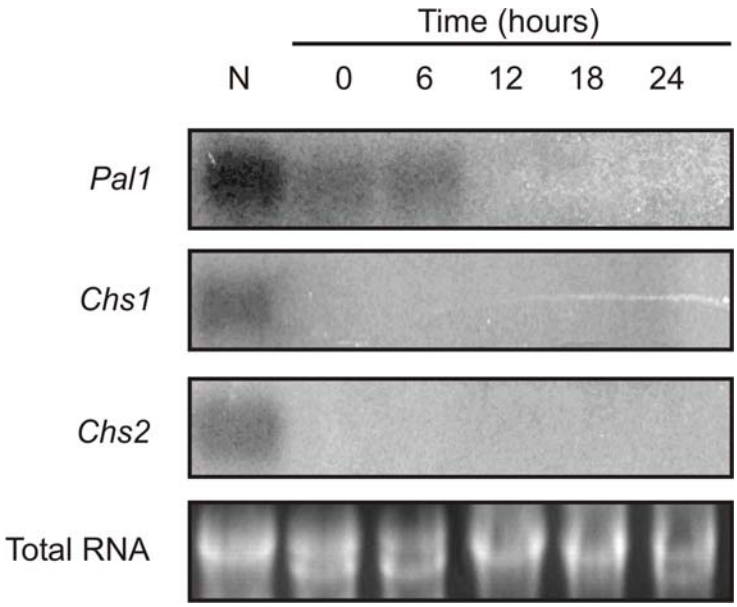

Figure 5.2.8. Expression analysis of *P. pinaster Pal1, Chs1 and Chs2* during time course of elicitation of suspended cells with *B. cinerea* spores, and in needles of adult trees (N). Total RNA samples were separated on a denaturing formaldehyde gel, blotted and hybridized with the corresponding ^{32}P-labeled cDNA homologous probes. Total RNA was used as loading control.

In the present work, the lack of *P. pinaster Chs1* and *Chs2* expression is consistent with the phenolics component of maritime pine cells being composed of simple phenolic acids, as detected by HPLC analysis. The absence of *P. pinaster Chs1* and *Chs2* transcripts, together with the decrease in *Pal1* transcript levels in pine elicited cells could account for a reduction in the synthesis of antimicrobial compounds through phenylpropanoid pathway, which agrees with the results of soluble phenolics quantification presented in figure 5.2.2. Downregulation of *P. pinaster Pal1* during elicitation by *B. cinerea* contrasts with the generally accepted mechanism of PAL

increase during plant defence. Beyond the involvement in cell wall reinforcement and phytoalexin production, phenylpropanoids correlate with the plant sensitivization mechanism designated systemic acquired resistance (SAR) (Ryals *et al.* 1996; Smith-Becker *et al.* 1998). SAR induction is mediated by salicylic acid, acting as the signalling molecule between infected and target tissues (Shirasu *et al.* 1997; Dempsey *et al.* 1999). As depicted in figure 5.2.1., salicylic acid biosynthesis occurs downstream of PAL. In light of this, PAL inhibition during the *P. pinaster-B. cinerea* interaction supports the observation made by Grovin and Levine (2002) that *B. cinerea*-challenged *Arabidopsis* plants were incapable of accumulating SA in both inoculated and secondary leaves, and were thus incapable of inducing SAR to *Pseudomonas syringae* secondary challenging (Govrin and Levine 2002). These authors also suggested that *Arabidopsis* plants that were SAR-activated by other pathogens developed increased resistance to *B. cinerea* secondary challenging, and concluded that SAR-mediated phenylpropanoid pathway activation was likely to contribute to resistance.

Taken together, results suggest that the defence response to *B. cinerea* might favour the infection process, by impairing SA biosynthesis and SAR activation. This response to *B. cinerea* elicitation can be explained in light of the increasing evidence that SAR is preferably induced after biotroph attack (Thomma *et al.* 1998; Ton *et al.* 2002), with necrotroph responses being preferably operated by the jasmonate-dependant SAR-like mechanism of induced systemic response (ISR).

Due to its nature, plant suspended cell culture constitute a model for studying plant responses in what concerns elicited cells only. However, defence responses can came also from surrounding cells of elicited ones in a plant organ. Therefore, the importance of the phenylpropanoid metabolism in the localised response of maritime pine to necrotroph challenging should not be underrated. For instance, *Pinus sylvestris* seedlings were shown to promote phytoalexin biosynthesis in response to *B. cinerea* challenging, by increasing the content of the stilbene pinosylvin (Preisig-Müller *et al.* 1999). Further elicitation studies using all-plants will be needed for the evaluation of tissue-level responses and of the role of cells adjoining HR sites in the defence process.

5.3. Effect of salicylic acid on the regulation of the expression of *P. pinaster* chloroplastic *Cu,Zn-Sod*

Adapted from:

Azevedo H, Lino-Neto, Tavares RM. 2004. Salicylic acid up-regulates the expression of chloroplastic Cu,Zn-superoxide dismutase in needles of maritime pine (*Pinus pinaster* Ait.). *Annals of Forest Science* 61: 847-850.

5.3.1. Introduction

Salicylic acid (SA) has been referred as playing a role in modulating plant responses to abiotic and biotic stresses. Accordingly, SA has been reported to increase thermotolerance and heat acclimation (Dat *et al.* 1998), chilling tolerance (Janda *et al.* 1999), salt and osmotic stress responses (Borsani *et al.* 2001). SA has also been described as being an endogenous signal for the activation of plant defenses during pathogen attack, mediating the oxidative burst that leads to cell death in the hypersensitive response, and acting as a signal for the development of systemic acquired resistance (SAR) (Shirasu *et al.* 1997; Dempsey *et al.* 1999). The transduction of the resistance signal by SA could be achieved by the inhibition of the major H_2O_2-scavenging enzymes, such as ascorbate peroxidase and catalase, leading to an increased level of H_2O_2 (reviewed by (Dempsey *et al.* 1999). More recently, it has been suggested that H_2O_2 functions upstream rather than, or in addition to, acting downstream of SA, since SA-treated plants showed no differences in catalase or ascorbate peroxidase activity (Dempsey *et al.* 1999). SA-enhanced H_2O_2 levels could also

be attributed to an increased activity of H_2O_2–producing enzymes, as reported for Cu,Zn-superoxide dismutase (Rao *et al.* 1997).

The superoxide dismutase (SOD) protein family comprises metal containing enzymes responsible for the dismutation of superoxide radical into oxygen and hydrogen peroxide. This family is divided in three groups differing in their active site metal ion (Cu/Zn, Fe and Mn). Cu,Zn-SOD isoforms are structurally unrelated to the remaining groups; most of them form an homodimer and each subunit binds a copper and zinc ion (Kanematsu and Asada 1994). In plants, Cu,Zn-SODs are mainly located in the cytosol and in the chloroplast stroma, although other locations have been reported (Bowler *et al.* 1994). The extracellular location of this isoform in Scots pine is possibly related to the transmission of systemic signal in wounding or in pathogen responses (Karpinska *et al.* 2001).

Here, the effect of SA was studied in what concerns the chloroplastic form of Cu,Zn-SOD from *Pinus pinaster*.

5.3.2. Results and Discussion

5.3.2.1. *Analysis of* P. pinaster chlCu,Zn-Sod *cDNA*

A full-length cDNA (961 bp; acc. no. AF434186) containing a putative 648 bp open reading frame was identified after screening a *P. pinaster* cDNA library with a chloroplastic *Cu,Zn-Sod* fragment from *Zantedeschia aethiopica* (acc. no. AF054151). The predicted protein of 215 amino acid residues has a molecular mass of 22.1 kDa and a 6.41 isoelectric point. Multiple nucleotide sequence alignment using ClustalW indicated the presence of a putative N-terminal signaling peptide (figure 5.3.1.). Indeed, chloroplast targeting of the protein was predicted by TargetP and PSORT, allowing the recognition of the first cDNA encoding a putative chloroplastic Cu,Zn-SOD in gymnosperms. The amino acid sequence of the corresponding protein was analysed together with other chloroplastic and cytosolic SODs (figure 5.3.2.), using the

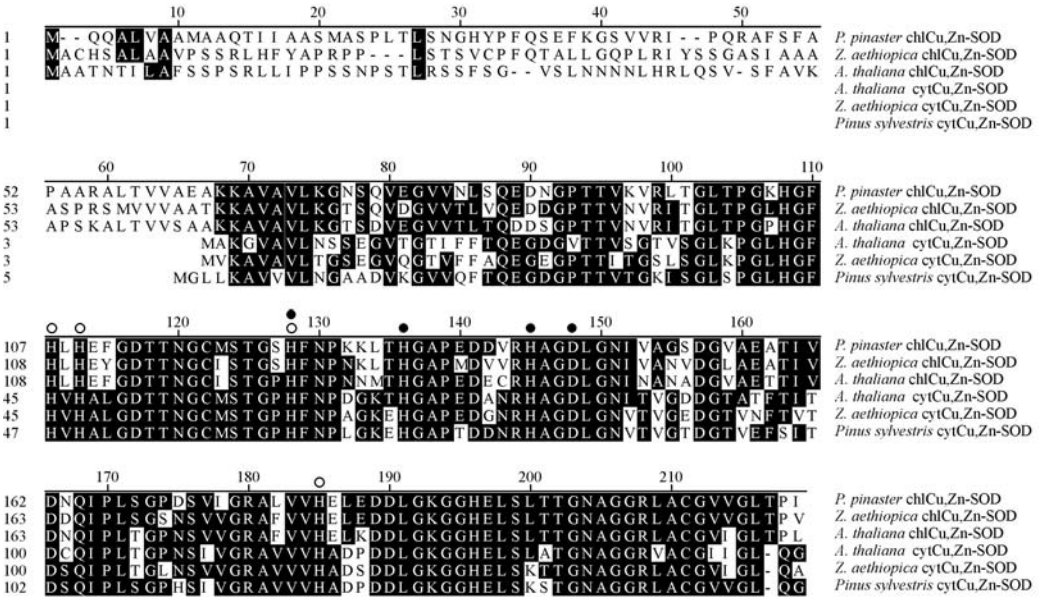

Figure 5.3.1. Amino acid sequence analysis of *P. pinaster* chlCu,Zn-SOD (acc. no. AF434186) with other higher plant chloroplastic and cytosolic Cu,Zn-SOD sequences. Multiple alignment was done using ClustalW. Cu-binding residues (○) and Zn-binding residues (●) are indicated. (*Zantedeschia aethiopica* chlCu,Zn-SOD – acc no. AF054151; *Zantedeschia aethiopica* cytCu,Zn-SOD – acc no. AF054150; *Arabidopsis thalina* chlCu,Zn-SOD – acc no. AF061519; *Arabidopsis thalina* cytCu,Zn-SOD – acc no. X60935; *Pinus sylvestris* chlCu,Zn-SOD – acc no. X58578).

Jones-Taylor-Thorton model of maximum likelihood as the criteria of inference (Doyle and Gaut 2000). PROML and DrawTree from the PHYLIP software package (Felsenstein 1989) were used for algorithm computation and unrooted tree plotting, respectively.

Analysis of the tree clearly established the *P. pinaster* deduced protein within the chloroplastidic Cu,Zn-SODs, yet indicating the natural divergence from all angiosperm species in the clade (the *P. pinaster* deduced protein showed between 46.2% and 70.8% similarity to angiosperm sequences). While pointing towards the divergence between cytosolic and chloroplastic Cu,Zn-SODs occurring early in plant evolution (Bowler *et al.* 1994), branch distance also indicates that chloroplastic Cu,Zn-SOD have much higher variability in nucleotide substitution rates than their cytosolic paralogues. This observation has already been found in other plant gene families (Doyle and Gaut 2000). In addition, *cytCuZn-Sod*s were already shown to be highly conserved (Lino-Neto 2001). Both isoforms display markedly different catalytic properties,

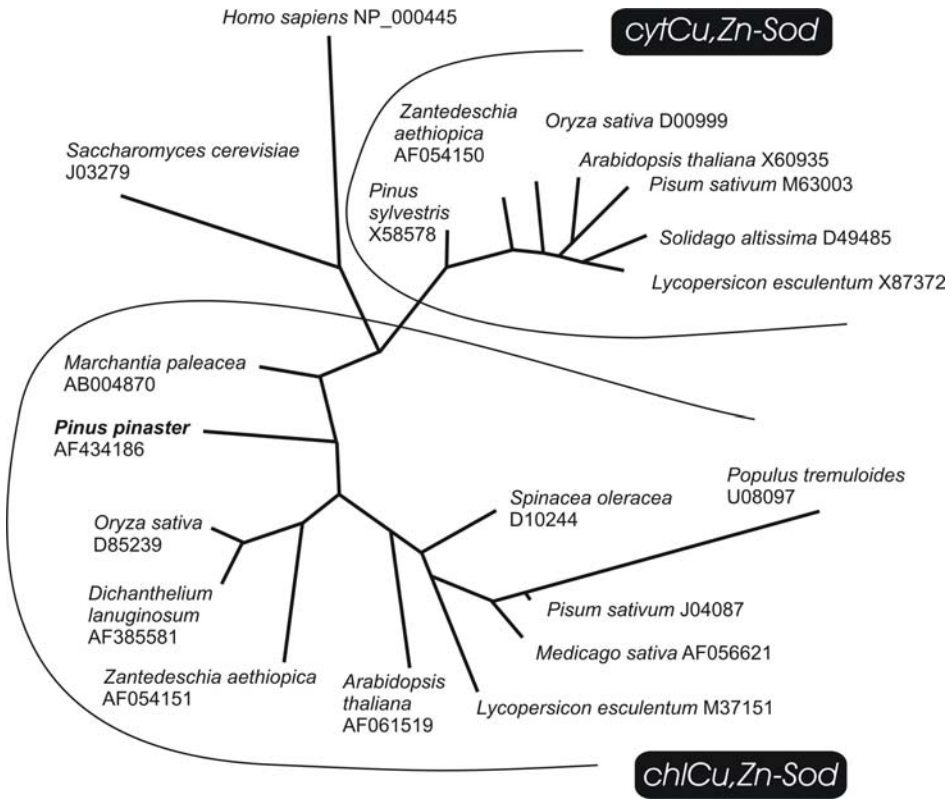

Figure 5.3.2. Unrooted tree representing the phylogenetic relationship between *Pinus pinaster* Cu,Zn-SOD (acc. no. AF434186) and cytosolic and chloroplastic Cu,Zn-SOD forms from higher plants. Inference was determined using the PHYLIP package (URL no. 9).

stability and proteolytic digestion patterns, which account for substantial differences in the structure of the proteins (Kwiatowski and Kaniuga 1986). Chloroplastic Cu,Zn-SODs are likely to have evolved from cytosolic precursor (Lino-Neto 2001), and the increased resistance to H_2O_2 which was necessary in chloroplasts has been pointed as a possible evolutionary motor for the higher divergence rate (Kanematsu and Asada 1994).

5.3.2.2. Evidences for the up-regulation of P. pinaster chlCu,Zn-Sod *by salicylic acid*

The expression of maritime pine chloroplastic *Cu,Zn-Sod* was evaluated in two month-old seedlings by Northern analysis. While high levels of transcripts were detected in needles, low levels of expression were observed in roots and stems, corroborating the chloroplastic location of this protein

(figure 5.3.3.-A). For studying the effect of SA on chloroplastic *Cu,Zn-Sod* expression, *P. pinaster* seedlings were sprayed with 5 mM salicylic acid and transcript levels were analyzed along time. The results indicate that maritime pine needles treated with SA exhibit a transient increase in chloroplastic *Cu,Zn-Sod* transcript levels (figure 5.3.3.-B).

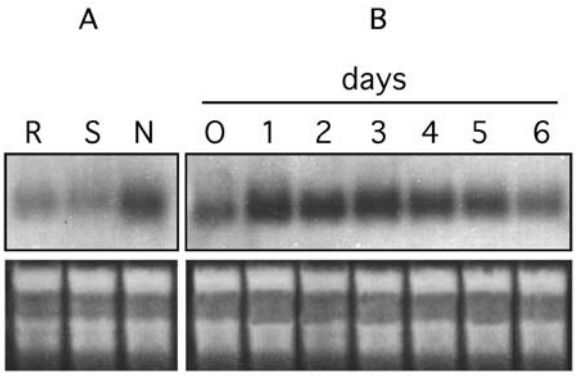

Figure 5.3.3. Expression analysis of *P. pinaster* chloroplastic *Cu,Zn-Sod* mRNA by Northern analysis. Aliquots (20 µg) of total RNA were separated in formaldeyde-agarose gel, blotted and hybridized with ^{32}P-labelled *P. pinaster Cu,Zn-Sod* probe. The amount of RNA was determined using ethidium bromide-stained RNA. **A** – Expression analysis in different plant organs: roots (R), stems (S) and needles (N). **B** – Time course expression analysis in needles after treatment with 5 mM salicylic acid.

While it has been hypothesized that SA could serve as the long-distance SAR signal that moves from inoculated leaf to uninoculated portions of the plant, it was also suggested that H_2O_2 produced during the oxidative burst that occurs in incompatible plant-pathogen interactions could be the signal responsible for the induction of SAR (Dempsey *et al.* 1999). Several studies reported the effects of SA on the activity of H_2O_2-scavenging enzymes; however its role on the regulation of the expression of enzymes responsible for H_2O_2 production is not well understood. Our results are in accordance with those reported by Rao *et al.* (1997), in which SA-enhanced H_2O_2 levels were related to the increased activity of Cu,Zn-SOD. We suggest that due to SA-mediated up-regulation of chloroplastic *Cu,Zn-Sod* expression, chloroplasts might play a role in the increase of H_2O_2 levels that are associated to the systemic microbursts occurring in uninfected cells.

Chapter 6

Effect of *Botrytis cinerea* elicitation on glucose transport in *Pinus pinaster* suspended cultured cells

6. Effect of *Botrytis cinerea* elicitation on glucose transport in *Pinus pinaster* suspended cultured cells

6.1. Introduction

Co-evolution of plants and pathogens has led to the development of a complex array of plant defence mechanisms. The increasing knowledge has revealed that the essentials for resistance lie at the cellular level, and are set upon two principles: prompt recognition of the pathogen, and subsequent triggering of the defence repertoire. Recognition of the pathogen usually culminates in a programmed cell death event (PCD) of both infected and adjoining plant cells, a process known as the hypersensitive response (HR). The not so obvious role of carbon metabolism in the overall defence response has nonetheless been substantiated (Truernit *et al.* 1996; Ehness *et al.* 1997; Bourque *et al.* 2002), suggesting that sugar mobilization and uptake might be crucial for the HR and the activation of defence mechanisms.

The importance of sugar in the regulation of various aspects of plant physiology other than carbon metabolism has been well documented (Koch 1996). In recent years, some advances have been made towards understanding the relationships between sugar metabolism and the complex defence process of plants to pathogen challenging. For infected plants, coping with the induction of several defence responses requires energy, as was demonstrated by the increase in mitochondrial activity in challenged sweet potato roots (Greksak *et al.* 1972). In sink tissues this demand must be met by exogenous supplies. During challenging both plant and pathogen cells compete for the

same nutrients and the importance of controlling carbon availability has been previously highlighted (Clark and Hall 1998; Sutton *et al.* 1999). The role of genes encoding proteins associated to sugar metabolism, such as extracellullar invertase and sugar transporters, have been studied in plant-pathogen interactions.

In higher plants sucrose is generally the main carbon source translocated from source to sink tissues. The assimilation of carbon in heterotrophic tissues can occur through direct sucrose uptake. More frequently though, sucrose is hydrolised by extracellular or cell-wall bound invertases (Masuda *et al.* 1988). Carbon uptake can then be mediated by the sugar carrier family of monosaccharide transporters (MST), energy-dependent H^+-symporters which are responsible for the transport of a wide range of monosaccharides (Büttner and Sauer 2000; Williams *et al.* 2000). MST are present in large gene families: at least 26 genes are present in the *Arabidopsis thaliana* genome, with others already isolated in several species, including the conifer *Picea abies*. Some genes like *MST1* in tobacco show sink tissue specificity (Sauer and Stadler 1993). Conserved motifs in MST promoter regions suggest that these genes are differentially regulated by various transduction signals, including stress responsive pathways. Despite indications that plant MSTs are highly regulated in response to wounding and pathogen attack (Lalonde *et al.* 1999; Delrot *et al.* 2000; Delrot *et al.* 2001), there is little knowledge on how this regulation occurs and how it coordinates with sink metabolism signalling.

Most of the physiological characterization of plant monosaccharide transporters has resorted to simplified heterologous expression systems, due to the inherent difficulties of plant material and the presence of complex sugar transport kinetics (Delrot *et al.* 2000). The use of a unicellular system such as plant cell suspension cultures presents several advantages for physiological studies, the main of which being the possibility of concerted cellular responses which minimize variability (Eshita *et al.* 2000). Heterotrophic suspension cells were previously used to study the kinetics and energetics of glucose transport in *Olea europaea* (Oliveira *et al.* 2002), and have proved to be an adequate model to study the kinetics and regulation of monosaccharide uptake in plant-microbe interactions (Truernit *et al.* 1996).

Here we describe the study of glucose transport in *P. pinaster* suspended cells and its regulation by glucose availability and *B. cinerea* challenging.

6.2. Results and Discussion

6.2.1. P. pinaster *suspended cells display activity for a H^+-monosaccharide symporter at low sugar supply*

Uptake of glucose was determined over a concentration range of 0.02–0.5 mM, and at pH 5.0 to impose a transmembrane electrochemical proton gradient. The initial D-[^{14}C]glucose uptake rates are depicted in figure 6.1. The results showed that in cells

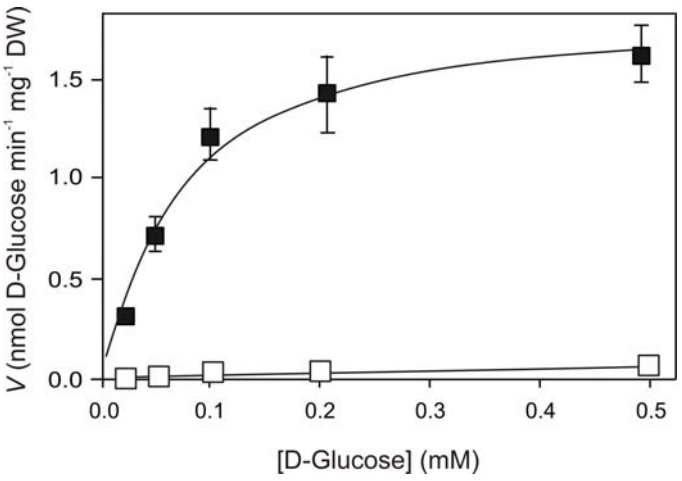

Figure 6.1. Initial uptake rates of D-[^{14}C]glucose, at pH 5.0, by *P. pinaster* suspended cells cultivated with an initial glucose concentration of 3%, harvested when glucose concentration in the medium had fallen to 2% (□) and 0.02% (■). The best fitting transport kinetics was determined by the application of GraphPad software (San Diego, Calif.).

cultivated with an initial glucose concentration of 3%, and harvested at late exponential growth phase ([glucose]$_{medium} \approx 0.02\%$), initial uptake rates of D-[^{14}C]glucose followed a Michaelis-Menten kinetics, suggesting the presence of a carrier mediated transport. By the application of computer-assisted non-linear regression analysis (GraphPad software), the following kinetic parameters were obtained: K_m, 70±15 μM glucose; V_{max}, 1.92±0.17 nmol glucose min^{-1} mg^{-1} DW. The K_m value is of the same order of magnitude of that described for *Daucus carota* (Krook *et al.* 2000), *Nicotiana tabacum* (Verstappen *et al.* 1991), *Olea europaea* (Oliveira *et al.* 2002) and *Pisum sativum* (Ritte et al. 1999) sugar carriers.

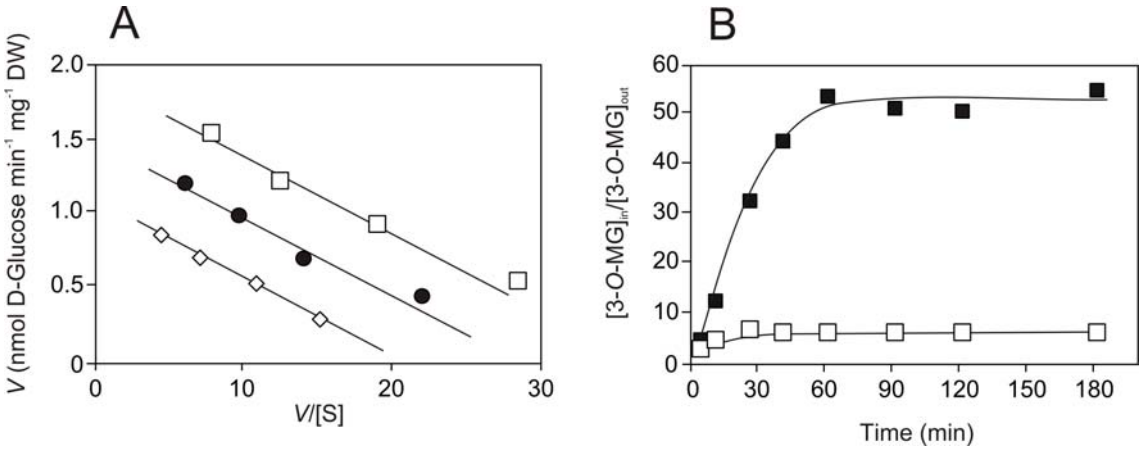

Figure 6.2. Energetics of the *P. pinaster* monosaccharide carrier. **A** – Eadie-Hofstee plots of initial uptake rates of D-[^{14}C]glucose, at pH 5.0, in the absence (□) or in the presence of 0.05 mM CCCP (◇) and 10 mM TPP^+(●). **B** – Accumulation of labelled 3-*O*-MG at pH 5.0 in the absence (■) and in the presence (□) of 0.05 mM CCCP.

To ascertain the involvement of a proton-dependent monosaccharide transport system, the initial uptake rates of 0.02–0.2 mM D-[^{14}C]glucose were measured in the presence of the protonophore carbonyl cyanide m-chlorophenylhydrazone (CCCP) (figure 6.2.-A). The presence of 50 μM CCCP inhibited up to 50% sugar transport, pointing towards a glucose-proton symport mechanism. Sugar transport was further evaluated in the presence of the lipophilic cation tetraphenylphosphonium (TPP^+) (figure 6.2.-A), which dissipates the transmembrane electric potential, thus interfering with the net influx of positive charges into the cells. The initial uptake rates of D-[^{14}C]glucose were reduced in about 30%, indicating that the transmembrane electrical gradient has a significant contribution to the driving force for sugar transport by the carrier. To evaluate the accumulative capacity of the carrier, the non-metabolizable glucose analog 3-*O*-MG was used, since, as shown in figure 6.3., it is a substrate for the monosaccharide carrier. According to figure 6.2.-B, the 3-*O*-methyl-D-[^{14}C]glucose was accumulated intracellulary to levels of about 50-fold, and the protonophore CCCP prevented 3-*O*-MG accumulation.

All together, glucose transport in pine cells growing with low sugar concentration appeared to involve a H^+-dependent monosaccharide carrier. These results are in accordance with what is described for other types of plant cells where most co-transporters utilize the electrochemical gradient of protons generated by the H^+-ATPase to drive the transport of substrates across the plasma membrane.

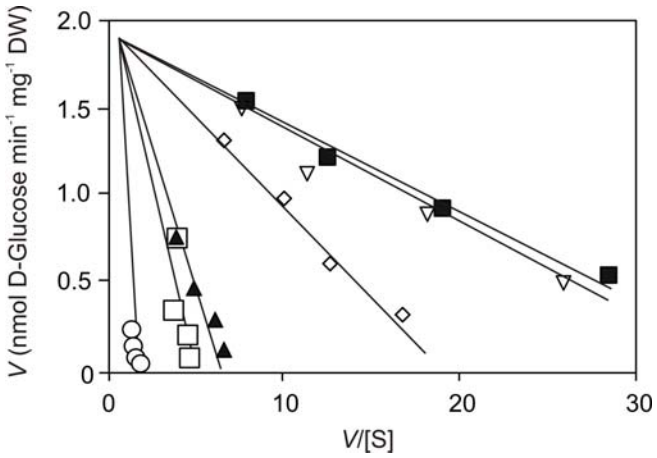

Figure 6.3. Specificity of the *P. pinaster* monosaccharide carrier. Eadie-Hofstee plots of initial uptake rates of D-[^{14}C]glucose in the absence of other sugars (■) and in the presence of 10 mM D-fructose (▲), 5 mM xylose (◇) and 5 mM mannitol (Δ), or in the presence of the following glucose analogs: 0.5 mM 2-deoxy-D-glucose (□) and 0.5 mM 3-*O*-MG (○).

The specificity of the glucose carrier was evaluated by estimating the initial uptake rates of 0.02–0.2 mM D-[^{14}C]glucose in the presence of other sugars (figure 6.3). Results indicated that D-fructose, D-xylose and D-galactose (not shown) behaved as competitive inhibitors, suggesting that they share the same carrier. The affinity of the monosaccharide carrier was in the order galactose < fructose < xylose. D-mannitol and D-arabinose (not shown) had no effect on glucose transport, appearing not to be recognized by the carrier. The D-glucose carrier is also able to accept the analogs 2-deoxy-D-glucose and 3-*O*-MG. These results, together with those regarding kinetics and energetics, suggest that the *P. pinaster* monosaccharide carrier is a member of the MST family, which comprises sugar transporters with a broad specificity, transporting a range of hexoses and pentoses with K_m values for the preferred substrate typically between 10-100 μM (Büttner and Sauer 2000).

6.2.2. P. pinaster *H^+-monosaccharide symporter is regulated by glucose levels*

As can be seen in figure 6.1., in cells cultivated with an initial glucose concentration of 3%, harvested at mid exponential growth phase ($[glucose]_{medium} \approx 2\%$), there is a linear relationship between D-[^{14}C]glucose uptake rates and the sugar concentration, suggesting that carrier-mediated transport was not present. The same

result was obtained when transport studies were performed with glucose concentrations up to 50 mM (not shown). Results suggested that the activity of the H^+-monosaccharide symporter of *P. pinaster* is repressed by high sugar levels in the culture medium, as permease activity was only measured when sugar concentration dropped to residual levels.

To demonstrate the induction of transport activity in response to the decrease of glucose concentration, the accurate dependence of the permease activity on sugar levels in the medium was evaluated. For this purpose, cells were grown in a medium with 1.5% glucose and the uptake of D-[^{14}C]glucose was measured in cell aliquots harvested from the culture at the time periods indicated in figure 6.4. Growth of cell suspension and sugar consumption from the medium are also depicted.

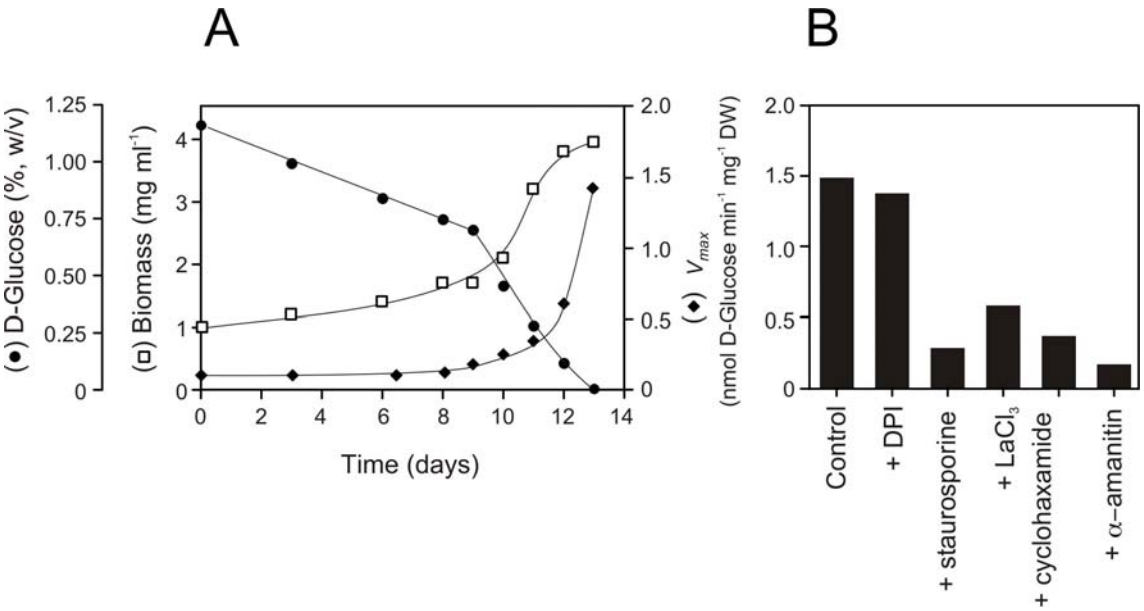

Figure 6.4. Regulation of *P. pinaster* H^+-monosaccharide symporter activity by sugar levels. **A** - Dry weight (□), glucose concentration (●) and activity of the H^+-monosaccharide symporter (◆) in suspension cultured cells of *P. pinaster* grown in mineral medium with 1.5% (w/v) glucose. **B** - DPI (50 µM), staurosporine (5 µM), LaCl (1 mM), cyclohexamide (50 µg ml^{-1}) and α-amanitin (250 µM) were added to the culture medium at day 12 and D-[^{14}C]glucose transport was measured in cell aliquots at day 13.

Glucose disappeared from the medium within 13 days, and the decline of sugar content was associated with the arrest of cell growth. In addition, once the external levels of glucose had fallen to around 0.7% (day 10), the activity of the monosaccharide carrier was significantly increased from basal levels. The maximal activity of the

permease (V_{max}=1.5 nmol min^{-1} mg^{-1} DW) was observed at day 13, when glucose was completely exhausted from the culture medium. At day 14 it was observed extensive loss in cell viability and subsequent decrease in carrier activity (data not shown). Overall results indicate that *P. pinaster* suspended cells seem to adapt the glucose transport capacity to the sugar concentration in the culture, a carrier with high affinity being operational when growth is carried out with low sugar supply.

Proton-coupled sugar transporter activity can be regulated in two major ways: (i) indirectly, by regulating H^+-ATPase activity, or (ii) more specifically by controlling the expression of sugar transporters at the transcriptional and post-transcriptional levels (Lalonde *et al.* 1999). It is believed that genes encoding monosaccharide transporters are differently regulated by sugars in higher plants. For instance, in *V. vinifera* berry flesh cells the *Vvht1* gene (hexose transporter 1) is up-regulated by sugar (Fillion *et al.* 1999), whereas MST activity in *O. europaea* suspended cells is sugar repressed (Oliveira *et al.* 2002). In contrast, hexose transporter genes of photoautotrophic *Chenopodium rubrum* suspensions are constitutively expressed and are not regulated by sugars (Roitsch and Tanner 1994).

The regulation of the *P. pinaster* H^+- monosaccharide symporter by glucose was further characterized by studying the effect of staurosporine (MAPK inhibitor), DPI (NAPH oxidase inhibitor), $LaCl_3$ (calcium influx inhibitor), α-amanitin (transcription inhibitor) and cycloheximide (inhibitor of protein synthesis) on carrier derepression mediated by glucose depletion. For this purpose, cells were collected at day 12 in the conditions described in figure 6.4.-A and incubated in the presence of the inhibitors for 24 h. As can be seen in figure 6.4.-B, from all the compounds tested, only DPI did not inhibit carrier derepression.

6.2.3. Evidences for P. pinaster *H^+-monosaccharide symporter regulation by* B. cinerea *elicitation*

As emphasised before, abiotic and biotic stresses can severely influence carbon partitioning and source-sink relationships. Yet, knowledge is still scarce on how stress-derived signalling pathways influence the regulation of sink genes. During plant-microbe interactions the pathogenic agents become an additional sink tissue, and a competition for solutes is set in the apoplast. The use and control of host carbon sources can be fundamental to the pathogen (Clark and Hall 1998; Sutton *et al.* 1999). Despite

some knowledge on the mechanisms of solute transport from host to pathogen (Bourque *et al.* 2002), very little is know on resistance mechanisms of the plant cells to sugar sequestration. Nonetheless, it is clear that sugars should play a major role in the outcome of infection.

To evaluate the role of *B. cinerea* elicitation on the regulation of *P. pinaster* glucose transport, suspended cells were incubated in the presence of different spore concentrations, up to 6.10^4 spores ml^{-1}. The results showed that in elicitation experiments performed when glucose concentration in the medium was higher than 1%, *B. cinerea* failed to induce monosaccharide transporter activity, probably because of the overlapping effect of sugar repression. However, in cells cultivated when glucose concentration in the medium was bellow 1%, the addition of fungal spores always promoted the increase of glucose carrier activity. To overcome the interference of carrier induction mediated by sugar depletion, elicitation was performed in pine

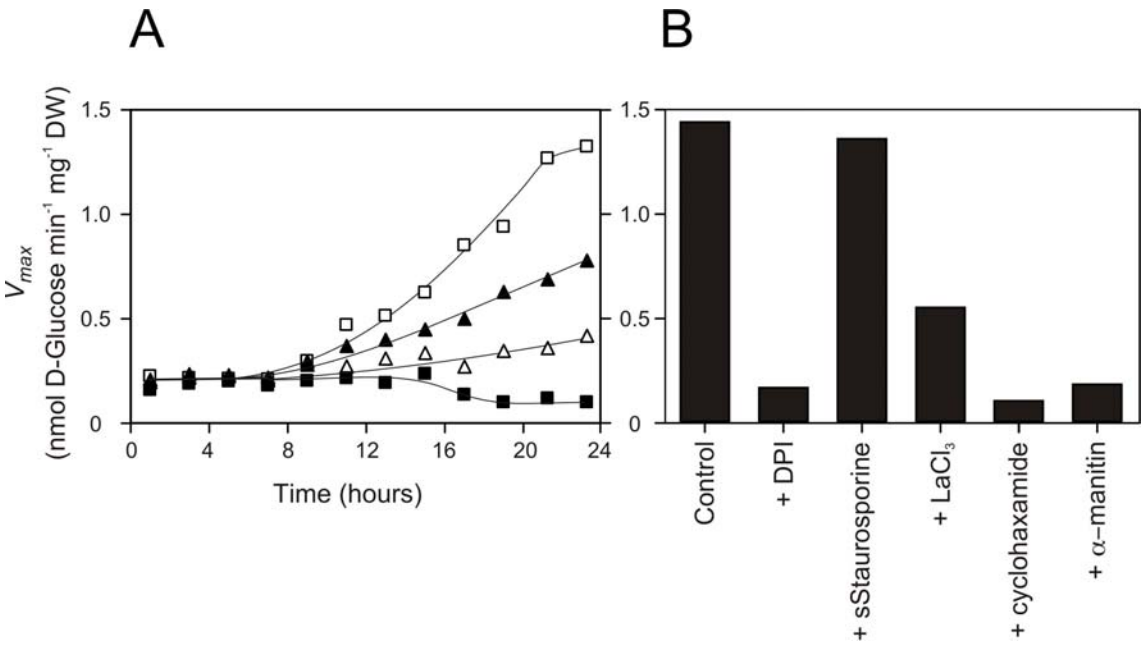

Figure 6.5. Effect of the elicitation of *P. Pinaster* suspended cells with *B. cinerea* spores on the activity of the H^+-monosaccharide symporter. **A** – Cells were washed after 9 days in culture, as indicated in figure 6.4.A., and the activity of the glucose carrier was determined in cells resuspended in mineral medium without sugar, in the absence (Δ) and presence of 2.10^4 spores ml^{-1} (▲) and 6.10^4 spores ml^{-1} (□). The activity of the glucose carrier was also determined in cells ressuspended in a medium containing 2% glucose and 6.10^4 spores ml^{-1} (■). **B** – Activity of the glucose carrier, at time t=24 h, in elicited cells (6.10^4 spores ml^{-1}) plus DPI (50 μM), staurosporine (5 μM), $LaCl_3$ (1 mM), cyclohexamide (50 μg ml^{-1}) or α-amanitin (250 μM).

suspended cells collected at day 9, in the conditions described in figure 6.4.-A, when glucose in the medium had fallen to around 0.7% (w/v). The cells were washed and resuspended in media with or without sugar, in the presence or absence of spores (figure 6.5.-A). When *B. cinerea* spores were added to cells incubated in sugar-free medium, there was a up to 3-fold increase in glucose carrier activity over to non-elicited cultures 24 h after elicitation, and a 14-fold increase over to elicited cells resuspended with 2% glucose.

To compare the mechanisms underlying the increase of H^+-monosaccharide symporter activity mediated by fungal elicitation and by glucose depletion, the effects of staurosporine, DPI, $LaCl_3$, α-amanitin and cycloheximide were also evaluated in glucose-starved cells elicited with *B. cinerea* (figure 6.5. -B). From all the compounds tested, only staurosporine had no effect on the increase of carrier activity mediated by fugal challenging. By comparing the results depicted in figures 6.4. -B and 6.5. -B, both responses appeared to be dependent on transcription and protein synthesis, because they were strongly inhibited by α-amanitin and cycloheximide, respectively. Also, calcium influx seems to be involved in the increase of carrier activity promoted by either glucose depletion or by fugal elicitation, as $LaCl_3$ markedly inhibited both responses. Calcium influx is an important component of most signal transduction cascades, and has been associated with source-sink regulation (Barker *et al.* 1998; Iwata *et al.* 1998) as well as biotic stress (Knight *et al.* 1991; Pugin *et al.* 1997; Blume *et al.* 2000; Lecourieux *et al.* 2002). Taken together, the results suggest that NADPH oxidases and MAPK are differentially involved on H^+-monosaccharide symporter regulation by glucose depletion and by *B. cinerea* challenging. Activity of plasma membrane NADPH oxidase was shown to be required for elicitation-dependent increase of glucose carrier capacity, but as expected, was not involved on glucose derepression of the symporter mediated by glucose depletion. The activity of MAPK appeared to be involved on glucose derepression of the symporter mediated by glucose exhaustion, but was not required for elicitation-dependent increase of glucose carrier capacity. The conserved mitogen-activated protein kinase cascades have been shown to play a fundamental role in signal transduction pathways of all eukariotes (Kim *et al.* 2003). They can be activated upon a vast array of signals (Hirt 1997), including sugar (Ehness *et al.* 1997) and biotic and abiotic stresses (Suzuki *et al.* 1995; Agrawal *et al.* 2003). Ehness and *et al.* (1997) showed that different MAPKs were activated during the sugar and defence

responses in *C. rubrum* suspensions, due to the differential effect of staurosporine on invertase and *Pal* expression.

In the present work, the increase of glucose carrier activity started 12 h after challenging, reaching a maximum after 24 h (figure 6.4.-A). Previous results indicated that within 12 h, *P. pinaster* suspended cells were already capable of mediated response to infection, which included HR activation and bursts of ROS production. Accordingly, Ehness and *et al.* (1997) showed that in challenged *Chenopodium rubrum* suspensions, expression of sink-specific (invertase) and defence-specific (*Pal*) genes was coordinated.

Evidences on the role of sugar transporters in the defence response are contradictory. Our results are in accordance to those of Truernit and *et al.* (1996), and Fotopoulos *et al.* (2003) who analysed the expression of *Arabidopsis AtSTP4*, a gene encoding a high affinity H^+-monosaccharide symporter with transcript specificity for heterotrophic tissues. *AtSTP4* expression is rapidly induced in the presence of fungal or bacterial elicitors, as well as after wounding. On the contrary, Bourque and co-workers (2002) showed that challenging tobacco suspension cells with the fungal elicitor cryptogein blocks glucose transport. During challenging, pathogenic fungi can respond by releasing toxins and proteinaceous elicitors that directly or indirectly alter the plasma membrane (PM) H^+-ATPase activity and cause PM depolarization (Bourque *et al.* 2002). As a consequence, PM permeability and H^+ dependent co-transporters can be affected at the beginning of infection. These authors demonstrated, however, that blocking of the glucose transporter was accompanied by phosphorylation of the carrier and took place prior to PM depolarization, but it is still unclear weather the proteinaceous elicitor cryptogein might present cell toxicity at a level other than PM depolarization. It was also suggested that this is a host mechanism to halt the cell metabolism, triggering the hypersensitive response cell death. In this work, the results obtained with *P. pinaster* cells agree with the hypothesis that host cells undergoing HR increase their capacity to absorb carbon and energy sources (Truernit and *et al.* 1996; Fotopoulos *et al.* 2003). This hypothesis is further supported by studies where extracellullar invertase activity increases after pathogen challenging (Sturm and Chrispeels 1990; Ehness *et al.* 1997).

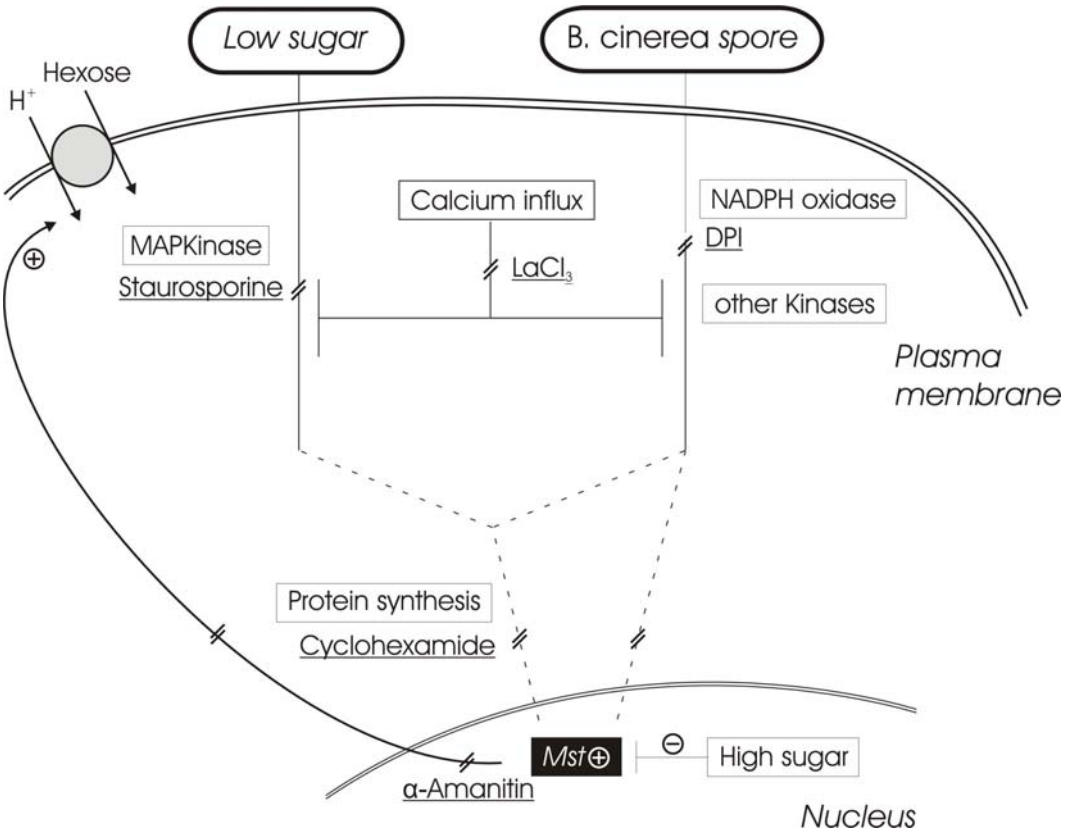

Figure 6.6. Model for the regulation of *P. pinaster* H^+-monocaccharide transporter activity by sugar and by *B. cinerea* spore elicitation. Fungal spores and low glucose levels can induce glucose activity. The involvement of different transduction pathways at the early stages of signalling is suggested by the differential involvement of MAPK and NAPH oxidase, as supported by inhibition studies. Calcium influx is a component of both signalling events. MST induction requires *de novo* transcription and protein synthesis. These transduction pathways might converge, leading to the induction of *Mst* gene(s).

An increase of sugar uptake by host cells mediated by pathogen elicitation can be related with the activation of the defence response to infection, the decrease of sugar availability to the pathogen, and the recover of leaked nutrients.

Based on overall data, a model is proposed for the signal transduction pathways involved in the regulation of hexose carrier activity by sugar and *B. cinerea* elicitation (figure 6.6.). Both signals are apparently able to increase glucose carrier activity. The involvement of different transduction pathways at the early stages of signalling is suggested by the differential involvement of MAPK and NAPH oxidase. Calcium influx seems to be a component of both signalling events. Increase in glucose carrier activity requires gene transcription and protein synthesis. These transduction pathways might converge, leading to the induction of *Mst* gene(s) expression.

Chapter 7

Final considerations and future perspectives

7. Final considerations and future perspectives

7.1. Final considerations

An intricate network of defence mechanisms allows most plants to be resistant to most pathogens despite the difficulty of having to defend against such diverse organisms as viruses, bacteria, fungi, or even animals (Dangl and Jones 2001). Non-host resistance accounts for most of the plants defence capability, by providing broad spectrum resistance (Heath 2000). In contrast to gene-for-gene resistance, the diversity of mechanisms involved in non-host resistance results from multi-genic traits (Heath 1996; Holub and Cooper 2004),

In the present work, different approaches were used to provide insights on the mechanisms involved in determining resistance of *Pinus pinaster* (maritime pine) to the non-host necrotrophic pathogen *Botrytis cinerea*. To study the cellular responses of *P. pinaster* to challenging by a necrotrophic pathogen it was required the establishment of an elicitation model system with maritime pine suspensions. In fact woody species such as pines possess inherent limitations to the use of plant material for experimentation. On the other hand, the applicability of woody species suspension cells as a model system has been well supported (Butland *et al.* 1998; Chiron *et al.* 2000; Cooney *et al.* 2000; Fornalè *et al.* 2002; Oliveira *et al.* 2002). An efficient method for obtaining heterotrophic stable pine cell suspension cultures was developed and growth was characterized in what concerned biomass production, pH variation, cell viability

and the uptake of the main nutrients present in the medium. Uptake kinetics of sugar, phosphate and nitrogen sources suggest increased nutrient consumption in the early stage of pine cultures, which might account for the absence of a lag phase. Stationary growth phase was extremely short and was followed by a pronounced death phase. Taking into consideration that phosphate was the first limiting nutrient followed immediately by sugar depletion, it was studied the response of maritime pine cells to phosphate and sugar depletions. Results evidenced that sugar starvation was responsible for the induction of a programmed cell death (PCD) response in maritime pine suspended cells. The induction of DNA cleavage, as detected by TUNEL, and the increase in hydrolytic capacity of the cells, as suggested by the increase in acid phosphase activity suggests that an autophagy type of PCD is likely to occur in sugar-starved *P. pinaster* cells (Van Doorn and Woltering 2005).

Using pine suspended cells as an elicitation model, it was possible to evaluate the responses undergone strictly by elicited cells, in opposition to all-plant models, were cells neighbouring the infection site are often taken into consideration, and the differential response between challenged and neighbouring cells is disregarded.

Challenging of maritime pine cells with *Botrytis cinerea* spores resulted in the induction of two intracellular bursts of ROS production. In contrast, mycelium from *B. cinerea* and from the necrotrophic fungi *Lophodermium seditiosum* were uncapable of inducing a response in maritime pine cells, suggesting that recognition of *B. cinerea* is specific to the spore cell wall.

The inhibition of signal transduction components (Ca^{2+} influx, MAPK, NADPH oxidase) known to be involved in elicitor signalling suggested that in *P. pinaster* elicited cells, phase I of ROS production was strictly dependant on calcium influx. This result was in accordance with the occurrence of a calcium influx event within 30 min of *B. cinerea* challenging, and points towards the involvement of calcium signalling on the induction of the defence response, as referred by others authors (Knight *et al.* 1991; Pugin *et al.* 1997; Blume *et al.* 2000; Lecourieux *et al.* 2002). How Ca^{2+} acts as a common signal transduction component of such a diverse set of responses has been an area of intense research for many years. It has been hypothesized that specificity is achieved by differences in the temporal and spatial nature and the amplitude of calcium signatures (Lecourieux *et al.* 2002). In elicited maritime pine cells, phase I oxidative burst did not seem to be dependent on the activation of MAPKs or NADPH oxidase, contrarily to reported evidence concerning the involvement of both components in early

ROS production during plant-pathogen interactions (Tenhaken *et al.* 1995; Kovtun *et al.* 2000; Suzuki 2002). It can be suggested that in pine cells, phase I ROS production may result from mechanisms other than NADPH oxidase, as suggested by Aple and Hirt (2004) and Gara *et al.* (2003). Contrarily to what was observed for phase I, MAPKs and NADPH oxidase seem to play a role in the activation of phase II oxidative burst in maritime pine suspended cells elicited with *B. cinerea*.

ROS generation, namely H_2O_2, has been implicated as a local threshold trigger for the induction of programmed cell death HR in challenged plant cells (Tenhaken *et al.* 1995). Accordingly, maritime pine suspended cells were shown to exhibit hypersensitive response (HR) when elicited with *B. cinerea* spores, as evidenced by the detection of DNA cleavage by TUNEL reaction. HR was observed following the phase II oxidative burst and was maximum within 24 h of challenging. According to the model for non-host resistance proposed by Mysore and Ryu (2004), where differences between Type I and Type II non-host responses are based on the occurrence of HR only in type II, resistance of maritime pine to *B. cinerea* challenging may fall into the category of Type II non-host resistance. A different perspective on plant defence mechanisms considers the existence of a basal resistance, whose function is containing pathogen progression once disease has set in the plant (Dangl and Jones 2001). The function of *R* gene-mediated signalling would be to speed up and optimize the activation of the defence mechanisms shared by the basal and host resistances (McDowell and Dangl 2000). Under this context, type II non-host resistance might be considered a broad-spectrum recognition mechanism, with identical function and working in parallel to the more specific host resistance mechanism. This is supported be the fact that resistance genes/pathogen recognition genes *RPS4* and *RPS5* from *Arabidopsis* were shown to play a part in non-host resistance (Holub 2001).

Results evidenced that both oxidative bursts observed in *P. pinaster* elicited cells involved the simultaneous accumulation of H_2O_2 and $O_2^{\cdot-}$. As the levels of both reactive species are maintained by the balance between SODs and H_2O_2-scavenging enzymes (De Gara *et al*. 2003, Mittler *et al.* 2004), results obtained in *P. pinaster* suggested that ROS-scavenging metabolism was subjected to fine regulation, since simultaneous increase of both ROS was observed. It was previously suggested that plant cells were overwhelmed with the levels of ROS generated during oxidative bursts (Lamb and Dixon 1997). In contrast, some authors have recently pointed out that an absolute requirement for the coordinated production of ROS and the down-regulation of ROS

scavenging mechanisms is required for hypersensitive response cell death to be observed during plant-pathogen interactions (De Gara *et al.* 2003; Apel and Hirt 2004). It has been described that *B. cinerea*, can use HR and ROS-mediated cellular disruption to promote pathogen progression in infected tissues (Williamson *et al.* 1995; ten Have *et al.* 1998; Muckenschnabel *et al.* 2002)**.** Therefore, this fungal necrotroph is putatively equipped to trigger a beneficial response from maritime pine cells. Taking into account that infection by non-host pathogens only occurs when a parasite has developed pathogenicity factors that allow it to overcome the multiple steps of non-host resistance (Heitefuss 2001), it can be suggested that resistance of maritime pine to *B. cinerea* might involve mechanisms operating at tissue level.

Challenged *P. pinaster* suspended cells were analysed in terms of the response of key ROS scavenging enzymes to *B. cinerea* challenging. The decline in CAT and SOD activity together with the down-regulation of *Fe-Sod*, *chlCu,Zn-Sod* and *csApx* genes, strongly suggest that a coordinated response is induced towards the decrease of ROS-scavenging capacity of maritime pine cells during *B. cinerea* challenging. The requirement for a suppression of ROS-scavenging mechanisms during elicitor-induced PCD raises the question of weather plants with improved ROS-scavenging mechanisms have indeed an added agricultural value as was previously suggested (Van Camp *et al.* 1994), with enzymes such as superoxide dismutases forming a desired target for engineering stress tolerance in plants. Even though several published reports referred discrepancies on the oxidative stress protection conferred by overexpression of *Sod* genes (Tepperman and Dunsmuir 1990; Pitcher *et al.* 1991), it is true that increased tolerance to oxidative stress was achieved by *Sod* overexpression (Bowler *et al.* 1991; Pitcher and Zilinskas 1996; Van Camp *et al.* 1996). In view of the present data, engineering of increased ROS-scavenging capability in plants should take into consideration a putative down-effect of determining increased susceptibility to pathogen attack.

Plants constitutively produce a multitude of secondary metabolites (phytoalexins), that create a hostile environment to pathogens due to their anti-microbial activity (Dixon 2001). In addition, phytoalexin production in response to pathogen challenge is part of the defence arrays induced during both host and non-host resistance (Dixon 2001; Mysore and Ryu 2004). Taken together the reduction in phenolics content, the decrease of cell-wall lignin content, the non-detected *Chs* transcripts levels and the down-regulation of *Pal*, it can be suggested that *B. cinerea-e*licited maritime

pine cells are not able to trigger defence responses dependant upon phenylpropanoid metabolism (e.g. production of phenylpropanoid-derived phytoalexin, cell wall reinforcement by lignification) and, possibly, nor the increase of salicylic acid (SA) levels, thus conditioning the induction of the systemic acquired resistance (SAR). It was reported that *B. cinerea*-infected *Arabidopsis* plants were incapable of inducing SA increase and were thus SAR-impaired (Govrin and Levine 2000), which agrees with hypothesis suggesting that SAR and ISR differ on the spectrum of pathogens they are targeted to, with ISR protecting against necrotrophic pathogens and SAR conferring resistance to biotrophic pathogens (Thomma *et al.* 1998; Ton *et al.* 2002). In fact, a reclassification of biotrophs and necrotrophs was recently proposed by Oliver and Ipcho (2004) based on the deployment of defence against fungal pathogens via the salicylate or jasmonate/ethylene pathways, respectively.

The involvement of SA on the sensitivization of *P. pinaster* seedlings was evaluated in what concerns the response of ROS-scavenging. The results obtained after SA application to *P. pinaster* seedlings showed that *chlCu,Zn-Sod* expression was transiently increased in response to SA. The transduction of the systemic resistance signal mediated by SA was shown to involve an increase of H_2O_2 levels (Rao 97, Dempsey 99). Results suggest that the induction of *Cu,Zn-Sod* in chloroplasts might be involved in the SA-mediated increment of H_2O_2 levels.

The role of sugar metabolism during defence responses and the regulation of genes associated to sink metabolism by biotic stress signals is still poorly understood. In this work, results from the study of glucose transport in *P. pinaster* suspended cells and its regulation by glucose and by *B. cinerea* challenging evidence that in the presence of low sugar in the medium, a H^+-monosaccharide symporter was involved in glucose transport into pine cells. The dependence of glucose carrier on sugars levels seems to indicate that carrier repression by high sugar levels takes place, which is in accordance with what was reported for the regulation by glucose carrier in *O. europaea* suspended cells (Oliveira *et al.* 2002). In addition, when conditions for sugar repression of monosaccharide carrier activity were not present, results indicated that elicitation of *P. pinaster* suspended is able to increase sugar carrier activity, suggesting that elicited pine cells are able to increase sugar mobilization. These results are in accordance with those reported by Truernit *et al.* (1996) and Fotopoulos *et al.* (2003), but do not agree to what was described by Bourque *et al.* (2002) where glucose uptake seems to be rapidly inhibited after challenging.

Signal transduction components known to take part in the sink and elicitor signals were analysed for their involvement in regulating elicitation-dependent glucose carrier induction. NADPH oxidase was shown to be specific of fungal challenging-mediated sugar carrier induction, whereas MAPK was only involved in the increase of MST activity induced by low sugar levels. These results suggest that sink-specific and elicitor-specific signals may be involved in different signal transduction pathways that regulate derepression of monosaccharide carrier, and agree with what was previously suggested by Ehness *et al.* (1997). Several hypotheses can be formulated as to the function of monosaccharide carrier induction during plant-pathogen interactions, that relate with the activation of the defence response to infection, the decrease of sugar availability to the pathogen, and the recover of leaked nutrients. However, the induction of MST activity is likely to correlate with increasing the sugar availability to challenged plants cells, since the deployment of plant defences and the induction of programmed cell death are likely to require increasing energetic needs in both source and sink tissues (Greksak *et al.* 1972; Lino-Neto 2001). This poses new questions as to the correlation between source-sink relationships and the carbon metabolic needs with the cellular events undertaken during pathogen challenge.

7.2. Future perspectives

Different research lines can be suggested based on the work carried out in the present thesis:

i) In what concerns ROS metabolism, identification of genes encoding other ROS-scavenging enzymes (*e.g.* other SOD, CAT and APX isoforms; glutathione peroxidase) and expression analysis in elicited pine cells. The use of RT-PCR for cloning purposes will take advantage of the recent *P. pinaster* EST program (URL no. 13) for primer design. In addition, further insights should be given on how ROS-generating mechanisms determine phase I oxidative burst and how the down-regulation of ROS-scavenging metabolism accounts for the phase II oxidative burst, and determines the triggering of hypersensitive response cell death during the maritime pine response to *B. cinerea*.

ii) Studies on the involvement of jasmonic acid in deploying ISR and sensitizing maritime pine plants to necrotroph attack is also justified. Further studies could include determination of phytoalexin content in elicited pine seedlings, and the study of the role of key-enzymes belonging the phytoalexin-producing pathways. However the importance of SA should not be minimized and its role of SAR induction should also be studied.

iii) It would be important to complement the study on the regulation of pine hexose carrier activity during biotic challenging with gene transcript profiling. For this purpose, isolation of maritime pine monosaccharaide transporter (MST) nucleotide sequences using a degenerate primer strategy is underway. This will allow the functional characterization of pine *Mst* genes. Since *B. cinerea* is considered as a non-host pathogen for *Arabidopsis* further studies should also consider the use of *Arabidopsis*, since mutants, affected in key points of sugar sensing, carbon metabolism and defence response are available.

References

Able, A J, Guest, D I and Sutherland, M W. (1998). Use of a new tetrazolium-based assay to study the production of superoxide radicals by tobacco cell cultures challenged with avirulent zoospores of *phytophthora parasitica* var *nicotianae*. *Plant Physiol* **117:** 491-499.

Able, A J. (2003). Production of reactive oxygen species during non-specific elicitation, non-host resistance and field resistance expression in cultured tobacco cells. *Funct. Plant Biol.* **30:** 91–99.

Adam, A, Farkas, T, Somlayai, G, Hevesi, M and Kiraly, Z. (1989). Consequence of O_2– generation during bacterially induced hypersensitive reaction in tobacco: deterioration of membrane lipids. *Physiol Mol Plant Pathol* **34:** 13-26.

Adams, V. (1991). Water and wastewater examination manual (Chelsea: Lewis Publishers).

Agrawal, G K, Agrawal, S K, Shibato, J, Iwahashi, H and Rakwal, R. (2003). Novel rice MAP kinases *OsMSRMK3* and *OsWJUMK1* involved in encountering diverse environmental stresses and developmental regulation. *Biochem Biophys Res Commun* **300:** 775-783.

Alía, R and Martín, S. (2003). Technical guidelines for genetic conservation and use: *Pinus pinaster*. (Rome: EUFORGEN).

Allan, A C, Lapidot, M, Culver, J N and Fluhr, R. (2001). An early tobacco mosaic virus-induced oxidative burst in tobacco indicates extracellular perception of the virus coat protein. *Plant Physiol* **126:** 97-108.

Alting-Mees, M, Hoener, P, Ardourel, D, Sorge, J A and Short, J M. (1992). New lambda and phagemid vectors for prokaryotic and eukaryotic expression. *Strategies Mol. Biol.* **5:** 58-61.

Altschul, S F, Madden, T L, Schäffer, A A, Zhang, J, Zhang, Z, Miller, W and Lipman, D J. (1997). Gapped BLAST and PSI-BLAST: a new generation of protein database search programs. *Nucleic Acids Res* **25:** 3389-3402.

Amor, Y, Babiychuk, E, Inzé, D and Levine, A. (1998). The involvement of poly(ADP-ribose) polymerase in the oxidative stress responses in plants. *FEBS Lett* **440:** 1-7.

Andres, C and Ojeda, F. (2002). Effects of afforestation with pines on woody plant diversity of Mediterranean heathlands in southern Spain. *Biodivers Conserv* **11:** 1511-1520.

Anthony, R G, Henriques, R, Helfer, A, Meszaros, T, Rios, G, Testerink, C, Munnik, T, Deak, M, Koncz, C and Bogre, L. (2004). A protein kinase target of a PDK1 signalling pathway is involved in root hair growth in *Arabidopsis*. *EMBO J* **23:** 572-581.

Apel, K and Hirt, H. (2004). Reactive oxygen species: Metabolism, oxidative stress, and signal transduction. *Ann Rev Plant Biol* **55:** 373-399.

Asada, K. (1994). Production and action of active oxygen species in photosynthetic tissues. In *Causes of photooxidative stress and amelioration of defense systems in plants*, C H Foyer and P M Mullineaux, eds (Boca Raton: CRC Press), pp. 77-104.

Asada, K. (1999). The water-water cycle in chloroplasts: Scavenging of active oxygens and dissipation of excess photons. *Annu Rev Plant Physiol Plant Mol Biol* **50:** 601-639.

Asai, T. (2002). MAP kinase signalling cascade in *Arabidopsis* innate immunity. *Nature* **415:** 977–983.

Ashman, T L and Schoen, D J. (1994). How long should flowers live? *Nature* **371:** 788-791.

Ausubel, F M, Brent, R, Kingston, R E, Moore, D D, Seidman, J G, Smith, J A and Struhl, K. (1996). Current Protocols in Molecular Biology. (New York: Grenn Publishing Associates and Wiley Interscience.).

Avila, C and Cánovas, F M. (2000). An improved and rapid method for the isolation of RNA isolation from adult maritime pine needles. *Plant Mol Biol Rep* **10:** 117-122.

Baba, M, Takeshige, K, Baba, N and Ohsumi, Y. (1994). Ultrastructural analysis of the autophagic process in yeast: detection of autophagosomes and their characterization. *J Cell Biol* **124:** 903-913.

Baehrecke, E H. (2003). Autophagic programmed cell death in *Drosophila*. *Cell Death Differ* **10:** 940–945.

Baier, M, Noctor, G, Foyer, C H and Dietz, K J. (2000). Antisense suppression of 2-cysteine peroxiredoxin in *Arabidopsis* specifically enhances the activities and expression of enzymes associated with ascorbate metabolism but not glutathione metabolism. *Plant Physiol* **124:** 823-832.

Baker, B, Zambryski, P, Staskawicz, B and Dinesh-Kumar, S P. (1997). Signaling in plant-microbe interactions. *Science* **276:** 726-733.

Baker, C J and Orlandi, E W. (1995). Active oxygen in plant pathogenesis. *Annu Rev Phytopathol* **33:** 299–321.

Barker, L D P, Templeton, M D and Ferguson, I B. (1998). A 67-kDa plasma membrane-bound Ca^{2+}-stimulated protein kinase active in sink tissue of higher plants. *Planta* **205:** 197-204.

Baxter-Burrell, A, Yang, Z, Springer, P S and Bailey-Serres, J. (2002). RopGAP4-dependent Rop GTPase rheostat control of *Arabidopsis* oxygen deprivation tolerance. *Science* **296:** 2026-2028.

Beauchamp, C and Fridovich, I. (1971). Superoxide dismutase: improved assay and an assay applicable to acrylamide gels. *Anal. Biochem.* **44:** 276-286.

Becana, M, Paris, F J, Sandalio, L M and del Río, L A. (1989). Isoenzymes of superoxide dismutase in nodules of *Phaseolus vulgaris* L., *Pisum sativum* L., and *Vigna unguiculata* (L.) Walp. *Plant Physiol* **68:** 275-278.

Bedell, J P, Chalot, M, Garnier, A and Botton, B. (1999). Effects of nitrogen source on growth and activity of nitrogen-assimilating enzymes in Douglas-fir seedlings. *Tree Physiol* **19:** 205-210.

Bellincampi, D, Dipierro, N, Salvi, G, Cervone, F and Lorenzo, G D. (2000). Extracellular H_2O_2 induced by oligogalacturonides is not involved in the inhibition of the auxin-regulated *rolB* gene expression in tobacco leaf explants. *Plant Physiol* **122:** 1379-1385.

Bernards, M A, Susag, L M, Bedgar, D L, Anterola, A M and Lewis, N G. (2000). Induced phenylpropanoid metabolism during suberization and lignification: a comparative analysis. *J Plant Physiol* **157:** 601-607.

Bestwick, C, Adam, A L, Puri, N and J.W. Mansfield. (2001). Characterization and changes to pro– and anti-oxidant enzyme activities during the hypersensitive reaction in lettuce (*Lactuca sativa* L.),. *Plant Sci* **61:** 497–506.

Bi, Y-M, Cammue, B P A, Goodwin, P H, KrishnaRaj, S and Saxena, P K. (1999). Resistance to *Botrytis cinerea* in scented geranium transformed with a gene encoding the antimicrobial protein Ace-AMP1. *Plant Cell Rep* **18:** 835–840.

Blume, B, Nürnberger, T, Nass, N and Scheel, D. (2000). Receptor-mediated increase in cytoplasmic free calcium required for activation of pathogen defense in parsley. *Plant Cell* **12:** 1425-1440.

Bohlmann, J, Meyer-Gauen, G and Croteau, R. (1998). Plant terpenoid synthases: molecular biology and phylogenetic analysis. *Proc Natl Acad Sci USA* **95:** 4126-4133.

Bolwell, G P, Butt, V S, Davies, D R and Zimmerlin, A. (1995). The origin of the oxidative burst in plants. *Free Radic Res* **23:** 517–532.

Bolwell, G P, Blee, K A, Butt, V S, Davies, D R, Gargner, S L, Gerrish, C, Minibayeva, F, Rowntree, E G and Wojtaszek, P. (1999). Recent advances in understanding the origin of the apoplastic oxidative burst in plant cells. *Free Radic Res* **31:** 137-145.

Borsani, O, Valpuesta, V and Botella, M A. (2001). Evidence for a role of salicylic acid in the oxidative damage generated by NaCl and osmotic stress in *Arabidopsis* seedlings. *Plant Physiol* **126:** 1024-1030.

Bortolotti, C, Murillo, I, Fontanet, P, Coca, M and Segundo, B S. (2005). Long-distance transport of the maize pathogenesis-related PRms protein through the phloem in transgenic tobacco plants. *Plant Sci* **168:** 813–821.

Bosnes, M, Deggerdal, A, Rian, A, Korsnes, L and Larsen, F. (1997). Magnetic separation in molecular biology. In *Scientific and Clinical Applications of Magnetic Carriers*, U Häfeli, W Schütt, J Teller and M Zborowski, eds (New York: Plenum Press), pp. 269-285.

Bourque, S, Lemoine, R, Sequeira-Legrand, A, Fayolle, L, Delrot, S and Pugin, A. (2002). The elicitor cryptogein blocks glucose transport in tobacco cells. *Plant Physiol* **130:** 2177-2187.

Bowler, C, Slooten, L, Vandenbranden, S, Derycke, R, Botterman, J, Sybesma, C, Vanmontagu, M and Inzé, D. (1991). Manganese superoxide-dismutase can reduce cellular-damage mediated by oxygen radicals in transgenic plants. *EMBO J* **10:** 1723-1732.

Bowler, C, Van Camp, W, Van Montagu, M and Inzé, D. (1994). Superoxide dismutase in plants. *Crit Rev Plant Sci* **13:** 199-218.

Bowler, C and Fluhr, R. (2000). The role of calcium and activated oxygens as signals for controlling cross-tolerance. *Trends Plant Sci* **5:** 241-246.

Bridges, S M and Salin, M L. (1981). Distribution of iron-containing superoxide dismutase in vascular plants. *Plant Physiol* **68:** 275-278.

Brown, I. (1998). Localization of components of the oxidative cross-linking of glycoproteins and of callose synthase in papillae formed during the interaction between non-pathogenic strains of *Xanthomonas campestris* and French bean mesophyll cells. *Plant J* **15:** 333–343.

Brown, T A. (1995). Gene Cloning: an introduction. (London: Chapman & Hall).

Bunkelmann, J R and Trelease, R N. (1996). Ascorbate peroxidase: A prominent membrane protein in oilseed glyoxysomes. *Plant Physiol* **110:** 589-598.

Burges, N A, Heywood, V H, Tutin, T G and Walters, S M. (1964). *Flora Europae* vol.1. (Cambridge: Cambridge University Press).

Butenko, R G, Lipsky, A K, Chernyak, N D and Arya, H C. (1984). Changes in culture-medium pH by cell-suspension cultures of *Dioscorea deltoidea*. *Plant Sci Lett* **35:** 207-212.

Butland, S L, Chow, M L and Ellis, B E. (1998). A diverse family of phenylalanine ammonia-lyase genes expressed in pine trees and cell cultures. *Plant Mol Biol* **37:** 15-24.

Büttner, M and Sauer, N. (2000). Monosaccharide transporters in plants: structure, function and physiology. *Biochim Biophys Acta* **1465:** 263-274.

Campbell, M M and Ellis, B E. (1992). Fungal elicitor-mediated responses in pine cell cultures: cell wall-bound phenolics. *Phytochemistry* **31:** 737-742.

Carrier, D J, Cosentino, G, Neufeld, R, Rho, D, Weber, M and Archambault, J. (1990). Nutritional and hormonal requirements of *Ginkgo biloba* embryo-derived callus and suspension cell-culture. *Plant Cell Rep* **8:** 635-638.

Cathcart, R, Schwiers, E and Ames, B N. (1983). Detection of picomole levels of hydroperoxides using a fluorescent dichlorofluorescein assay. *Anal Biochem* **134:** 111–116.

Cazale, A C, Rouet-Mayer, M A, Barbier-Brygoo, H, Mathieu, Y and Lauriere, C. (1998). Oxidative burst and hypoosmotic stress in tobacco cell suspensions. *Plant Physiol* **116:** 659-669.

Chagné, D, Brown, G, Lalanne, C, Madur, D, Pot, D, Neale, D and Plomion, C. (2003). Comparative genome and QTL mapping between maritime and loblolly pines. *Mol Breed* **12:** 185–195.

Chang, S, Puryear, J and Cairney, J. (1993). Simple and efficient method for isolating RNA from pine trees. *Plant Mol Biol Rep* **11:** 113-116.

Chen, H and Chen, F. (2000). Effect of yeast elicitor on the secondary metabolism of Ti-transformed *Salvia miltiorrhiza* cell suspension cultures. *Plant Cell Rep* **19:** 710–717.

Chen, S X and Schopfer, P. (1999). Hydroxylradical production in physiological reactions. A novel function of peroxidase. *Eur. J. Biochem.* **260:** 726–735.

Chiron, H, Drouet, A, Claudot, A C, Eckerskorn, C, Trost, M, Heller, W, Ernst, D and Sandermann, H. (2000). Molecular cloning and functional expression of a stress-induced multifunctional O-methyltransferase with pinosylvin methyltransferase activity from Scots pine (*Pinus sylvestris* L.). *Plant Mol Biol* **44:** 733-745.

Cho, S and Muehlbauer, F J. (2004). Genetic effect of differentially regulated fungal response genes on resistance to necrotrophic fungal pathogens in chickpea (*Cicer arietinum* L). *Physiol Mol Plant Pathol* **64:** 57–66.

Choi, G J, Lee, H J and Cho, K Y. (1997). Involvement of catalase and superoxide dismutase in resistance of *Botrytis cinerea* to dicarboximide fungicide vinclozolin. *Pest Biochem Physiol* **59:** 1–10.

Clark, J I M and Hall, J L. (1998). Solute transport into healthy and powdery mildew-infected leaves of pea and uptake by powdery mildew mycelium. *New Phytol* **140:** 261-269.

Clarke, P G H. (1990). Developmental cell death: morphological diversity and multiple mechanisms. *Anat Embryol* **181:** 195–213.

Claros, M G and Cánovas, F M. (1998). Rapid high quality RNA preparation from pine seedlings. *Plant Mol Biol Rep* **16:** 9-18.

Clough, S J, Fengler, K A, Yu, I, Lippok, B, Smith Jr., R K and Bent, A F. (2000). The *Arabidopsis dnd1* "defense, no death" gene encodes a mutated cyclic nucleotide-gated ion channel. *Proc Natl Acad Sci USA* **97:** 9323-9328.

Collins, N S. (2003). SNARE-protein-mediated disease resistance at the plant cell wall. *Nature* **425:** 973–977.

Cooney, A M, Hotter, G S and Lauren, D R. (2000). Biotransformation of the *Trichoderma* metabolite 6-n-pentyl-2H-pyran-2-one by cell suspension cultures of *Pinus radiata*. *Phytochemistry* **53:** 447-450.

Costa, P, Pionneau, C, Bauw, G, Dubos, C, Bahrmann, N, Kremer, A, Frigerio, J-M and Plomion, C. (1999). Separation and characterization of needle and xylem maritime pine proteins. *Electrophoresis* **20:** 1098-1108.

Crowell, D N and Amasino, R M. (1991). Induction of specific mRNAs in cultured soybean cells during cytokinin or auxin starvation. *Plant Physiol* **95:** 711-715.

Csaikl, U M, Bastian, H, Brettschneider, R, Gauch, S, Meir, A, Schauerte, M, Scholz, F, Sperisen, C, Vrnam, B and Ziegenhagen, B. (1998). Comparative analysis of different DNA extraction protocols: a fast, universal maxi-preparation of high quality plant DNA for genetic evaluation and phylogenetic studies. *Plant Mol Biol Rep* **16:** 69-86.

Cunningham, I. (1992). Biomagnetic separation. *Today´s Life Sci***:** 50-58.

Damon, S, Hewitt, J, Nieder, M and Bennett, A B. (1988). Sink metabolism in tomato fruit. II. Phloem unloading and sugar uptake. *Plant Physiol* **87:** 731-736.

Dangl, J L and Jones, J D G. (2001). Plant pathogens and integrated defense responses to infection. *Nature* **411:** 826-833.

Dangl, J L, Dietrich, R A and Thomas, H. (2000). Senescence and programmed cell death. In *Biochemistry and Molecular Biology of Plants*, B B Buchanan, W Gruissem and R L Jones, eds (Rockville: American Society of Plant Physiologists), pp. 1044-1100.

Dat, J F, Lopez-Delgado, H, Foyer, C H and Scott, I M. (1998). Parallel changes in H_2O_2 and catalase during thermotolerance induced by salicylic acid or heat acclimation in mustard seedlings. *Plant Physiol* **116:** 1351-1357.

Dat, J F, Pellinen, R, Beeckman, T, Van de Cotte, B, Langebartels, C, Kangasjarvi, J, Inzé, D and Van Breusegem, F. (2003). Changes in hydrogen peroxide homeostasis trigger an active cell death process in tobacco. *Plant J* **33:** 621-632.

De Gara, L, De Pinto, M C and Tommasi, F. (2003). The antioxidant systems vis-à-vis reactive oxygen species during plant–pathogen interaction. *Plant Physiol Biochem* **41:** 863–870.

Deighton, N, Muckenschnabel, I, Goodman, B A and Williamson, B. (1999). Lipid peroxidation and the oxidative burst associated with infection of *Capsicum annuum* by *Botrytis cinerea*. *Plant J* **20:** 485-492.

Delaney, T P, Uknes, S and Vernooij, B. (1984). A central role of salicylic-acid induced plant disease resistance. *Science* **266:** 1247–1250.

Delrot, S, Atanassova, R and Maurousset, L. (2000). Regulation of sugar, amino acid and peptide plant membrane transporters. *Biochim Biophys Acta* **1465:** 281-306.

Delrot, S, Atanassova, R, Gomès, E and Coutos-Thévenot. (2001). Plasma membrane transporters: a machinery for uptake of organic solutes and stress resistance. *Plant Sci* **161:** 391-404.

Dempsey, D A, Shah, J and Klessig, D F. (1999). Salicylic acid and disease resistance. *Crit. Rev. Plant Sci.* **18:** 547-575.

Desikan, R, Hancock, J T, Coffey, M J and Neill, S J. (1996). Generation of active oxygen in elicited cells of *Arabidopsis thaliana* is mediated by a NADPH oxidase-like enzyme. *FEBS Lett* **382:** 213-217.

Desikan, R, Clarke, A, Atherfold, P, Hancock, J T and Neill, S J. (1999). Harpin induces mitogen-activated protein kinase activity during defence responses in *Arabidopsis thaliana* suspension cultures. *Planta* **210:** 97-103.

Devaux, C, Baldet, P, Joubès, J, Dieuaide-Noubhani, M, Just, D, Chevalier, C and Raymond, P. (2003). Physiological, biochemical and molecular analysis of sugar-starvation responses in tomato roots. *J Exp Bot* **54:** 1143-1151.

Dias, A. (2000). Produção de metabolitos secundários por plantas *in vivo* e culturas *in vitro* de *Hypericum perforatum* L. e *Hypericum androsaemum* L. (Ph D. Thesis, University of Minho, Braga, Portugal).

Dixon, R A, Harrison, M J and Paiva, N L. (1995). The isoflavonoid phytoalexin pathway: from enzymes to genes to transcription factors. *Physiol Plant* **93:** 385-392.

Dixon, R A. (2001). Natural products and plant disease resistance. *Nature* **411:** 843–847.

Doehlert, D C. (1989). Separation and characterization of four hexokinases from developing maize kernels. *Plant Physiol* **89:** 1042–1048.

Doyle, J J and Doyle, J L. (1990). Isolation of plant DNA from fresh tissue. *Focus* **12:** 13-15.

Doyle, J J and Gaut, B S. (2000). Evolution of genes and taxa: a primer. *Plant Mol Biol* **42:** 1-23.

Dretzen, G, Bellard, M, Sassone-Corsi, P and Chambon, P. (1981). A reliable method for the recovery of DNA fragments from agarose and acrylamide gels. *Anal. Biochem.* **112:** 295-298.

Droillard, M J and Paulin, A. (1990). Isozymes of superoxide dismutase in mitochondria and peroxisomes isolated from petals of carnation (*Dianthus caryophyllus*) during senescence. *Plant Physiol* **94:** 1187-1192.

Drumm, H and Schopfer, P. (1974). Effect of phytochrome on development of catalase activity and isoenzyme pattern in mustard (*Sinapsis alba* L.) seedlings. A reinvestigation. *Planta* **120:** 13-30.

Durbin, M L, McCaig, B and Clegg, M T. (2000). Molecular evolution of the chalcone synthase multigene family in the morning glory genome. *Plant Mol Biol* **42:** 79-92.

Durzan, D. (1976). Biochemical changes during gymnosperm development. *Acta Hortic* **56:** 183-194.

Dvornyk, V, Sirviö, A, Mikkonen, M and Savolainen, O. (2002). Low nucleotide diversity at the *pal1* locus in the widely distributed *Pinus sylvestris*. *Mol Biol Evol* **19:** 179-188.

Eaton, A D, Clesceri, L S and Greenberg, A E. (1995). Standard methods for the examination of water and wastewater (Washington DC: American Public Health Association).

Ehness, R, Ecker, M, Godt, D E and Roitsch, T. (1997). Glucose and stress independently regulate source and sink metabolism and defense mechanisms via signal transduction pathways involving protein phosphorylation. *Plant Cell* **9:** 1825-1841.

Emanuelsson, O, Nielsen, H, Brunak, S and Heijne, G. (2000). Predicting subcellullar localization of proteins based on their N-terminal amino acid sequence. *J Mol Biol* **300:** 1005-1016.

Eshita, S M, Kamalay, J C, Gingas, V M and Yaussy, D A. (2000). Establishment and characterization of American elm cell suspension cultures. *Plant Cell Tissue Organ Cult* **61:** 245-249.

Evans, D E. (2003). Aerenchyma formation. *New Phytol* **161:** 35–49.

Farjon, A. (1998). World Checklist and Bibliography of Conifers. (Richmond, U.K.: Royal Botanical Gardens at Kew).

Farzad, M, Soria-Hernanz, D F, Altura, M, Hamilton, M B, Weiss, M R and Elmendorf, H G. (2005). Molecular evolution of the chalcone synthase gene family and identification of the expressed copy in flower petal tissue of *Viola cornuta*. *Plant Sci In press*.

Felsenstein, J. (1989). PHYLIP - Phylogeny Inference Package (Version 3.2). *Cladistics* **5:** 164-166.

Fernandes, P and Botelho, H. (2004). Analysis of the prescribed burning practice in the pine forest of northwestern Portugal. *J Environ Manage* **70:** 15-26.

Figueiral, I. (1995). Charcoal analysis and the history of *Pinus pinaster* (cluster pine) in Portugal. *Rev Paleobot Palynol* **89:** 441-454.

Fillion, L, Ageorges, A, Picaud, S, Coutos-Thévenot, P, Lemoine, R, Romieu, C and Delrot, S. (1999). Cloning and expression of a hexose transporter gene expressed during the ripening of grape berry. *Plant Physiol* **120:** 1083–1093.

Flaig, H and Mohr, H. (1992). Assimilation of nitrate and ammonium by the scots pine (*Pinus sylvestris*) seedling under conditions of high nitrogen supply. *Physiol Plant* **84:** 568-576.

Fornalè, S, Esposti, D D, Navia-Osorio, A, Cusidò, R M, Palazòn, J, Piñol, M T and Bagni, N. (2002). Taxol transport in *Taxus baccata* cell suspension cultures. *Plant Physiol Biochem* **40:** 81-88.

Forster, B and Staub, T. (1996). Basis for use strategies of anilinopyrimidine and phenylpyrrole fungicides against *Botrytis cinerea*. *Crop Prot* **15:** 529-537.

Fotopoulos, V, Gilbert, M J, Pittman, J K, Marvier, A C, Buchanan, A J, Sauer, N, Hall, J L and Williams, L E. (2003). The monosaccharide transporter gene, *AtSTP4*, and the cell-wall invertase, *Atβfruct1*, are induced in *Arabidopsis* during infection with the fungal biotroph *Erysiphe cichoracearum*. *Plant Physiol* **132:** 821–829.

Frugoli, J A, Zhong, H H, Nuccio, M L, McCourt, P, McPeek, M A, Thomas, T L and McClung,
C R. (1996). Catalase is encoded by a multigene family in *Arabidopsis thaliana* (L.) Heynh. *Plant Physiol* **112:** 327-336.

Frye, C A and Innes, R W. (1998). An *Arabidopsis* mutant with enhanced resistance to powdery mildew. *Plant Cell* **10:** 947–956.

Frye, C A, Tang, D and Innes, R W. (2001). Negative regulation of defense responses in plants by a conserved MAPKK kinase. *Proc Natl Acad Sci USA* **98:** 373–378.

Gahan, P B. (1982). Cytochemical and ultrastructural changes in cell senescence and death. In *Growth Regulators in Plant Senescence*, Monograph 8, M B Jackson, ed (British Plant Growth Regulator Group), pp. 47–57.

Gamborg, O L, Miller, R A and Ojima, K. (1968). Nutrient requirements of suspension cultures of soybean root cells. *Exp Cell Res* **50:** 151-158.

Gavrieli, Y, Sherman, Y and Ben-Sasson, S A. (1992). Identification of programmed cell death in situ via specific labeling of nuclear DNA fragmentation. *J Cell Biol* **119:** 493-501.

Gidrol, X, Lin, W S, Dégousée, N, Yip, S F and Kush, A. (1994). Accumulation of reactive oxygen species and oxidation of cytokinin in germinating soybean seeds. *Eur J Biochem* **224:** 21-28.

Gilchrist, D G. (1998). Programmed cell death in plant disease: the purpose and promise of cellular suicide. *Annu Rev Phytopathol* **36:** 393-414.

Glazebrook, J, Chen, W J, Estes, B, Chang, H S, Nawrath, C, Metraux, J P, Zhu, T and Katagiri, F. (2003). Topology of the network integrating salicylate and jasmonate signal transduction derived from global expression phenotyping. *Plant J* **34:** 217–228.

Govrin, E M and Levine, A. (2000). The hypersensitive response facilitates plant infection by the necrotrophic pathogen *Botrytis cinerea*. *Curr Biol* **10:** 751–757.

Govrin, E M and Levine, A. (2002). Infection of *Arabidopsis* with a necrotrophic pathogen, *Botrytis cinerea*, elicits various defense responses but does not induce systemic acquired resistance (SAR). *Plant Mol Biol* **48:** 267-276.

Granot, D, Levine, A and Dor-Hefetz, E. (2003). Sugar-induced apoptosis in yeast cells. *FEMS Yeast Res* **4:** 7-13.

Green, P. (1994). The ribonucleases of higher plants. *Annu Rev Plant Physiol* **45:** 421-445.

Greksak, M, Asahi, T and Uritani, I. (1972). Increase in mitochondrial activity in diseased sweet potato root tissue. *Plant Cell Physiol* **13:** 1117-1121.

Grey, D, Stepan-Sarkissian, G and Fowler, M W. (1987). Biochemistry of Forest tree species in culture. In *Cell and Tissue Culture in Forestry*, J M Bonga and D J Durzan, eds (Martinus Nijhoff Publishers), pp. 31-60.

Griffin, H G and Griffin, A M. (1994). PCR Technology: Current Innovations. (Boca Raton: CRC Press).

Groom, Q J, Torres, M A, Fordham-Skelton, A P, Hammond-Kosack, K E, Robinson, N J and Jones, J D G. (1996). rbohA a rice homologue of the mammalian gp91phox respiratory burst oxidase gene. *Plant J* **10:** 515–522.

Guan, L and Scandalios, J G. (1996). Molecular evolution of maize catalases and their relationship to other eukaryotic and prokaryotic catalases. *J Mol Evol* **42:** 570-579.

Gupta, R and Luan, S. (2003). Redox control of protein tyrosine phosphatases and mitogen-activated protein kinases in plants. *Plant Physiolology* **132:** 1149–1152.

Hahlbrock, K and Kuhlen, E. (1972). Relationship between growth of parsley and soybean cells in suspension cultures and changes in conductivity of culture Mmedium. *Planta* **108:** 271-278.

Hammerschmidt, R. (2004). Resistance to necrotrophs: is there a predictable defense pattern? *Physiol Mol Plant Pathol* **64:** 55-56.

Hammond-Kosack, K E, Silverman, P, Raskin, I and Jones, J D. (1996). Race-specific elicitors of *Cladosporium fulvum* induce changes in cell morphology and the synthesis of ethylene and salicylic acid in tomato plants carrying the corresponding *Cf* disease resistance gene. *Plant Physiol* **110:** 1381-1394.

Hammond-Kosack, K E and Jones, J D G. (1997). Plant disease resistance genes. *Annu Rev Plant Physiol Plant Mol Biol* **48:** 2–45.

Hammond-Kosack, K E and Jones, J D G. (2000). Responses to Plant Pathogens. In *Biochemistry and Molecular Biology of Plants*, B B Buchanan, W Gruissem and R L Jones, eds (Rockville: American Society of Plant Physiologists), pp. 1102-1156.

Hausbeck, M K and Moorman, G W. (1996). Managing *Botrytis* in greenhouse-grown flower crops. *Plant Disease* **80:** 1212–1219.

Heath, M C. (1996). Plant resistance to fungi. *Can J Plant Pathol* **18:** 469–475.

Heath, M C. (2000a). Nonhost resistance and nonspecific plant defenses. *Curr Opin Plant Biol* **3:** 315–319.

Heath, M C. (2000b). Hypersensitive response-related death. *Plant Mol Biol* **44:** 321-334.

Heerden, P S, Towers, G H N and Lewis , N. (1996). The nitrogen metabolism of lignifying *Pinus taeda* cell cultures. *J Biol Chem* **271:** 12350-12355.

Heitefuss, R. (2001). Defence reactions of plants to fungal pathogens: principles and perspectives, using powdery mildew on cereals as an example. *Naturwissenschaften* **88:** 273–283.

Henzler, T and Steudle, E. (2000). Transport and metabolic degradation of hydrogen peroxide in *Chara corallina*: model calculations and measurements with the pressure probe suggest transport of H_2O_2 across water channels. *J Exp Bot* **51:** 2053-2066.

Hilber, U W and Hilber-Bodmer, M. (1998). Genetic basis and monitoring of resistance of *Botryotinia fuckeliana* to anilinopyrimidines. *Plant Disease* **82:** 496-500.

Hirt, H. (1997). Multiple roles of MAP Kinases in plant signal transduction. *Trends Plant Sci* **2:** 11-15.

Hoeberichts, F A, Have, A t and Woltering, E J. (2003). A tomato metacaspase gene is upregulated during programmed cell death in *Botrytis cinerea*-infected leaves. *Planta* **217:** 517–522.

Holmes, D S and Quigley, M. (1981). A rapid boiling method for the preparation of bacterial plasmids. *Anal. Biochem.* **114:** 193-197.

Holub, E B. (2001). The arms race is ancient history in *Arabidopsis*, the wild flower. *Nat. Rev. Genet* **2:** 516–527.

Holub, E B and Cooper, A. (2004). Matrix, reinvention in plants: how genetics is unveiling secrets of non-host disease resistance. *Trends Plant Sci* **9:** 211-214.

Hornes, E and Korsnes, L. (1990). Magnetic DNA hybridization properties of oligonucleotide probes attached to superparamagnetic beads and their use in the isolation of poly(A) mRNA from eukaryotic cells. *Genetical Analytical Techniques Applications* **7:** 145-150.

Hotter, G S. (1997). Elicitor-induced Oxidative burst and phenylpropanoid metabolism in Pinus radiata cell suspension cultures. *Aust. J. Plant Physiol* **24:** 797-804.

Huckelhoven, R. (2001). Non-host resistance of barley is associated with a hydrogen peroxide burst at sites of attempted penetration by wheat powdery mildew fungus. *Mol Plant Pathol* **2:** 199–205.

Hutcheson, S W. (2001). The molecular biology of hypersensitivity to plant pathogenic bacteria. *J Plant Pathol* **83:** 151–172.

Ilieva, M and Pavlov, A. (1997). Rosmarinic acid production by *Lavandula vera* MM cell-suspension culture. *Appl Microbiol Biotechnol* **47:** 683-688.

Ingram, B and Mavituna, F. (2000). Effect of bioreactor configuration on the growth and maturation of *Picea sitchensis* somatic embryo cultures. *Plant Cell Tissue and Organ Culture* **61:** 87-96.

Ishii, K and Teasdale, R D. (1997). Effects of xylooligosaccharides on suspension-cultured cells and protoplasts of *Pinus radiata*. *Plant Cell Tissue and Organ Culture* **49:** 189-193.

Ishikawa, T, Yoshimura, K, Sakai, K, Tamoi, M, Takeda, T and Shigeoka, S. (1998). Molecular characterization and physiological role of a glyoxysome-bound ascorbate peroxidase from spinach. *Plant Cell Physiol* **39:** 23-34.

Iwamoto, M, Maekawa, M, Saito, H, Higo, H and Higo, K. (1998). Evolutionary relationship of plant catalase genes inferred from exon-intron structures: isozyme divergence after the separation of monocots and dicots. *Theor Appl Genet* **97:** 9-19.

Iwata, Y, Kuriyama, M, Nakakita, M, Kojima, H, Ohto, M-A and Nakamura, K. (1998). Characterization of a calcium-dependent protein kinase of tobacco leaves that is associated with the plasma membrane and is inducible by sucrose. *Plant Cell Physiol* **39:** 1176-1183.

Janda, T, Szalai, G, Tari, I and Páldi, E. (1999). Hydroponic treatment with salicylic acid decreases the effects of chilling injury in maize (*Zea mays* L.) plants. *Planta* **208:** 175-180.

Jarvis, W R. (1980). Taxonomy. In *The biology of* Botrytis, J R Coley-Smith, K Verhoef and W R Jarvis, eds (London: Academic press), pp. 1-18.

Jeanmougin, F, Thompson, J D, Gouy, M, Higgins, D G and Gibson, T J. (1998). Multiple sequence alignment with Clustal X. *Trends Biochem Sci* **23:** 403-405.

Jelaska, S. (1987). European pines. In *Cell and Tissue Culture in Forestry*, J M Bonga and D J Durzan, eds (Martinus Nijhoff Publishers), pp. 42-60.

Jerpseth, B, Greener, A, Short, J M, Viola, J and Kretz, P L. (1992). XL1-Blue MRF' *E. coli* cells: McrA-, McrCB-, McrF-, Mrr-, HsdR- derivative of XL1-Blue cells. *Strategies Mol Biol* **5:** 81-83.

Jung, W, Yu, O, Lausm, S M, O'Keefe, D P, Odell, J, Fader, G and McGonigle, B (2000). Identification and expression of isoflavone synthase, the key enzyme for biosynthesis of isoflavones in legumes. *Nat Biotechnol* **18:** 208-212.

Kaiser, W M. (1979). Reversible inhibition of the Calvin cycle and activation of the oxidative pentose phosphate cycle by hydrogen peroxide. *Planta* **145:** 377-382.

Kaminaka, H, Morita, S, Yokoi, H, Masumura, T and Tanaka, K. (1997). Molecular cloning and characterization of a cDNA for plastidic copper/zinc-superoxide dismutase in rice (*Oryza sativa* L.). *Plant Cell Physiol* **38:** 65-69.

Kaminaka, H, Morita, S, Tokumoto, M, Yokoyama, H, Masumura, T and Tanaka, K. (1999). Molecular cloning and characterization of a cDNA for an iron-superoxide dismutase in rice (*Oryza sativa* L.). *Biosci Biotechnol Biochem* **63:** 302-308.

Kanematsu, S and Asada, K. (1994). Superoxide dismutase. In *Molecular Aspects of Enzyme Catalysis*, T Fukui and K Soda, eds (Tokyo: VCH Publishers), pp. 191-210.

Karpinska, B, Karlsson, M, Schinkel, H, Streller, S, Süss, K-H, Melzer, M and Wingsle, G. (2001). A novel superoxide dismutase with a high isoelectric point in higher plants. Expression, regulation, and protein localization. *Plant Physiol* **126:** 1668-1677.

Kato, A and Nagai, S. (1979). Energetics of tobacco cells, *Nicotiana tabacum* L., growing on sucrose medium. *Eur J Appl Microbiol* **7:** 219-225.

Katou, S, Yamamoto, A, Yoshioka, H, Kawakita, K and Doke, N. (2003). Functional analysis of potato mitogen-activated protein kinase kinase, StMEK1. *J Gen Plant Path* **69:** 161–168.

Kaul, K and Hoffman, S A. (1993). Ammonium ion inhibition of *Pinus strobus* L callus growth. *Plant Sci* **88:** 169-173.

Keegstra, K, Olsen, L J and Theg, S M. (1989). Chloroplastic precursors and their transport across the envelope membranes. *Annu Rev Plant Physiol Plant Mol Biol* **40:** 471-501.

Keith, R C. (2003). Alginate gene expression by *Pseudomonas syringae* pv. tomato DC3000 in host and non-host plants. *Microbiology* **149:** 1127–1138.

Kerr, J F, Wyllie, A H and Currie, A R. (1972). Apoptosis: a basic biological phenomenon with wide-ranging implications in tissue kinetics. *Br J Cancer* **26:** 239-257.

Kim, J-A, Agrawal, G K, Rakwal, R, Han, K-S, Kim, K-N, Yun, C-H, Heu, S, Park, S-Y, Lee, Y-H and Jwa, N-S. (2003). Molecular cloning and mRNA expression analysis of a novel rice (*Oryza sativa* L.) MAPK kinase kinase, *OsEDR1*, an ortholog of *Arabidopsis AtERD1*, reveal its role in defense/stress signalling pathways and development. *Biochem Biophys Res Commun* **300:** 868-876.

King, P J, Mansfield, K J and Street, H E. (1973). Control of growth and cell division in plant cell suspension cultures. *Can J Bot* **51:** 1807-1823.

Kitayama, K, Kitayama, M, Osafune, T and Togasaki, R K. (1999). Subcellular localization of iron and manganese superoxide dismutase in *Chlamydomonas reinhardtii* (Chlorophyceae). *J Phycol* **35:** 136-142.

Klement, Z. (1999). Symptomless resistant response instead of the hypersensitive reaction in tobacco leaves after infiltration of heterologous pathovars of *Pseudomonas syringae*. *J Phytopathol* **147:** 467–475.

Klionsky, D J, Cregg, J M, Dunn, W A J, Emr, S D, Sakai, Y, Sandoval, I V, Sibirny, A, Subramani, S, Thumm, M, Veenhuis, M and Ohsumi, Y. (2003). A unified nomenclature for yeast autophagy-related genes. *Dev Cell* **5:** 539–545.

Knight, M R, Campbell, A K, Smith, S M and Trewavas, A J. (1991). Transgenic plant aequorin reports the effects of touch and coldshock and elicitors on cytoplasmic calcium. *Nature* **352:** 524–526.

Kobayashi, I. (1992). Recognition of a pathogen and a nonpathogen by barley coleoptile cells. III. Responses of microtubules and actin filaments in barley coleoptile cells to penetration attempts. *Can J Bot* **70:** 1815–1823.

Koch, K. (2004). Sucrose metabolism: regulatory mechanisms and pivotal roles in sugar sensing and plant development. *Curr Opin Plant Biol* **7:** 235–246.

Koch, K E. (1996). Carbohydrate-modulated gene expression in plants. *Annu Rev Plant Physiol Plant Mol Biol* **47:** 509-540.

Koch, W, Wagner, C and Seitz, H U. (1998). Elicitor-induced cell death and phytoalexin synthesis in *Daucus carota* L. *Planta* **206:** 523-532.

Kovtun, Y, Chiu, W L, Tena, G and Sheen, J. (2000). Functional analysis of oxidative stress-activated mitogen-activated protein kinase cascade in plants. *Proc Natl Acad Sci USA* **97:** 2940-2945.

Krieg, P A. (1996). A Laboratory Guide to RNA: Isolation, Analysis and Synthesis. (New York: Wiley-Liss, Inc.).

Krook, J, Vreugdenhil, D and Plas, L H W v d. (2000). Uptake and phosphorylation of glucose and fructose in *Daucus carota* cell suspensions are differently regulated. *Plant Physiol. Biochem.* **38:** 603-612.

Kumar, A and Ellis, B E. (2001). The phenylalanine ammonia-lyase gene family in raspberry. Structure, expression and evolution. *Plant Physiol* **127:** 230-239.

Kurepa, J, Hérouart, D, Van Montagu, M and Inzé, D. (1997). Differential expression of CuZn- and Fe-superoxide dismutase genes of tobacco during development, oxidative stress, and hormonal treatments. *Plant Cell Physiol* **38:** 463-470.

Kuzniak, E and Sklodowska, M. (1999). The effect of *Botrytis cinerea* infection on ascorbate glutathione cycle in tomato leaves. *Plant Sci* **148:** 69–76.

Kwiatowski, J and Kaniuga, Z. (1986). Isolation and characterization of cytosolic and chloroplast isoenzymes of Cu,Zn-superoxide dismutase from tomato leaves and their relationships to other Cu,Zn-superoxide dismutases. *Biochim Biophys Acta* **874:** 99-115.

Lalonde, S, Boles, E, Hellmann, H, Barker, L, Patrick, J W, Frommer, W B and Ward, J M. (1999). The dual function of sugar carriers: transport and sugar sensing. *Plant Cell* **11:** 707–726.

Lam, E, Pontier, D and del Pozo, O. (1999). Die and let live-programmed cell death in plants. *Curr Opin Plant Biol* **2:** 502-507.

Lam, E, Kato, N and Lawton, M. (2001). Programmed cell death, mitochondria and the plant hypersensitive response. *Nature* **411:** 848-853.

Lamb, C and Dixon, R A. (1997). The oxidative burst in plant disease resistance. *Annu Rev Plant Physiol Plant Mol Biol* **48:** 251-275.

Lange, B M, Trost, M, Heller, W, Langebartels, C and Sandermann, H. (1994). Elicitor-induced formation of free and cell-wall-bound stilbenes in cell-suspension cultures of Scots Pine (*Pinus sylvestris* L). *Planta* **194:** 143-148.

Lange, B M, Wildung, M R, McCaskill, D and Croteau, R. (1998). A novel family of transketolases that directs isoprenoid biosynthesis via a mevalonate-independant pathway. *Proc Natl Acad Sci USA* **95:** 2100-2104.

Lebourgeois, F, Levy, G, Becker, M and Lefevre, Y. (1997). Effects of mineral nutrition and water site conditions on radial growth of Corsican pine in western France. *Ann Sci Forest* **54:** 279-300.

Lecourieux, D, Mazars, C, Pauly, N, Ranjeva, R and Pugin, A. (2002). Analysis and Effects of Cytosolic Free Calcium Increases Response to Elicitors in *Nicotiana plumbaginifolia* Cells. *Plant Cell* **14:** 2627–2641.

Leustek, E G K and Lee, M S. (1987). Nitrogen nutrition. In *Cell and Tissue Culture in Forestry*, J M Bonga and D J Durzan, eds (Martinus Nijhoff Publishers), pp. 67-88.

Lincoln, J E, Richael, C, Overduin, B, Smith, K, Bostock, R and Gilchrist, D G. (2002). Expression of the antiapoptotic baculovirus p35 gene in tomato blocks programmed cell death and provides broadspectrum resistance to disease. *Proc Natl Acad Sci USA* **99:** 15217–15221.

Lindgren, P B. (1986). Gene cluster of *Pseudomonas syringae* pv. phaseolicola controls pathogenicity on bean plants and hypersensitivity on nonhost plants. *J Bacteriol* **168:** 512–522.

Lino-Neto, T. (2001). Role of oxidative stress enzymes during *Zantedeschia aethiopica* spathe whitening and regreening. (Ph D. Thesis, University of Minho, Braga, Portugal).

Liu, J, Yeo, H C, Doniger, S J and N, A B. (1997). Assay of aldehydes from lipid peroxidation: gas chromatography-mass spectrometry compared to thiobarbituric acid. *Anal Biochem* **245:** 161-166.

Logemann, J, Schell, J and Willmitzer, L. (1987). Improved method for the isolation of RNA from plant tissues. *Anal Biochem* **163:** 16-20.

Loomis, W D. (1974). Overcoming problems of phenolics and quinones in the isolation of plant enzymes and organelles. *Meth Enzymol* **31:** 528-545.

López-Gómes, R and Gómes-Lim, M A. (1992). A method for extracting intact RNA from fruits rich in polysaccharides using ripe mango mesocarp. *HortScience* **27:**440-442.

Loreto, F and Velikova, V. (2001). Isoprene produced by leaves protects the photosynthetic apparatus against ozone damage, quenches ozone products and reduces lipid peroxidation of cellular membranes. *Plant Physiol* **127:** 1781-1787.

Lu, M. (2001). *Arabidopsis NHO1* is required for general resistance against *Pseudomonas* bacteria. *Plant Cell* **13:** 437–447.

Lucas, J A. (1998). Plant Pathology and Plant Pathogens. (Oxford: Blackwell Science).

Lüttge, U and Ratajczak, R. (1997). The physiology, biochemistry and molecular biology of the plant vacuolar ATPase. *Adv Bot Res* **25:** 253-296.

Martin, S M and Rose, D. (1976). Growth of plant cells (*Ipomoea*) suspension cultures at controlled pH levels. *Can J Bot* **54:** 1264-1270.

Masuda, H, Takahashi, T and Sugawara, S. (1988). Acid and alkaline invertases in suspension-cultures of sugar-beet cells. *Plant Physiol* **86:** 312-317.

Matsumoto, T, Okunishi, K, Nishida, K, Noguchi, M and Tamaki, E. (1971). Studies on culture conditions of higher plant cells in suspension culture .2. Effect of nutritional factors on growth. *Agr Biol Chem* **35:** 543-551.

Matta, A. (1969). Accumulation of phenols in tomato plants infected by different activities and the consequence of stress induced resistance to *Fusarium* wilt of tomato. *Phytopathology* **59:** 512–513.

Mazel, A and Levine, A. (2002). Induction of glucosyltransferase transcription and activity during superoxide-dependent cell death in *Arabidopsis* plants. *Plant Physiol Biochem* **40:** 133–140.

McCabe, P F and Leaver, C J. (2000). Programmed cell death in cell cultures. *Plant Mol Biol* **44:** 359–368.

McDonell, M W, Simon, M N and Studier, F W. (1977). Analysis of restriction fragments of T7 DNA and determination of molecular weights by electrophoresis in neutral and alkaline gels. *J Mol Biol* **110:** 119-146.

Mehdy, M C. (1994). Active oxygen species in plant defense against pathogens. *Plant Physiol* **105:** 467–472.

Mittler, R and Zilinskas, B A. (1991). Molecular cloning and nucleotide sequence analysis of a cDNA encoding pea cytosolic ascorbate peroxidase. *FEBS Lett* **289:** 257-259.

Mittler, R, Feng, X and Cohen, M. (1998). Post-transcriptional suppression of cytosolic ascorbate peroxidase expression during pathogen-induced programmed cell death in tobacco. *Plant Cell* **10:** 461-473.

Mittler, R, Herr, E H, Orvar, B L, Van Camp, W, Willekens, H, Inzé, D and Ellis, B E. (1999). Transgenic tobacco plants with reduced capability to detoxify reactive oxygen intermediates are hyperresponsive to pathogen infection. *Proc Natl Acad Sci USA* **96:** 14165-14170.

Mittler, R. (2002). Oxidative stress, antioxidants and stress tolerance. *Trends Plant Sci* **7:** 405-410.

Mittler, R, Vanderauwera, S, Gollery, M and Van Breusegem, F. (2004). Reactive oxygen gene network of plants. *Trends Plant Sci* **9:** 490-498.

Moerschbacher, B M. (1990). Hypersensitive lignification response as the mechanism of non-host resistance of wheat against oat crown rust. *Physiol. Plant.* **78:** 609–615.

Moore, T, Martineau, B, Bostock, R M, Lincoln, J E and Gilchrist, D G. (1999). Molecular and genetic characterization of ethylene involvement in mycotoxin-induced plant cell death. *Physiol Mol Plant Pathol* **54:** 73–85.

Morard, P, Fulcheri, C and Henry, M. (1998). Kinetics of mineral nutrient uptake by *Saponaria officinalis* L. suspension cell cultures in different media. *Plant Cell Rep* **18:** 260-265.

Morel, J-B and Dangl, J L. (1997). The hypersensitive response and the induction of cell death in plants. *Cell Death Diff* **4:** 671-683.

Moriyasu, Y and Ohsumi, Y. (1996). Autophagy in tobacco suspension-cultured cells in response to sucrose stravation. *Plant Physiol* **111:** 1233-1241.

Muckenschnabel, I, Williamson, B, Goodman, B A, Lyon, G D, Stewart, D and Deighton, N. (2001). Markers for oxidative stress associated with soft rots in French beans (*Phaseolus vulgaris*) infected with *Botrytis cinerea*. *Planta* **212:** 376-381.

Muckenschnabel, I, Goodman, B A, Williamson, B, Lyon, G D and Deighton, N. (2002). Infection of leaves of *Arabidopsis thaliana* by *Botrytis cinerea*: changes in ascorbic acid, free radicals and lipid peroxidation products. *J Exp Bot* **53:** 207-214.

Mühlbach, H P. (1998). Use of plant cell cultures in biotechnology. In Biotechnology Annual Review, M El-Gewely, ed,pp. 113-175.

Murashige, T and Skoog, F. (1962). A Revised Medium for Rapid Growth and Bio Assays with Tobacco Tissue Cultures. *Physiol Plant* **15:** 473-&.

Murphy, T M and Auh, C K. (1996). The superoxide synthases of plasma membrane preparations from cultured rose cells. *Plant Physiol* **110:** 621–629.

Mysore, K S. (2002). Comprehensive transcript profiling of Pto and Prf-mediated host defense responses to infection by *Pseudomonas syringae* pv. tomato. *Plant J* **32:** 299–315.

Mysore, K S and Ryu, C-M. (2004). Nonhost resistance: how much do we know? *Trends Plant Sci* **9:** 97-104.

Nakai, K and Kanehisa, M. (1992). A knowledge base for predicting protein localization sites in eukaryotic cells. *Genomics* **14:** 897-911.

Naton, B, Hahlbrock, K and Schmelzer, E. (1996). Correlation of rapid cell death with metabolic changes in fungus-infected, cultured parsley cells. *Plant Physiol* **112:** 433-444.

Neill, S, Desikan, R and Hancock, J. (2002). Hydrogen peroxide signalling. *Curr Opin Plant Biol* **5:** 388-395.

Nicholson, R L and Hammerschmidt, R. (1992). Phenolic compounds and their role in disease resistance. *Annu Rev Phytopatol* **30:** 369–389.

Nickstadt, A, Bart, P H J, Thomma, I F, Kangasjärvi, J, Zeier, J, Loeffler, C, Scheel, D and Berger, S. (2004). The jasmonate-insensitive mutant *jin1* shows increased resistance to biotrophic as well as necrotrophic pathogens. *Mol Plant Pathol* **5:** 425-434.

Noctor, G and Foyer, C. (1998). Ascorbate and glutathione: keeping active oxygen under control. *Ann Rev Plant Physiol Plant Mol Biol* **49:** 249-279.

Noodén, L D. (1988). The phenomenon of senescence and aging. In *Senescence and Aging in Plants*, L D Noodén and A C Leopold, eds (London: Academic Press), pp. 1-50.

Nurnberger, T and Brunner, F. (2002). Innate immunity in plants and animals: emerging parallels between the recognition of general elicitors and pathogen-associated molecular patterns. *Curr Opin Plant Biol* **5:** 318–324.

Obara, K, Kuriyama, H and Fukuda, H. (2001). Direct evidence of active and rapid nuclear degradation triggered by vacuole rupture during programmed cell death in zinnia. *Plant Physiol* **125:** 615–626.

Oliveira, J, Tavares, R M and Gerós, H. (2002). Utilization and transport of glucose in *Olea europaea* cell suspensions. *Plant Cell Physiol* **43:** 1510-1517.

Oliver, R P and Ipcho, S V S. (2004). *Arabidopsis* pathology breathes new life into the necrotrophs-vs.-biotrophs classification of fungal pathogens. *Mol Plant Pathol* **5:** 347-352.

op den Camp, R G L, Przybyla, D, Ochsenbein, C, Laloi, C, Kim, C H, Danon, A, Wagner, D, Hideg, E, Gobel, C, Feussner, I, Nater, M and Apel, K. (2003). Rapid induction of distinct stress responses after the release of singlet oxygen in *Arabidopsis*. *Plant Cell* **15:** 2320-2332.

Orozco-Cardenas, M L, Narvaez-Vasquez, J and Ryan, C A. (2001). Hydrogen peroxide acts as a second messenger for the induction of defense genes in tomato plants in response to wounding, systemin, and methyl jasmonate. *Plant Cell* **13:** 179–191.

Orrenius, S, Zhivotovsky, B and Nicotera, P. (2003). Regulation of cell death: the calciumapoptosis link. *Nat Rev Mol Cell Biol* **4:** 552–565.

Otto, G P, Wu, M Y, Kazgan, N, Anderson, O R and Kessin, R H. (2003). Macroautophagy is required for multicellular development of the social amoeba *Dictyostelium discoideum*. *J Biol Chem* **278:** 17636–17645.

Overmyer, K, Brosche, M and Kangasjarvi, J. (2003). Reactive oxygen species and hormonal control of cell death. *Trends Plant Sci* **8:** 335-342.

Palma, D A, Blumwald, E and Plaxtona, W C. (2000). Upregulation of vacuolar H^+-translocating pyrophosphatase by phosphate starvation of *Brassica napus* (rapeseed) suspension cell cultures. *FEBS Lett* **486:** 155-158.

Parsons, H L, Yip, J Y H and Vanlerberghe, G C. (1999). Increased respiratory restriction during phosphate-limited growth in transgenic tobacco cells lacking alternative oxidase. *Plant Physiol* **121:** 1309–1320.

Patrick, J W. (1990). Sieve element unloading: cellular pathway, mechanism and control. *Physiol Plant* **78:** 298–308.

Patrick, J W. (1997). Phloem unloading: sieve element unloading and post-sieve element transport. *Annu Rev Plant Physiol Plant Mol Biol* **48:** 191–222.

Peart, J R. (2002). Ubiquitin ligase-associated protein SGT1 is required for host and nonhost disease resistance in plants. *Proc Natl Acad Sci USA* **99:** 10865–10869.

Pellinen, R, Palva, T and Kangasjarvi, J. (1999). Subcellular localization of ozone-induced hydrogen peroxide production in birch (*Betula pendula*) leaf cells. *Plant J* **20:** 349-356.

Pesce, A, Capasso, C, Battistoni, A, Folcarelli, S, Rotilio, G, Desideri, A and Bolognesi, M. (1997). Unique structural features of the monomeric Cu,Zn superoxide dismutase from *Escherichia coli*, revealed by X-ray crystallography. *J Mol Biol* **274:** 408-420.

Petersen, D R, Reichard, J, Kolaja, K L and Hartley, D P. (1999). 4-Hydroxynonenal and malondialdehyde heatic protein adducts in rats treated with carbon tetrachloride: immuno-chemical dection and lobular localization. *Toxicol Appl Pharmacol* **161:** 23-33.

Petit, R J, Bahrman, N and Baradat, P. (1995). Comparison of genetic differentiation in maritime pine (*Pinus pinaster* Ait.) estimated using isozyme, total protein and terpenic loci. *Heredity* **75:** 382–389.

Pieterse, C M J and VanLoon, L C. (1999). Salicylic acid-independent plant defense pathways. *Trends Plant Sci* **4:** 52-58.

Piffanelli, P, Devoto, A and Schulze-Lefert, P. (1999). Defence signalling pathways in cereals. *Curr Opin Plant Biol* **2:** 295-300.

Pinto, I, Pereira, H and Usenius, A. (2004). Heartwood and sapwood development within maritime pine (*Pinus pinaster* Ait.) stems. *Trees* **18:** 284–294.

Popp, M P, Lesney, M S and Davis, J M. (1996). Defense responses elicited in pine cell suspension cultures. *Plant Cell Tissue and Organ Culture* **47:** 199-205.

Preisig-Müller, R, Schwekendiek, A, Brehm, I, Reif, H-J and Kindl, H. (1999). Characterization of a pine multigene family containing elicitor-responsive stilbene synthase genes. *Plant Mol Biol* **39:** 221–229.

Pugin, A, Frachisse, J-M, Tavernier, E, Bligny, R, Gout, E, Douce, R and Guernb, J. (1997). Early events induced by the elicitor cryptogein in tobacco cells: involvement of a plasma membrane NADPH oxidase and activation of glycolysis and the pentose phosphate pathway. *Plant Cell* **9:** 2077-2091.

Rao, M V, Paliyath, G, Ormrod, D P, Murr, D P and Watkins, C B. (1997). Influence of salicylic acid on H_2O_2 production, oxidative stress, and H_2O_2-metabolizing enzymes. Salicylic acid-mediated oxidative damage requires H_2O_2. *Plant Physiol* **115:** 137-149.

Rea, P A and Poole, R J. (1993). Vacuolar H^+-translocating pyrophosphatase. *Annu Rev Plant Physiol Plant Mol Biol* **44:** 157-180.

Rentel, M C, Lecourieux, D, Ouaked, F, Usher, S L, Petersen, L, Okamoto, H, Knight, H, Peck, S C, Grierson, C S, Hirt, H and Knight, M R. (2004). OXI1 kinase is necessary for oxidative burst-mediated signalling in *Arabidopsis*. *Nature* **427:** 858-861.

Ribeiro, M M, Plomion, C, Petit, R, Vendramin, G G and Szmidt, A E. (2001). Variation in chloroplast single-sequence repeats in Portuguese maritime pine (*Pinus pinaster* Ait.). *Theor Appl Genet* **102:** 97–103.

Richardson, D M. (1998). Ecology and Biogeography of *Pinus*. (Cambridge University Press).

Rizhsky, L, Hallak-Herr, E, Van Breusegem, F, Rachmilevitch, S, Barr, J E, Rodermel, S, Inzé, D and Mittler, R. (2002). Double antisense plants lacking ascorbate peroxidase and catalase are less sensitive to oxidative stress than single antisense plants lacking ascorbate peroxidase or catalase. *Plant J* **32:** 329-342.

Rizhsky, L, Liang, H J and Mittler, R. (2003). The water-water cycle is essential for chloroplast protection in the absence of stress. *J Biol Chem* **278:** 38921-38925.

Roitsch, T and Tanner, W. (1994). Expression of a sugar-transporter gene family in a photoautotrophic suspension culture of *Chenopodium rubrum*. *Planta* **194:** 365–371.

Rolland, F, Winderickx, J and Thevelein, J. (2001). Glucose-sensing mechanisms in eukaryotic cells. *Trends Bio Sci* **26:** 310-317.

Rose, D and Martin, S M. (1975). Effect of ammonium on growth of plant-cells (*Ipomoea* Sp) in suspension cultures. *Can J Bot* **53:** 1942-1949.

Rosslenbroich, H-J and Stuebler, D. (2000). *Botrytis cinerea* - history of chemical control and novel fungicides for its management. *Crop Prot* **19:** 557-561.

Rouhier, N and Jacquot, J-P. (2002). Plant peroxiredoxins: alternative hydroperoxide scavenging enzymes. *Photosynthesis Res* **74:** 259–268.

Ryals, J A, Neuenschwandler, U H, Willits, M G, Molina, A, Steiner, H Y and Hunt, M D. (1996). Systemic acquired resistance. *Plant Cell* **8:** 1809-1819.

Sagi, M, Davydov, O, Orazova, S, Yesbergenova, Z, Ophir, R, Stratmann, J W and Fluhr, R. (2004). Plant respiratory burst oxidase homologs impinge on wound responsiveness and development in *Lycopersicon esculentum*. *Plant Cell* **16:** 616-628.

Saier, M H, Beatty, J T, Goffeau, A, Harvey, K T, Heijne, W H, Huang, S C, Jack, D L, Jahn, P S, Lew, K, Liu, J, Pao, S S, Paulsen, I T, Tseng, T T and Virk, P S. (1999). The major facilitator superfamily. *J Mol Microbiol Biotech.* **1:** 257-279.

Salin, M L. (1988). Plant superoxide dismutases: a means of coping with oxygen radicals. *Curr Top Plant Biochem Physiol* **7:** 188-200.

Salisbury, F B and Ross, C W. (1994). *Plant Physiol*. (Belmont: Wadsworth Publishing Company).

Salvador, L, Alía, R, Agúndez, D and Gil, L. (2000). Genetic variation and migration pathways of maritime pine (*Pinus pinaster* Ait) in the Iberian peninsula. *Theor Appl Genet* **100:** 89–95.

Sambrook, J, Fritsch, E F and Maniatis, T. (1989). Molecular Cloning: a Laboratory Manual. (Cold Spring Harbor, New York: Cold Spring Harbor Laboratory Press).

Sargent, P A and King, J. (1974). Investigations of growth-promoting factors in conditioned soybean root cells and in liquid-medium in which they grow - ammonium, glutamine, and amino-acids. *Can J Bo* **52:** 1747-1755.

Sauer, N and Stadler, R. (1993). A sink-specific H+/monosaccharide cotransporter from *Nicotiana tabacum*: Cloning and heterologous expression in baker's yeast. *Plant J* **4:** 601-610.

Schenk, P M, Kazank, K, Wilson, I, Anderson, J P, Richmond, T, Somerville, S C and Manners, J M. (2000). Coordinated plant defense responses in *Arabidopsis* revealed by microarray analysis. *Proc Natl Acad Sci USA* **97:** 11655–11660.

Schröder, J. (2000). The family of chalcone synthase-related proteins: functional diversity and evolution. In *Evolution of metabolic pathways*, J T Romeo, R K Ibrahim, L Varin and V De Luca, eds (Amsterdam: Pergamon Press), pp. 55-89.

Sedmak, J J and Grossberg, S E. (1977). A rapid, sensitive, and versatile assay for protein using Coomassie Brilliant Blue G250. *Anal. Biochem.* **79:** 544-552.

Sgonc, R, Boeck, G, Dietrich, H, Gruber, J, Recheis, H and Wick, G. (1994). Simultaneous determination of cell surface antigenes. *Trends Gen* **10:** 41-42.

Shan, L. (2000). A cluster of mutations disrupt the avirulence but not the virulence function of AvrPto. *Mol Plant Microbe Interact* **13:** 592–598.

Shimon-Kerner, N, Mills, D and Merchuk, J C. (2000). Sugar utilization and invertase activity in hairy-root and cell-suspension cultures of *Symphytum officinale*. *Plant Cell Tissue Organ Cult* **62:** 89-94.

Shirasu, K, Nakajima, H, Rajasekhar, V K, Dixon, R A and Lamb, C. (1997). Salicylic acid potentiates an agonist-dependent gain control that amplifies pathogen signals in the activation of defense mechanisms. *Plant Cell* **9:** 261-270.

Short, J M, Fernandez, J M, Sorge, J A and Huse, W D. (1988). λ ZAP: a bacteriophage λ expression vector with *in vivo* excision properties. *Nucleic Acids Res* **16:** 7583-7600.

Short, J M and Sorge, J A. (1992). *In vivo* excision properties of bacteriophage λ ZAP expression vectors. *Meth Enzymol* **216:** 495-508.

Singh, U P, Sarma, B K and Singh, D P. (2003a). Effect of plant growth-promoting Rhizobacteria and culture filtrate of *Sclerotium rolfsii* on phenolic and salicylic acid contents in chickpea (*Cicer arietinum*). *Curr Microbiol* **46:** 131-140.

Singh, V K, Wood, S M, Knowles, V L and Plaxton, W C. (2003b). Phosphite accelerates programmed cell death in phosphate-starved oilseed rape (*Brassica napus*) suspension cell cultures. *Planta* **218:** 233-239.

Smart, C M. (1994). Gene expression during leaf senescence. *New Phytol* **126:** 419-449.

Smirnoff, N. (1993). The role of active oxygen in the response of plants to water deficit and desiccation. *New Phytol* **125:** 27-58.

Smit, F and Dubery, I A. (1997). Cell wall reinforcement of cotton hypocotyls in response to a *Verticillium dahliae* elicitor. *Phytochemistry* **44:** 811-815.

Smith, F A. (1984). Regulation of the cytoplasmic pH of *Chara corallina* - response to changes in external pH. *J Exp Bot* **35:** 43-50.

Smith-Becker, J, Marois, E, Huguet, E J, Midland, S L, Sims, J J and Keen, N T. (1998). Accumulation of salicylic acid and 4-hydroxybenzoic acid in phloem fluids of cucumber during systemic acquired resistance is preceded by a transient increase in phenylalanine ammonia-lyase activity in petioles and stems. *Plant Physiol* **116:** 231-238.

Sousa, E M and Trigueiros, J J. (2001). Protecção integrada do pinheiro bravo na região de Entre-Douro e Minho. *PAMAF 4054*.

Speirs, J and Longhurst, T. (1993). RNA extraction and fractionation. In *Methods in Plant Biochemistry* (Academic Press), pp. 1-32.

Srinivasan, V, Pestchanker, L, Moser, S, Hirasuna, T J, Taticek, R A and Shuler, M L. (1995). Taxol production in bioreactors - kinetics of biomass accumulation, nutrient-uptake, and taxol production by cell-suspensions of *Taxus baccata*. *Biotechnol Bioeng* **47:** 666-676.

Sticher, L, Mauch-Mani, B and Metraux, J P. (1997). Systemic acquired resistance. *Ann Rev Phytopathol* **35:** 235–270.

Sturm, A and Chrispeels, M J. (1990). cDNA cloning of carrot extracellular β-fructosidase and its expression in response to wounding and bacterial infection. *Plant Cell* **2:** 1107-1119.

Suarez, M F, Avila, C, Gallardo, F, Canton, F R, Garcia-Gutierrez, A, Claros, M G and Canovas, F M. (2002). Molecular and enzymatic analysis of ammonium assimilation in woody plants. *J Exp Bot* **53:** 891-904.

Sussman, M R. (1994). Molecular analysis of proteins in the plant plasma membrane. *Annu Rev Plant Physiol Plant Mol Biol* **45:** 211-234.

Sutton, P N, Henry, M J and Hall, J L. (1999). Glucose, and not sucrose, is transported from wheat to wheat powdery mildew. *Planta* **208:** 426-430.

Suzuki, K, Fukuda, Y and Shinshi, H. (1995). Studies on elicitor-signal transduction leading to differential expression of defense genes in cultured tobacco cells. *Plant Cell Physiol* **36:** 281-289.

Suzuki, K. (2002). MAP kinase cascades in elicitor signal transduction. *J Plant Res* **115:** 237–244.

Taiz, L and Zeiger, E. (1998). Plant Physiology (Sunderland, Massachusetts: Sinauer Associates).

Tanaka, K, Otsubo, T and Kondo, N. (1982). Participation of hydrogen peroxide in the inactivation of Calvin cycle SH enzymes in SO_2-fumigated spinach leaves. *Plant Cell Physiol* **23:** 1009-1018.

Tang, W and Ouyang, F. (1999). Plant regeneration via organogenesis from six families of loblolly pine. *Plant Cell Tiss Organ Cult* **58:** 223-226.

Tao, Y. (2003). Quantitative nature of *Arabidopsis* responses during compatible and incompatible interactions with the bacterial pathogen *Pseudomonas syringae*. *Plant Cell* **15:** 317–330.

Tavernier, E, Wendehenne, D, Blein, J P and Pugin, A. (1995). Involvement of free calcium in action of cryptogein, a proteinaceous elicitor of hypersensitive reaction in tobacco cells. *Plant Physiol* **109:** 1025–1031.

Tenhaken, R, Levine, A, Brisson, L F, Dixon, R A and Lamb, C. (1995). Function of the oxidative burst in hypersensitive disease resistance. *Proc Natl Acad Sci USA* **92:** 4158-4163.

Thomas, H and Stoddard, J L. (1980). Leaf senescence. *Annu Rev Plant Physiol* **31:** 83-111.

Thomma, B J, Eggermont, K, Penninckx, I A, Mauch-Mani, B, Vogelsang, R, Cammue, B A and Broekaert, W F. (1998). Separate jasmonate-dependent and salicylate-dependent defense-response pathways in *Arabidopsis* are essential for resistance to distinct microbial pathogens. *Proc Natl Acad Sci USA* **95:** 15107–15111.

Thomma, B J, Penninckx, I A, Cammue, B A and Broekaert, W F. (2001). The complexity of disease signaling in *Arabidopsis*. *Curr Opin Immunol* **13:** 63-68.

Thompson, J E, Legge, R L and Barber, R F. (1987). The role of free radicals in senescence and wounding. *New Phytol* **105:** 317-344.

Thompson, M R and Thorpe, T A. (1987). Metabolic and non-metabolic roles of carbohydrates. In *Cell and Tissue Culture in Forestry*, J M Bonga and D J Durzan, eds (Martinus Nijhoff Publishers), pp. 89-124.

Thordal-Christensen, H. (2003). Fresh insights into processes of nonhost resistance. *Curr Opin Plant Biol* **6:** 351–357.

Thorpe, T A. (1980). Organogenesis In vitro: structural, physiological and biochemical aspects. In International Review of Cytology, Supplement 11A, Perspectives in Plant Cell and Tissue Culture, I V ed., ed (New York: Academic Press), pp. 71-112.

Ton, J, Van Pelt, J A, VanLoon, L C and Pieterse, C M J. (2002). Differential effectiveness of salicylate-dependent and jasmonate/ethylene-dependent induced resistance in *Arabidopsis*. *Mol Plant Microbe Interact* **15:** 27–34.

Torimitsu, K, Yazaki, Y, Nagasuka, K, Ohta, E and Sakata, M. (1984). Effect of external pH on the cytoplasmic and vacuolar pHs in mung bean root-tip cells - a P-31 nuclear magnetic-resonance study. *Plant Cell Physiol* **25:** 1403-1409.

Trewavas, A J and Malhó, R. (1998). Ca^{2+} signalling in plant cells: The big network! *Curr Opin Plant Biol* **1:** 428–433.

Truernit, E, Schmid, J, Epple, P, Illig, J and Sauer, N. (1996). The sink-specific and stress-regulated *Arabidopsis STP4* gene: enhanced expression of a gene encoding a monosaccharide transporter by wounding, elicitors, and pathogen challenge. *Plant Cell* **8:** 2169-2182.

Tsang, E W T, Bowler, C, Hérouart, D, Van Camp, W, Villaroel, R, Genetello, C, Van Montagu, M and Inzé, D. (1991). Differential regulation of superoxide dismutase in plants exposed to environmental stress. *Plant Cell* **3:** 783-792.

Van den Ende, W, Coninck, B D and Van Laere, A. (2004). Plant fructan exohydrolases: a role in signaling and defense? *Trends Plant Sci* **9:** 523-528.

Van Doorn, W G, Balk, P A, van Houwelingen, A M, Hoeberichts, F A, Hall, R D, Vorst, O, Van der Schoot, C and Van Wordragen, M F. (2003). Gene expression during anthesis and PCD in *Iris* flowers. *Plant Mol Biol* **53:** 885–903.

Van Doorn, W G and Woltering, E J. (2005). Many ways to exit? Cell death categories in plants. *Trends Plant Sci In press*.

Van Leeuwen, W, Ökrész, L, Bögre, L and Munnik, T. (2004). Learning the lipid language of plant signalling. *Trends Plant Sci* **9: 378**-384.

VanEtten, H, Mansfield, J W, Bailey, J A and Farmer, E E. (1994). Two classes of plant antibiotics: phytoalexins versus "phytoanticipins". *Plant Cell* **6:** 1191-1192.

Vendramin, G G, Anzidei, M, Madaghiele, A and Bucci, G. (1998). Distribution of genetic diversity in *Pinus pinaster* Ait. as revealed by chloroplast microsatellites. *Theor Appl Genet* **97:** 456-463.

Verniquet, F, Gaillard, J, Neuberger, M and Douce, R. (1991). Rapid inactivation of plant aconitase by hydrogen peroxide. *Biochem J* **276:** 643-648.

Verstappen, R, Ranostaj, S and Rausch, T. (1991). The hexose transporters at the plasma membrane and the tonoplast of transformed plant cells: kinetic characterization of two distinct carriers. *Biochim Biophys Acta* **1073:** 366-373.

Vleeshouwers, V. (2000). The hypersensitive response is associated with host and nonhost resistance to *Phytophthora infestans*. *Planta* **210:** 853–864.

Volokita, M. (1991). The carboxy-terminal end of glycolate oxidase directs a foreign protein into tobacco leaf peroxisomes. *Plant J* **1:** 361-366.

Vranova, E, Atichartpongkul, S, Villarroel, R, Van Montagu, M, Inzé, D and Van Camp, W. (2002). Comprehensive analysis of gene expression in *Nicotiana tabacum* leaves acclimated to oxidative stress. *Proc Natl Acad Sci USA* **99:** 10870-10875.

Wakayima, I, Newton, R, Johnston, J S and Price, H J. (1993). Genome size and environmental factors in the genus *Pinus*. *Am J Bot* **80:** 1235–1241.

Wang, J W and Wu, J Y. (2004). Involvement of nitric oxide in elicitor-induced defense responses and secondary metabolism of *Taxus chinensis* cells. *Nitric Oxide* **11:** 298–306.

Warren, C R and Adams, M A. (2002). Phosphorus affects growth and partitioning of nitrogen to Rubisco in *Pinus pinaster*. *Tree Physiol* **22:** 11-19.

Waterhouse, P M, Wang, M-B and Lough, T. (2001). Gene silencing as an adaptative defence against viruses. *Nature* **411:** 834-842.

Waterman, P G and Mole, S. (1994). Analysis of phenolic plant metabolites. (London: Blackwell).

Webb, R P and Allen, R D. (1995). Isolation and characterization of a cDNA for spinach cytosolic ascorbate peroxidase. *Plant Physiol* **108:** 1325.

Wendel, J F and Weeden, N F. (1989). Visualization and interpretation of plant isozymes. In *Isozymes in Plant Biology*, D E Soltis and P S Soltis, eds (London: Chapman and Hall), pp. 5-45.

Whistler, C A, Corbell, N A, Sarniguet, A, Ream, W and Loper, J E. (1998). The two component regulators GacS and GacA influence accumulation of the stationary phase sigma factor sigmaS and the stress response in *Pseudomonas fluorescens* Pf-5. *J Bacteriol* **180:** 6635–6641.

Wilkins, T and Smart, L B. (1996). Isolation of RNA from plant tissue. In *A Laboratory Guide to RNA - isolation, analysis and synthesis*, P Krieg, ed (New York: Wiley-Liss), pp. 21-42.

Willekens, H, Langebartels, C, Tiré, C, Van Montagu, M, Inzé, D and Van Camp, W. (1994a). Differential expression of catalase genes in *Nicotiana plumbaginifolia* (L.). *Proc Natl Acad Sci USA* **91:** 10450-10454.

Willekens, H, Villarroel, R, Van Montagu, M, Inzé, D and Van Camp, W. (1994b). Molecular identification of catalases from *Nicotiana plumbaginifolia* (L.). *FEBS Lett* **352:** 79-83.

Williams, L E, Lemoine, R and Sauer, N. (2000). Sugar transporters in higher plants - a diversity of roles and complex regulation. *Trends Plant Sci* **5:** 283-290.

Wilson, S B. (1971). Studies of growth in culture of plant cells. 13. Properties of mitochondria isolated from batch cultures of *Acer pseudoplatanus* cells. *J Exp Bot* **22:** 725-&.

Woolhouse, H W. (1984). The biochemistry and regulation of senescence in chloroplasts. *Can J Bot* **62:** 2934-2942.

Xu, N, Johns, B, Pullman, G and Cairney, J. (1997). Rapid and reliable differential display from minute amounts of tissue: mass cloning and characterization of differentially expressed genes from loblolly pine embryos. *Plant Mol Biol Rep* **15:** 377-391.

Yamaguchi, K, Mori, H and Nishimura, M. (1995). A novel isoenzyme of ascorbate peroxidase localized on glyoxysomal and leaf peroxisomal membranes in pumpkin. *Plant Cell Physiol* **36:** 1157-1162.

Yamakaki, Y, Suh, D-Y, Sitthithaworn, W, Ishiguro, K, Kobayashi, Y, Shibuya, M, Ebizuka, Y and Sankawa, U. (2001). Diverse chalcone synhase superfamily enzymes from the most primitive vascular plant, *Psilotum nudum*. *Planta* **214:** 75-84.

Yang, Y, Shah, J and Klessig, D F. (1997). Signal perception and transduction in plant defence responses. *Genes Dev* **11:** 1621-1639.

Yanish-Perron, C, Viera, J and Messing, J. (1985). Improved M13 phage cloning vectors and host strains: nucleotide sequences of the M13mp18 and pUC19 vectors. *Gene* **33:** 103-119.

Yen, C-H and Yang, C-H. (1998). Evidence for programmed cell death during leaf senescence in plants. *Plant Cell Physiol* **39:** 922-927.

Yu, S-M. (1999). Cellular and genetic responses of plants to sugar starvation. *Plant Physiol* **121:** 687-693.

Zhang, W, Seki, M, Furusaki, S and Middelberg, A P J. (1998). Anthocyanin synthesis, growth and nutrient uptake in suspension cultures of strawberry cells. *J Ferment Bioeng* **86:** 72-78.

Zhao, D X, Xing, J M, Li, M Y, Lu, D P and Zhao, Q. (2001). Optimization of growth and jaceosidin production in callus and cell suspension cultures of *Saussurea medusa*. *Plant Cell Tissue Organ Cult* **67:** 227-234.

URL

1. EUFORGEN – European Forest Genetics, Conifer Network
http://www.ipgri.cgiar.org/networks/euforgen/Networks/Conifers/CN_home.asp

2. Gymnosperm Database
http://www.conifers.org/pi/pin/pinaster.htm

3. DGRF – Direcção Geral dos Recursos Florestais
http://www.dgf.min-agricultura.pt/

4. Canadian Forest Services
http://www.nrcan.gc.ca/cfs-scf/index_e.html

5. CECT Spanish Type Culture Collection
http://www.cect.org/

6. NCBI - Genbank
http://www.ncbi.nlm.nih.gov/Genbank/

7. NCBI - Entrez
http://www.ncbi.nlm.nih.gov/Entrez/index.html

8. NCBI – Blast
http://www.ncbi.nlm.nih.gov/BLAST/
9. PHYLIP software package
http://evolution.genetics.washington.edu/phylip.html

10. GenomeNet ClustalW server
http://clustalw.genome.jp/

11. TargetP
http://www.cbs.dtu.dk/services/TargetP/

12.PSORT
http://psort.nibb.ac.jp/

13. *Pinus pinaster* EST programme
http://www.pierroton.inra.fr/genetics/